CHEMOMETRIC AND METABOLOMIC INVESTIGATIONS OF THERMAL TREATMENT-INDUCED CHEMICAL AND METABOLIC EVENTS IN HEAT STRESS, PREPARATION AND CONSUMPTION OF HEATED VEGETABLE OILS

A DISSERTATION
SUBMITTED TO THE FACULTY OF
UNIVERSITY OF MINNESOTA
BY

LEI WANG

IN PARTIAL FULFILLMENT OF THE REQUIREMENTS
FOR THE DEGREE OF
DOCTOR OF PHILOSOPHY

DR. CHI CHEN, ADVISOR

DECEMBER 2016

© LEI WANG 2016

Acknowledgements

Firstly, I would like to thank my adviser, Dr. Chi Chen for his constant guidance and support. Without his advice and encouragement, I would not have completed my studies and research projects. It is my great honor and fortune to work with him.

Second, I want to express my gratitude to my committee members, Drs. Gerald Shurson, Brian Kerr, A. Saari Csallany, and Daniel Gallaher. I want to thank them for their insightful advice and generous help to my projects.

I also want to thank my lab members, Dana Yao, Xiaolei Shi, Yuwei Lu, Yiwei Ma, Feng Ding, John Kurtz, Qingqing Mao, and Dr. Zheting Bi for their helps and advice for my experiments. I would like to thank Zhaohui Luo, who provided countless help for the animal studies and statistical analysis. I also want to express my great appreciation to Dr. Andrea Hanson, for her generous help to my research projects. I am also very grateful for the advice from Dr. Pedro Urriola.

Finally, I want to thank all my friends here in Minnesota for their encouragements and helps. I would like to thank all of my family. Their constant love, encouragement and support, are the priceless treasure for me. To my fiancee, Yue Ding, I appreciate everything from you.

ABSTRACT

Temperature is a fundamental parameter in nature that determines the physical properties of materials, the rate and extent of chemical reactions, and the scale and direction of thermal radiation. Energy associated with high temperature can affect the survival and wellbeing of a living organism, directly through heat stress, and indirectly through exposure and consumption of thermally-processed food and chemicals. In this project, the direct influences of thermal energy on a biological system were examined by the metabolomic analysis of heat stress (HS)-elicited metabolic effects in pigs, while the indirect influences of thermal energy on a biological system were investigated by the chemometric analysis of heating-induced chemical changes in frying oils and the metabolomic analysis of metabolic changes induced by the consumption of thermally-oxidized cooking oils in mice. The results of these metabolomics and chemometric analyses are summarized as follows: (1) HS greatly affected diverse metabolites associated with amino acid, lipid, and microbial metabolism, including urea cycle metabolites, essential amino acids, phospholipids, medium-chain dicarboxylic acids, fatty acid amides, and secondary bile acids. More importantly, many changes in these metabolite markers were correlated with both acute and adaptive responses to heat stress. (2) Thermal stress-elicited degradation of triacylglycerols and formation of lipid oxidation products (LOPs) in vegetable oils occurred simultaneously at frying temperature. Specific aldehydes and aldehyde clusters could be more effective indicators of lipid oxidation status for frying oils and fried foods than many traditional markers. (3) Feeding heated soybean oil (HSO) significantly altered the composition of the

metabolome by introducing diverse LOPs and altering the metabolism of lipids, amino acids, and antioxidants. Among these metabolic changes, the decrease of serum tryptophan and the increase of urinary tryptophan metabolites were caused by HSO-elicited activation of tryptophan-NAD^+ catabolic pathway. Overall, these results from metabolomic and chemometric analyses provide mechanistic insights on thermal energy-induced chemical and metabolic events.

Table of Contents

List of Tables

List of Figures

CHAPTER 1. LITERATURE REVIEW

Part of this chapter is modified from the manuscript:
Wang, L.; Chen, C. Emerging applications of metabolomics in studying chemopreventive phytochemicals. *The AAPS journal*. 2013, *15*, 941-950.

1.1 TEMPERATURE AND METABOLISM

Metabolism, including catabolic and anabolic processes, sustains the life through numerous enzyme-dependent or -independent chemical reactions. All chemical reactions comprise substrates, reaction medium, and products, while enzyme-dependent chemical reactions also require enzymes and cofactors. Temperature, as a fundamental parameter in nature, can affect metabolism through its influences on all these elements of chemical reactions, and therefore plays a decisive role in the survival and wellbeing of a living organism. For the metabolic system of humans and animals, high temperature directly alters the functions and reactivity of enzymes, subtracts, products, and reaction media in metabolic reactions as well as genes, proteins, and signaling pathways responsible for the execution and regulation of these metabolic reactions. Moreover, high temperature induces chemical changes in food and feeds consumed by humans and animals [1, 2], and therefore indirectly affect the metabolic system through altered nutrients and newly formed bioactive compounds in food and feeds[3] (Figure 1.1).

In humans and animals, metabolites are the nutrients and chemicals transferred from food and feed intakes after digestion or the products of metabolic reactions in energy, nutrient, and even microbial metabolism. All the metabolites in a biological system construct a metabolome, which coexist and interact with genome, transcriptome, and proteome. Functioning as the end products of biological pathways, the building blocks of growth, and the regulators of wellbeing, the metabolites in a metabolome not only reflect the metabolic status of a biological system, but also carry diverse information on gene expression, protein function, and signal transduction events associated with the disruption and homeostasis of a biological system, especially after nutritional and xenobiotic

challenges or pathophysiological disturbances. Therefore, examining the composition and changes in the metabolome offers the opportunities to understand the metabolic phenotype of a biological system as well as their underlying mechanisms.

In this study, thermal energy-elicited chemical and metabolic events in food and animals were examined using chemometrics- and metabolomics-based approaches. Three specific aims of this study are:

1. To identify and characterize the metabolic effects of heat stress in animals.
2. To identify and characterize the chemical changes in cooking oils at frying temperature.
3. To identify and characterize the biotransformation and metabolic effects of thermally-oxidized oils in animals.

New information and valuable insights from this study could serve as a knowledge base for alleviating the adverse effects of high temperature on food, feeds, and health through chemical prevention or pharmacological intervention.

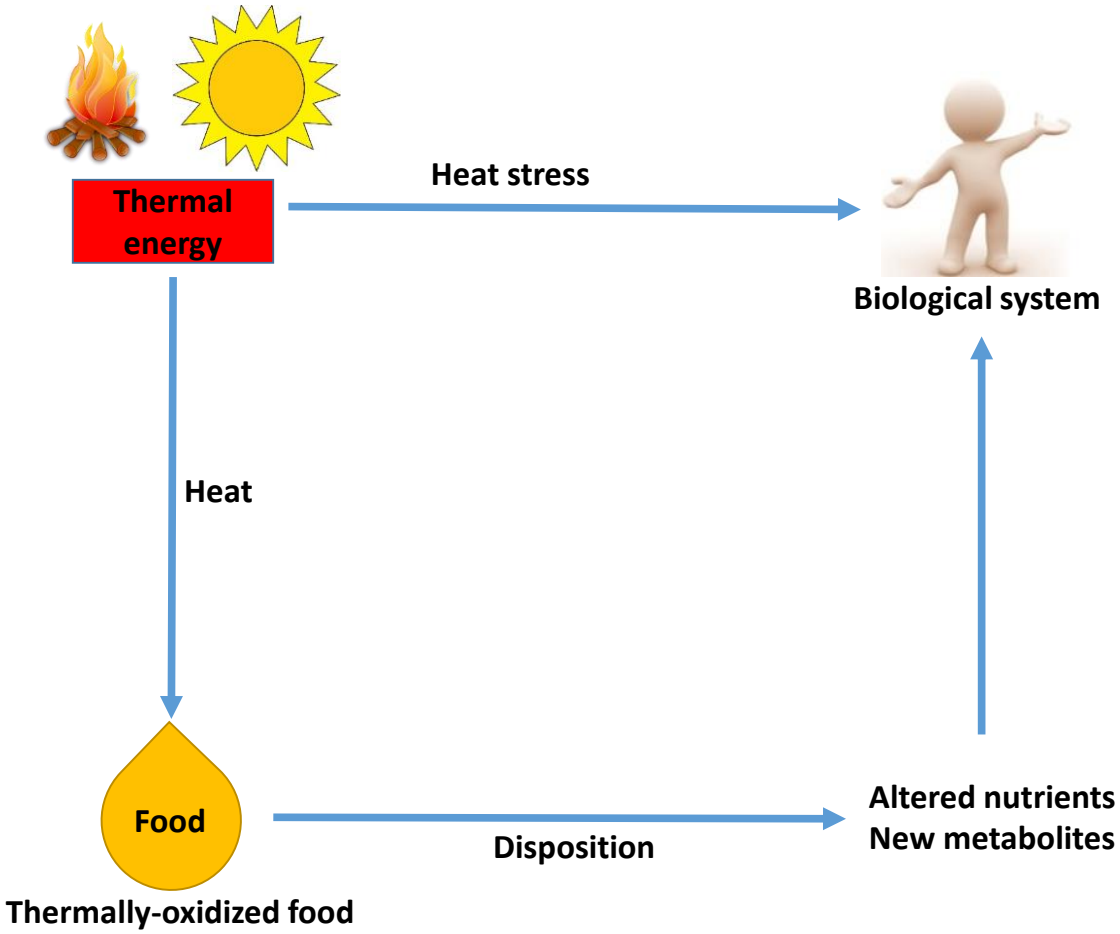

Figure 1.1. Direct and indirect influences of thermal energy on a biological system. Energy associated with high temperature can affect the survival and wellbeing of humans and animals, directly through heat stress and hyperthermia, or indirectly through the exposure and consumption of thermally-processed food and chemicals.

1.2 HEAT STRESS

1.2.1 Adverse effects of heat stress on humans and animals

High ambient temperature-elicited heat stress (HS) is a detrimental pathophysiological event that directly affects the homeostasis of living organisms[4-7]. In humans and animals, heat stress-induced illness can progress from heat exhaustion, which is accompanied with heavy sweating and rapid breathing, to heat stroke when the core body temperature exceeds a threshold, such as 104°F for humans[8]. Heat stroke can

cause lasting damages to organ functions and is associated with a high risk of early mortality[4, 5, 9]. As one of natural hazards, extreme high temperature has significant impacts on public health. The heat waves in France and Athens caused 14,802 and 2,000 deaths in August, 2003 and July, 1987, respectively[8, 10]. The heat waves have also been occurring annually in different regions of the United States, such as the 1995 Chicago heat wave[11], and are expected to be more frequent and intense according to the current climate trends. Besides being a health threat to humans, HS negatively affects the growth performance, reproduction, and health status of farm animals and has caused average annual loss of 1.7 billion dollars for dairy, beef, swine, and poultry industries[6, 7, 12]. Severe HS is predicted to be an increasing problem for animal industry in near future because of global warming progression[13]. The report from an intergovernmental panel on climate change has shown that the earth temperature has been increased by 0.2°C per decade, and the global average surface temperature is predicted to raise 1.4-5.8°C by the end of this century[14]. This situation will cause more heat illness in humans and animals and heat stress-elicited damages to the ecosystem and agriculture in near future [14].

1.2.2 Heat stress-induced biological effects

Elevated core body temperature caused by HS leads to extensive systemic changes and physiological responses, such as the changes in cardiovascular and respiratory systems, and systemic inflammatory responses[15-18]. One hallmark event in HS is the elevated cardiac and respiratory rates[15, 16]. In cellular level, HS inhibits DNA synthesis and transcription, and triggers denaturation and degradation of proteins, as well as disruption of cytoskeletal structure[19, 20]. HS decreases the number of mitochondria, causing dramatic decrease of ATP synthesis[21, 22]. HS also altered the membrane

permeability by changing the ratio of protein to lipids, leading to an imbalance of Na^+, H^+, and Ca^{2+} between intracellular and extracellular spaces[23, 24]. In the digestive tract, HS can compromise the tight junctions among intestinal epithelial cells, resulting in the translocation of bacteria and endotoxins[17, 18]. The metabolic system is also greatly affected by HS. HS induces the changes in metabolism-related hormones, such as thyroid and growth hormones, and decreases the basal metabolic rate[25-30]. At the same time, HS alters the expression of genes and proteins involving in energy and nutrient metabolism[28-30]. Changes in individual metabolites such as amino acids, lipid, and carbohydrate have been observed in HS[25, 31-33]. However, HS-induced global changes in the metabolome were seldom evaluated.

1.2.3 Molecular events in heat stress

The composition and dynamics of membrane lipids play an important role in the cellular responses to HS[34]. The membrane structures of cells and intracellular organelles are sensitive to thermal stress due to their lipid contents[35]. The lipid membranes are responsible for the integrity of cells and organelles, and also convey the signals for heat shock response (HSR). Under HS, the lipid metabolizing enzymes convert the membrane lipid species to their downstream signaling metabolites. Together, membrane lipids and their metabolites constitute a complex lipid signaling network responsive to the HS[36]. One of the main targets of this complex signaling network is the heat shock proteins (Hsps) which are highly expressed under the HS. Hsps function as intracellular chaperones that can stabilize the folding structures of proteins and prevent the unwanted protein aggregation[37]. Hsps contain five major families including Hsp70s, Hsp90s, Hsp100s, Hsp60s, and small Hsps[24].

Based on the duration and temperature, HS could be classified into three categories: mild (39.5 ± 1°C), severe (42.5 ± 1°C), and deleterious (45 ± 1°C) (Figure 1.2). Under mild HS, no protein denaturation occurs inside the cells. Fever and free radicals from mild HS could trigger the functional changes in cellular membranes and then release the signal lipids for the HSR, which further induces the synthesis of Hsps (Figure 1.2). Under severe HS, denatured proteins start to accumulate in the cytoplasm, resulting in stress responses. In response, the calcium level is greatly increased and the signal lipids are accumulated in severe HS, triggering much higher expression of Hsps than mild HS to protect against the HS-induced protein denaturation (Figure 1.2). Furthermore, the changes of membrane lipids in severe HS also disturb the electron transport chain and oxidative phosphorylation (Figure 1.2). Under deleterious HS, the signals for cytoprotection, including the increased levels of Ca^{2+} and signal lipids, such as free fatty acids and ceramide, reach their upper limits. In fact, the excessive ceramide can initiate apoptosis[38]. Moreover, the perturbation of the mitochondrial membrane and the oxidation of phosphatidylserine also contribute to the programmed cell death[39, 40]. At the same time, extensive protein denaturation occurs while Hsps synthesis is inhibited due to the suppressive effects of hyperthermia on protein synthesis. All together, these events activate the apoptosis and autophagy pathways in HS-affected cells[41] (Figure 1.2).

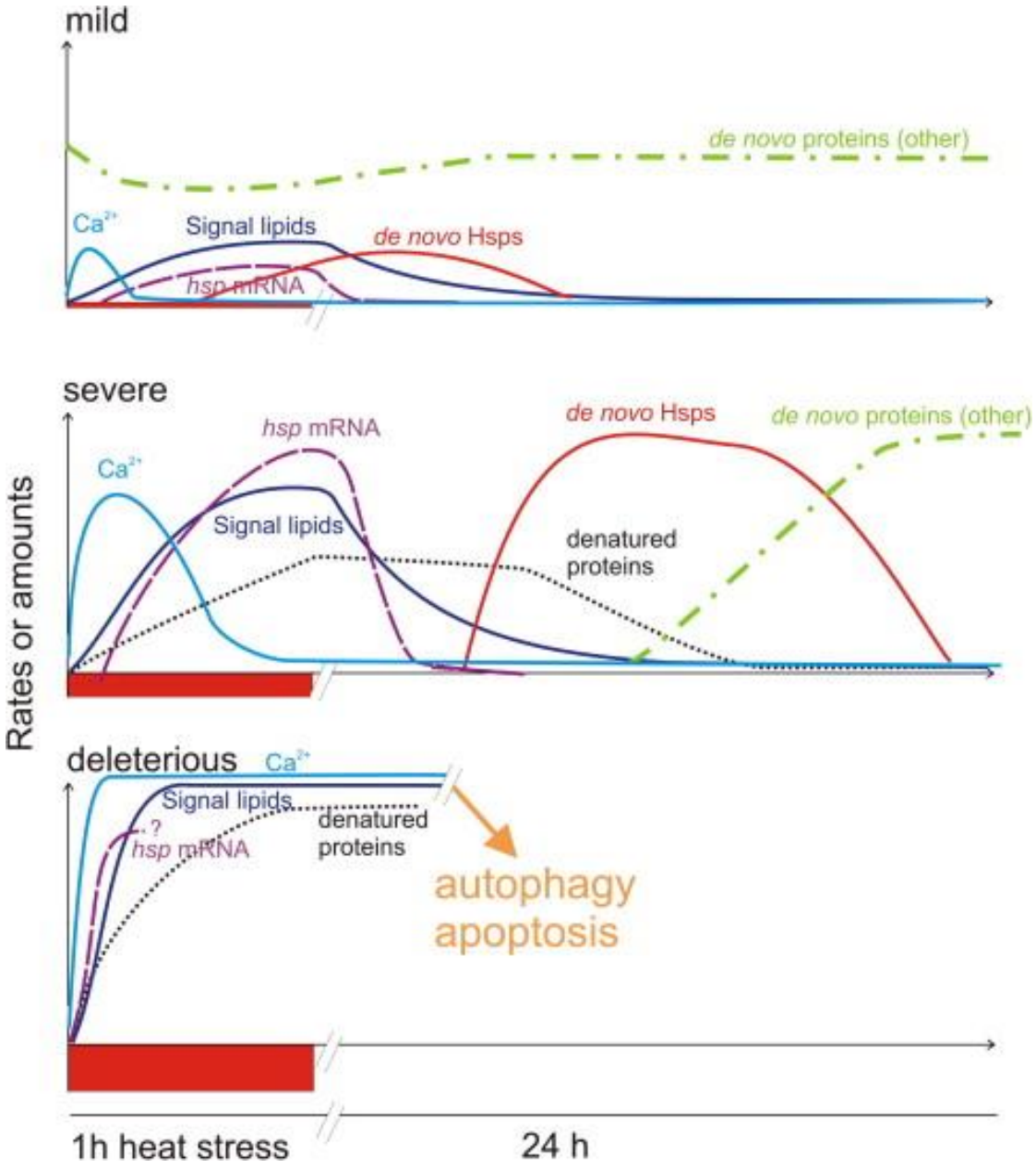

Figure 1.2. The sequence of events during and after heat stress in mammalian cells (adapted from Balogh et al, 2013)[36].

1.2.4 Dietary intervention of heat stress

Dietary supplementation has been explored as a practice to protect against the HS. Supplementation of ascorbic acid and lipoic acid alleviated negative effects of HS on the growth performance and meat quality of broilers[42]. The uses of ascorbic acid and lipoic

acid in HS are mainly based on their antioxidant properties as well as their functions as enzymatic cofactors[43-45]. Chromium supplementation improved the production and reduced HS-induced lipolysis and the elevation of plasma non-esterified fatty acids (NEFAs) levels in dairy cows and broilers, potentially due to its functions as insulin activator and the stabilizer of proteins and nucleic acids[46-48]. Zinc (Zn) is commonly supplemented in animal feeds to maintain health status and achieve optimal growth performance. Recently, zinc oxide (ZnO) and zinc sulfate ($ZnSO_4$), as well as organic zinc have also been explored as the supplements for protecting animals against the adverse effects of HS[49-53]. The protective effects of Zn are attributed to its antioxidant property and its cofactor role in metabolizing enzymes[54].

Overall, despite numerous studies that have been carried out to investigate the effects of HS, many questions remain unsolved with regarding to the initiation and progression of HS-induced adverse health effects. Human-induced climate changes make those questions even more important since human society will likely face more extreme temperatures and severe HS in near future[55].

1.3 CHEMISTRY AND BIOLOGICAL EFFECTS OF THERMALLY-OXIDIZED OILS

In typical American diet, nearly the half of daily lipid intake comes from consuming thermally-oxidized cooking oils in food. In addition, waste cooking oils are recycled by the rendering industry as a source of energy in animal feeds and thus could affect humans indirectly through consuming animal products. Adverse health effects of consuming large quantities of thermally-oxidized oils and fats have been observed in animal experiments,

leading to the hypothesis that thermally-oxidized cooking oils could be a contributing factor in human morbidities.

1.3.1 Thermally-oxidized oils in human diet and animal feed

The most commonly used cooking oils are the mixtures of triacylglycerols (TAGs) extracted from plant seeds, such as soybean, corn, canola, and sunflower seeds. These vegetable oils are used for frying, baking, and other cooking activities due to their flavors, low cost, and availability. Less commonly in modern society, animal-derived and synthetic fats, which exist in solid forms at ambient temperature, are also used in cooking. Deep frying is one of the most popular food preparations methods in the world. In the United States, the economy of commercial deep frying, mainly fast food restaurants, is estimated to be 83 billion dollars per year, which is more than twice the amount for the rest of the world[56]. Food processing using different heating temperatures could significantly change the nutrient profile of foods[1, 2] and their biological effects in the body[3]. In a typical deep frying procedure, the food is submerged in the oils and the temperatures range from 150 to 190°C. Frying time, surface area, moisture content, and oil type determine the amount of oil transferred to the food.

Triacylglycerols, which are commonly called as fat, are important nutrient components in typical American diet. About 1/3 of daily energy intake in the US comes from fat[57, 58]. More importantly, the half of total daily fat intake is thermally-oxidized oils from baked and fried food, which is equivalent to daily 36-gram intake[59, 60]. Besides humans, animals are also widely exposed to heavily thermally-oxidized oils through rendering practices since yellow grease or used cooking oil recovered from commercial or industrial cooking operations is commonly used as a source of energy in livestock

feed. Through this practice, the compounds in used cooking oils could affect the wellbeing of animals and reach to humans indirectly through meat consumption. The estimated annual yellow grease production in the U.S. was about 2.6 billion pounds from 1995 to 2000, while the estimated annual production in Minnesota ranges from 16 million to 48 million pounds[61].

1.3.2 Thermal stress-induced chemical changes in cooking oils

Deep frying is a widely applied food preparation procedure, in which food is prepared in cooking oils at high temperature (150-190°C). During deep frying, thermal stress can extensively transform the chemical composition of frying oils, especially the vegetable oils enriched with polyunsaturated fatty acids (PUFAs), altering their nutritional value and toxicological profile[62, 63]. Diverse chemical events, such as hydrolysis, radical formation, peroxidation, cyclization, polymerization, hemolytic and heterolytic cleavage, occur in this process, converting TAGs in frying oils to free fatty acids, mono- and di-acylglycerols, hydroperoxide primary lipid oxidation products (LOPs), and diverse secondary LOPs, such as cyclic fatty acids, polymeric products, aldehydes, ketones, alcohols, dienes, and acids[64].

1.3.2.1 Hydrolysis of oil

In deep frying, the moisture in food forms steam and then evaporate as bubbles. The hydrolysis of TAGs occurs when water reacts with the ester bonds of TAGs, producing di- and mono-acylglycerols, glycerol, and free fatty acids [65]. In general, the free fatty acid content in frying oils is positively correlated with the temperature, and duration in frying, and thus is a quality indicator of frying oils[66]. Due to their higher solubility in water, the oils enriched with short-chain and unsaturated fatty acids are more susceptible to

hydrolysis than the ones with long-chain and saturated fatty acids. Other factors that facilitate the hydrolysis of oil include water content[67] and the contamination of alkalis, such as the reagents from cleaning the fryers[68]. It has been reported that the free fatty acid content in cooking oils increases from less than 0.15 to 4% by frying before discarding[69-72].

1.3.2.2 Polymerization of oil

Formation of dimers, trimers, oligomers, and polymers of TAGs occur in heating and frying[73, 74]. Polymerization reactions also occur to PUFAs and the decomposed products of TAGs. Without oxygen, polymers can be formed by new -C-C- bonds, while with oxygen, polymers can also be formed by new -C-O-C- and -C-O-O-C- bonds[69, 75, 76].

1.3.2.3 Oxidation of oil

Oxygen and temperature are two essential factors in the autoxidation of oils and the formation of LOPs[77]. The formation rate of LOPs is relatively slow in the induction period of frying, but is rapidly increased along with the frying time[78]. The peroxidation reactions initiate the formation of diverse primary LOPs, including lipid hydroperoxides, epoxy hydroperoxides, keto hydroperoxides, cyclic peroxides, and their degradation products, i.e. secondary LOPs, including alcohol, aldehyde, ketone, ester, furan and lactone structures[64, 79-81]. The mechanism of thermal oxidation involves the initiation, propagation, and termination of the reaction (Figure 1.3)[82].

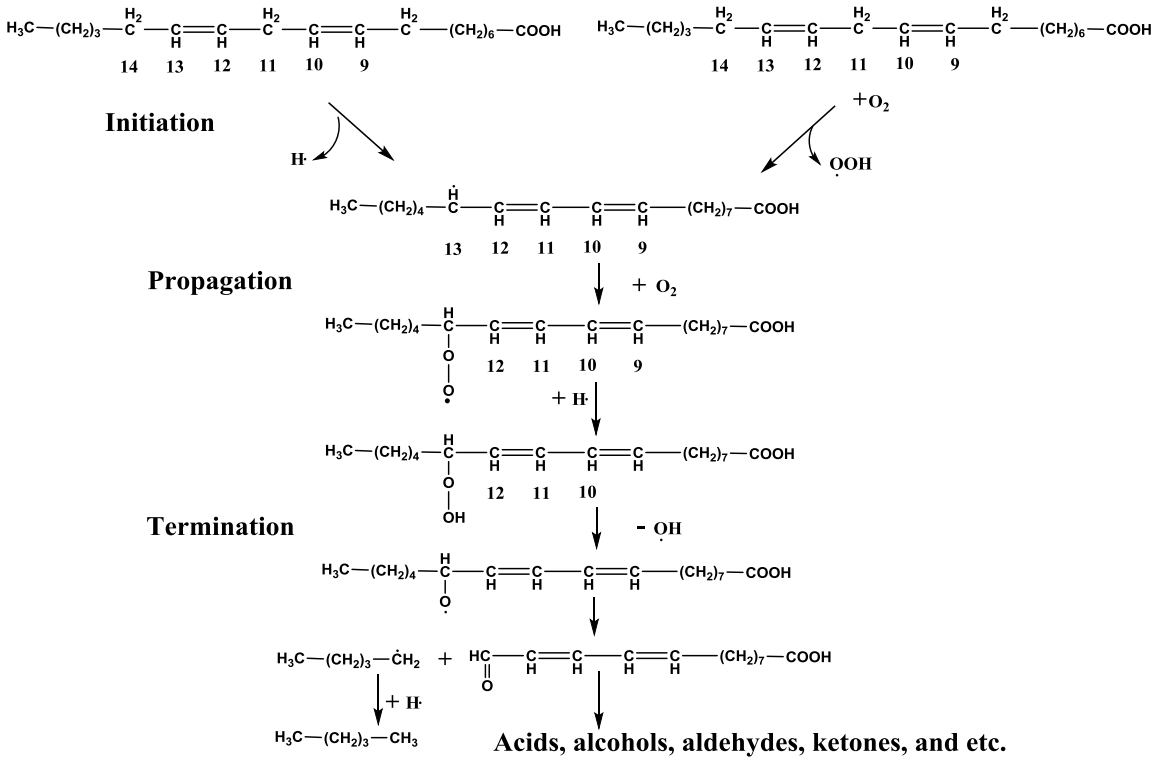

Figure 1.3. The peroxidation process of linoleic acid in cooking oils to produce primary and secondary LOPs. The formation of the alkyl radical from a fatty acid molecule by removing hydrogen is the initiation step in the oxidation reaction of oil. Generally, the carbon-hydrogen bond on carbon 11 of linoleic acid is the weakest and will be broken first to form a radical. The radical at carbon 11 will be rearranged to form conjugated pentadienyl radical at carbon 13 or carbon 9. Then, alkyl radicals react with oxygen to form peroxy radicals. The peroxy radical abstracts hydrogen from another oil molecule forming new hydroperoxide and another alkyl radical. This chain reaction is the propagation step and accelerates the thermal oxidation of oil. There are two types of terminations. One is the formation of non-polar dimers and polymers by reactions between alkyl radicals, alkoxy radicals, and peroxy radicals. The other is the formation of non-radical volatile and nonvolatile compounds at the end of oxidation. Volatile compounds contain aldehydes, ketones, acids, hydrocarbons, alcohols, esters, lactones and aromatic compounds.

1.3.2.4 Chemical changes of oil during frying process

Heating-induced reactions, including hydrolysis, oxidation, and polymerization, transform a TAGs-dominant chemical profile to a profile that is much more diverse and complex because it contains acylglycerols, free fatty acids, peroxides, polar materials, volatile compounds, polymeric materials, and many other chemical entities. The most

prominent features of chemical changes in the time course of frying include transient increase of peroxides and volatile compounds, progressive decrease of unsaturated level, and progressive increases of foaming, darkness, viscosity, free fatty acids, polar and polymeric products (Figure 1.4)[62].

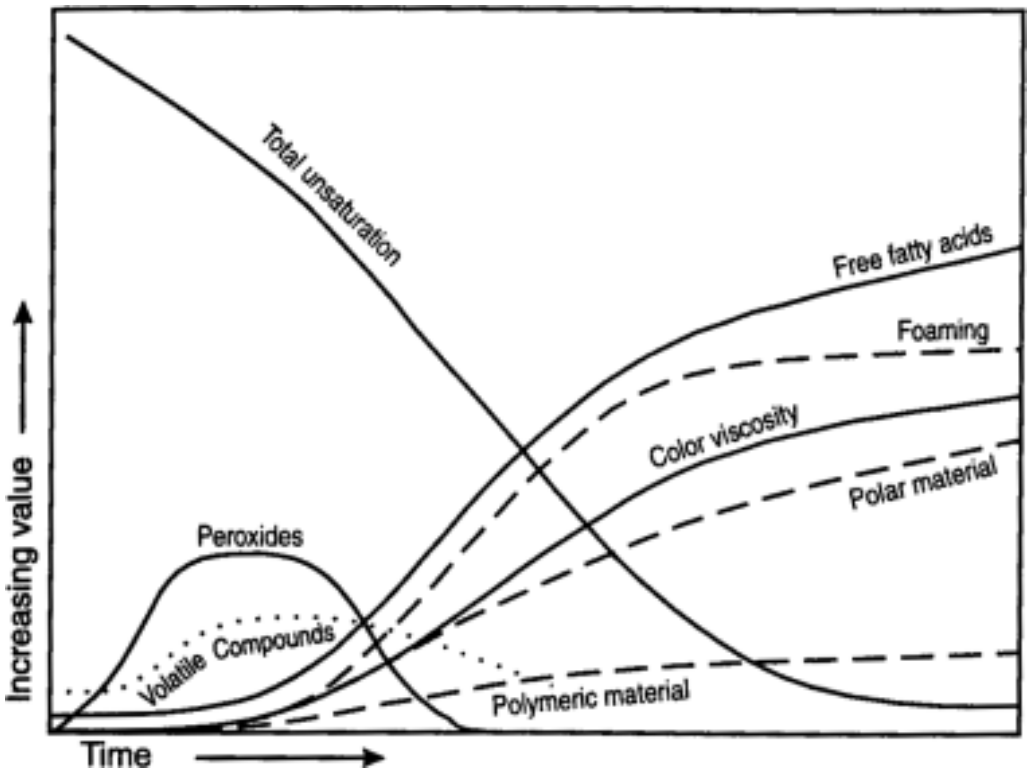

Figure 1.4. Physical and chemical changes of oil during deep-fat frying (adapted from Choe and Min, 2007)[62].

1.3.3 Evaluation of lipid oxidation

Accurate assessment of lipid oxidation status of frying oils is important for evaluating their quality and biological effects, but remains to be a challenge in spite of the availability of various assays for determining the status of lipid oxidation[83, 84]. This situation can be largely attributed to the following facts: (1) under thermal stress, various lipid oxidation products production originates from multiple precursors and multiple degradation routes, resulting in unstable composition of lipid oxidation products in frying

oils; and (2) in contrast to the chemical complexity of lipid oxidation products, these established assays are targeted in nature and thus are incapable of detecting and analyzing multiple LOPs simultaneously. The features of common evaluation assays on the chemical changes in frying oils are reviewed as follows.

1.3.3.1 Peroxide value (PV)

The PV assays are mainly based on the redox properties of hydroperoxides. Iodide is used as the reactant in the American Oil Chemists' Society (AOCS) official method for measuring the PV of oils. In the presence of peroxides, iodide ion is oxidized to iodine. In the presence of starch, the black color of the solution changes into colorless when iodine is titrated with sodium thiosulfate. This method has been criticized for its tediousness. Compared to the AOCS official method, ferrous oxidation method is simpler. In this method, Fe (II) is oxidized to Fe (III) by hydroperoxides in acidic media. Fe (III) then forms the complexes with thiocyanate or xylenol orange (FOX), which could be measured with a visible spectrophotometer at 500 and 560 nm, respectively. Other methods, including chemiluminescent method[85], flow-injection method[86], and high-performance liquid chromatography (HPLC) analysis[87], are also available for PV measurement. Overall, PV measurement is widely used to evaluate lipid oxidation and lots of methods are available. However, PV has limited value in reflecting the real status of lipid oxidation in frying oils. This conclusion is based on the fact that the production and decomposition of primary LOPs occur simultaneously in frying oils. Previous studies have showed that the transient increase of PV in heated ethyl linolenate[88] and low PV in extensively oxidized frying oils[89]. These results indicate that when evaluate frying oil, a low PV may not solely represent a low level of oxidation (Figure 1.4)

1.3.3.2 Thiobarbituric acid reactive substances (TBARS)

The TBARS assay aims to measure malondialdehyde (MDA), a secondary LOP[90]. In this assay, MDA react with thiobarbituric acid (TBA) adduct to form an adduct with maximum absorbance at 530-540 nm wavelength[91]. The TBARS value is widely used parameter in the evaluation of lipid oxidation, but is also criticized for the lack of sensitivity and specificity. The concern is partially based on the fact that TBA could react with diverse compounds besides MDA, including 2-alkenals, 2,4-alkedienals, sugars, and amino acids, and these reactions are expected to interfere MDA measurement[92]. For frying oils, the results of TBARS assay might not reflect the MDA level because many TBA-reactive compounds are generated from the frying process[93].

1.3.3.3 p-Anisidine value (AnV)

The AnV assay detects secondary LOPs, such as 2-alkenals and 2,4-alkedienals. In the assay, the reactions between the carbonyl group in aldehydes and the amino group in *p*-anisidine produce Schiff bases ($R_2C=NR'$) that have maximum absorbance at 350 nm. It has been shown that AnV is correlated with TBARS value, the levels of aldehydes, and the sensory odors of fried foods[94, 95]. However, AnV assay can be interfered by other compounds in testing samples. In addition, unsaturated aldehydes have higher reactivity to *p*-anisidine than saturated aldehydes[96].

1.3.3.4 TOTOX value

TOTOX value is a calculated as the sum of AnV and two PVs (TOTOX = AnV + 2PV)[91]. Even though TOTOX value is widely used to evaluate frying oil[97-99], it inherits the limitations of PV and AnV in the quality evaluation of frying oils.

1.3.3.5 Total polar material (TPM)

Neutral lipids, mainly TAGs, are the major components of frying oil. The remaining polar compounds in frying oils are referred as the total polar materials (TPM). In the frying process, the reciprocal changes occur to the percentages of neutral lipids and TPM, and are affected by temperature, time, and fatty acid composition. Because aldehydes are the major components of TPM in frying oils and are responsible for the toxicity of frying oils[100, 101], the level of TPM in frying oil and fried goods is an indicator of potential health risk. The limit of TPM in frying oil is set as 25% in several European countries[102]. Several methods are available to determine the level of TPM in frying oil. As the standard methods for determination of TPM, both AOCS official method Cd 20-91and IUPAC method 2.507 use silica gel column chromatography for measurement. Those two methods, together with some other similar methods are time-consuming[103]. Other methods such as high performance liquid chromatography–size exclusion chromatography (HPLC-SEC) and accelerated solvent extraction (ASE) were developed in TPM measurement[103, 104].

1.3.3.6 Polymerized TAGs (PTGs)

PTGs are a major group of newly formed compounds in used frying oils[105]. Heating induces the modification of fatty acyl groups, mostly through the oxidation reactions. Modified fatty acyl groups and non-modified ones in different TAG species can the react with each other to form PTGs, including the monomers, dimers and oligomers of TAGs. These PTGs can be analyzed by size exclusion chromatography (SEC) and gel permeation chromatography Fourier transform infrared (GPC-FTIR) analysis[105, 106]. For example, PTGs, oxidized triacylglycerols, and diacylglycerols were separated by HPLC-

SEC[107]. Since the formation of PTGs is well correlated to the TPM[106, 108], PTGs is becoming more adopted for the quality evaluation of frying oil[109, 110].

1.3.3.7 Hexanal, pentanal, and 2,4-decadienal

As the components of secondary LOPs, aldehydes such as hexanal, pentanal, and 2,4-decadienal are used for evaluation of lipid oxidation levels[91]. The levels of those compounds can be quantified by gas chromatography–mass spectrometry (GC-MS) and near-infrared spectroscopy (NIR) spectroscopy[111, 112]. However, the fatty acid profile of the lipid may be considered before certain aldehyde is used to evaluate lipid oxidation of lipids. For example, hexanal is generally considered as a reliable indicator of lipid oxidation in lipids rich in linoleic acid because it mainly comes from linoleic acid during oxidation[84].

1.3.3.8 Active oxygen method (AOM)

The AOM is a method for predicting lipid stability, in which the lipids are keep at 98 to 100^0C under constant air flow. The stability of the lipids is determined by either measuring the time required to reach the PV of 100 meq O_2/kg lipid or measuring the PV at a preset time point. Since PV is the target of AOM, the limitations of PV assay, such as the lack of reproducibility and the tediousness of analytical procedure, are also applicable to AOM.

1.3.3.9 Oil stability index (OSI)

The OSI is another method for predicting lipid stability, in which the lipids are keep between 110 and 130°C under constant air flow. The volatile compounds produced from this process are carried by the air and subsequently dissolved in a reservoir of water. The dissolution of volatile compounds in water increases the conductivity of water, which is

monitored in this process. The OSI value is defined as the time required to reach a preset value of conductivity. Compared to AOM, the conductivity measurement in OSI is more reliable and reproducible, and the OSI value is better correlated with the stability[84, 113, 114]. However, to obtain detectable volatile acids, the temperature used in the OSI measurement (110 or 130°C) is higher than the temperature in many food preparation procedures, resulting in the concerns on the prediction power of OSI in these procedures[115].

1.3.3.10 The need to develop new markers of lipid oxidation

Based on extensive research on the chemical components and properties of frying oils, diverse chemical assays have been developed and established to characterize frying oils[116]. Among these assays, iodine value, AOM, and OSI assays, predict the stability of unprocessed frying oils and their susceptibility to stresses by measuring the unsaturation level of frying oils or the production of peroxides and volatile compounds under the designated conditions[117, 118]. While the majority of indicative assays determine the status of processed frying oils by measuring the end products of hydrolysis and oxidation reactions, such as free acid content, PV, AnV, TOTOX value, TBARS, TPM, PTGs, hexanal and 2, 4-decadienal levels[118, 119]. Despite the availability of a large selection of analytical methods for defining the status and susceptibility of frying oils, one reliable lipid oxidation marker easy to measure is still missing, mainly due to the undefined global profile of thermally-stressed frying oils and the kinetics of thermal stress-induced changes. This knowledge gap is mainly due to two facts: (1) all established analytical methods only measure a fraction of frying oils and do not cover the chemical diversity of frying oils; (2) under thermal stress, the composition and status of frying oils are not

stable. Due to the above reasons, TAGs were not characterized to define and monitor the status and quality of frying oils. Furthermore, large variety of secondary LOPs have also not been studied for their correlation with lipid oxidation of oils. Thus, application new and powerful detection platform is a promising strategy for discovering reliable lipid oxidation markers.

Table 2.1. Summary of evaluation methods for lipid oxidation.

Oils and fats undergo frying							
Reactions	Products	Indicative tests			Predictive tests		
		Test	Test target	Principle	Test	Test target	Principle
Polymerization	Dimer, polymer	Polymerized triacylglycerols	Polymerized triacylglycerols	HPLC-SEC GPC-FTIR			
Hydrolysis	Free fatty acids, Diacylglycerols	Free fatty acids					
Oxidation	Peroxides, hydroperoxides, secondary oxidation products (aldehydes, ketones, carboxylic acids)	Peroxide value (PV)	Peroxides, hydroperoxides	Iodide ion, starch solution, sodium thiosulphate	Active oxygen method (AOM)	Peroxides, hydroperoxides	Measure the time to get to the preset PV
		Anisidine value (AnV)	Aldehydes	Anisidine-aldehyde has absorbance at 350 nm	Oxygen stability index (OSI)	Volatile acids	Measure the time to reach a preset value of conductivity
		TOTOX value(= 2 × PV + AnV)	Peroxides, hydroperoxides, Aldehydes				
		TBARs	MDA	Thiobarbituric acid-MDA adduct has absorbance at 532 nm			
		Hexanal, pentanal, 2,4-decadienal	Individual aldehyde	GC/MS, LC/MS			
		Total polar material (TPM)	Polar compounds	HPLC-SEC			

1.3.4 Disposition of thermally-oxidized oils *in vivo*

The fate of consumed thermally-oxidized oils in humans and animal is determined by the disposition processes, which include digestion, absorption, distribution, metabolism and excretion.

1.3.4.1 Digestion of thermally-oxidized oils.

TAGs in thermally-oxidized oils are digested by lingual lipases in oral cavity, gastric lipases in the stomach, and then by pancreatic lipases in the duodenum with the assistance of bile salts and colipase[120]. Compared to TAGs, PTGs are much more resistant to enzymatic digestion. In addition, digestion is not necessary for the absorption of LOPs.

1.3.4.2 Absorption of thermally-oxidized oils.

Animal feeding studies have shown that heating process affects the absorption of cooking oils[121, 122]. Free fatty acids and monoacylglycerols, as the products of triglyceride digestion, are effectively absorbed into the enterocyte through free diffusion. As for other compounds in thermally-oxidized oils, polymers are resistant to transmembrane absorption[123-125], and the absorption of primary LOPs is limited by slow hydrolysis in the gut[126, 127]. In contrast, secondary LOPs, such as 4-hydroxynonal (4-HNE), 4-oxononenal (4-ONE), and 4,5-epoxy-2-decenals, are absorbed efficiently as shown by their appearance in the circulation system and the detection of their metabolites in the urine[128-132].

1.3.4.3 Distribution of thermally-oxidized oils.

Once inside intestinal enterocytes, majority of absorbed free fatty acids and monoacylglycerols are reassembled to TAGs through *de novo* synthesis, and then

distributed to target tissues through lipoproteins, including chylomicrons, VLDL, IDL, LDL, and HDL. Owing to their poor absorption, primary LOPs have limited distribution in the body. In contrast, secondary LOPs could reach the systemic circulation after ingestion and then are distributed to various organs, among which the liver has the highest concentrations of absorbed LOPs[133].

1.3.4.4 Metabolism of thermally-oxidized oils.

At target tissue, triacylglycerols are broken down by specific lipoprotein lipases to glycerol and fatty acids for either anabolic or catabolic metabolism. Glycerol can enter glycolysis, gluconeogenesis, and lipid synthesis pathways. Besides being a component of triacylglycerols and other lipids, free fatty acids are transported into mitochondrion or peroxisomes for β-oxidation reactions to generate energy and bioactive intermediates. As for the secondary LOPs, their reactive structures could lead to the reactions with various functionally biomolecules *in vivo*. Therefore, the biotransformation of these molecules *in vivo*, especially detoxification reactions, could play a decisive role on whether they could produce adverse effects inside the body. For example, MDA is metabolized to carbon dioxide[134] or its lysine adduct[135], while *trans*-2-alkenals, including 4-HNE and 4-ONE, are metabolized by aldehyde dehydrogenases (ALDHs), aldo-keto reductases (AKR), and glutathione s-transferases (GST)[128, 136-138]. However, due to the structural and functional diversity of LOPs, their metabolic fates in the body still remain poorly defined.

1.3.4.5 Excretion of thermally-oxidized oils.

Through catabolic metabolism, the TAGs in thermally-oxidized oils are mostly converted to carbon dioxide and water. LOPs have different excretion routes because the rate and extent of their *in vivo* absorption from the gut into the systemic circulation are

different. Most of primary LOPs, such as methyl and ethyl esters of linoleate hydroperoxide are excreted in feces. The excretion fate of secondary LOPs of oils is more diverse. About 50% of an oral dose of secondary LOPs are excreted through feces. Within absorbed secondary LOPs, 50% of them were excreted as CO_2, 25% in urine[132].

1.3.4.6 Function of ALDHs in the metabolism of LOPs

Aldehydes, especially α, β-unsaturated aldehydes, are produced as major secondary LOPs in thermally-oxidized cooking oils[139]. Due to the reactivity and toxicity associated with these compounds, the enzymes responsible for their biotransformation inside the body are expected to significantly affect the biological effects of thermally-oxidized oils. Among these enzymes, ALDHs, using NAD^+ or $NADP^+$ as the cofactor, are capable of converting both endogenous and exogenous reactive aldehydes to their corresponding carboxylic acids, which in general are much less reactive than their aldehyde precursors. ALDHs are ubiquitous in all organisms and also in almost all intracellular organelles, including cytoplasm, nucleus, mitochondria, and endoplasmic reticulum. More than 500 ALDH genes have been identified in microorganisms, plants, and animals. The human genome contains 19 functional ALDH genes that have been classified into 10 families and 13 subfamilies[140, 141]. Because the substrates of ALDHs have diverse functions in numerous physiological, pathological, and pharmacological events, the ALDHs-mediated reactions could affect cell proliferation, differentiation, and survival. However, at present, the role of ALDHs in the disposition and biological effects of thermally-oxidized oils remains largely unknown.

1.3.5 Biological effects of consuming thermally-oxidized oils

The health risks of consuming thermally-oxidized oils have been examined in epidemiological, clinical, and animal studies. The results from these studies suggested that moderately-oxidized oils had either limited or no detrimental effects on animals[122, 142]. However, feeding highly-oxidized oils led to apparent toxicities, including loss of appetite, diarrhea, growth retardation, elevated kidney and liver weights, altered fatty acid composition of tissue lipids[132, 143-148]. The LOPs in thermally-oxidized oils have been considered as major contributors to observed toxic effects[149]. For example, primary LOPs, such as conjugated lipid hydroperoxydienes, are acutely toxic to rodents[150], while secondary LOPs, such as 2-alkenals, can covalently bind to proteins and DNA, resulting in protein inactivation and DNA damage[101]. In addition, primary and secondary LOPs could react with amino acids and lipids in the GI tract, thereby decreasing the digestibility of proteins and complex lipids[151].

Among the LOPs in thermally-oxidized oils, the biological activities of 4-HNE have been extensively investigated. 4-HNE, as an endogenous metabolite of regular lipid metabolism, could mediate cell proliferation and differentiation at the physiological and non-toxic concentrations (below 1 μM)[152, 153]. However, at pathophysiological concentrations, 4-HNE can react with proteins and nucleic acids to form adducts, disrupting the functions of enzymes and proteins, and modulating gene expression[154-159]. Other LOPs, including 4-ONE, 4,5-epoxy-*trans*-2-decenal, and 9,12-dioxo-trans-10-dodecenoic acid, are also capable of forming DNA-adducts and generating pro-mutagenic lesions that can contribute to the etiology of cancer[131, 136, 160]. In addition, the pro-apoptotic effects of 4-HNE, 4-ONE and 4,5-epoxy-*trans*-2-decenal on endothelial cells suggest a potential role for secondary LOPs in cardiovascular pathogenesis[161].

Despite previous research efforts on the biological effects of thermally-oxidized oils, many issues remain undefined, such as how thermally-oxidized oils affect nutrient metabolism *in vivo*. Traditional biomarkers such as TAGs and cholesterol in the blood are inefficient to explain the mechanisms behind complexity of metabolic events induced by thermally-oxidized oils. Comprehensive evaluation of the effect of thermally oxidized oil on metabolome which could reflect the changes in metabolism as a whole picture, was not carried out previously.

1.3.6 Regulation of gene expression by oxidized lipids

Even though the health risk of thermally-oxidized oils was widely recognized, consumption of thermally-oxidized oils may be considered to be beneficial with regarding to its effects of lowering concentrations of hepatic and blood triacylglycerols and cholesterol[162-164]. The mechanism behind this phenomenon was recognized as the activation of peroxisome proliferator-activated receptor α (PPARα) as well as a series of its target genes. A set of genes involved in fatty acid and lipoprotein metabolism were upregulated by the PPARα including acyl-CoA thioesterases (ACOT), acyl-CoA oxidase (ACO), cytochrome P450 isoenzyme 4A1 (CYP4A1), carnitine-palmitoyltransferase I (CPT I), CPT II, carnitine-acylcarnitine translocase (CACT), medium-chain acyl-CoA dehydrogenase, long-chain acyl-CoA dehydrogenase, and 3-ketoacyl-CoA dehydrogenase when the animal consume thermally-oxidized oils[163-167]. The potent ligands and activators of PPARα from the thermally-oxidized oil were proposed to be hydroxylated fatty acids and cyclic fatty acids monomers[168, 169]. At the same time, animals fed with oxidized fat developed a symptom of liver enlargement[163-165], which were recognized as a typical response to PPARα agonist inducing peroxisome

proliferation[170, 171]. Organic cation transporter 2 (OCTN2), another PPARα target gene, was also upregulated by consumption of thermally-oxidized oils. OCTN2 plays the most important role as the carnitine transporter, taking part in reabsorption and distribution of carnitine. Consumption of oxidized fat was found to increase the carnitine concentration in the liver of rats, most likely due to the upregulation of OCTN2 mediated by PPARα[172](Figure 1.5). The cholesterol lowering effect of oxidized fat was attributed to the inhibition of sterol regulatory element-binding protein (SREBP-2) in previous study[173]. Administration of the thermally-oxidized oils could lower the transcript levels of SREBP-2 and then reduce the transcription of low-density lipoprotein receptor and 3-hydroxy-3-methylglutaryl-CoA reductase genes, subsequently[173].

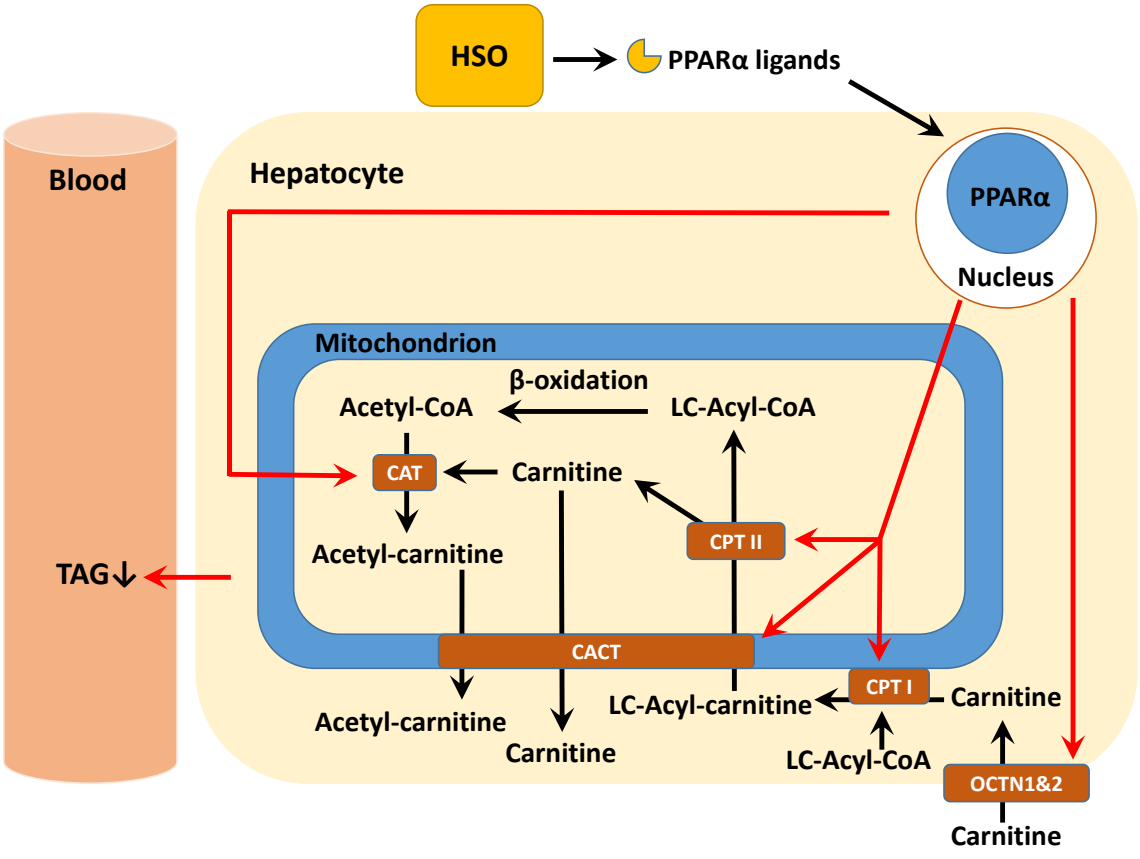

Figure 1.5. **Roles of PPARα in HSO-induced fatty acid oxidation (**modified based on AOCS lipid library: http://lipidlibrary.aocs.org/content.cfm?ItemNumber=39222).

1.4 CHEMOMETRICS AND METABOLOMICS

Though information on high temperature-induced HS, as well as changes in oil quality and biological effects associated with consumption of frying oils are available, there are still knowledge gaps with regarding to those information. For example, many issues related to chemical profile and biological effects of thermally-oxidized oil, such as how heating affects the chemical composition of cooking oils, how the body processes thermally-oxidized oils, and how thermally-oxidized oils affect nutrient metabolism *in vivo*, remain undefined. To fill up those gaps, traditional methodology is insufficient to provide advanced information. However, those information could be provided by high throughput methodology such as chemometircs and metabolomics. Chemometircs and metabolomics, which is a powerful methodology served as markers finder by measuring small-molecule metabolite profiles in samples, has been applied to find mechanisms in many scientific fields[174-178]. Thus, as a highly effective tool to examine chemical changes in a reaction system or metabolic changes in a biological system, chemometircs and metabolomics should be capable of detecting newly-formed chemicals in thermally-oxidized oils and defining the changes in metabolome after the direct exposure of heat stress and the indirect exposure through thermally-oxidized oils (Figure 1.6).

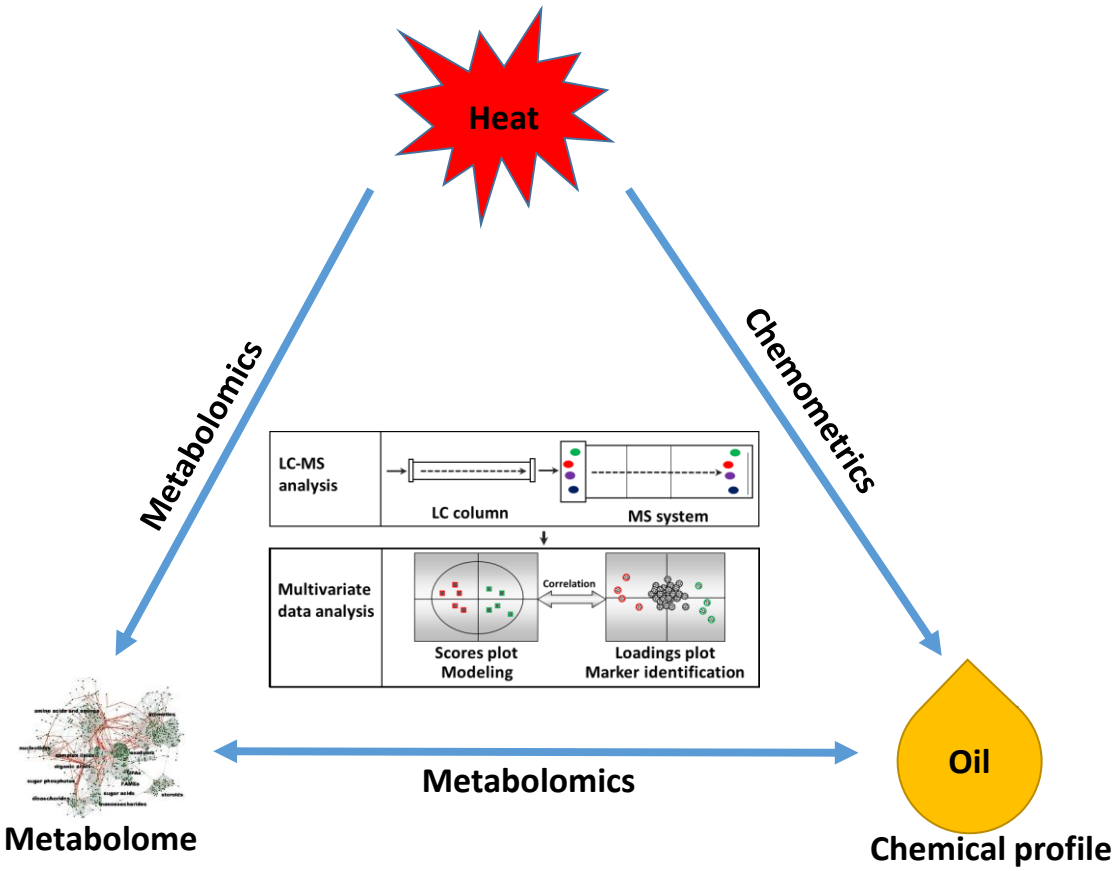

Figure 1.6. Roles of chemometrics and metabolomics in studying thermal energy-induced chemical and biological changes in food, feed, animals, and humans.

At present, LC is the most commonly used platform in MS-based metabolomics owing to its good compatibility with the metabolites in a biological system. LC-MS data comprise retention time (RT), mass-to-charge ratio (*m/z*), and signal intensity. To conduct untargeted metabolomic analysis, deconvolution is required to convert these data into a data matrix suitable for multivariate data analysis. After LC-MS analysis, chromatographic and spectral data need to be properly processed before being used in multivariate data analysis. The procedure includes data condensation and reduction by centroiding and deisotoping mass spectra, chromatographic alignment for peak identification, and filtering for removing noise or isotope signals[179]. To reduce the influence of systematic and sample biases, MS data can be normalized by either the parameters of whole dataset (such as total ion count or median ion count) or the intensities of single or multiple internal standards (such as creatinine in the case of urine)[180]. After all these procedures, a multivariate data matrix containing information about sample identities, ion identities (RT and *m/z* values) and normalized ion intensities can be generated. This dataset can be either directly used for multivariate data analysis, or be further statistically transformed and scaled according to the properties of data and the purpose of multivariate data analysis. To identify latent components or principal components in a complex dataset, data are projected onto a new coordinate system based on pattern recognition algorithm[181]. Thereafter, a model containing one or multiple principal components can be established to represent a large portion of examined dataset (Figure 1.7). In contrast to other statistical techniques, such as *t*-test and ANOVA, an established multivariate data analysis model and its principal components can be presented in the scores plot, in which sample- principal components and sample-sample

relationships can be visualized. In LC-MS-based metabolomics, the spatial distance between two samples in the scores plot reflects their differences in chemical composition. When a clear sample clustering is observed in the scores plot, the contribution of individual ions to principal components and to the group separation can be further examined in the loadings plot, in which the relationships between ions and principal components are depicted. Two major categories of multivariate data analysis methods, unsupervised and supervised multivariate data analysis, have been widely used in metabolomic data analysis. In unsupervised multivariate data analysis, sample classification is unknown or intentionally blinded to the analytical software, while in supervised multivariate data analysis this information is provided to the software for the purpose of model construction. The most popular unsupervised method is principal components analysis (PCA). Because of its indiscriminate nature, the markers identified in a robust PCA model can usually be validated. Supervised multivariate data analysis encompasses many methods, including partial least squares (PLS), orthogonal partial least squares (OPLS), and partial least squares-discriminant analysis (PLS-DA)[182]. The selection of supervised multivariate data analysis method is determined by the data properties and the aim of multivariate data analysis. In metabolomics analysis, when a clear separation of different treatments is observed in the scores plot, metabolites can be conveniently identified in the loadings plot through their correlation with the principal components that separate sample groups (Figure 1.7). The concentrations or relative abundances of identified metabolite markers in examined samples can be presented in the heat maps generated by the R program (http://www.R-project.org), and the correlations among these metabolite markers can be defined by hierarchical clustering analysis

(HCA). Subsequently, chemical identities of metabolite markers can be determined by accurate mass measurement, elemental composition analysis, MS/MS fragmentation and searches of metabolite and spectral databases, such as Kyoto Encyclopedia of Genes and Genomes (KEGG, http://www.genome.jp/kegg/), Human Metabolome Database (http://www.hmdb.ca/), Lipid Maps (http://www.lipidmaps.org/), METLIN database (http://metlin.scripps.edu/), BioCyc (http://biocyc.org/), Spectral Database for organic compounds (http://sdbs.riodb.aist.go.jp). Recent development in bioinformatics has further facilitated metabolite annotation in metabolomics studies[183, 184]. The relevant pathway analysis of metabolite markers can be performed by online databases such as MetaboAnalyst 3.0 (www.metaboanalyst.ca) using KEGG pathway database.

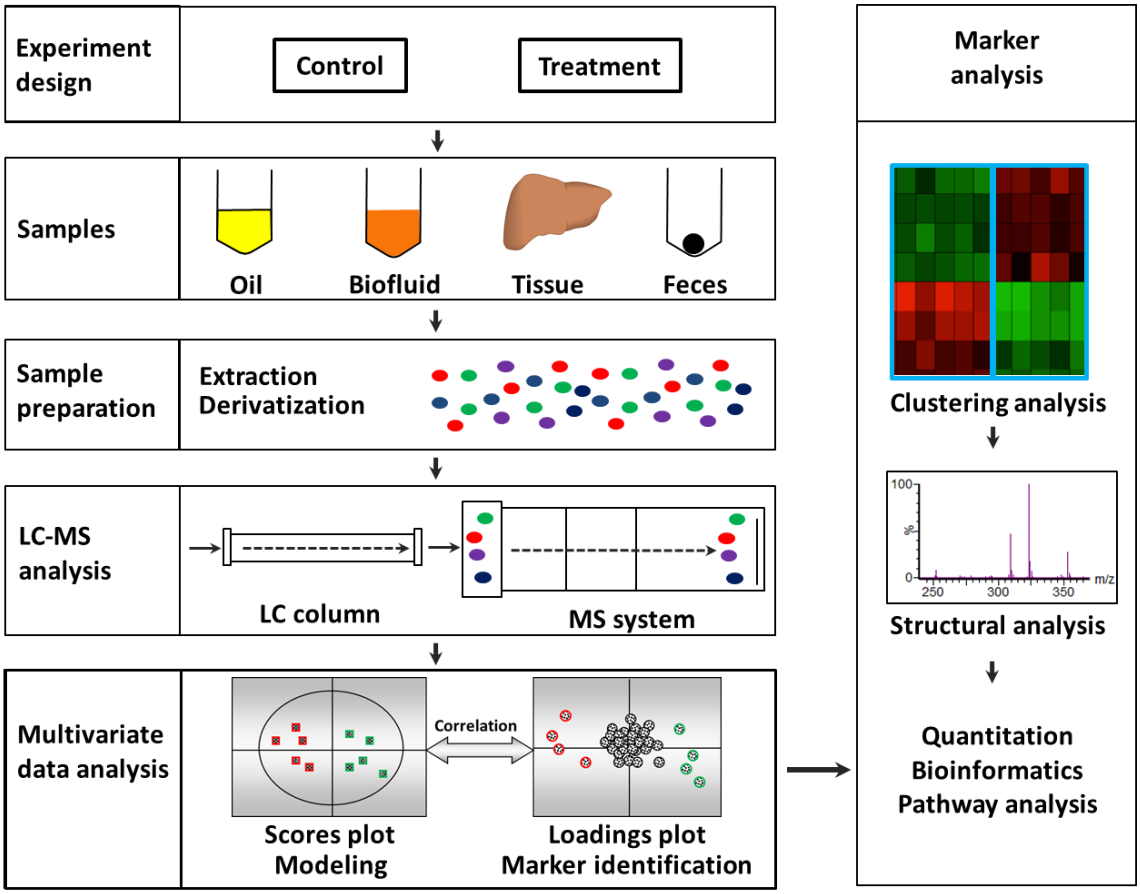

Figure 1.7. The work flow of untargeted chemometrics or metabolomics. Samples from diverse sources need to be processed appropriately to make them compatible with MS-based chemometrics or metabolomic analysis. Chemical derivatization can be performed to facilitate the chromatographic separation of metabolites and increase the sensitivity of metabolite detection in LC-MS systems. Spectral data acquired by MS need to be deconvoluted to a data matrix compatible to multivariate data analysis. Subsequently, a multivariate model can be established in which the scores plot illustrates the principal or latent components of the model as well as sample classification while the loadings plot presents the contribution of each ion to sample classification in the model. Marker analysis is based on clustering and structural analysis. The confirmed markers could be further used for quantitation, bioinformatics and pathway analysis.

CHAPTER 2. EFFECTS OF DIURNAL HEAT STRESS AND ZINC SUPPLEMENTATION ON SWINE METABOLOME

This chapter is modified from the manuscript:
Wang, L.; Urriola, P. E.; Luo, Z. H.; Rambo, Z. J.; Wilson, M. E.; Torrison, J. L.; Shurson, G. C.; Chen, C. Metabolomics revealed diurnal heat stress and zinc supplementation-induced changes in amino acid, lipid, and microbial metabolism. *Physiological Reports.* 2016, *4*, e12676.

2.1 SUMMARY

Heat stress (HS) dramatically disrupts the events in energy and nutrient metabolism, many of which requires zinc (Zn) as a cofactor. In this study, metabolic effects of HS and Zn supplementation were evaluated by examining growth performance, blood chemistry, and metabolomes of crossbred gilts fed with ZnNeg (no Zn supplementation), ZnIO (120 ppm $ZnSO_4$), or ZnAA (60 ppm $ZnSO_4$ + 60 ppm zinc amino acid complex) diets under diurnal HS or thermal-neutral (TN) condition. The results showed that growth performance was reduced by HS but not by Zn supplementation. Among measured serum biochemicals, HS was found to increase creatinine but decrease blood urea nitrogen (BUN) level. Metabolomic analysis indicated that HS greatly affected diverse metabolites associated with amino acid, lipid, and microbial metabolism, including urea cycle metabolites, essential amino acids, phospholipids, medium-chain dicarboxylic acids, fatty acid amides, and secondary bile acids. More importantly, many changes in these metabolite markers were correlated with both acute and adaptive responses to HS. Relative to HS-induced metabolic effects, Zn supplementation-associated effects were much more limited. A prominent observation was that ZnIO diet, potentially through its influences on microbial metabolism, yielded different responses to HS compared to two other diets, which included higher levels of short-chain fatty acids (SCFAs) in cecal fluid and higher levels of lysine in the liver and feces. Overall, comprehensive metabolomic analysis identified novel metabolite markers associated with HS and Zn supplementation, which could guide further investigation on the mechanisms of these metabolic effects.

KEYWORDS: Heat stress, metabolism, metabolomics, zinc supplementation.

ABBREVIATIONS: ADFI, average daily feed intake; ADG, average daily gain; BPM,

breaths per minute; BUN, blood urea nitrogen; BW, body weight; D, day; DC, dansyl chloride; DG, daily gain; FAA, free amino acid; Fe, iron; FI, feed intake; G:F, gain:feed; H, hour; HCA, hierarchical clustering analysis; HMDB, human metabolome database; HPLC, high performance liquid chromatography; HQ, 2-hydrazinoquinoline; HS, heat stress; IACUC, Institutional Animal Care and Use Committee; KEGG, Kyoto encyclopedia of genes and genomes; LC-MS, liquid chromatography-mass spectrometry; LysoPC, lyso-phosphatidylcholines; m/z, mass to charge ratio; PC, phosphatidylcholines; PCA, principal components analysis; PE, phosphatidylethanolamine; QTOF, quadrupole time of flight mass spectrometry; RR, respiratory rate; RT, rectal temperature; SIC, single ion counts; SM, sphingomyelins; T, temperature; TIC, total ion counts; TN, thermal neutral; UPLC, ultra-performance liquid chromatography; Zn, zinc.

2.2 INTRODUCTION

High ambient temperature-elicited heat stress (HS) is a detrimental pathophysiological event. Besides its threat to human health[4, 5], HS also negatively affects the growth performance, reproduction, and health status of farm animals[6, 7]. Annual cost of HS on the US swine industry is over $300 million[12]. Under high ambient temperature, inadequate release of body heat elevates core body temperature, leading to extensive systemic changes and physiological responses. In cardiovascular and respiratory systems, HS elevates cardiac and respiratory rates and causes cutaneous vasodilation[15, 16]. Systemic inflammatory responses could also be triggered by HS-induced translocation of bacteria and endotoxins across compromised tight junctions in the gut[17, 18]. The metabolic system is also greatly affected by HS-induced alterations in metabolism-related hormones, genes, proteins, and metabolites[25, 26]. The well-known effects of HS on metabolism-related hormones, genes, and proteins include attenuated releases of thyroid and growth hormones, which decrease basal metabolic rate[26, 27], and alter expression of genes and proteins involving in energy and nutrient metabolism[28, 29, 185]. The effects of HS on metabolites have also been examined by both metabolomics[31, 32] and targeted analysis of specific metabolites in AA, lipid, and carbohydrate metabolic pathways[25, 33]. However, the short-term exposure in these metabolomics studies aimed to mimic acute exposure in humans but not extended exposure in animals, while targeted metabolite analysis lacks the capacity to cover the metabolome and to identify novel metabolic changes. Therefore, the metabolic responses to reoccurring diurnal HS remains largely unexplored.

Zinc (Zn), as an essential mineral, is commonly supplemented in animal feeds to maintain health status and achieve optimal growth performance. Inorganic Zn, mainly zinc oxide (ZnO) and zinc sulfate ($ZnSO_4$), are widely used for this purpose, though the use of organic zinc has also been explored in recent years after observing synergistic effects of AAs in Zn absorption[51-53]. In practice, the pharmacological levels of Zn have been widely used to improve the growth performance of young pigs[186]. Zn has also been explored as a supplement for protecting animals against the adverse effects of HS[49, 50]. The protective effects of Zn have been partially attributed to its antioxidant property[54], while its growth promotion effects are likely due to its functions as the cofactor of insulin, transcriptional factors, and metabolic enzymes[187-189]. Despite these established functions of Zn in metabolism, whether Zn supplementation could affect HS-induced metabolic changes is largely unknown.

Through growth performance, blood chemistry, and liquid chromatography-mass spectrometry (LC-MS)-based metabolomic analysis of serum, hepatic extract, cecal fluid, fecal extract, and urine samples, the present study aims to characterize metabolic effects of diurnal HS challenge as well as to determine whether Zn supplementation could affect metabolic responses to HS. Comprehensive examination of the metabolomes in these biological samples led to identification of time- and site-specific metabolite markers that are associated with HS and Zn-induced changes in AA, lipid, and microbial metabolism.

2.3 MATERIALS AND METHODS

2.3.1 Chemicals

LC-MS-grade water and acetonitrile (ACN) (Fisher Scientific, Houston, TX). 2-Hydrazinoquinoline (HQ) and triphenylphosphine (TPP) (Alfa Aesar, Ward Hill, MA).

2,2′-Dipyridyl disulfide (DPDS) (MP Biomedicals, Santa Ana, CA). Dansyl chloride (DC) and n-butanol (Sigma-Aldrich, St. Louis, MO). The metabolite standards used for structural confirmation were from Sigma-Aldrich, Fisher Scientific, Alfa Aesar, Ark Pharm **(**Libertyville, IL), Frontier Scientific (Logan, UT), and Steraloids (Newport, RI), respectively.

2.3.2 Animals and feeds

The animal study protocol was reviewed and approved by the Iowa State University Institutional Animal Care and Use Committee (IACUC). Forty eight crossbred gilts (pre-breeding female pigs) in growing phase, with initial body weight (BW) of 71 ± 9 kg, were assigned to 1 of 6 treatments in a 2 temperatures × 3 feeds factorial design (8 pigs/treatment) at the Iowa State University Swine Nutrition Farm (Ames, IA). All 3 feeds (ZnNeg: no Zn supplementation; ZnIO: 120 ppm $ZnSO_4$; and ZnAA: 60 ppm $ZnSO_4$ + 60 ppm Availa®Zn zinc AA complex) were prepared by mixing three mineral premixes with corn-soybean meal, respectively. The nutrient contents in formulated diets met or exceeded the National Research Council (NRC) requirements (2012) for energy, essential AAs, minerals and vitamins (Table 2.1). The mineral contents of premixes and feeds were measured by the Minnesota Valley Testing Lab (New Ulm, MN).

2.3.3 Animal experiment

The feeding experiment was divided into 3 periods (Figure 2.1A**)**. From day -14 to -4, pigs were housed in group pens and fed with one of assigned diets. From day -3 to 0, pigs were moved to two separate environment rooms and acclimated to the individual pens for 4 days under thermal neutral (TN) condition (21°C room temperature). From day 1 to 7, diurnal HS (12 h 25°C + 12 h 37°C) was applied in one environment room while TN was

maintained in the other room (Figure 2.1B). During whole experiment, pigs were *ad libitum* access to water and diet. For pigs under HS treatment, rectal temperature (RT) and respiratory rate (RR) were monitored five times daily at 9 AM, 11 AM, 1 PM, 3 PM and 5 PM for the first three days. RT was measured using a digital thermometer. RR was determined by counting flank movements for 1 minute. BW was measured on day -14, -4, and 0, and then daily during day 1 to 7. Feed intake was measured between day -4 and 0, and then daily from day 1 to 7.

2.3.4 Sample collection

Blood samples were collected via jugular venipuncture using Vacutainer tubes (Becton Dickinson, Franklin Lakes, NJ) at 1 PM of the sampling days (day 0, 2 and 7 of TN treatment; day 0, 1, 2, 5, and 7 of HS treatment). After the collection, the samples were allowed to clot at room temperature for 20 min, and then placed on ice. Serum were obtained by centrifugation of blood samples at 1,400 × *g* for 10 min and stored at -80°C. On day 7, liver, cecal fluid, and fecal samples were collected immediately after sacrifice and snap-frozen in liquid nitrogen. Urine samples were drawn from bladder using syringes. All these samples were stored at -80°C until further analysis.

2.3.5 Blood chemistry

The levels of cholesterol, triglycerides, glucose, creatinine, blood urea nitrogen (BUN), and iron in serum samples were measured using the reagent kits (Pointe Scientific, Canton, MI). Serum Zn level was determined using a reagent kit (Sigma-Aldrich).

2.3.6 Metabolomics

LC-MS-based metabolomic analysis comprises sample preparation, chemical derivatization, LC-MS analysis, data deconvolution and processing, multivariate data analysis, and marker characterization and quantification[190].

2.3.6.1 Sample preparation

For serum samples, deproteinization was conducted by mixing one volume of serum with 19 volumes of 66% aqueous ACN and then centrifuging at 18,000 × *g* for 10 min to obtain the supernatants. Liver tissue samples were fractionated using a modified Bligh and Dyer method[191]. Briefly, 100 mg of liver sample was homogenized in 0.5 mL of methanol and then mixed with 0.5 mL of chloroform and 0.4 mL of water. After 10 min centrifugation at 18,000 × *g*, upper aqueous fraction was harvested while chloroform fraction was dried by nitrogen and then reconstituted in n-butanol. After precipitating insoluble content by centrifugation, cecal fluid samples were further diluted with 4 volumes of 50% aqueous ACN and then centrifuged at 18,000 × *g* for 10 min to obtain the supernatants. Feces samples were mixed with 50% aqueous ACN in 1:9 (w/v) ratio and then centrifuged at 18,000 × *g* for 10 min to obtain fecal extract supernatants. Urine samples were processed by mixing one volume of urine with 4 volumes of 50% aqueous ACN and then centrifuged at 18,000 × *g* for 10 min to obtain the supernatants.

2.3.6.2 Chemical derivatization

For detecting the metabolites containing amino functional group in their structures, the samples were derivatized with DC prior to the LC-MS analysis. Briefly, 5 μL of sample or standard was mixed with 5 μL of 100 μM *p*-chlorophenylalanine (internal standard), 50 μL of 10 mM sodium carbonate, and 100 μL of DC solution (3 mg/mL in acetone). The mixture was incubated at 25°C for 15 min and centrifuged at 18,000 × *g* for

10 min, the supernatant was transferred into a HPLC vial for LC-MS analysis. For detecting carboxylic acids, aldehydes and ketones, the samples were derivatized with HQ prior to the LC-MS analysis[192]. Briefly, 2 µL of sample was added into a 100 µL of freshly-prepared ACN solution containing 1 mM DPDS, 1 mM TPP and 1 mM HQ. The reaction mixture was incubated at 60°C for 30 min, chilled on ice and then mixed with 100 µL of ice-cold H_2O. After centrifugation at 18,000 × *g* for 10 min, the supernatant was transferred into a HPLC vial for LC-MS analysis.

2.3.6.3 LC-MS analysis

A 5 µl of aliquot prepared from serum, hepatic extract, cecal fluid, fecal extract, or urine sample, was injected into an Acquity ultra-performance liquid chromatography (UPLC) system (Waters, Milford, MA) and separated in a BEH C18 column (Waters). The mobile phase for underivatized and DC-derivatized samples used a gradient ranging from water to 95% aqueous ACN containing 0.1% formic acid over a 10 min run, while the mobile phase for HQ-derivatized samples contained A: H_2O containing 0.05 % acetic acid (v/v) and 2 mM ammonium acetate; B: H_2O:ACN = 5:95 (v/v) containing 0.05 % acetic acid (v/v) and 2 mM ammonium acetate. LC eluant was introduced into a Xevo-G2-S quadrupole time-of-flight mass spectrometer (QTOFMS, Waters) for accurate mass measurement and ion counting. Capillary voltage and cone voltage for electrospray ionization was maintained at 3 kV and 30 V for positive-mode detection, or at -3 kV and -35 V for negative-mode detection, respectively. Source temperature and desolvation temperature were set at 120°C and 350°C, respectively. Nitrogen was used as both cone gas (50 L/h) and desolvation gas (600 L/h), and argon as collision gas. For accurate mass measurement, the mass spectrometer was calibrated with sodium formate solution with

mass-to-charge ratio (*m/z*) of 50-1,000 and monitored by the intermittent injection of the lock mass leucine enkephalin ($[M+H]^+$ = *m/z* 556.2771 and ($[M-H]^-$ = *m/z* 554.2615) in real time. Mass chromatograms and mass spectral data were acquired and processed by MassLynx™ software (Waters) in centroided format. Additional structural information was obtained tandem MS (MSMS) fragmentation with collision energies ranging from 15 to 40 eV.

2.3.6.4 Data deconvolution and processing

After data acquisition in the UPLC-QTOFMS system, chromatographic and spectral data of samples were deconvoluted by MarkerLynx™ software (Waters). A multivariate data matrix containing information on sample identity, ion identity (retention time and *m/z*) and ion abundance was generated through centroiding, deisotoping, filtering, peak recognition and integration. The intensity of each ion was calculated by normalizing the single ion counts (SIC) *versus* the total ion counts (TIC) in the whole chromatogram.

2.3.6.5 Multivariate data analysis

The processed data matrix was exported into SIMCA-P+™ software (Umetrics, Kinnelon, NJ), transformed by *Pareto* scaling, and then analyzed by unsupervised PCA and supervised partial least squares-discriminant analysis (OPLS-DA). Major latent variables in the data matrix were determined as the principal components of PCA model, and the relationships among examined samples were described in the scores scatter plot. Metabolite markers of HS exposure and Zn supplementation were identified by analyzing ions contributing to sample separation in OPLS-DA model. After Z score transformation, the concentrations or relative abundances of identified metabolite markers in examined samples were presented in the heat maps generated by the R program (http://www.R-

project.org), and the correlations among these metabolite markers were defined by hierarchical clustering analysis (HCA).

2.3.6.6 Marker characterization and quantification

The chemical identities of metabolite markers were determined by accurate mass measurement, elemental composition analysis, searching Human Metabolome Database (HMDB), Kyoto Encyclopedia of Genes and Genomes (KEGG), and Lipid Maps databases using MassTRIX search engine (http://masstrix3.helmholtz-muenchen.de/masstrix3/)[193], MSMS fragmentation, and comparisons with authentic standards if available. Individual metabolite concentrations were determined by calculating the ratio between the peak area of metabolite and the peak area of internal standard and fitting with a standard curve using QuanLynx^{TM} software (Waters).

2.3.7 Statistics

The statistical significances among diet and treatment groups were analyzed using the PROC MIXED procedure of SAS version 9.1 (SAS Institute, Cary, NC). Data are reported as least squares means (LSMEANS). Student's *t*-test was used for pairwise comparisons of two time points within a treatment. The PROC GLM procedure of SAS was used to compare three diet groups. Differences are considered significant if $P < 0.05$ and as a tendency if $0.05 \geq P \leq 0.10$.

2.4 RESULTS

2.4.1 Diet analysis

The concentrations of minerals in the premixes and diets were measured. The Zn levels in ZnIO and ZnAA were comparable (Table 2.2). The presence of low-level Zn in

ZnNeg diet suggested that corn and soybean meal provided about 30 ppm Zn in all three experimental diets (Table 2.2).

2.4.2 Physiological responses and growth performance

Under TN condition, average RT of pigs was 39.0 ± 0.4°C, and their average RR was 75 ± 8 breaths per minute (BPM). After diurnal HS challenge, average RT and RR were greatly increased (Figure 2.2A,B). On day 1 of HS, average RT rose up to 40.5 ± 0.6°C after 2 h of 37°C HS, and average RR became 183 ± 25 BPM (Figure 2.2A,B). Furthermore, after 4 h of 37°C exposure on day 1, half of all 24 pigs under HS challenge had their RT higher than 41°C, which is the threshold temperature for the mitigation treatment required by approved IACUC protocol. This situation led to the adjustment of ambient temperature to 35-36°C on day 1-3 to avoid heat stroke. However, on day 4 to 7, RT of HS group became comparable to that of TN group, and hence ambient temperature was maintained at 37°C during daily 12-h HS challenge (Figure 2.2A). In contrast, RR of HS group was still significantly higher than its value in TN group (Figure 2.2B). Overall, these observations suggested that HS led to an initial acute response followed by a gradual physiological acclimation.

HS reduced average daily gain (ADG), average daily feed intake (ADFI), and gain:feed ratio (G:F ratio) (Figure 2.3A,B, Table 2.3) while Zn supplementation did not significantly alter live performance metrics (Figure2.3C,D, Table 2.3).

2.4.3 Blood chemistry

Despite some day-to-day fluctuation, serum glucose, triglycerides, and cholesterol levels were not significantly affected by either HS or Zn supplementation during 1-week treatment (Figure 2.4A-C, Table 2.4). In contrast, serum BUN level was gradually

decreased by HS from day 1 to 5, while serum creatinine level was significantly higher on day 1 and 7 of HS than its level on day 0 (Figure 2.5A,B, Table 2.4). Furthermore, serum iron level was also not affected by Zn supplementation and HS during 1-week treatment (Figure 2.6A, Table 2.4). Serum Zn level on day 0 and 7 was comparable among all treatment groups (Figure 2.6B, Table 2.4).

2.4.4 Metabolomics

Daily metabolic responses to HS challenge were examined by metabolomic analysis of multiple serum samples collected during one week of diurnal HS challenge, while the metabolic effects of one-week HS exposure were determined by metabolomic analysis of liver, cecal content, feces, and urine samples.

2.4.4.1 Daily effects of HS and Zn supplementation on serum metabolome

Effect on serum free amino acids (FAAs). Considering the potential association between amino acids and observed changes in BUN and creatinine, the influences of HS and Zn supplementation on the composition of FAAs and other amino-containing metabolites in serum were examined by LC-MS analysis and PCA modeling. The distribution of serum samples in an unsupervised PCA model revealed that HS induced dramatic changes in serum metabolome, especially on day 1 of HS, since the principal component 1 of the model mainly define the differences between day 0 and day1 HS samples (Figure 2.7A,B). It is also noticeable that the time-dependent differences existed in TN groups, but in much smaller scale than HS groups. Furthermore, Zn did not significantly affected the composition of serum metabolome since the samples were not grouped based on Zn supplementation (Figure 2.7A,B). The serum metabolites affected by HS exposure were identified in an S-plot from an OPLS-DA-based comparison

between HS and TN samples. As expected, major contributors to the separation of HS from TN samples are FAAs (Figure 2.7C). The concentrations of major free proteinogenic and nonproteinogenic AAs in serum were examined by HCA (Figure 2.7D) and then quantified (Figure 2.8, 2.9, Table 2.5).

After one week of experiment, serum AAs profile was affected by HS×Zn supplementation interaction, HS or Zn supplementation. *1)* Treatment by diet interaction occurred on serum methionine (Table 2.5). Under TN condition, ZnAA had lower level of methionine than ZnIO. *2)* Compared to TN, HS led to higher levels of tryptophan, phenylalanine, glutamate, taurine, citrulline and 4-hydroxyproline. On the other side, HS had lower levels of alanine, tyrosine, lysine, histidine, asparagine, serine, proline, ornithine, isoleucine, leucine, and total FAAs (Table 2.5). *3)* ZnIO led to higher tryptophan and tyrosine compared to ZnAA, while higher tryptophan, tyrosine, lysine, arginine, and citrulline compared to ZnNeg. ZnAA led to higher valine and proline compared to ZnNeg, while higher glutamine and proline compared to ZnIO (Table 2.5).

The distribution patterns of individual AAs in the heat map and their concentrations (Figure 2.7D, 2.8, 2.9) further revealed the following conclusions on the daily effects of HS and Zn supplementation: *1)* Majority of examined FAAs were affected by HS. In comparison, the FAA profile of TN samples was much more stable despite some day-to-day variances. *2)* The most dramatic changes induced by HS occurred on day 1. Afterwards, some of those changes were attenuated. This pattern of changes was consistent to the acute responses and the acclimation to HS. *3)* The level of total FAAs tended to increase on day 1 of HS and then was decreased afterwards, but this pattern of change was not followed by individual FAAs. Among essential AAs, lysine and histidine

were persistently decreased by HS while tryptophan, valine, and isoleucine were transiently increased by HS. Among AAs that are closely related by specific metabolic reactions, glycine was increased on day 1while serine, the precursor metabolite of glycine, was decreased by HS. Similarly, 4-hydroxyproline was increased while proline, its precursor, was decreased by HS. Among urea cycle-related AAs, arginine, citrulline, glutamate, and glutamine were increased while ornithine was decreased by HS.

Effect on serum lipids. Besides amino-containing metabolites, serum lipidome was also examined by LC-MS analysis and multivariate data analysis modeling. Based on the distribution pattern of examined samples in an unsupervised PCA model, HS induced dramatic changes in serum lipidome, especially on day 1 of exposure (Figure 2.10A,B). Moreover, Zn supplementation appeared to affect the metabolic responses to HS since the changes occurred in ZnIQ samples were not very similar to ZnAA and ZnNeg samples after HS exposure (Figure 2.10B).

The lipids responsive to HS were identified in an S-plot from an OPLS-DA model on HS and TN samples (Figure 2.10C), and their structural identities as phospholipids, including phosphatidylcholines (PC), lyso-phosphatidylcholines (LysoPC), and sphingomyelins (SM), were defined by MSMS fragmentation. Based on their distribution patterns in the heat map generated by HCA, the serum lipid markers can be roughly classified into 4 groups, containing the phospholipids that were transiently decreased, persistently decreased, transiently increased, or persistently increased during one-week of HS exposure (Figure 2.10D). A prominent feature of those persistently-decreased PCs is the presence of odd chain fatty acids (pentadecanoic acid and heptadecanoic acid) in their structures while those persistently-increased markers contain

either very long chain fatty acid (carbon number ≥ 22) or stearic acid. Furthermore, two SM species were transiently increased in the first two days of HS while multiple PC species containing palmitic acid or linoleic acid were transiently decreased by HS (Figure 2.10D).

2.4.4.2 Weekly effects of HS and Zn supplementation on the metabolomes

Compared to serum samples harvested on multiple days during 1 week of diurnal HS, liver, cecal contents, feces and urine samples were collected at the end of 1-week HS. Therefore, metabolomic analyses of these samples potentially reveal accumulative effects of HS exposure and Zn supplementation. Major classes of metabolites in these samples, such as bile acids, short-chain fatty acids, lipids, and amino acids, were analyzed by corresponding LC-MS methods.

Markers contributing the separation of HS and TN samples were characterized by elemental composition analysis, database, MSMS fragmentation, and confirmation with authentic standards if available. However, because of the limitations in accuracy of database library and availability of standards, not all of the markers acquired though metabolomics models were confirmed and discussed in the following statement. The markers whose identities were acquired though database and standard confirmation were listed in the result. But the ones whose identities cannot be found though database were not listed in the result even though some of them were contributors to the model separation. The biological importance of these markers is worth further evaluations with regarding to understand effects of HS.

Summary model of hepatic, cecal, fecal, and urinary metabolomes after one-week HS challenge. For each type of sample, the LC-MS data from different LC-MS runs were

pooled and then analyzed by PCA. Clear separations of HS and TN samples were observed in the PCA models on hepatic, cecal, and fecal metabolomes, but not in the model on urine metabolome (Figure 2.11A-D). Another noticeable feature is that HS-ZnIO samples were more separated from TN samples than HS-ZnAA and HS-ZnNeg samples in PCA models of hepatic and cecal metabolomes (Figure 2.11A,B). Markers contributing the separation of HS and TN samples were summarized based on their structures and biochemical functions (Table 2.7).

*Liver***.** After one week of experiment, liver AAs profile was affected by HS×Zn supplementation interaction, HS or Zn supplementation. *1)* There was a treatment by diet interaction ($P < 0.05$) on level of glycine, arginine, asparagine, glutamine, methionine, threonine, and 4-hydroxyproline (Table 2.6). For arginine, glutamine, methionine and threonine, after Tukey adjustment, the differences were not significant. Under TN condition, ZnNeg had higher level of glycine than ZnIO. TN-ZnNeg had higher level of asparagine than HS-ZnAA and HS-ZnNeg. For 4-hydroxyproline, TN-ZnNeg had higher level of it than HS and TN-ZnIO, while TN-ZnAA had higher level of it than HS-ZnAA. *2)* Compared to TN, HS only had higher level of lysine, but lower levels of alanine, valine, tyrosine, histidine, glutamate, methionine, serine, taurine, proline, ornithine, and isoleucine. *3)* ZnIO led to higher level of lysine compared to ZnAA and ZnNeg (Figure 2.12**,** Table 2.6). Since the levels of many FAAs in the liver were decreased by HS, total FAAs was consequently decreased in the liver. In fact, this phenomenon is consistent with the decrease of total FFAs in serum on day 7 of HS. Opposite to this change in total FFAs, hepatic ammonia level was increased by HS (Figure 2.12). Multiple PCs and PEs in the liver were affected by HS. Similar to the changes in serum lipidome, the PCs

decreased by HS contain odd-chain fatty acids (pentadecanoic acid and heptadecanoic acid) while the PCs increased by HS contain palmitic acid and stearic acid (Figure 2.12).

*Cecal fluid***.** HS decreased the levels of oleic acid and linoleic acid, as well as the level of fatty acid amide (oleamide). Stercobilin, a bacterial degradation product of bilirubin, was increased by HS. The levels of cecal hyodeoxycholic acid and deoxycholic acid, two major secondary bile acids in pigs, were also increased by HS. Interestingly, inosine, a purine nucleoside, was increased in cecal fluid by HS, accompany with the decrease of xanthine, a degradation product of inosine (Figure 2.13A). As major metabolites of microflora, SCFAs in cecal fluids were quantified. HS led to higher acetic acid versus TN. ZnIO led to higher propionic acid compared to ZnNeg, higher acetic acid compared to ZnAA and ZnNeg, and higher butyric acid compared to ZnAA and ZnNeg (Figure 2.13B-D). The higher concentrations of SCFAs in ZnIO-HS group suggested that ZnIO might promote SCFAs production under HS condition.

Feces. Higher level of lysine was observed in ZnIO-HS fecal samples. Furthermore, HS also increased citrulline and ornithine in feces. Moreover, HS decreased the levels of oleic acid and linoleic acid, but increased the levels of medium-chain dicarboxylic acids (suberic acid and sebacic acid). Stercobilin, was also increased by HS in feces. Levels of LysoPE(16:0), LysoPC(16:0), LysoPC(18:2) and 2,8-dihydroxyquinoline were decreased by HS (Figure 2.14).

*Urine***.** HS increased the level of creatinine, but decreased the level of kynurenic acid (Figure 2.15).

Beside different types of sample, the markers were summarized and discussed separately based on their biochemical functions (Table 2.7).

---*AAs and associated metabolites (summarized in Table* 2.7*)*: The levels of many FAAs in the liver were decreased by HS, leading to the decrease of total FAAs in the liver (Table 2.6). In fact, this phenomenon is consistent with the decrease of total FAAs in serum on day 7 of HS (Figure 2.8A). Opposite to this change in total FAAs, hepatic lysine levels were increased by HS (Table 2.6). However, the increase in lysine mainly occurred in ZnIO diet under HS. Interestingly, the higher level of lysine was also observed in ZnIO-HS fecal samples (Figure 2.14). Furthermore, HS also increased citrulline and ornithine in feces and creatinine in urine, but decreased kynurenic acid in urine (Figure 2.14, 2.15).

---*Fatty acids, phospholipids and associated metabolites (summarized in Table* 2.7*)*: Multiple PCs and phosphatidylethanolamines (PEs) in the liver were affected by HS (Figure 2.12). Similar to the changes in serum lipidome (Figure 2.10D), the PCs decreased by HS contain odd-chain fatty acids (pentadecanoic acid and heptadecanoic acid) while the PCs increased by HS contain palmitic acid and stearic acid (Figure 2.12). Moreover, in cecal and fecal samples, HS decreased the levels of oleic acid and linoleic acid, as well as fatty acid amide such as oleamide, but increased the levels of suberic acid and sebacic acid, which are medium-chain dicarboxylic acids (Figure 2.13A, 2.14).

---*Microbial metabolites (summarized in Table* 2.7*)*: Stercobilin, a bacterial degradation product of bilirubin, was increased by HS in both cecal and fecal samples (Figure 2.13A, 2.14). The levels of cecal hyodeoxycholic acid and deoxycholic acid, two major secondary bile acids in pigs, were also increased by HS (Figure 2.13A). Interestingly, inosine, a purine nucleoside, was increased in cecal fluid by HS,

accompanying with the decrease of xanthine, a degradation product of inosine (Figure 2.13A). As major metabolites of microflora, SCFAs in cecal fluids were quantified. The higher concentrations of SCFAs, especially acetic acid and propionic acid, in ZnIO-HS group suggested that ZnIO might promote SCFAs production under HS condition (Figure 2.13).

2.5 DISCUSSION

Metabolites are both the building blocks of animal growth and the regulators of animal health. In both HS exposure and Zn supplementation, metabolism is expected to play a central role in determining animal's growth performance and health status. Through metabolomic analysis in this study, diverse metabolites affected by HS and Zn were identified and characterized. The changes in these metabolites were often time (transient or persistent) and site (different samples)-specific. Discussions on the significance of these changes are based on the biochemistry of these metabolites, the physiology of HS and Zn supplementation, and metabolic functions of gut microflora.

Effects of HS on swine metabolome

Almost all biological processes in living entities, i.e. humans, animals, plants, and microbes, are conducted within a narrow range of temperature. High ambient temperature affects energy and nutrient metabolism through its influences on thermogenesis and thermoregulation as well as the functions of biomolecules, such as enzymatic activity, protein folding, and lipid membrane integrity. In this study, the disruptive effects of HS on metabolic system were reflected indirectly by the changes in physiological parameters (RT and RR) and the decrease in growth performance (Figure 2.2, 2.3, Table 2.3), and also directly by the metabolic changes detected by blood chemistry and metabolomic

analysis (Figure 2.4 to 2.15, Table 2.4 to 2.7). The results from metabolomic analysis of diverse samples, including serum, liver, cecal fluid, feces and urine, not only reconfirmed the comprehensive impacts of HS on metabolic systems through multivariate modeling, but also revealed previously unreported changes in amino acid, fatty acid, phospholipid, and microbial metabolism through identification and quantitation of metabolite markers (Figure 2.5 to 2.15, Table 2.5 to 2.7). Among these metabolites, FAAs, even though a minor fraction of total AA pool in the body, are useful indicators of nutritional and metabolic status since their levels are commonly controlled by dynamic equilibrium among different metabolic pathways[194]. Several interesting features were identified among many changes in FFAs and their associated metabolites: *1)* Even though feed intake was reduced by HS, the total FAA level in serum tended to increase on day 1 of HS. Protein degradation, as a prominent consequence of HS, is likely contribute to this phenomenon. For example, the increase of 4-hydroxyproline, a major component of collagen, could be due to increased activity of collagenase under HS[195], while the increase of branched-chain AAs (BCAAs: leucine and isoleucine) could originate from hyperthermia-induced muscle degradation as BCAAs account for one-third of muscle proteins[196, 197]. *2)* Multiple metabolites in urea cycle were greatly affected by HS. Urea (BUN) and ornithine (serum and liver), as the products of urea cycle, were decreased by HS. In contrast, the nitrogen donors and carriers, including glutamate (serum), ammonia (liver), citrulline (serum), and arginine (serum) were increased by HS (Figure 2.7D, 2.12, Table 2.5, 2.6). This pattern of changes suggests that HS can significantly disrupt urea cycle, potentially through negative regulation on arginase. It has been shown that HS-induced vasodilation is correlated with the increase of nitric oxide (NO) biosynthesis[198],

which in return could inhibit the activity of arginase[199]. Whether this is a contributing mechanism on observed changes in urea cycle requires further studies. *3)* Besides urea cycle, other changes in amino acid catabolism and biotransformation might also contribute to the changes in individual FFAs. For example, tryptophan in serum was greatly increased by HS (Figure 2.7D, Table 2.5**)**, while kynurenic acid, a major catabolic metabolite of tryptophan, was decreased in urine (Figure 2.15, Table 2.7). Since kynurenine pathway connects these two metabolites, the down-regulation of this pathway provides a plausible explanation for this observation. Furthermore, the decrease in proline and the increase of 4-hydroxyproline could be contributed by the oxidation reaction between them, while the decrease in serine and the increase in glycine could also be associated with the one-carbon metabolism between them. Further mechanistic studies are required to examine the validity of these hypothesis. *4)* Lysine, as the first limiting AA in swine diet, was consistently decreased in serum during 1-week HS (Figure 2.7D), but its level in the liver and feces, especially in ZnIO-HS pigs, was increased after HS (Table 2.6, 2.7). This observation could be due to the changes in absorption and utilization of lysine, or microflora-mediated lysine biosynthesis in pigs[200]. Further studies are required to determine the underlying mechanism.

With regard to HS-induced changes of phospholipids in the liver and serum (Figure 2.10D, 2.12, Table 2.7), the implication of these changes is likely to be the alteration or disruption of plasma membrane since PCs, PEs, and SMs are its major components[201]. This is largely consistent to the reported sensitivity of plasma membrane to heat stress[202]. Examining the pattern of HS-responsive phospholipid markers suggested that the transient changes in some of these markers are consistent with the general feature of

physiological response to HS, such as RT, which proceeds from acute response to acclimation (Figure 2.2). Among them, SMs identified in the present study could be closely related to the induction of Hsps in response to HS[36]. In contrast, the decrease of PCs containing pentadecanoic acid or heptadecanoic acid in serum persisted during 7 days of HS (Figure 2.10D). Considering microbial origin of these two odd-chain fatty acids[203], this pattern of change is consistent with the feature associated with the disruption of microflora, which yields more lasting effects than acute physiological responses. Furthermore, HS also increased multiple stearic acid-containing PCs in the liver and serum. Since heptadecanoic acid is formed by α-oxidation of stearic acid[204], it is possible that HS might suppress this biotranformation process, resulting in different distribution of fatty acids in phospholipids.

Besides observing the changes of fatty acid composition in phospholipids, examining cecal and fecal metabolomes also revealed the changes in fatty acid metabolism by observing the increases of medium-chain dicarboxylic acids (suberic acid and sebacic acid) and the decreases of unsaturated fatty acids (oleic acid and linoleic acid) and their amides (oleamide) after HS (Figure 2.13A, 2.14, Table 2.7). Since medium-chain dicarboxylic acids are likely the oxidation products of unsaturated fatty acids[205], the imbalance between these two types of fatty acids further implicates the potential effects of HS on microflora-mediated fatty acid metabolism.

The influences of HS on GI function and microbial metabolism were also reflected by other cecal and fecal metabolites (Figure 2.13A, 2.14, Table 2.7). For example, the observed increases of secondary bile acids (hyocholic acid and deoxycholic acid) and bilirubin metabolite (sterobilin and sterobiligen) could be due to reduced reabsorption in

GI tract or more active microbial metabolism. Moreover, the increase of inosine and the decrease of xanthine in cecal samples suggest purine degradation in microflora was negatively affected by HS.

Effects of Zn supplementation on swine metabolome

Zn supplementation in this study did not significantly affect serum Zn level (Figure 2.6B), growth performance (Figure 2.3C,D), and blood chemistry (Figure 2.4, 2.5, 2.6). The lack of diet-induced changes in serum Zn level could be explained by the existence of robust regulation of Zn homeostasis in the body[206]. Previous studies have shown that serum and whole-body Zn levels in humans and animals are relatively stable even under a wide range of dietary Zn intake, since higher Zn intake is commonly translated into reduced absorption efficiency and higher fecal excretion[207-209]. Therefore, significant change in serum Zn level may only occur under extremely low or high Zn intake when there is insufficient Zn input or Zn overload for the exchangeable pool in Zn homeostasis[210]. These two scenarios did not occur in this study since 30 ppm Zn was detected in ZnNeg diet while 120 ppm Zn in ZnIO and ZnAA diets is not expected to overwhelm the body.

Even though HS-induced metabolic changes are dominant in defining the differences among sample groups in this study, Zn supplementation also elicited subtle metabolic differences among pigs under HS challenge. This conclusion is based on both the multivariate data analysis models on the metabolomes and the HS-induced changes in individual metabolites. A prominent feature is that ZnIO diet appears to elicit stronger metabolic responses to HS than ZnAA and ZnNeg diets. As shown in both unsupervised PCA models of hepatic and cecal metabolomes (Figure 2.11A,C), HS-ZnIO samples were

further away from TN samples than HS-ZnAA and HS-ZnNeg samples. Moreover, the PCA model of serum lipids (Figure 2.10A,B) also showed that the time-dependent changes in HS-ZnIQ samples did not share a similar pattern with HS-ZnAA and HS-ZnNeg samples, especially in the first 2 days of HS. On individual metabolites, HS-induced increase of serum tryptophan in ZnIO pigs was much greater than that in ZnAA and ZnNeg pigs (Table 2.5). Furthermore, under HS, ZnIO pigs had higher level of lysine in the liver and feces than ZnAA and ZnNeg pigs (Figure 2.12, 2.14, Table 2.7). HS also increased the level of acetic acid in cecal fluids from ZnIO pigs (Figure 2.13B). Since SCFAs in cecal fluid originate from microbial fermentation, this observation suggested that $ZnSO_4$ in ZnIO diet might elevate these fermentation activities, especially the formation of acetic acid. The underlying mechanism of this selective activity requires further investigation. However, the function of inorganic Zn, including ZnO and $ZnSO_4$, as modulation agents for the stability of microflora and the growth of pathogenic microbes have been shown in previous studies[211, 212].

Values and challenges of metabolomics

Targeted analyses of specific metabolites have been performed in numerous studies on HS exposure and Zn supplementation. Despite their merits in confirming expected metabolic changes or revealing general metabolic status of study subjects, targeted analyses are incapable of defining global profile of metabolic system or identifying unexpected metabolic events. Adopting untargeted metabolomics in this study addressed these limitations of targeted analyses, resulting in the identification of amino acids, lipids, and microbial metabolites responsive to HS challenge or Zn supplementation. The procedures of LC-MS-based untargeted metabolomics platform, which include sample

preparation, LC-MS analysis, multivariate analysis, marker identification and characterization, have been extensively reviewed[177, 213]. In this study, the values and challenges of individual metabolomic analysis procedures in discovering metabolite markers are evident and can be summarized as follows. *1)* In sample preparation, besides adopting respective extraction methods for each type of samples, chemical derivatization, using DC and HQ, had greatly extended the coverage of LC-MS analysis and facilitated the quantitation of interested metabolites in this study. Considering chemical derivatization is a requisite step in GC-MS-based metabolomics, the application of chemical derivatization in LC-MS-based metabolomics remains to be limited and can be greatly expanded[214]. *2)* PCA and HCA, two multivariate methods, were adopted to process complex LC-MS data in this study. Besides revealing the treatment- and diet-associated grouping of examined samples, PCA modeling was also able to show time-dependent events, including acute response and acclimation to HS, based on sample distribution in the score plots (Figure 2.7B, 2.10B). Subsequently, the metabolite markers identified by PCA were processed by HCA, which produced the heat maps revealing both the correlations among multiple as well as time-dependent changes (Figure 2.7D, 2.10D). This combination of PCA and HCA facilitated data visualization and marker identification, and is an efficient approach for examining complex metabolomics datasets. *3)* Despite the progresses in constructing metabolomic databases and bioinformatics tools, marker identification remains to be a bottleneck in many metabolomics efforts[215]. In this study, multiple candidate structures with the same elemental composition were commonly enlisted for interested metabolites by accurate mass-based database search, which reduced the choices for further structural elucidation. However, unambiguous

structural identification of these metabolite markers was still achieved by the comparison of authentic standards or the analysis of MSMS fragmentograms, which in many cases corrected the structure proposed by initial analysis. Since many recent published metabolomics works heavily relied on bioinformatics-based structural identification, the experience in this study highlights the need to be cautious when processing the results from database search.

2.6 CONCLUSION

In conclusion, comprehensive metabolomic analysis of diverse biological samples in this study revealed HS-induced dramatic metabolic effects and Zn supplementation-associated subtle metabolic changes in finishing pigs. Identified metabolite markers and their responses to HS and Zn indicate that disruption of urea cycle, amino acid biotransformation, fatty acid profile, and microbial metabolism occurred during diurnal HS challenge while Zn supplementation, especially ZnIO, affect microbial metabolism under HS (Figure 2.16). All these observations warrant further investigations on the causes of identified metabolic events as well as their roles in physiological responses to HS and Zn supplementation.

Table 2.1. Ingredients and formulation of three experimental diets

Parameter	Diet		
	ZnIO	ZnAA	ZnNeg
Ingredients (%)			
Corn	88.94	88.94	88.94
Soybean meal	8.41	8.41	8.41
L-lysine HCl	0.30	0.30	0.30
Monocalcium phosphate	0.71	0.71	0.71
Limestone	0.75	0.75	0.75
Salt	0.40	0.40	0.40
Vitamin premix	0.25	0.25	0.25
Trace mineral premix*	0.24	0.24	0.24
Total	100.00	100.00	100.00
*Trace mineral premix			
Zinpro trace mineral premix (no zinc)†	0.12	0.12	0.12
Zinc sulfate, monohydrate	0.12	0.06	-
Zinpro - AvailaZn	-	0.06	-
Carrier (rice hull)	-	-	0.12

†Provided the following per kg of diet: Fe, 100 mg; Mn, 10 mg; Cu, 10 mg; Iodine, 0.20 mg; Se, 0.30 mg.

Table 2.2. Concentrations of minerals in premixes and diets

Mineral (%)	Trace mineral premix			Diet		
	ZnIO	ZnAA	ZnNeg	ZnIO	ZnAA	ZnNeg
Calcium	16.95	13.57	21.81	0.66	0.57	0.60
Copper	0.78	0.56	1.14	0.0012	0.0013	0.0015
Iron	5.54	6.28	9.59	0.021	0.022	0.026
Magnesium	0.46	0.40	0.61	0.11	0.11	0.11
Manganese	0.81	0.70	1.11	0.0022	0.0019	0.0018
Phosphorus	0.03	0.05	< 0.02	0.42	0.45	0.48
Potassium	0.22	0.16	0.032	0.46	0.45	0.44
Sodium	0.089	0.063	0.047	0.17	0.16	0.15
Zinc	8.79	7.20	0.097	0.0154	0.0143	0.0030

Table 2.3. Effects of HS and Zn Supplementation on growth performance parameters

	Groups						Treatments		Diets			*P*		
Parameter	TN-ZnIO	TN-ZnAA	TN-ZnNeg	HS-ZnIO	HS-ZnAA	HS-ZnNeg	TN	HS	ZnIO	ZnAA	ZnNeg	T x D	Diet	Trt
ADG (kg)	1.088	1.179	1.254	0.346	0.504	0.461	1.174[a]	0.437[b]	0.717	0.841	0.857	0.830	0.294	<0.0001
ADFI (kg)	3.261	3.208	3.614	2.032	2.184	1.971	3.361[a]	2.062[b]	2.646	2.696	2.792	0.083	0.559	<0.0001
G:F ratio	0.334	0.370	0.347	0.152	0.223	0.216	0.350[a]	0.197[b]	0.243	0.297	0.282	0.784	0.356	<0.0001

[a,b,c]Within groups, treatments or diets, the values with different letter labels are statistically different ($P < 0.05$).

Table 2.4. Effects of HS and Zn Supplementation on blood chemistry parameters

Parameter	Groups						Treatments		Diets			*P*		
	TN-ZnIO	TN-ZnAA	TN-ZnNeg	HS-ZnIO	HS-ZnAA	HS-ZnNeg	TN	HS	ZnIO	ZnAA	ZnNeg	T x D	Diet	Trt
Glucose (mg/dL)	109.01	118.89	111.53	108.70	111.84	113.04	113.11	111.18	108.85	115.34	112.28	0.608	0.349	0.598
Cholesterol (mg/dL)	95.54	98.83	97.92	88.45	94.60	97.78	97.42	93.53	91.93	96.69	97.85	0.717	0.363	0.284
Triglyceride (mg/dL)	27.27	29.40	27.94	26.83	28.17	29.45	28.20	28.14	27.05	28.78	28.69	0.762	0.589	0.971
BUN (mg/dL)	15.98	14.90	15.97	12.98	13.09	12.30	15.61[a]	12.79[b]	14.44	13.98	14.08	0.325	0.739	<0.0001
Creatinine (mg/dL)	0.89	0.95	1.00	1.04	1.05	1.15	0.95[a]	1.08[b]	0.96	1.00	1.08	0.803	0.039	0.0004
Iron (µg/dL)	190.41	191.75	195.18	190.93	185.75	191.66	192.44	189.43	190.68	188.73	193.41	0.884	0.783	0.582
Zn (µM)	8.06	8.66	8.81	9.03	8.27	9.85	8.51	9.05	8.54	8.46	9.33	0.283	0.167	0.191

[a,b,c]Within groups, treatments or diets, the values with different letter labels are statistically different ($P < 0.05$).

Table 2.5. Serum FAAs concentration*

FAAs (μM)	Groups						Treatments		Diets			*P*†		
	TN-ZnIO	TN-ZnAA	TN-ZnNeg	HS-ZnIO	HS-ZnAA	HS-ZnNeg	TN	HS	ZnIO	ZnAA	ZnNeg	T x D	Diet	Trt
Alanine	505.53	494.13	484.73	448.41	504.87	447.87	494.72^{a}	466.33^{b}	476.13	499.50	465.91	0.142	0.153	0.049
Glycine	865.34	828.97	807.14	823.98	904.51	876.29	833.64	867.93	844.53	866.33	841.36	0.073	0.637	0.142
Valine	196.59	189.82	182.82	197.28	208.49	184.34	189.67	196.45	196.94^{ab}	198.94^{a}	183.57^{b}	0.266	0.021	0.168
Phenylalanine	85.47	81.30	85.47	85.47	92.59	89.29	84.03^{a}	89.29^{b}	85.47	86.96	86.96	0.101	0.830	0.022
Tyrosine	59.37	48.31	50.20	48.44	40.28	39.81	52.52^{a}	42.75^{b}	53.76^{a}	44.20^{b}	44.85^{b}	0.901	0.001	<0.0001
Tryptophan	44.37	35.17	35.14	64.34	52.82	55.38	38.10^{a}	57.41^{b}	53.89^{a}	43.54^{b}	44.69^{b}	0.893	0.0004	<0.0001
Arginine	168.28	152.15	141.43	158.5	150.78	142.52	153.96	150.60	163.39^{a}	151.47^{ab}	141.98^{b}	0.651	0.003	0.505
Histidine	85.17	84.26	86.69	63.58	72.89	70.75	85.38^{a}	69.07^{b}	74.38	78.57	78.72	0.055	0.067	<0.0001
Lysine	302.45	266.87	256.49	182.66	193.12	158.64	275.27^{a}	178.14^{b}	242.56^{a}	230.00^{ab}	207.57^{b}	0.095	0.004	<0.0001
Aspartic acid	7.93	8.70	7.53	8.07	8.44	7.25	8.05	7.91	8.00	8.57	7.39	0.886	0.053	0.728
Asparagine	96.14	90.78	87.66	65.67	72.46	62.29	91.49^{a}	66.74^{b}	80.18	81.37	74.43	0.168	0.073	<0.0001
Glutamate	130.99	139.83	139.17	169.83	176.94	154.42	136.61^{a}	166.80^{b}	149.16	157.29	146.60	0.273	0.370	<0.0001
Glutamine	562.32	579.86	564.63	536.71	599.80	553.06	568.91	562.88	549.44^{a}	589.79^{b}	558.84^{ab}	0.360	0.037	0.649
Methionine	28.36^{a}	23.49^{b}	25.94^{ab}	22.30^{b}	25.11^{ab}	23.76^{b}	25.89^{a}	23.71^{b}	25.23	24.30	24.84	0.002	0.674	0.012
Serine	175.83	168.45	164.53	128.56	133.15	122.06	169.58^{a}	127.88^{b}	151.27	150.29	142.51	0.526	0.191	<0.0001
Threonine	71.81	59.87	61.69	62.20	58.59	56.88	64.25	59.19	66.83	59.22	59.24	0.508	0.031	0.056
Taurine	82.32	74.34	72.62	90.38	88.10	84.34	76.36^{a}	87.59^{b}	86.30	81.07	78.37	0.725	0.111	0.0004
Proline	283.35	299.23	282.05	204.36	228.10	205.37	288.10^{a}	212.34^{b}	240.64^{a}	261.26^{b}	240.66^{a}	0.688	0.023	<0.0001
Citrulline	51.82	49.49	43.49	58.82	52.69	51.81	48.20^{a}	54.40^{b}	55.27^{a}	51.08^{ab}	47.56^{b}	0.434	0.002	0.0005
Ornithine	111.40	99.78	106.79	85.34	86.19	80.01	105.89^{a}	83.80^{b}	97.50	92.74	92.43	0.201	0.374	<0.0001
Isoleucine	88.62	78.52	80.67	73.13	70.22	62.97	82.49^{a}	68.63^{b}	80.50	74.25	71.27	0.548	0.140	0.0004
Leucine	222.43	220.75	217.45	209.39	214.95	195.88	220.21^{a}	206.74^{b}	215.91	217.85	206.67	0.478	0.186	0.012
Hydroxyproline	73.06	74.55	68.09	87.19	86.15	86.90	73.06^{a}	86.75^{b}	79.81	80.14	76.92	0.356	0.439	<0.0001
Total	4339.64	4198.64	4101.42	3934.00	4186.94	3881.05	4213.24^{a}	4000.66^{b}	4136.82	4192.79	3991.24	0.149	0.118	0.010

*The FAA concentrations are the means of serum samples belonging to the same groups, treatments, or diets.

†Statistical significance is calculated by the PROC MIXED procedure of SAS.

[a,b,c]Within groups, treatments or diets, the values of individual AAs with different letter labels are statistically different ($P < 0.05$).

Table 2.6. Liver FAAs concentration*

	Groups						Treatments		Diets			*P*†		
FAAs	TN-ZnIO	TN-ZnAA	TN-ZnNeg	HS-ZnIO	HS-ZnAA	HS-ZnNeg	TN	HS	ZnIO	ZnAA	ZnNeg	T x D	Diet	Trt
Alanine	2405.47	2430.86	2754.52	2166.35	2079.54	2092.89	2525.51^{a}	2112.65^{b}	2282.67	2248.46	2400.90	0.318	0.486	0.0004
Glycine	2722.50^{a}	3098.50^{ab}	3171.00^{b}	3034.60^{ab}	2910.30^{ab}	2876.90^{ab}	2997.33	2940.60	2878.55	3004.40	3023.95	0.010	0.306	0.496
Valine	330.40	369.80	358.00	350.80	361.10	330.90	362.93^{a}	337.37^{b}	355.90	350.10	344.45	0.576	0.713	0.029
Phenylalanine	154.00	153.50	162.20	160.70	157.80	158.90	156.57	159.13	157.35	155.65	160.55	0.789	0.806	0.679
Tyrosine	86.10	81.62	111.46	86.59	54.33	53.97	92.19^{a}	63.32^{b}	86.35	66.59	77.56	0.143	0.364	0.015
Tryptophan	48.30	42.10	45.40	49.60	46.30	40.00	45.27	45.30	48.95	44.20	42.70	0.351	0.164	0.990
Arginine	45.67	48.50	58.85	61.81	45.23	45.40	50.70	50.25	53.13	46.84	51.69	0.0499	0.506	0.924
Histidine	663.30	639.90	677.00	521.30	572.10	593.10	660.07^{a}	562.17^{b}	592.30	606.00	635.05	0.268	0.195	<0.0001
Lysine	278.70	240.30	236.10	324.50	281.80	259.80	251.70^{a}	288.70^{b}	301.60^{a}	261.05^{b}	247.95^{b}	0.736	0.002	0.004
Aspartic acid	982.70	1175.09	1156.55	1041.69	1031.43	978.58	1101.25	1016.89	1011.81	1100.92	1063.80	0.389	0.624	0.268
Asparagine	410.30^{ab}	457.20^{ab}	497.80^{a}	429.10^{ab}	364.80^{b}	373.80^{b}	455.10^{a}	389.23^{b}	419.70	411.00	435.80	0.026	0.641	0.004
Glutamate	2971.10	3503.30	3802.20	2918.00	2926.30	2985.70	3425.53^{a}	2943.33^{b}	2944.55	3214.80	3393.95	0.225	0.138	0.011
Glutamine	2543.51	2965.79	3076.97	2934.52	2775.82	2547.84	2852.64	2748.20	2732.03	2869.23	2800.07	0.042	0.747	0.479
Methionine	83.20	89.50	101.90	88.00	80.90	77.60	91.53^{a}	82.17^{b}	85.60	85.20	89.75	0.032	0.641	0.037
Serine	974.30	1089.90	1135.00	883.20	861.10	831.20	1066.44^{a}	858.50^{b}	928.75	975.50	983.10	0.218	0.628	0.0001
Threonine	206.30	216.50	235.20	233.90	205.80	201.80	219.33	213.83	220.10	211.15	218.50	0.033	0.703	0.555
Taurine	1142.30	1217.80	1116.33	1025.67	889.54	949.94	1158.06^{a}	953.46^{b}	1082.47	1040.75	1029.78	0.188	0.660	0.0002
Proline	620..70	700.00	693.10	467.30	458.80	447.20	671.27^{a}	457.77^{b}	544.00	579.40	570.15	0.434	0.658	<0.0001
Citrulline	17.90	15.50	15.00	13.60	10.80	11.80	16.13	12.07	15.75	13.15	13.40	0.960	0.574	0.073
Ornithine	482.80	435.28	440.41	291.55	280.00	283.13	452.37^{a}	284.86^{b}	375.18	349.11	353.12	0.856	0.498	<0.0001
Isoleucine	268.50	278.20	264.20	218.90	220.10	222.80	270.30^{a}	220.60^{b}	243.70	249.15	243.50	0.766	0.854	<0.0001
Leucine	503.80	484.10	479.40	494.30	475.00	464.20	489.10	477.83	499.05	479.55	471.80	0.983	0.320	0.456
Hydroxyproline	74.20^{ac}	87.20^{ab}	98.90^{b}	73.50^{ac}	67.00^{c}	70.60^{ac}	86.77^{a}	70.37^{b}	73.85^{a}	77.10^{ab}	84.75^{b}	0.008	0.042	<0.0001
Total	18174	19945	20873	18009	17235	16983	19664^{a}	17409^{b}	18092	18590	18928	0.025	0.461	0.0002

*Unit is nmol/g liver.

†Statistical significance is calculated by the PROC MIXED procedure of SAS.

^{a,b,c}Within groups, treatments or diets, the values of individual AAs with different letter labels are statistically different ($P < 0.05$).

Table 2.7. Effects on HS and Zn supplementation on hepatic, cecal, fecal, and urinary metabolomes*.

	Markers of HS	Markers of Zn supplementation
AAs & associated metabolites	**Increased by HS**: Creatinine^{U}, Lys$^{L, F}$, Cit^{F}, Orn^{F} **Decreased by HS**: Ala^{L}, Tyr^{L}, Val^{L}, His^{L}, Asp^{L}, Glu^{L}, Met^{L}, Ser^{L}, Tau^{L}, Pro^{L}, Orn^{L}, Ile^{L}, Hyp^{L}, Kynurenic acid^{U}	Lys^{L} (ZnIO > ZnAA, ZnIO > ZnNeg), Lys^{F} (ZnIO-HS > ZnAA-HS > ZnNeg-HS)†
Phospholipids	**Increased by HS**: PE(16:0/18:2)^{L}, PC(16:0/16:0)^{L}, PC(16:0/18:2)^{L}, PC(18:2/18:0)^{L}, PC(18:0/20:3)^{L}, PC(18:0/20:2)^{L}, PC(18:0/22:6)^{L} **Decreased by HS**: PC(15:0/18:2)^{L}, PC(15:0/18:1)^{L}, PC(17:0/18:2)^{L}, PC(17:0/18:1)^{L}, PE(18:1/18:0)^{L}, PE(18:1/20:4)^{L}, PC(18:1/20:4)^{L}, PC(18:0/22:3)^{L}, LysoPE(16:0)^{F}, LysoPC(16:0)^{F}, LysoPC(18:2)^{F}	PC(18:0/22:3)^{L} (ZnIO < ZnNeg), PC(16:0/18:2)^{L} (ZnIO-HS > ZnNeg-HS)†
Microbial metabolites	**Increased by HS**: Suberic acid^{F}, Sebacic acid^{F}, Hyodeoxycholic acid^{C}, Deoxycholic acid^{C}, Inosine^{C}, Acetic acid^{C}, Stercobilin$^{C, F}$ **Decreased by HS**: Oleic acid^{F}, Linoleic acid$^{C, F}$, Oleamide^{C}, Xanthine^{C}, 2,8-Dihydroxyquinoline^{F}	Acetic acid^{C} (ZnIO > ZnAA, ZnIO > ZnNeg), Propionic acid^{C} (ZnIO > ZnNeg), Butyric acid^{C} (ZnIO > ZnAA, ZnIO > ZnNeg)

*Enlisted metabolites are the ones that were significantly affected by HS or Zn supplementation and also had their structures identified by either authentic standards or MSMS fragmentograms. The distribution of these markers in liver, cecum, feces or urine was indicated by the superscripts "L", "C", "F", "U", respectively.

PE, phosphatidylethanolamine; PC, phosphatidylcholines; LysoPE, lysophosphatidylethanolamine; LysoPC, lysophosphatidylcholine.

$^{\dagger}P < 0.05$ from the PROC GLM procedure of SAS on the data of HS group.

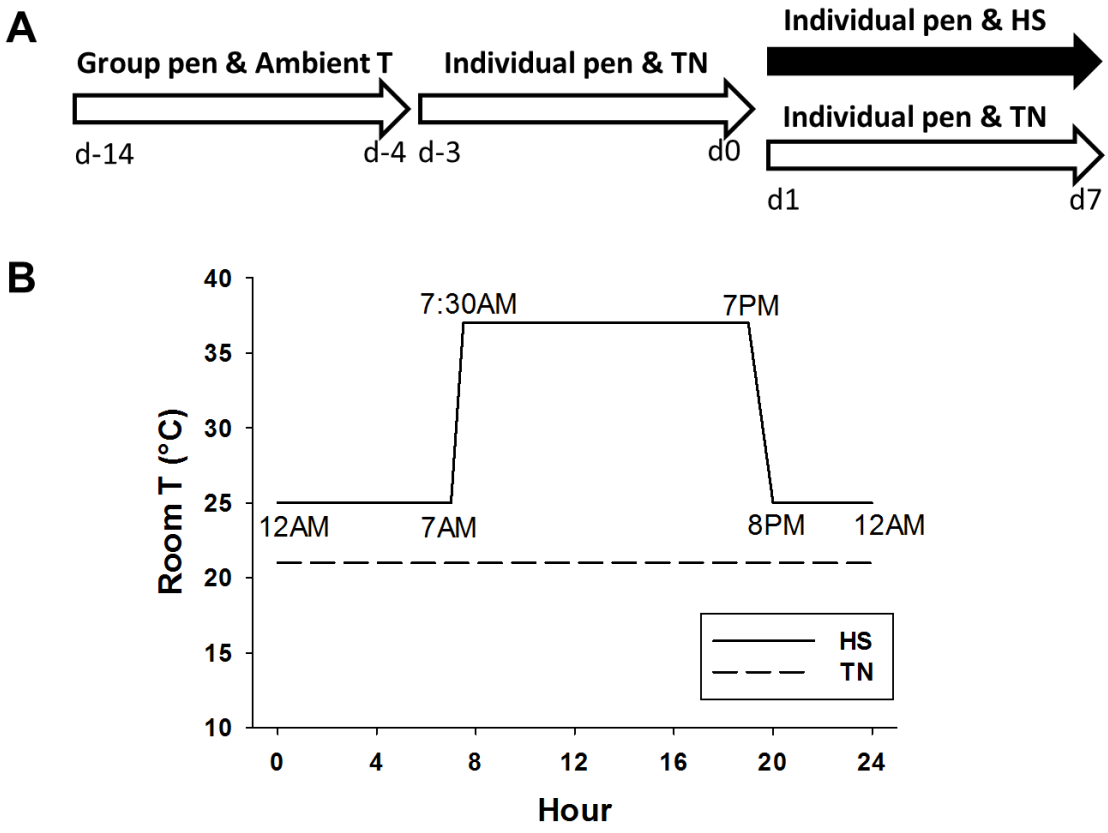

Figure 2.1. Experiment design. ***A.*** Timeline of 21-day feeding experiment. Pigs had ad libitum access to water and diet and were fed with one of assigned diets (ZnNeg, ZnIO, or ZnAA) through entire feeding experiment. ***B.*** Designed daily temperature settings in TN and HS treatments.

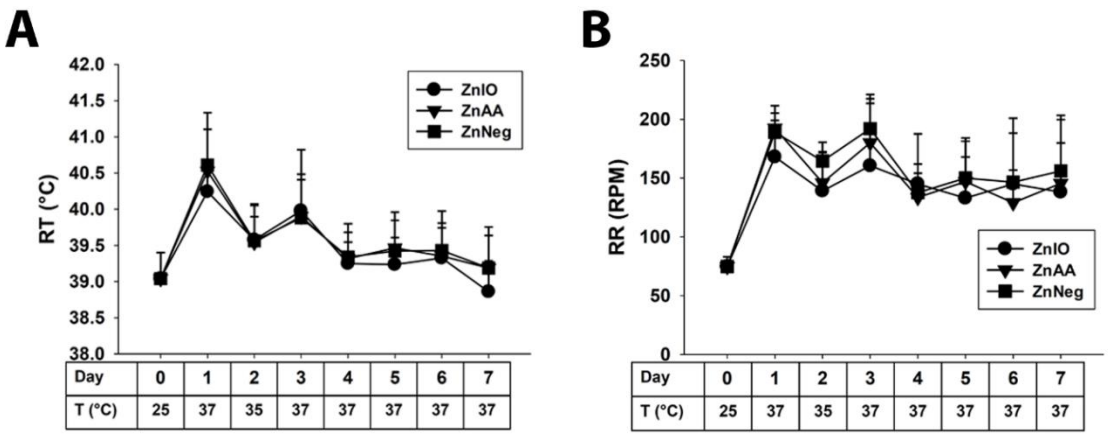

Figure 2.2. Effects of HS and Zn supplementation on physiological parameters of pigs. T is the room temperature when RT and RR were measured. ***A.*** Average RT of pigs after 2 h of HS. ***B.*** Average RR of pigs after 2 h of HS.

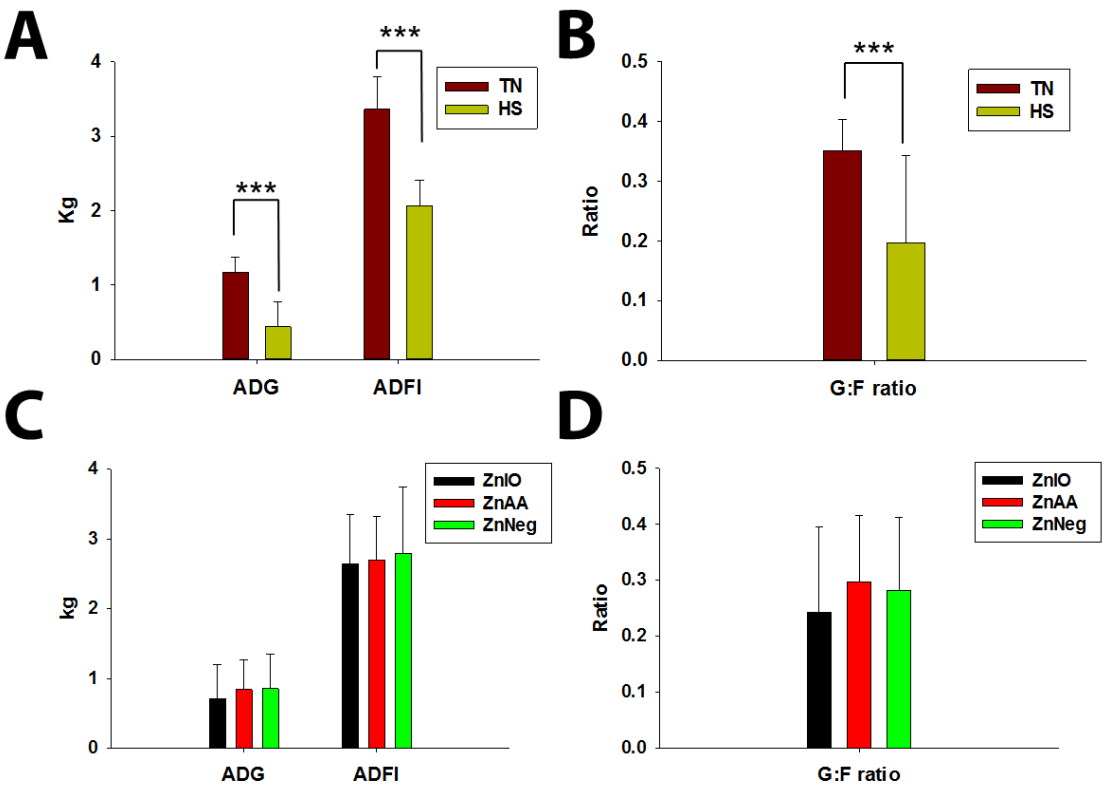

Figure 2.3. Effects of HS and Zn supplementation on growth performance of pigs. *A.* Effects of HS on ADG and ADFI. Significant differences are labeled as *** ($P < 0.001$). ***B.*** Effects of HS on G:F ratio. Significant differences are labeled as *** ($P < 0.001$). ***C.*** Effects of Zn supplementation on ADG and ADFI. ***D.*** Effects of Zn supplementation on G:F ratio.

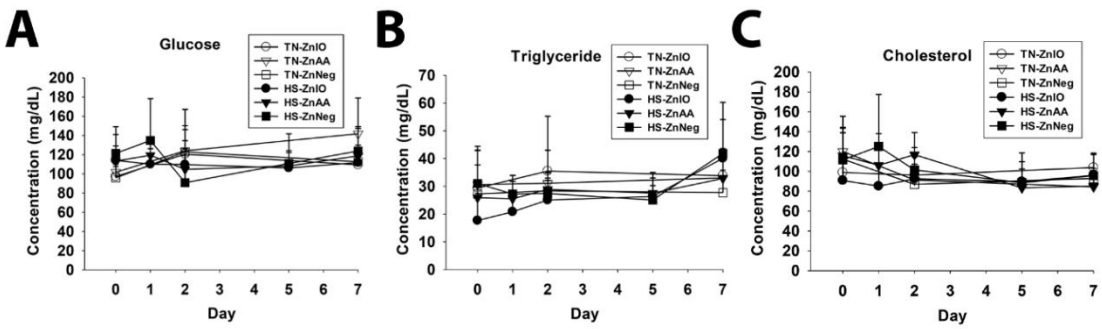

Figure 2.4. Effects of HS and Zn supplementation on serum level of glucose, cholesterol, and triglycerides of pigs. *A.* Serum glucose. ***B.*** Serum triglyceride. ***C.*** Serum cholesterol.

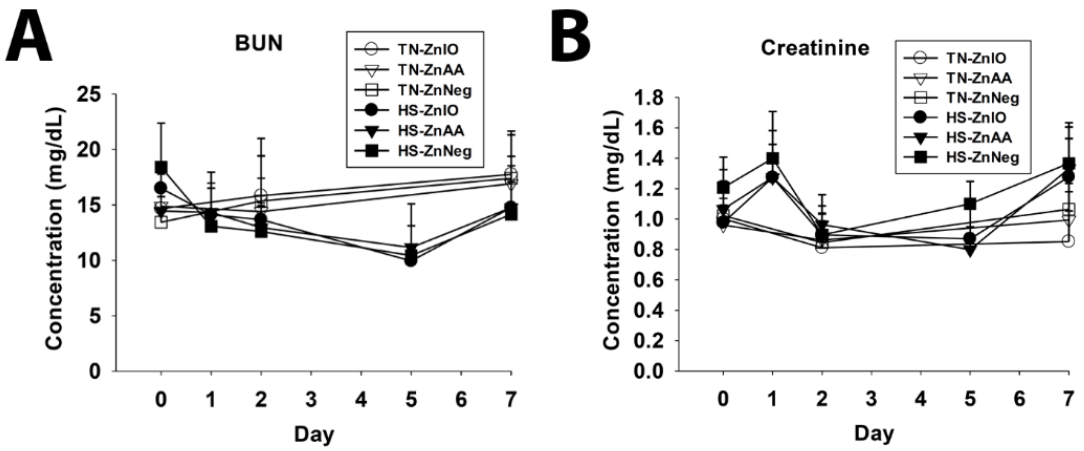

Figure 2.5. Effects of HS and Zn supplementation on serum level of creatinine and BUN of pigs. ***A.*** Serum BUN. ***B.*** Serum creatinine.

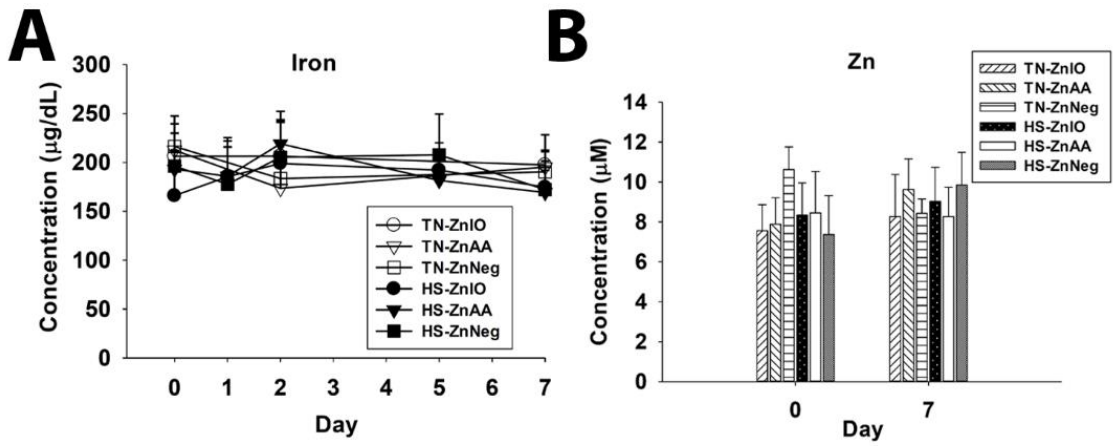

Figure 2.6. Effects of HS and Zn supplementation on serum level of iron and Zn of pigs. ***A.*** Serum iron. ***B.*** Serum Zn.

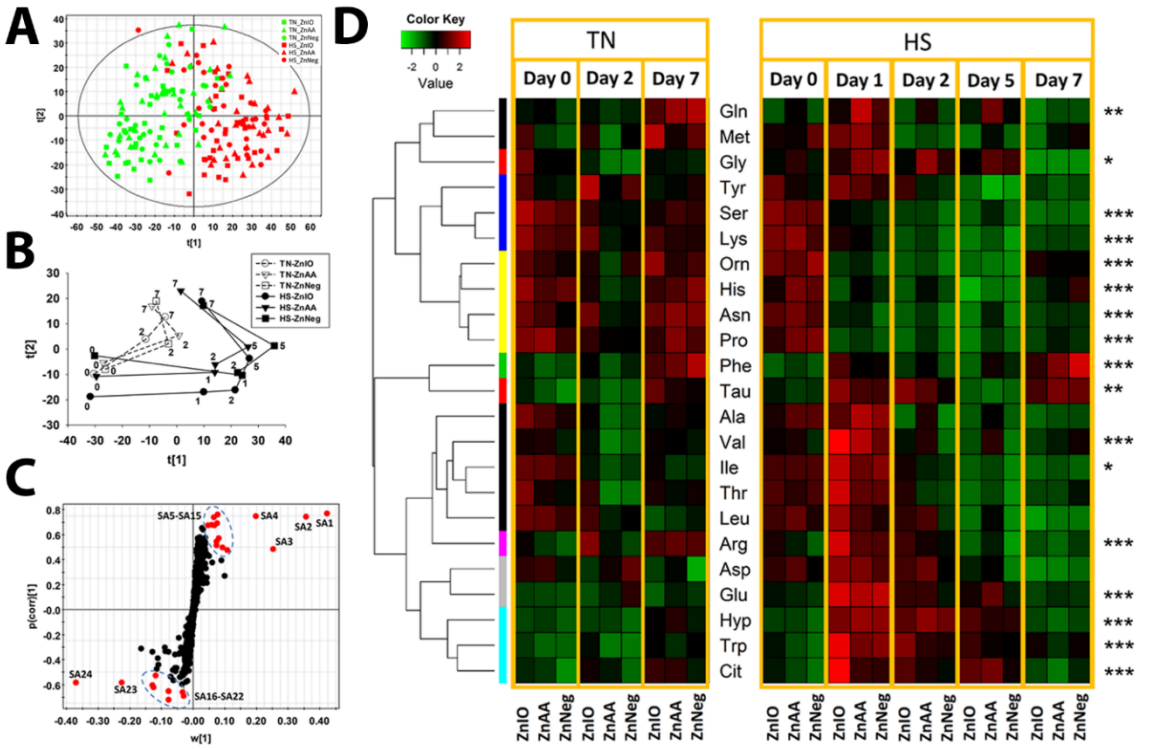

Figure 2.7. Metabolomics analysis of FAAs metabolites in serum samples. ***A.*** The scores plot from PCA analysis on serum metabolome. The t[1] and t[2] values represent the scores of each sample in the principal component 1 and 2, respectively. ***B.*** The scores plot from PCA analysis on serum metabolome. The t[1] and t[2] values of each sample group are the average scores of 8 samples in principal components 1 and 2, respectively. The numbers of days of each sample group under HS are labeled. ***C.*** The S-loadings plot on the ions contributing to the separation of HS and TN samples in an OPLS-DA model. Major contributing metabolites are labeled. ***D.*** The heat map on serum FAAs during 1-week HS and Zn supplementation. FAAs were grouped by HCA. Concentration of each AA at different time points and in different sample groups were compared by its Z scores and are presented according to inlaid color keys. Significant differences are labeled as * ($P < 0.05$), ** ($P < 0.01$), and *** ($P < 0.001$) when compare day 0 to day 1 within HS group using student's t-test.

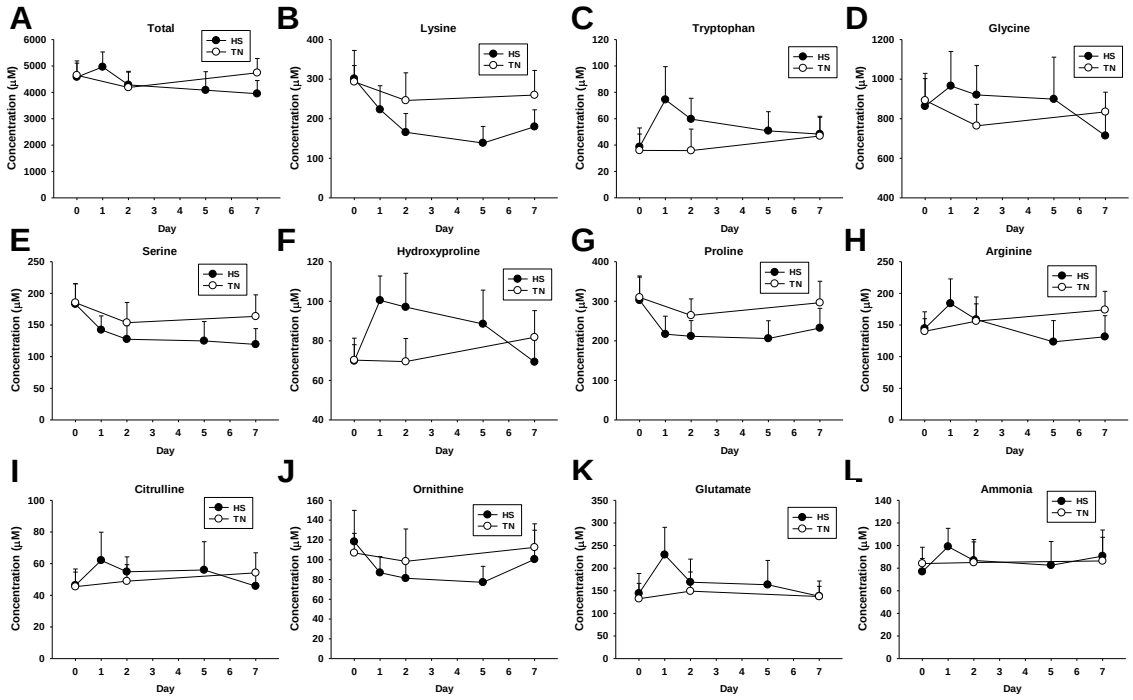

Figure 2.8. The concentrations of total, individual AAs, and ammonia in HS and TN groups. ***A.*** Total AAs. ***B.*** Lysine. ***C.*** Tryptophan. ***D.*** Glycine. ***E.*** Serine. ***F.*** Hydroxyproline. ***G.*** Proline. ***H.*** Arginine. ***I.*** Citrulline. ***J.*** Ornithine. ***K.*** Glutamate. ***L.*** Ammonia.

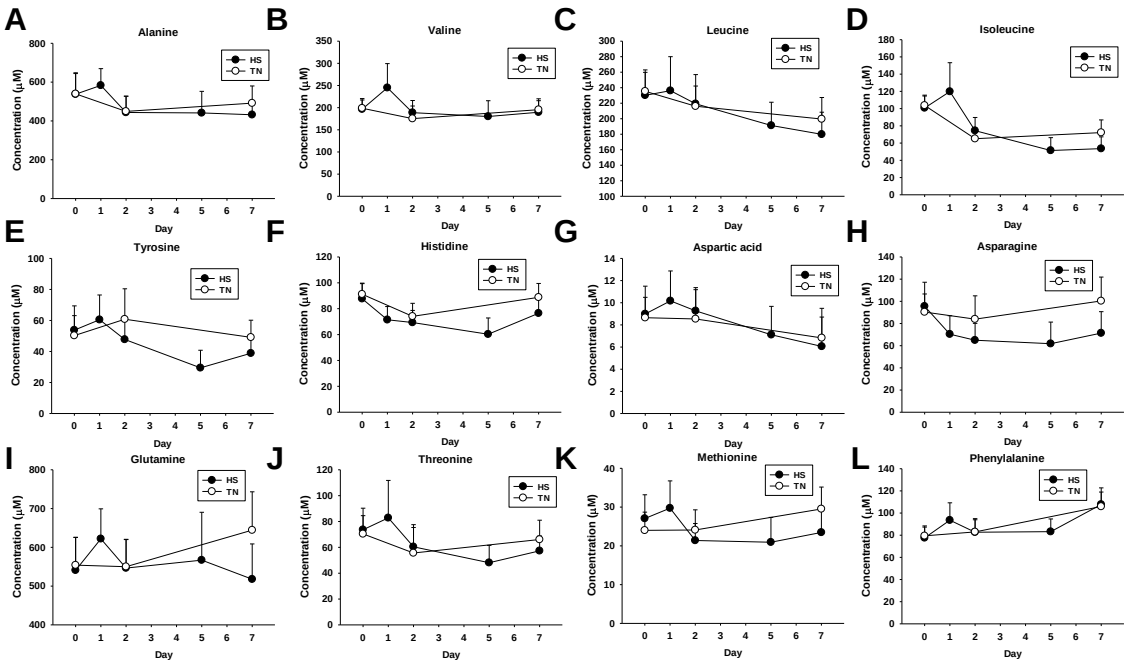

Figure 2.9. The concentrations of individual AAs in HS and TN groups. ***A.*** Alanine. ***B.*** Valine. ***C.*** Leucine. ***D.*** Isoleucine. ***E.*** Tyrosine. ***F.*** Histidine. ***G.*** Aspartic acid. ***H.*** Asparagine. ***I.*** Glutamine. ***J.*** Threonine. ***K.*** Methionine. ***L.*** Phenylalanine.

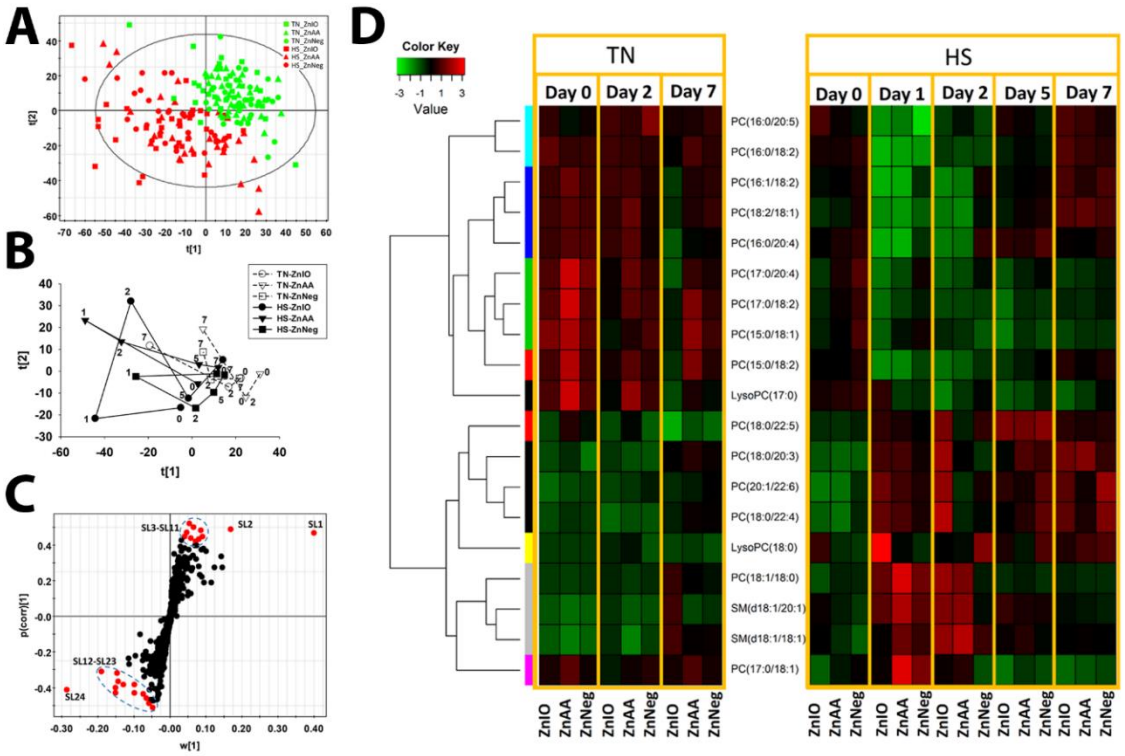

Figure 2.10. Metabolomics analysis of lipids metabolites in serum samples. ***A.*** The scores plot from PCA analysis on serum metabolome. The t[1] and t[2] values represent the scores of each sample in the principal component 1 and 2, respectively. ***B.*** The scores plot from PCA analysis on serum metabolome. The t[1] and t[2] values of each sample group are the average scores of 8 samples in principal components 1 and 2, respectively. The numbers of days of each sample group under HS are labeled. ***C.*** The S-loadings plot on the metabolites contributing to the separation of HS and TN samples in an OPLS-DA model. Major contributing lipid species are labeled. ***D.*** The heat map on lipid species during 1-week HS and Zn supplementation. Lipid species were grouped by HCA. Relative abundance of each lipid at different time points and in different sample groups were compared by its Z scores and are presented according to inlaid color keys.

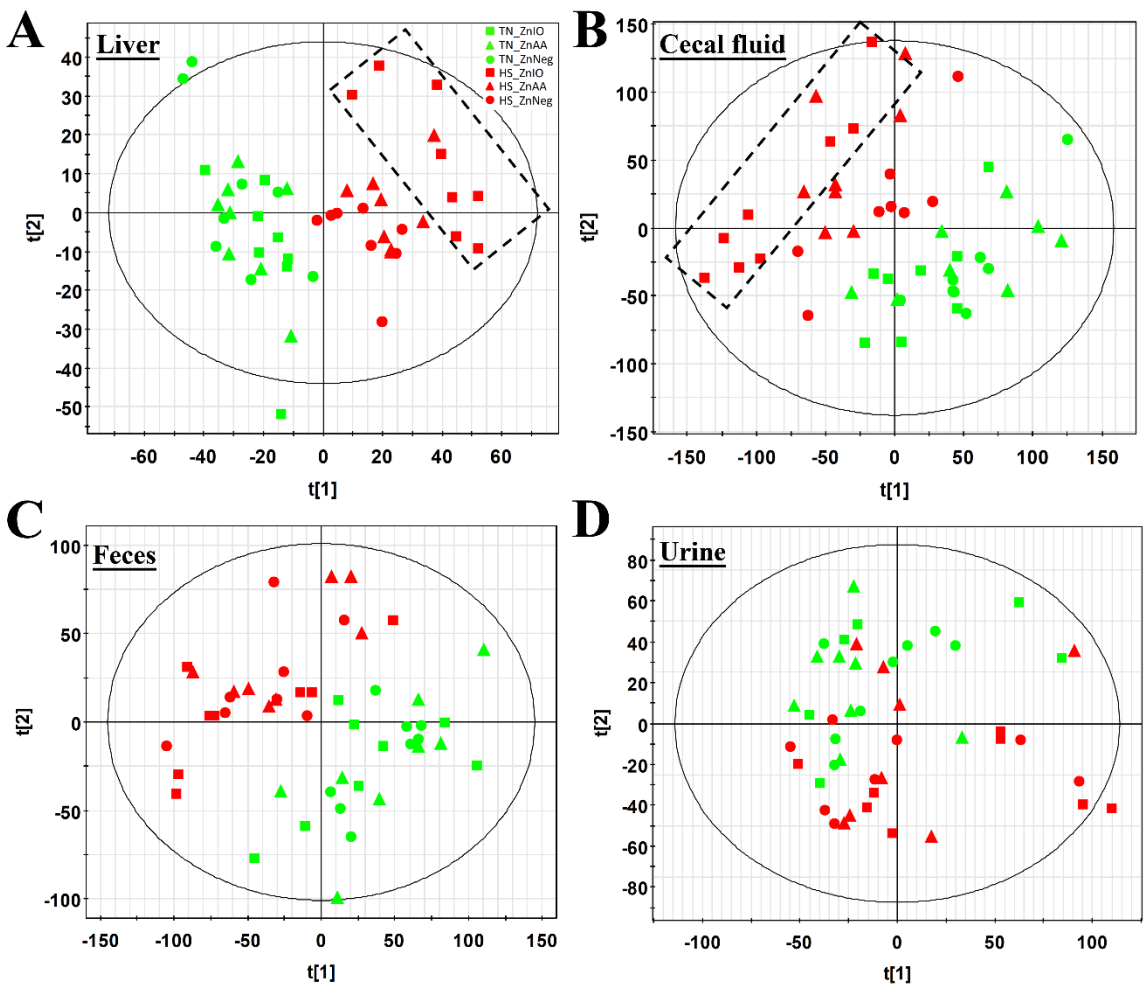

Figure 2.11. LC-MS-based metabolomic analysis of hepatic extract, cecal fluid, feces extract, and urine samples from pigs under HS and Zn supplementation. ***A.*** Scores plot of a PCA model on hepatic extracts. The distribution of HS-ZnIO samples in the model is illustrated by a rectangle. ***B.*** Scores plot of a PCA model on cecal fluid samples. The distribution of HS-ZnIO samples in the model is illustrated by a rectangle. ***C.*** Scores plot of a PCA model on feces extract samples. ***D.*** Scores plot of a PCA model on urine samples.

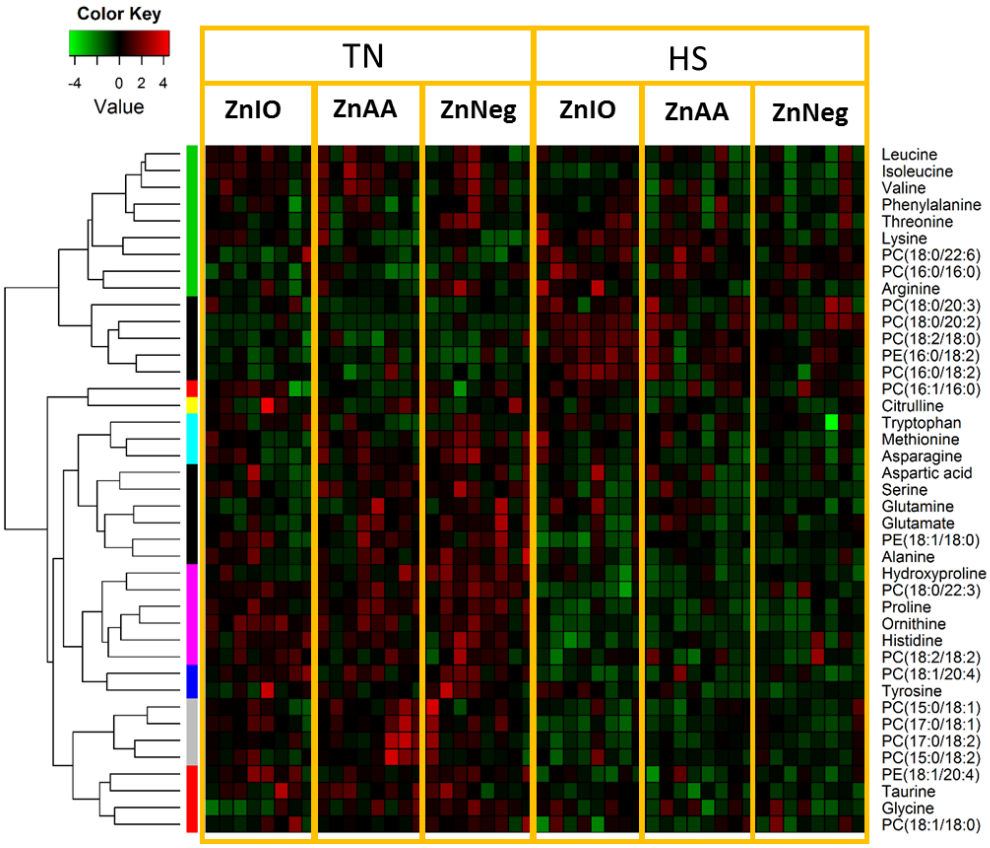

Figure 2.12. Metabolite markers from metabolomic analysis of hepatic extracts. In the heat map, the concentrations of FAAs and relative abundances of phospholipids in the liver are converted to the Z scores and presented according to inlaid color keys. All enlisted metabolites have been confirmed by authentic standards or MSMS fragmentation.

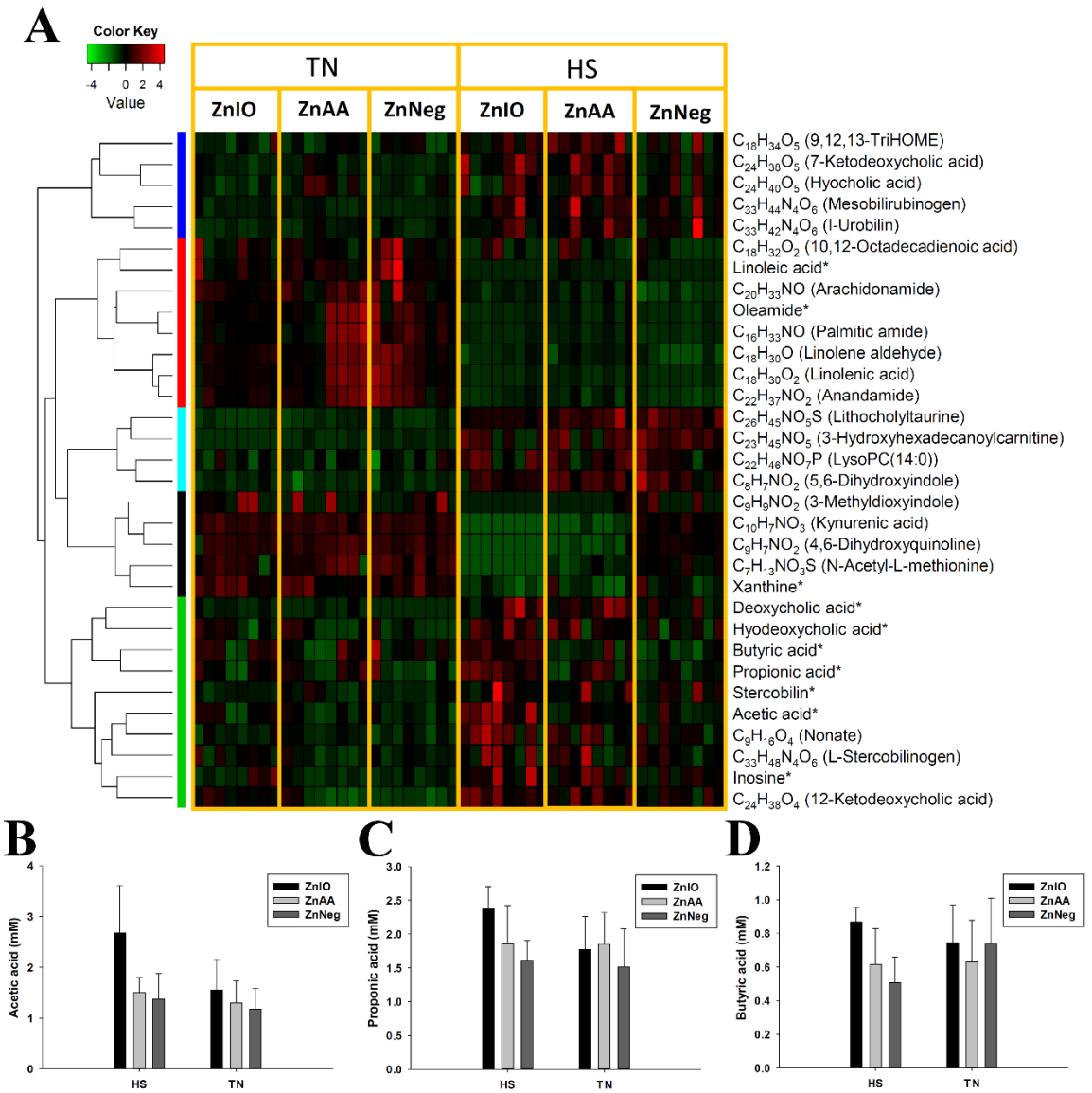

Figure 2.13. Metabolite markers of HS and Zn supplementation from metabolomic analysis of cecal fluid. The markers labeled with * were confirmed with authentic standards. Putative identities of other markers were based on database search. ***A.*** The heat map of cecal metabolite markers. The metabolites are grouped by HCA. Relative abundances of each metabolite across sample groups are converted to the Z scores and presented in the heat map according to inlaid color keys. ***B.*** The concentration of acetic acid in cecal fluid. ***C.*** The concentration of propionic acid in cecal fluid. ***D.*** The concentration of butyric acid in cecal fluid.

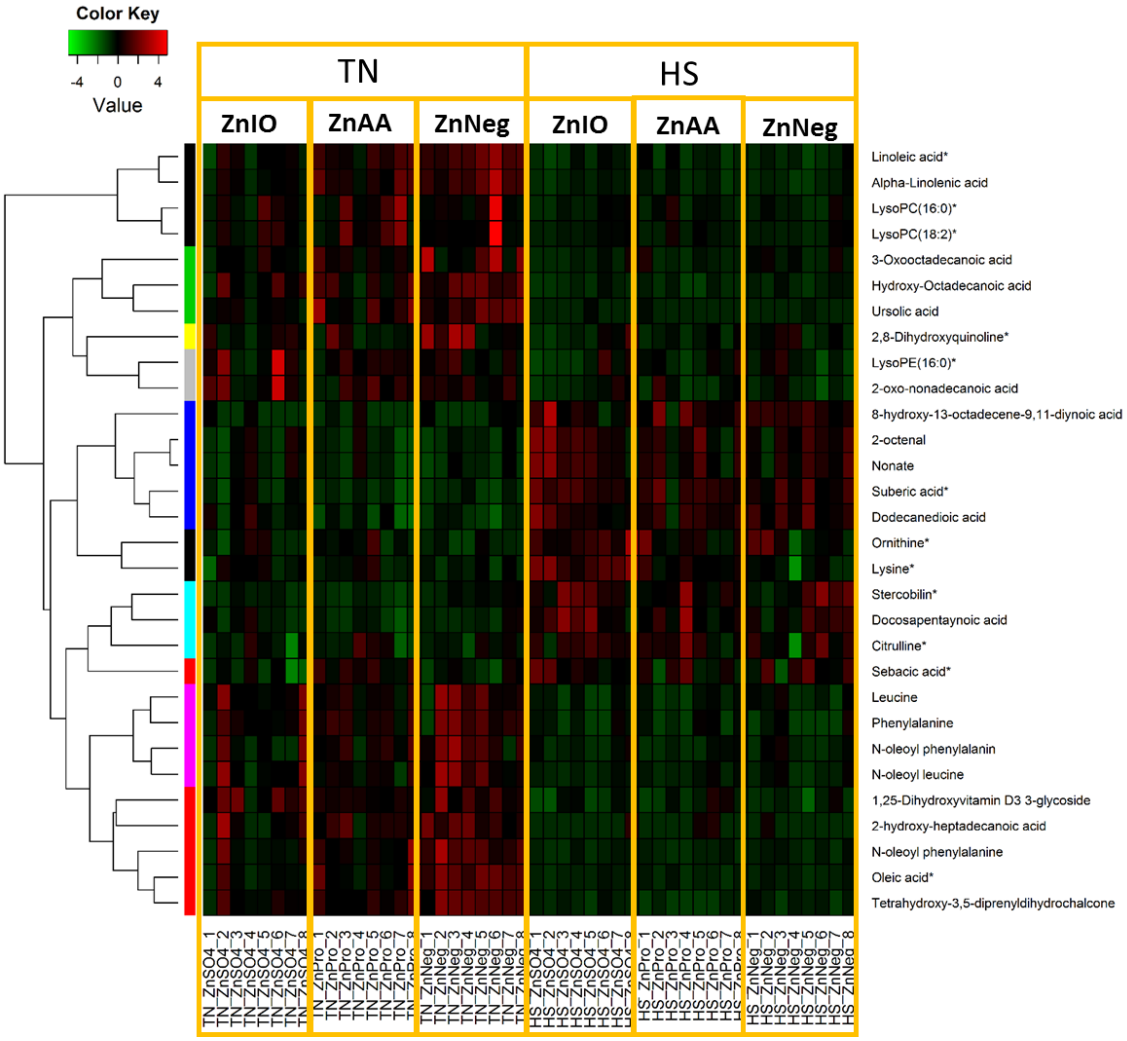

Figure 2.14. Metabolite markers in feces samples. The identities of markers with * were confirmed with authentic standards, while the others were acquired from HMDB and KEGG database.

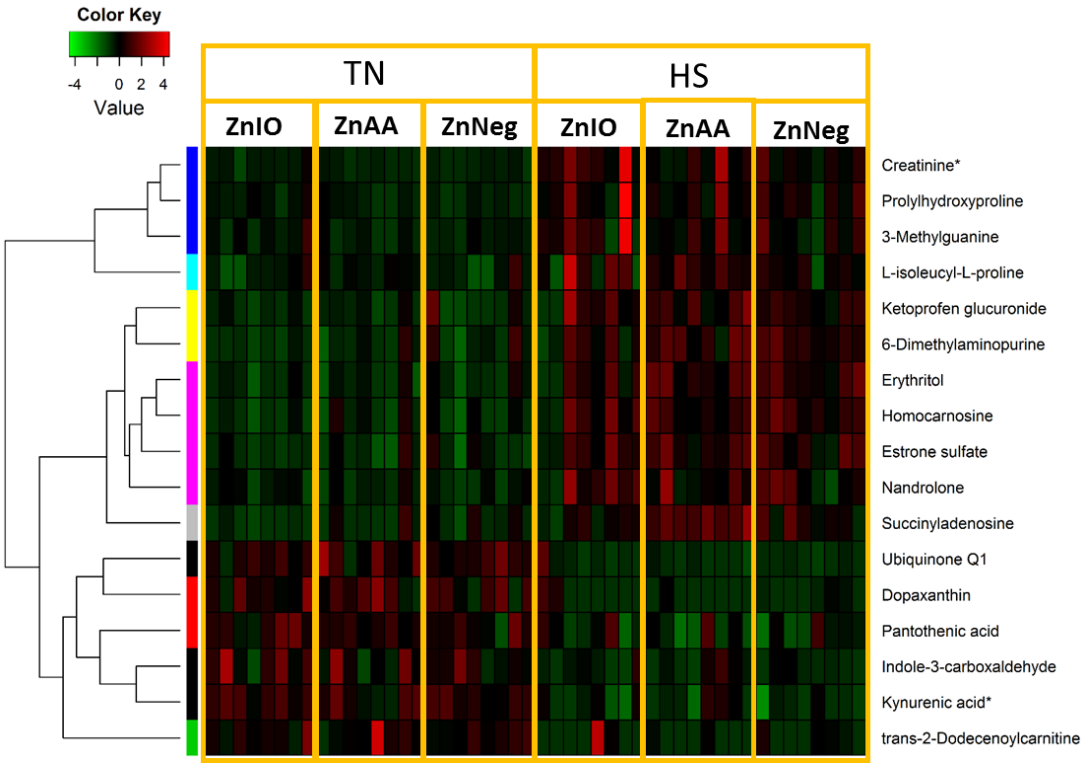

Figure 2.15. Metabolomics analysis of urine samples. The heat map on markers in urine after 1-week HS and Zn supplementation. The identities of markers with * were confirmed with authentic standards, while the others were acquired from HMDB and KEGG database.

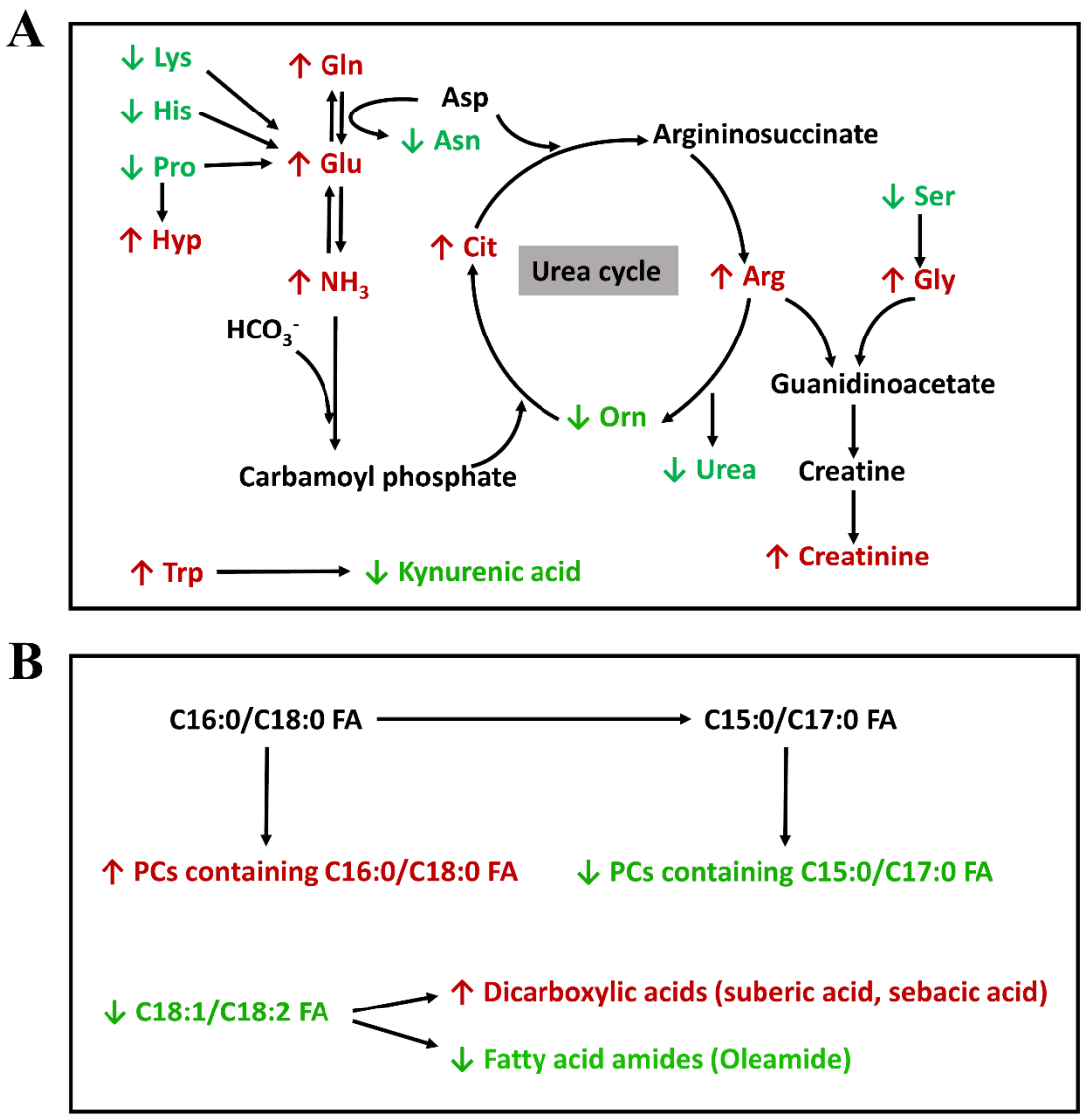

Figure 2.16. Summary of major HS-induced metabolic changes. ***A.*** HS-induced changes in the metabolites related to nitrogen and amino acid metabolism. ***B.*** HS-induced changes in fatty acids and phospholipids.

CHAPTER 3. IDENTIFICATION OF NOVEL LIPID OXIDATION MARKERS THROUGH LC-MS BASED CHEMOMETRIC PROFILING OF FRYING OILS

Part of this chapter is modified from the manuscript:
Wang, L.; Csallany, A. S.; Kerr, B. J.; Shurson, G. C.; Chen, C. Kinetics of forming aldehydes in frying oils and their distribution in French fries revealed by LC-MS-based chemometrics. *Journal of Agricultural and Food Chemistry.* 2016, *64*, 3881–3889.

3.1 SUMMARY

Deep-fat frying is a simple process in practice, but yields a complex mixture of chemicals with diverse physical, biological, and sensory properties in thermally-stressed cooking oils. Although the routes and reactions that generate reactive and bioactive species in this process have been extensively investigated, the sequences and kinetics of their formation remain poorly defined since traditional targeted analysis platforms lack the capacity to simultaneously define and monitor many changes induced by thermal stress. In this study, a platform combining customized sample preparations, high-resolution liquid chromatography-mass spectrometry (LC-MS) analysis, PCA, and HCA, was applied to compare the chemical profiles of multiple French fry oil extracts and to characterize the kinetics of degrading triacylglycerols (TAGs) and forming lipid oxidation products (LOPs) in heated soybean oil. Through the PCA modeling of LC-MS data, the likely sources of frying oils used in preparing fast food French fries were revealed, and thermal stress-induced changes in HSO were modeled. With LC-MS-based structural elucidation and quantification, this platform identified the acylglycerol, polar compound, and aldehyde markers of thermal stress and then characterized their distinctive kinetic profiles. Analyzing the clustering patterns of these markers in the HCA heat map further indicated that distinctive oxidation and degradation of individual fatty acids occurred at different stages of prolonged thermal stress. Overall, this LC-MS-based chemometrics platform has advantages over many traditional evaluation methods for its capacity to conduct both comprehensive profiling as well as specific characterization of frying oils.

KEYWORDS: TAGs, aldehydes, chemometrics, LC-MS, frying oil, French fries

ABBREVIATIONS: CSO, control soybean oil; DAGs, diacylglycerols; FA, fatty acid; HCA, hierarchical clustering analysis; HCAO, heated canola oil; HCO, heated corn oil; 13(*S*)-HODE, 13(*S*)-hydroxy-octadecadienoic acid; HPLC, high performance liquid chromatography; HQ, 2-hydrazinoquinoline; HSO, heated soybean oil; LC-MS, liquid chromatography-mass spectrometry; LOPs, lipid oxidation products; m/z, mass to charge ratio; PCA, principal components analysis; PV, peroxide value; PUFAs, polyunsaturated fatty acids; QTOF, quadrupole time of flight mass spectrometry; SIC, single ion counts; TAGs, triacylglycerols; TBARS, thiobarbituric acid reactive substance; TIC, total ion counts; TOTOX, total oxidation; UPLC, ultra-performance liquid chromatography.

3.2 INTRODUCTION

During deep frying of foods, thermal stress can extensively transform the chemical composition of frying oils, especially polyunsaturated fatty acids (PUFAs)-enriched vegetable oils, and alter their nutritional value and toxicological profile[62, 216]. Diverse reactions and chemical events, such as hydrolysis, radical formation, peroxidation, cyclization, polymerization, and homolytic and heterolytic cleavage occur in this process to convert triacylglycerols in frying oils to free fatty acids, mono- and di-acylglycerols, hydroperoxide primary lipid oxidation products (LOPs), and diverse secondary LOPs, such as cyclic fatty acids, polymeric products, aldehydes, ketones, alcohols, dienes, and acids[217]. Among these LOPs, aldehydes, due to their reactivity with proteins and DNA, have been defined as major contributors to the adverse effects induced by heated frying oils in animal and cell-based toxicity studies[100, 101]. Besides their bioreactivity, many aldehyde species possess organoleptic properties, contributing to the flavor of fried foods[218, 219].

Based on extensive research on the chemical components and properties of frying oils, diverse chemical assays have been developed and established to characterize frying oils[116]. Among these assays, iodine value, active oxygen method (AOM), and oxygen stability index (OSI) assays, predict the stability of unprocessed frying oils and their susceptibility to stresses by measuring the unsaturation level of frying oils or the production of peroxides and volatile compounds under the designated conditions[117, 118]. However, the majority of these assays determine the status of processed frying oils by measuring the end products of hydrolysis and oxidation reactions, such as free acid

content, peroxide value (PV), anisidine value (AnV), total oxidation (TOTOX) value, thiobarbituric acid reactive substance (TBARS), hexanal and 2,4-decadienal levels[118, 119].

Despite the availability of a large selection of analytical methods for defining the status and susceptibility of frying oils, the global profile of thermally-stressed frying oils and the kinetics of thermal stress-induced changes remains to be largely undefined. This is mainly due to two facts: (1) all established analytical methods only measure a fraction of frying oils and do not cover the chemical diversity of frying oils; (2) under thermal stress, the composition and status of frying oils are not stable. In addition, the correlations between the levels of individual triacylglycerols (TAGs), primary and secondary LOPs changes in frying oils and fried foods are also generally undefined.

In the study herein, a platform combining chemical derivatization, high-resolution liquid chromatography-mass spectrometry (LC-MS) analysis, and multivariate chemometric analysis was adopted to characterize the kinetics of TAGs, primary and secondary LOPs changes in vegetable oils heated at frying temperature and their distribution in French fries. The values of specific TAGs, polar compounds, aldehydes and aldehyde clusters as the markers of thermal stress and oxidative degradation were evaluated based on their kinetic profiles and distribution.

3.3 MATERIALS AND METHODS

3.3.1 Vegetable oils and Chemicals

Refined soybean, corn, and canola oils were purchased from local grocery stores (St. Paul, MN). Ammonium formate were purchased from Alfa Aesar (Ward Hill, MA). LC-MS-grade water, isopropanaol, and acetonitrile were purchased from Fisher Scientific

(Houston, TX). Dichloromethane were purchased from EMD Millipore (Billerica, MA). n-butanol was purchased from Sigma (St. Louis, MO). Hexanal, triphenylphosphine (TPP), and 2-hydrazinoquinoline (HQ) from Alfa Aesar (Ward Hill, MA); 2,2′-dipyridyl disulfide (DPDS) from MP Biomedicals (Santa Ana, CA); and LC-MS-grade water and acetonitrile from Fisher Scientific (Houston, TX). Aldehyde standards, including 2,4-decadienal, 2-undecenal, 2-decenal, 2,4-undecadienal, 2-octenal, pentanal, 2,4-heptadienal, and 2-heptenal were acquired from Bedoukian Research (Danbury, CT); acrolein from Sigma-Aldrich (St. Louis, MO); and 4-hydroxynonenal (4-HNE) from Cayman Chemical (Ann Arbor, MI).

3.3.2 Preparation of frying oil samples

Soybean oil (300 mL) was placed in a 500 mL round-bottom glass flask and then heated in an electric heating mantle with power controller. The temperature of soybean oil was gradually increased from room temperature (22^{o}C) to 185^{o}C in approximately 1 h with bubbling air (50 mL/min). Heated soybean oil (HSO) samples were collected at 45^{o}C, 65^{o}C, 85^{o}C, 105^{o}C, 125^{o}C, 145^{o}C, 165^{o}C, and 185^{o}C. Afterwards, the temperature was held constant at 185^{o}C for 6 h with samples collected at 5 min, 15 min, 30 min, 1 h, 2 h, 4 h, and 6 h of heating (Figure 3.1A,B). Corn and canola oils were heated by the same procedure, but sampled only at 0 min, 30 min, and 6 h of heating at 185^{o}C. Control soybean oil (CSO) was stored at room temperature (22^{o}C).

3.3.3 Oil extraction from French fries

Ten French fry samples were purchased separately from five brands of fast food restaurants (abbreviated as A, B, K, M, W) in St. Paul, Minnesota, representing two

samples from each brand. The oil contents in minced French fries were extracted twice by 2 volumes of dichloromethane (v/w). The extracts were filtered through a column packed with anhydrous sodium sulfate to remove water and insolubles. After evaporating the solvent by nitrogen, the samples were stored at -80^{o}C prior to further analysis.

3.3.4 Measurement of PV

The PV of oil samples were determined by a modified colorimetric assay[220]. Briefly, 10 µL of 20 mM $FeCl_2$ solution (in 200 mM HCl) and 1 µL of oil sample were added into 100 µL of 1 mM xylenol orange solution (in a 1:1 butanol-methanol mixture) in a 96-well plate. After 10 min of shaking and incubation at room temperature, the absorbance of reaction mix was measured at 560 nm using a Molecular Devices SpectraMax 250 microplate reader (Sunnyvale, CA). The standard curve was prepared with $FeCl_3$ with a linear range from 1 to 20 µg/mL.

3.3.5 Measurement of TBARS value

The TBARS values of oil samples were measured using a modified method[221]. Briefly, 20 µL of oil sample or malondialdehyde standard was added to 200 µL of a solution containing 15% w/v trichloroacetic acid, 0.375% w/v thiobarbituric acid, and 0.25 M HCl in a 2 mL screw-top tube, and then heated at 100^{o}C for 30 min. After cooling on ice, the reaction mixture was then centrifuged at 3,000 × *g* for 5 min. The aqueous phase was transferred to a 96-well plate and measured at 535 nm using a Molecular Devices SpectraMax 250 microplate reader. The TBARS values were calculated using a multivariate data analysis standard curve ranging from 2.5 to 200 µM.

3.3.6 LC-MS analysis of acylglycerols

Neutral lipid contents in vegetable oils and French fry oil extracts were examined by LC-MS analysis of their ammonium adducts[222]. Both oils and oil extracts were firstly dissolved in n-butanol by 10,000 × dilution, and then transferred to HPLC vials. Five µL of sample was injected into a Waters Acquity UPLC system (Milford, MA) and then separated by a BEH C18 column (Waters) using a gradient of mobile phase (A1: 40% aqueous acetonitrile containing 10 mM ammonium formate and 0.1 % formic acid; B1: isopropanol:acetonitrile = 9:1, v:v, containing 10 mM ammonium formate and 0.1 % formic acid) at 60°C over a 10-min run. The LC eluant was introduced into a Xevo-G2-S system for ionization and MS scan. Capillary voltage and cone voltage for electrospray ionization was maintained at 3 kV and 30 V for positive mode detection, respectively. Source temperature and desolvation temperature were set at 120 °C and 350 °C, respectively[150]. Nitrogen was used as both cone gas (50 liters/h) and desolvation gas (600 liters/h) and argon as collision gas. For accurate mass measurement, the mass spectrometer was calibrated with sodium formate solution (range *m/z* 50–1500) and monitored by the intermittent injection of the lock mass leucine enkephalin ($[M + H]^+$ = 556.2771 *m/z.* Mass chromatograms and mass spectral data were acquired and processed by MassLynx^{TM} software (Waters) in centroided format. Additional structural information was obtained by tandem MS (MS/MS) fragmentation with collision energies ranging from 15 to 60 eV.

3.3.7 LC-MS analysis of polar contents of oil samples

The polar contents of oil samples were extracted using isopropanol[223]. Briefly, 100 µL of oil sample was mixed with 100 µL of extract solution (90% isopropanal in water).

After vortex, the mixture was centrifuged at 18,000 × g for 10 min. The supernatant was 5 times diluted in isopropanol before introduced into UPLC-Xevo-G2-S-MS system for analysis. The sample was separated by a BEH C18 column (Waters) using a gradient of mobile phase (A2: H_2O containing 10 mM ammonium acetate, *p*H = 9; B2: H_2O:acetonitrile = 5:95, v:v, containing 10 mM ammonium acetate, *p*H = 9). The MS analysis was conducted in negative mode with capillary voltage and cone voltage set at -3 kV and -30 V, respectively.

3.3.8 LC-MS analysis of aldehydes in oil samples

Prior to the LC-MS analysis, aldehydes in oil samples were first derivatized by HQ using a modified method[192]. Briefly, 4 µL of oil sample was added into a 200 µL of freshly-prepared acetonitrile solution containing 1 mM DPDS, 1 mM TPP, 1 mM HQ, and 100 µM acetone-d_6 (internal standard). The reaction mixture was incubated at 60°C for 30 min, chilled on ice, and then centrifuged at 18,000 × *g* for 10 min. A 100 µL of supernatant was mixed with 100 µL of ice-cold H_2O. After centrifugation at 18,000 × *g* for 10 min, the supernatant was transferred into a HPLC vial for LC-MS analysis. The sample was separated by a BEH C18 column (Waters) using a mobile phase (A3: H_2O containing 0.05 % acetic acid, v:v, and 2 mM ammonium acetate; B3: H_2O:acetonitrile=5:95, v:v, containing 0.05 % acetic acid, v:v, and 2 mM ammonium acetate). The MS analysis was conducted in positive mode. Quantitative analysis of secondary LOPs were determined by the integration of peak area and fitting with the standard curve using QuanLynx^{TM} software (Waters).

3.3.9 Structural analysis of interested compounds in oil samples

The chemical identities of interested compounds were determined by accurate mass measurement, elemental composition analysis, database search using MassTRIX search engine (http://masstrix3.helmholtz-muenchen.de/masstrix3/)[193], MS/MS fragmentation, and comparisons with authentic standards if available.

3.3.10 Chemometric analysis and data visualization

After data acquisition in the UPLC-QTOFMS system, the chromatographic and spectral data of samples were deconvoluted by MarkerLynx™ software (Waters). A multivariate data matrix containing information on sample identity, ion identity (retention time and *m*/*z*), and ion abundance was generated through centroiding, deisotoping, filtering, peak recognition and integration. The intensity of each ion was calculated by normalizing the single ion counts (SIC) *versus* the total ion counts (TIC) in the whole chromatogram. The data matrix was exported into SIMCA-P+™ software (Umetrics, Kinnelon, NJ) and transformed by *Pareto* scaling. PCA was then performed to model the data matrix and define the correlations among the samples. The compounds contributing to the sample separation in the model were identified in the loadings plot of the model. After Z score transformation, the relative abundance of identified compounds in samples were presented in heat maps generated by the R program (http://www.R-project.org), and correlations among these compounds were defined by HCA[224].

3.3.11 Statistics

The statistical significances among frying oils were analyzed by one-way ANOVA and Tukey's multiple comparison tests using PROC GLM procedure of SAS version 9.1 (SAS Institute, Cary, NC). A P value of < 0.05 was considered as statistically significant.

3.4 RESULTS

3.4.1 Determining the composition and likely sources of frying oils in fast food French Fries through LC-MS-based chemometric analysis of acylglycerols

To determine the acylglycerol composition of frying oils in fast food products and also to identify their likely sources, the oil extracts of ten French fries samples from the restaurants of five fast food chains were compared with retail samples of soybean, corn, and canola oil. The composition of acylglycerols in these oils and oil extracts were evaluated by the LC-MS analysis and chemometric modeling. Visual examination of base peaks in the chromatograms of three vegetable oil samples revealed clear differences among them (Figure 3.2). Furthermore, the variances in the chromatograms of oil extracts suggested that diverse frying oils were used in the preparations of French fries (Figure 3.2). To clearly define the relationships among these samples, a three-component PCA model was constructed based on the LC-MS data (Figure 3.3). The sample distribution pattern in the scores plot showed the resemblances of K1, W1, B1 and B2 with soybean oil; the frying oils in K2, M1, M2, A1, A2, and W2 might originate from other sources or the mixtures of vegetable oils (Figure 3.3A). Individual diacylglyerols (DAGs) and TAGs contributing to the sample separation in the model (D1-D4 and T1-T16) were identified in the loadings plot (Figure 3.3B). The structural identities of these markers were elucidated by accurate mass measurement, elemental composition analysis, and analyzing the MSMS fragmentograms of ammonia adducts of DAGs and TAGs, in which the FA composition of individual acylglycerols were revealed by both the peaks from neutral loss of acyl groups and the fragment peaks of individual acyl groups (Table 3.1 and

Figure 3.4). For example, T2 (*m/z* = 896.7758) as TAG (18:2, 18:2, 18:2) on the sole presence of a fragment (*m/z*: 599.5085) caused by the neutral loss of linoleoyl group from the parent ion (Figure 3.4A), while the identity of T8 (*m/z* = 870.7574) as TAG (16:0, 18:3, 18:2) was partially based on its three fragments (*m/z*: 597.4886, 575.5043 and 573.4885) caused by respective neutral loss of palmitoyl, linoleoyl, and linolenoyl group from the parent ion in positive mode (Figure 3.4B). The relationships between these markers and all examined samples were further defined by clustering analysis and then visualized by a heat map, which covers the distribution of individual acylglycerol species as well as the hierarchical clustering of all examined samples (Figure 3.5). The taxonomical information revealed by the heat map on the oils and oil extracts (Figure 3.5) largely confirmed the conclusions from the PCA modeling (Figure 3.3A) on the likely sources of frying oils in French fries samples. In addition, the distribution of acylglycerol markers in the heat map (Figure 3.5) is also consistent with their distribution in the loadings plot (Figure 3.3B). The FA compositions of these markers are summarized as follows: (1) α-linolenic acid (18:3)-containing TAGs, including T1, T8, and T13, are more enriched in soybean oil, K1, and W1 samples; (2) oleic acid (18:1)- and eicosanoic acid-containing TAGs, including T4, T5, T14, and T16, are more enriched in canola oil, K2, M1 and M2 samples; (3) palmitic acid (16:0)-containing TAGs, including T9, T10, and T12, are more enriched in corn oil, B1 and B2; (4) DAGs are more enriched in A1, A2 and corn oil (Figure 3.5). Overall, these observations suggested that FA composition is not enough to reflect TAG composition in frying oils. LC-MS-based chemometrics are

effective in determining the neutral lipid profile of frying oils while PCA and HCA are effective to find latent markers.

3.4.2 LC-MS-based chemometric analysis of thermal stress-induced changes in TAG composition of soybean oil

Even though the likely sources of frying oils in French fries samples were effectively identified through the LC-MS-based chemometric comparisons of vegetable oils and French fries oil extracts, noticeable differences between individual oil extracts and their likely sources, such as K1 and W1 *versus* soybean oil, were also observed (Figure 3.3A and Figure 3.5). A plausible explanation is that thermal stress has been applied to the French fries samples but not to retail vegetable oil samples. Therefore, the LC-MS-based chemometric analysis was conducted to determine the impacts of thermal stress on the composition of TAGs in soybean oil by comparing CSO with K1, W1, and a series of heated soybean oil samples collected at the temperatures ranging from 25ºC to 185ºC or different time points after reaching 185ºC. The distribution of all examined samples in the scores plot of a PCA model indicated that the changes in TAG profile mainly occurred after 1 h of heating at 185ºC (Figure 3.6A). In addition, the proximity of W1 and K1 samples to HSO-6h samples in the model suggested that the frying oils in these two French fry samples might have been exposed to extended thermal stress (Figure 3.6A). Analyzing the TAGs in the loadings plot led to the identification of T1, T2, T6-T11 and T13 as the markers contributing to the sample separation in the model (Figure 3.6B). The distribution of these TAG markers were defined in a heat map (Figure 3.6C). Based on the FA composition of these markers, thermal stress-induced changes in TAGs

are summarized as follows: (1) the relative abundances of α-linolenic acid (18:3) containing TAGs, including T1, T2, and T8, while TAGs containing three linoleic acid (18:2), such as T13, are greatly reduced by the frying condition; (2) in contrast, the relative abundances of palmitic acid (16:0)-containing TAGs which were without α-linolenic acid, including T6, T7, T9, T10, and T11, are increased by the frying condition even though these TAGs also contain linoleic acid; (3) Major TAGs changes happened after 2 h of heating under 185°C. Similar TAG profiles between 6-h HSO and two French fries samples suggested that the designated experimental conditions could yield the samples that are comparable to the frying oils in human diet.

3.4.3 LC-MS-based chemometric analysis of thermal stress-induced production of polar compounds in soybean oil

Frying-induced hydrolysis and oxidation of TAGs yield polar compounds in cooking oils. The polar contents of CSO and HSO in this study were extracted by aqueous isopropanol and then examined by LC-MS analysis and PCA modeling. As shown in the scores plot of a PCA model, the samples were separated in a time-dependent pattern, showing: (1) the samples harvested from 45ºC to 165ºC remained close to the control (CSO); (2) the samples in the first hour of 185ºC heating mainly moved away from the control along the 2nd principal component; (3) the samples collected after 1 h of 185ºC heating were separated from the others mainly along the 1st principal component of the model (Figure 3.7A). This distribution pattern of oils samples in the PCA model suggested that different changes occurred in the early (within the 1st hour) and late periods of heating at the frying temperature. Subsequently, the compounds affected by

heating, which are also the ones contributing to the separation of samples in the PCA mode, were identified in the loading plot (Figure 3.7B, Table 3.2). The presence of free fatty acids in the polar fractions, including linoleic acid (P1), α-linolenic acid (P2), palmitic acid (P3), and oleic acid (P4), was confirmed by comparing with authentic standards (data not shown). Consistent to the expected susceptibility of PUFAs to thermal stress, the relative abundances of linoleic acid (P1) and α-linolenic acid (P2) decreased at 185ºC while the relative abundances of palmitic acid (P3) and oleic acid (P4) increased at the end of 6-h heating (Figure 3.7C-F). Together with palmitic acid (P1) and oleic acid (P2), four newly-formed keto- and hydroxy-fatty acids were also identified as the compounds contributing to the sample separation along the 1st principal component of the model (Figure 3.7B). Their structural identities as 13(S)-HODE (P5), 9-oxononanic acid (P6), hydroxy-octadecenoic acid (P7), and 13-oxo-9,11-tridecadienoic acid (P8) were based on elemental composition analysis, database search, MSMS fragmentation, comparisons with published MSMS fragmentograms, and examination of the products from lipoxygenase-catalyzed reactions on linoleic acid and α-linolenic acid (Figure 3.8A-D). Among them, the increase in hydroxy-octadecenoic acid (P7) and 13-oxo-9,11-tridecadienoic acid (P8) occurred more rapid within the first hour of heating at 185ºC than others (Figure 3.7I,J), while the increases in 13(S)-HODE (P5) and 9-oxononanic acid (P6) were stable during the heating (Figure 3.7G,H). Correspondingly, as the source of LOPs, α-linolenic acid and linoleic acid were found dramatically decrease, after 2h heating under 185ºC (Figure 3.7C,D). Moreover, a group of newly-formed compounds corresponding to the early changes in the heating (along the 2nd principal component of

the model) were also identified (Figure 3.7B), and their levels in the polar fraction peaked with in the first hour of heating at 185ºC but decreased dramatically afterwards (Figure 3.7K-N). However, the MS-based structural analyses were only able to offer some information on their elemental composition and functional groups, but did not yield more definite structures (data not shown). Since many of these newly-formed compounds are likely generated through the autooxidation reactions of hydroperoxides, the presence of linoleate and linolenate hydroperoxides (13-HPODE and HPOTrE) in the polar fractions was compared with their presence in the products formed by the lipoxygenase-catalyzed reactions on linoleic acid and α-linolenic acid. Even though both HPODE and HPOTrE were conveniently detected in the mixtures from lipoxygenase-catalyzed reactions on linoleic acid and α-linolenic acid, they were not detected in the polar factions of HSO samples (data not shown).

3.4.4 Lipid oxidation status in HSO based on kinetic changes of PV and TBARS concentrations

PV and TBARS value are two widely used indicators of the presence of primary and secondary LOPs in frying oils, respectively. In this study, soybean oil was sampled multiple times at different temperatures to determine changes in PV and TBARS values. The PV of soybean oil started to increase from 145ºC, peaked when heating temperature reached 185ºC, and then decreased rapidly thereafter (Figure 3.9A). This transient increase of PV in the early time points of heating is consistent with other PV profile results reported at various frying conditions[88, 225], suggesting that hydroperoxide primary LOPs are highly unstable within this temperature range. Compared to PV, the TBARS

value, which reflects the concentration of multivariate data analysis, a secondary LOP of PUFA, also increased at 145ºC and began to plateau within the first hour of heating at 185°C (Figure 3.9B). Overall, even though PV and TBARS values partially reflect heating-induced chemical changes in soybean oil, the transient increase of PV and the plateauing of TBARS value in their kinetic profiles do not allow an accurate assessment of the duration of thermal stress on frying oils or enable the establishment of dose-response relationships in toxicological evaluation of heated oils.

3.4.5 LC-MS-based chemometric analysis of thermal stress-induced production of aldehydes in soybean oil

Considering that reactive aldehydes are major secondary LOPs responsible for the adverse biological effects associated with frying oil consumption, the kinetics of forming aldehydes in HSO was examined by LC-MS-based chemometrics to determine whether individual aldehydes or the aldehyde profile may serve as better indicators of thermal stress exposure in frying oils. Because direct detection of aldehydes in LC-MS analysis is hampered by their poor retention in common C18 reverse-phase columns, and their insufficient ionization efficiency in electrospray MS system, HQ was adopted as the derivatization agent to facilitate chromatographic separation and MS detection of aldehydes[192]. As shown in the scores plot (Figure 3.10A), heating-induced changes in soybean oil are reflected by the distribution pattern of HQ-derivatized samples in the PCA model, and can be summarized as follows: (1) Increasing the temperature from 45ºC to 165ºC did not significantly increased aldehyde production because the samples collected in this temperature range were clustered together with CSO in the model

(Figure 3.10A). The increase of PV began at 145ºC (Figure 3.9A), which suggests that aldehyde production lagged behind the formation of hydroperoxides, which is consistent to the sequence of forming primary and secondary LOPs[62]; (2) Increasing the temperature from 165ºC to 185ºC triggered dramatic changes of aldehyde profile in HSO, which was reflected by the clear separation of samples collected at these two temperatures in the model (Figure 3.10A); (3) Time-dependent chemical changes in HSO occurred from 0 min to 6 h when HSO was held at 185ºC (Figure 3.10A). Subsequently, a group of aldehydes were identified as the major contributors to the separation of CSO and different HSO samples in a loadings plot (Figure 3.10B). Their structural identities were further determined as 2,4-decadienal (I), 2-undecenal (II), 2-decenal (III), 2,4-undecadienal (IV), 4-HNE (V), 2-octenal (VI), pentanal (VII), hexanal (VIII), acrolein (IX), 2,4-heptadienal (X), and 2-heptenal (XI) after comparing their retention time and MSMS fragmentograms with authentic standards (Table 3.3, Figure 3.11). In addition to confirming the structures of these aldehydes, other markers of thermal stress were also identified in the model. For example, compound XII was tentatively defined as a 4-oxononanal, based on its molecular formula of $C_9H_{16}O_2$ and MSMS fragmentogram, but was not confirmed due to the lack of a standard. Moreover, the distribution pattern of these aldehydes in the loading plot indicated that individual aldehydes had different contributions to principal components 1 and 2 of the PCA model, which underlie the temperature- and time-dependent sample separation. To further define the kinetics of aldehyde formation and thermal stress-induced changes, a HCA was performed on these aldehyde markers together with PV and TBARS. Twelve aldehydes were divided into

three clusters, named as A1, A2, and B based on the branching of dendrogram and their kinetic patterns in the heat map (Figure 3.10C). The TBARS was grouped with cluster A1 aldehydes, while PV was separated from others in the dendrogram due to its distinctive pattern of change (Figure 3.10C).

Quantitative analysis of these aldehyde markers further confirmed the conclusions on the kinetics of individual aldehydes from the PCA and HCA models (Figure 3.12A-L), and the results can be summarized as follows: (1) 2,4-Decadienal (I) was the most abundant among all identified aldehydes (Figure 3.12A); (2) Concentrations of cluster B aldehydes, including 2,4-hepatadienal (X), 2-heptenal (XI), and acrolein (IX), peaked at 30 min of heating at 185ºC and then decreased thereafter (Figure 3.12I-K); (3) In contrast to cluster B aldehydes, concentrations of aldehydes belonging to clusters A1 and A2 (I-VIII) increased continuously at 185ºC (Figure 3.12A-H). The increases of cluster A1 aldehydes, including hexanal (VIII), pentanal (VII), 2,4-decadienal (I), and 2-octenal (VI), were attenuated after 1 h of heating at 185ºC while the increases of cluster A2 aldehydes, including 2,4-undecadienal (IV), 2-decenal (III), 2-undecenal (II), and 4-HNE (V), were more sustained (Figure 3.10C, 3.12A-H); (4) Different from other aldehydes, pentanal (VII) and hexanal (VIII) existed in detectable amounts in CSO (Figure 3.12G,H), while 4-HNE (V) was formed at a relatively constant rate ($r^2 = 0.99$) during heating at 185ºC (Figure 3.12E). Overall, the total aldehyde concentrations in HSO, which is the sum of all eleven identified aldehydes, had a similar kinetic profile with cluster A1 aldehydes (Figure 3.12L). More importantly, analyzing the relative abundance of three aldehyde clusters in the total aldehydes indicated that the percentage of cluster

A1 was relatively stable across 6 h of heating while the increase of cluster A2 aldehydes as a proportion of total aldehydes was accompanied with a decrease of cluster B aldehydes (Figure 3.12M). The opposite trends of changes between cluster A2 and B aldehydes were further reflected by the values of A2/B ratio, which were in a good linear correlation ($r^2 = 0.96$) with the duration of thermal stress (Figure 3.12N).

3.4.6 LC-MS-based chemometric analysis of thermal stress-induced production of aldehydes in frying oils and their distribution in French fries

Soybean, corn and canola oils are three widely used vegetable oils for preparing fried food. To understand the distribution of aldehydes in these frying oils and fried foods, soybean, corn and canola oil samples collected before and during heating (0, 30, and 360 min at 185ºC) and ten French fry oil extract samples were derivatized by HQ and then compared by LC-MS-based chemometric analysis. The distribution of control oils, HSO, heated corn oil (HCO) and heated canola oil (HCAO) samples in the scores plot of a PCA model indicated that progressive and time-dependent changes in the chemical composition occurred in all of these oils (Figure 3.13A). More importantly, changes in HCAO were greatly different from that in the other two oils, while the changes in HCO and HSO were relatively comparable (Figure 3.13A). The aldehydes contributing to the separation of three frying oils in the PCA model were identified as two groups of compounds in the loadings plot (Figure 3.13B), in which 2-undecenal (II), 2-decenal (III), and 2,4-heptadienal (X) were better correlated to HCAO while 2,4-decadienal (I), hexanal (VIII), and 2-heptenal (XI) were better correlated to HSO and HCO (Figure 3.13B). Another prominent feature of this PCA model is the clear separation of French

fry extracts from frying oils (Figure 3.13A). The markers contributing to this separation were also identified in the loadings plot (Figure 3.13B) and likely contained oxo fatty acids such as 8-oxo-octanoic acid based on elemental composition analysis, MSMS, and database search (data not shown). This observation suggests that the chemical composition of French fry extracts was greatly different from that of heated oils.

The concentrations of aldehydes (I-XI) in three heated oils and ten French fry extracts were further quantified. Consistent to the results of PCA modeling, the formation and distribution of aldehydes differed greatly among the three heated oils, in which HCO had higher levels (P<0.05) of 2,4-decadienal (I), 2,4-undecadienal (IV), 2-octenal (VI), pentanal (VII), and hexanal (VIII); HSO had higher levels (P<0.05) of HNE (V) and 2-heptenal (XI); and HCAO had higher levels (P<0.05) of 2-undecenal (II), 2-decenal (III), acrolein (IX), and 2,4-hepatadienal (X) (Figure 3.14A-K). Despite these differences in their aldehyde profiles, the total aldehyde concentrations in the HCO and HCAO were comparable (Figure 3.14L). Moreover, a comparison between heated oils and French fry oil extracts revealed that the concentrations of the majority of identified aldehydes (I-VI and X-XI) in French fry extracts were at least one order of magnitude lower than their highest concentrations determined in heated oils (Figure 3.14A-F, Figure 3.14J,K). The exceptions were the concentrations of pentanal (VII), hexanal (VIII), and acrolein (IX) in the French fry extracts, which were of the same magnitude as the concentrations in heated oils (Figure 3.14G-I). Furthermore, the distribution of three aldehyde clusters in three heated oils was compared. Interestingly, although the relative abundance of three clusters in total aldehydes differed greatly among three heated oils, the percentage of

cluster A1 within individual oils was relatively stable at the three time points of sampling, while the proportion of increase of clusters A2 of total aldehydes was accompanied with a decrease of cluster B aldehydes (Figure 3.14M). The A2/B ratios of French fry extracts were also within comparable range of its values in the three heated oils (Figure 3.14N).

3.5 DISCUSSION

Strengths and challenges of a LC-MS-based chemometric platform for analyzing chemical and oxidative status of frying oils.

In complement to existing targeted chemical analyses of frying oils, chemometrics platform, especially partial least-squares regression (PLS), have been adopted in examining the data from gas chromatography(GC), refractive index detector (RID), fluorescence, near infrared/visible (NIR/VIS), Fourier transform infrared (FT-IR), FT-Raman spectroscopic procedures to monitor the quality and identify the adulteration[226-229]. However, a combination of LC-MS analysis and chemometrics has not been widely used on frying oils for the same purpose, potentially due to the challenges of detecting major chemicals species in frying oils using LC-MS platform as well as the challenges of processing large volume of data. In this study, the challenges of detecting major chemicals species in frying oils using LC-MS platform were handled by adopting appropriate sample preparation procedures, mobile phase (such as adding isopropanol and ammonium formate to facilitate the separation of acylglycerols in common C18 column and their ionization in the MS system), and MS conditions (such as accurate mass measurement and MSMS fragmentation), leading to the identification and structural

elucidation of a series of TAGs and LOPs that were differs by the sources of oils and affected by thermal stress. Compared to other oil analysis platforms in practice, the high-resolution LC-MS analysis has its strengths in structural identification and high-throughput data acquisition[230]. As for the challenges of processing large volume of data, the multivariate data analysis-based chemometrics, including PCA and HCA, were adopted in this study to define the thermal stress-induced changes in frying oil. Using the identities (RT and *m/z*) of individual ions as the variables, the unsupervised PCA constructed multivariate models on the LC-MS data matrices containing sample identities, ion identities, and normalized ion intensities, and then identify the principal components in the model to illustrate the relationships among the samples[177]. Furthermore, the relationships among the detected chemicals in frying oils were defined by HCA and then visualized by heat map. The efficacy of these multivariate data analysis approached was demonstrated by the revelation of potential sources of frying oils used in commercial French fries samples (Figure 3.3A, 3.5) and the characterization of kinetics of heating-induced changes in TAGs and LOPs (Figure 3.6C, 3.10C).

Novel information revealed by sample distribution pattern in PCA models, clustering of individual markers in heat map, and kinetics profiles of individual markers.

In this study, the status of soybean oil was determined by examining acylglycerols, polar compounds, and aldehydes, and then visualized by the PCA models. Based on the sample distribution and grouping patterns in these three models, heating-induced progressive changes in the chemical composition of soybean oil were clearly defined by

this experimental approach (Figure 3.6A, 3.7A, 3.10A), and the markers/compounds contributing to these patterns were identified accordingly (Figure 3.6B, 3.7B, 3.10B). Hierarchical clustering of identified markers from three PCA models revealed several important features of heating-induced changes in soybean oil (Figure 3.6C, 3.10C).

FA composition and the index associated with it such as unsaturated level and iodine value, have been used to evaluate oil for authenticity and oxidation susceptibility for a long term. In contrast, the profile of intact acylglycerols, especially TAGs, in edible oils is less commonly used for the same purposes, largely due to the diversity of TAG species and the challenges of structural elucidation. The progresses in LC-MS technology in recent years have facilitated the chromatographic separation and structural identification of TAGs in oils[226, 231, 232]. As shown in the present study, the acylglycerol profiles of French fries oil extracts and oil samples can be effectively defined by high resolution LC-MS analysis, leading to the revelation of likely sources of frying oils in French fry samples (Figure 3.3, 3.5) and the oxidation level of these samples (K1 and W1 in Figure 3.6). Therefore, compared to 10-20 features (number of FA species) in FA profile, hundreds features of acylglycerols obtained by LC-MS and chemometric analyses should make acylglycerol profile a better indicator of quality and authenticity. Certain amount of studies had checked TGs profiles to evaluate authentication and identification of adulteration[233-235]. However, the comparisons of the oils in previous studies are not as simple as the visualization of comparison in the present study which was shown by scores plot and heatmap. The markers identified by the loadings plots could be used for comparison between the frying oils from fast food chains and the retail oils such as

soybean, canola, and corn oil. For example, similar acylglcerols profiles shared by frying oil from K1 and soybean oil were easily shown by the PCA and HCA result (Figure3.3, 3.5). The platform used in the present study could be simply applied for authentication and identification of adulteration.

Meanwhile, the status of HSO was determined by examining TAGs and then visualized by the PCA model in the present study. Even though various kinds of chemicals had been evaluated in deep frying oils[62, 64], TAGs as the major component of frying oil, were seldom characterized. In the present study, based on the sample distribution and grouping patterns in the model, heating-induced progressive changes in the TAGs composition of soybean oil were clearly defined by this experimental approach (Figure 3.6A), and the markers/compounds contributing to these patterns were identified accordingly (Figure 3.6B). Changes in relative abundances of the identified markers suggest that TAGs containing α-linolenic acid or TAGs containing three linoleic acids were vulnerable to heating under frying condition. While TAGs containing palmitic acid were more resistant to heat induced lipid oxidation (Figure 3.6C).

The decrease of linoleic acid (Figure 3.7C) are well correlated with the increase of 9-oxononanoic acid, 13-HODE, and 4-HNE, (Figure 3.7G, H, 3.12E). The similar patterns among 4-HNE, 9-oxononanoic acid, and 13-HODE, are consistent with a proposed mechanism of HNE formation through Hock cleavage of C9-C10 bond[236-238], in which 13-HODE is an intermediate product from 13-HPODE while 9-oxononanoic acid is another product from Hock cleavage. Compounds U1, U2, U3, and U4 had a kinetics profile that is distinctively different from other newly formed compounds in HSO since

their levels peaked within the first hour and then decreased afterwards (Figure 3.7K-N). At present, the chemical identities of these compounds are still under the investigation. To best of our knowledge, their molecule formula did not match any reported compounds in frying oils.

Kinetic profiles of aldehydes and fatty acid degradation. Oleic acid, linoleic acid, and α-linolenic acid are major fatty acids in many vegetable-derived frying oils, including soybean, corn, and canola oils used in this study[63]. As the precursors of frying-derived aldehydes, these three unsaturated fatty acids not only have different susceptibilities to thermal stress-induced oxidation, but also yield different LOPs from this process[77]. In the present study, by analyzing the kinetics and composition of aldehydes in frying oils, this association between individual fatty acids and aldehyde production was clearly shown by the three clusters of aldehydes identified by the HCA (A1, A2, and B in Figure 3.10C).

----Linoleic acid as a major source of cluster A1 aldehydes: Concentrations of aldehydes in cluster A1, including 2,4-decadienal (I), 2-octenal (VI), pentanal (VII), and hexanal (VIII) increased continuously, but their relative abundance to total aldehydes remained relatively stable during 6 h of heating at 185ºC (Figure 3.12A, F-H, M). It is known that 2,4-decadienal, 2-octenal, pentanal, and hexanal are formed by hemolytic β-scission of 9-hydroperoxy and 13-hydroperoxy linoleic acid[77]. Furthermore, all of these aldehydes were present in greater concentrations in corn oil than those in soybean and canola oil after 6 h of heating at 185ºC, which are correlated with the greater concentrations of linoleic acid in corn oil (Figure 3.14A, F-H). It is known that PUFAs containing three or more double bonds are preferred precursors of malondialdehyde, the

target of TBARS assay[239]. However, peroxidized linoleic acid was also determined as a precursor for malondialdehyde[240]. Because soybean oil contains a greater concentration of linoleic acid than α-linolenic acid, linoleic acid may be a significant contributor of TBARS value in HSO.

---Oleic acid as a major source of cluster A2 aldehydes: In contrast to cluster A1, concentrations of aldehydes in cluster A2, including 2-undecenal (II), 2-decenal (III), 2,4-undecadienal (IV), and 4-HNE (V), and their relative abundance in total aldehydes, increased gradually in heated soybean oil (Figure 3.12B-E, M). According to their kinetic profiles, 4-HNE was further separated from other aldehydes in the dendrogram (Figure 3.10C). It is known that 2-undecenal and 2-decenal are produced by hemolytic β-scission of 8-hydroperoxy and 9-hydroperoxy oleic acid, respectively[241, 242]. Despite being a dienal structure, 2,4-undecadienal has also been identified as an oxidation product of triolein[218]. Furthermore, canola oil had much greater concentrations of 2-undecenal and 2-decenal than soybean and corn oil after 6 h of heating at 185ºC, which is correlated with the greater concentration of oleic acid in canola oil (Figure 3.14B-C). The exception in cluster A2 aldehydes was 4-HNE because linoleic acid is generally considered as the main precursor of 4-HNE. The reaction mechanism of 4-HNE formation may contribute to its separation from the cluster A1 aldehydes and other cluster A2 aldehydes in the dendrogram because 4-HNE is formed through Hock cleavage of C9-C10 bond in linoleic acid, instead of hemolytic β-scission routes in the formation of other aldehydes[236-238].

---Alpha-linolenic acid as a major source of cluster B aldehydes: Compared to cluster A2, concentrations of aldehydes in cluster B, including acrolein (IX), 2,4-hepatadienal

(X), and 2-heptenal (XI), increased rapidly at the beginning of 185ºC but decreased or plateaued later in heated soybean oil (Figure 3.12M). This kinetic profile matches the susceptibility of α-linolenic acid to thermal stress. It is known that α-linolenic acid is the major precursor of acrolein when heating vegetable oils[243]. Furthermore, α-linolenic acid is also a more preferred precursor of 2,4-heptadienal than linoleic acid[244]. This association was further supported by the quantitative comparisons of these aldehydes in soybean, corn, and canola oil, in which a greater concentration of α-linolenic acid (canola > soybean > corn) was correlated to greater concentrations of acrolein and 2,4-heptadienal (canola > soybean > corn) (Figure 3.14I,J). As for 2-heptenal, it can be generated from both linoleic acid and α-linolenic acid[218, 245]. However, the results from this study suggest that it shares a similar kinetic profile with acrolein and 2,4-heptadienal in HSO (Figure 3.12K).

Overall, combining the existing knowledge on the oxidative degradation of unsaturated fatty acids, the observed kinetic profiles of aldehydes suggests strong correlations between individual aldehydes and fatty acid precursors, and further supports the use of specific aldehydes and aldehyde profiles as more accurate markers of thermal stress than PV and TBARS.

Potentials of using 4-HNE and aldehyde profiles as markers of thermal stress for heated oils and fried foods. Chemometric modeling and quantitative analysis utilized in this study offers an opportunity to examine the benefits and limitations of some existing oxidation evaluation methods by comparing their kinetic profiles with the profiles of other aldehydes in heated oils. Four common markers of lipid oxidation including PV,

TBARS, hexanal, and 2,4-decadienal levels were evaluated. The kinetic profile of PV reflected the transient increase of lipid hydroperoxides in soybean oil, but it differed from the profiles of aldehyde LOPs greatly (Figure 3.9A, 3.10C). Thus, PV does not represent the actual oxidative status of heated oil, especially after prolonged thermal stress. The plateauing of the TBARS curve after 1 h of frying temperature also does not accurately reflect the actual status of forming LOPs in HSO (Figure 3.9B, 3.10C). The kinetic profiles of hexanal and 2,4-decadienal were similar to each other and also to the profiles of other linoleic acid-derived aldehydes in HSO (Figure 3.10C), but differed from the profiles of aldehydes derived from oleic acid and α-linolenic acid. Overall, these four markers, like many other established assays, only target the oxidation products from specific degradation pathways, and thus cannot reflect general oxidative status of heated oils[83, 89]. Furthermore, the lack of a linear correlation (time vs level) in the kinetic curves of these markers also diminishes their value as accurate indicators of the length of time that oils have been subjected to thermal-stress conditions.

Novel information obtained from profiling aldehydes in this study provide some insights on how to overcome the drawbacks of using traditional markers (i.e. PV, anisidine value, TOTOX value, TBARS, hexanal, and 2, 4-decadienal assays). Among all examined aldehydes, 4-HNE is an established marker of *in vivo* lipid peroxidation[246], and was only recently identified as a secondary LOP in heated oil[247, 248]. Compared to other identified aldehydes in this study, including 2,4-decadienal and hexanal, the concentration of 4-HNE in HSO had a greater linear correlation with the duration of thermal stress (Figure 3.12E), suggesting that 4-HNE may be a more accurate aldehyde

marker to use when monitoring the oxidation status of soybean oil, than 2,4-decadienal and hexanal. Moreover, 4-HNE was also detected in HCO and HCAO (Figure 3.14E), and its levels in both oils increased progressively at three sampling time points (0, 30, 360 min when heated at 185ºC). Besides 4-HNE, the ratio between cluster A2 aldehydes and cluster B aldehydes (A2/B ratio), also had a sound linear correlation with the duration of thermal stress in HSO (Figure 3.12N), and had its value increased progressively at three sampling time points (0, 30, 360 min heating at 185 ºC) in HCO and HCAO (Figure 3.14N). Considering oleic acid and α-linolenic acid are major contributors to A2 and B aldehyde clusters, respectively, the A2/B ratio reflects the sensitivities of oleic acid and α-linolenic acid to oxidative degradation. Overall, these observations warrant future studies on whether 4-HNE and A2/B ratio could function as general markers to assess oxidative stress for diverse frying oils.

Human exposure to aldehyde LOPs is mainly through consuming fried foods which comprise LOPs from both frying oils and inherent lipid content. To explore whether individual aldehydes or aldehyde profiles could serve as effective markers of oxidative status in fried foods, the concentrations and composition of aldehydes in the extracts of commercial French fry samples were examined. The majority of aldehydes had their concentrations in French fry extracts far below their concentrations in the heated oils prepared under current experimental conditions (Figure 3.14A-F, J-K), which was likely due to the reactions between unsaturated aldehydes in frying oil and the chemical components of the potatoes, such as primary amines[249-251]. Therefore, the concentrations of these aldehydes (I-VI and X-XI) in French fries might not reflect the actual oxidation

status of oils used in cooking. However, the concentrations of pentanal (VII), hexanal (VIII), acrolein (IX), and A2/B ratio were within the range of their values in the three heated vegetable oils (Figure 3.14G-I, 3.14N). This selective retention of pentanal and hexanal in French fries may be explained by the fact that these two saturated alkanals are much less reactive than other unsaturated alkenals, alkadienals, and hydroxyalkenal in heated oils[246], while significant presence of acrolein in French fries may be attributed to its multiple sources, because acrolein can be formed from carbohydrates, fatty acids, and amino acids[252]. As for the A2/B ratio, even though the levels of aldehydes comprising A2 and B clusters differed greatly between heated oils and French fry extracts (Figure 3.12, 3.14), its values in French fry extracts were still of the same magnitude as the ones in heated oils. The use of the A2/B ratio as an accurate marker for evaluating frying oil residuals in fried foods needs to be further evaluated using more defined experimental settings, such as measuring the kinetic profile of aldehydes in fried foods.

In summary, comparison of neutral acylglycerols, polar compounds, and aldehydes profiles in frying oils and distinctive kinetics of individual lipid oxidation markers in HSO, as well as the distribution of aldehydes in French fries were defined by high-resolution of LC-MS analysis and multivariate chemometrics. The results demonstrated the capacity of LC-MS-based chemometrics in both comprehensive profiling and specific characterization of these LOPs, making it a robust platform for authentication and monitoring lipid oxidation of heated oils. The observations of temperature-sensitive and time-dependent change of individual TG and formation of aldehyde in frying oils indicated the limitation of several traditional lipid oxidation assays for the lack of strong

correlation with the duration of thermal stress, and also suggested the potential of certain individual TAG, 13(S)-HODE, 4-HNE, and aldehyde clusters (A2/B ratio) as the markers of thermal stress for frying oils and fried foods.

Table 3.1. Major DG and TG species contributing to the classification of oils and oil extracts in the PCA model and clustering analysis.

ID	*m/z**	Formula	Acylglycerols (C: DB)†	FA composition	MSMS fragments
D1	*615.4962*	$C_{39}H_{66}O_5$	DG(36:5)		
D2	*617.5144*	$C_{39}H_{68}O_5$	DG(36:4)		
D3	*639.4964*	$C_{41}H_{66}O_5$	DG(38:7)		
D4	*641.5124*	$C_{41}H_{68}O_5$	DG(38:6)		
T1	894.7575	$C_{57}H_{96}O_6$	TG (54:7)	TG (18:3/18:2/18:2)	597,599
T2	896.7723	$C_{57}H_{98}O_6$	TG (54:6)	TG (18:2/18:2/18:2)	599
T3	898.7892	$C_{57}H_{100}O_6$	TG (54:5)	TG (18:2/18:2/18:1)	599,601
T4	900.8042	$C_{57}H_{102}O_6$	TG (54:4)	TG (18:2/18:1/18:1)	601,603
T5	902.8195	$C_{57}H_{104}O_6$	TG (54:3)	TG (18:1/18:1/18:1)	603
T6	848.7715	$C_{53}H_{98}O_6$	TG (50:2)	TG (16:0/16:0/18:2)	551,575
T7	850.7867	$C_{53}H_{100}O_6$	TG (50:1)	TG (16:0/16:0/18:1)	551,577
T8	870.7549	$C_{55}H_{96}O_6$	TG (52:5)	TG (16:0/18:3/18:2)	573,575,597
T9	872.7727	$C_{55}H_{98}O_6$	TG (52:4)	TG (16:0/18:2/18:2)	575,599
T10	874.7879	$C_{55}H_{100}O_6$	TG (52:3)	TG (16:0/18:2/18:1)	575,577,601
T11	876.8025	$C_{55}H_{102}O_6$	TG (52:2)	TG (16:0/18:1/18:1)	577,603
T12	*879.7443*	$C_{57}H_{98}O_6$	TG (54:6)	TG (18:3/18:2/18:1)	597,599,601
T13	892.7412	$C_{57}H_{94}O_6$	TG (54:8)	TG (18:3/18:3/18:2)	595,597
T14	904.8335	$C_{57}H_{106}O_6$	TG (54:2)	TG (18:1/18:1/18:0)	603,605
T15	928.8334	$C_{59}H_{106}O_6$	TG (56:4)	TG (18:2/18:2/20:0)	599,631
T16	930.8479	$C_{59}H_{108}O_6$	TG (56:3)	TG (18:2/18:1/20:0)	601,631,633

*The enlisted *m/z* values in this column are from protonated ammonia adducts of TGs (NH_4^+), except the *m/z* values (*italics*) of D1-D4 and T12, which are from protonated ions (H^+).

†C = carbon; DB = double bond.

Table 3.2. Identification of free fatty acids and LOP species contributing to the classification of CSO and HSO samples in the PCA model.

ID	*m/z* (-H)*	Formula	Compounds†	Linoleate(Δ)‡	Linolenate (Δ)‡
	163.0761	$C_{10}H_{12}O_2$	3-Phenylbutyric acid; Eugenol(D)	-	-
	167.1070	$C_{10}H_{16}O_2$	*trans*-4,5-epoxy-2(E)-Decenal(D)	-	-
	181.0862	$C_{10}H_{14}O_3$	(5E,8E)-10-Oxo-5,8-decadienoic acid(D)	-	-
	219.1020	$C_{13}H_{16}O_3$	Flossonol(D)	-	-
	235.1317	$C_{14}H_{20}O_3$	4-(Heptyloxy)benzoic acid (D)	-	-
	249.1101	$C_{14}H_{18}O_4$	Coenzyme Q_1 (D)	-	-
	263.1274	$C_{15}H_{20}O_4$	Abscisic acid(D)	-	-
P2	277.2170	$C_{18}H_{30}O_2$	α-linolenic acid	-	+
P1	279.2330	$C_{18}H_{32}O_2$	Linoleic acid	+	-
	363.1933	$C_{24}H_{28}O_3$		+	-
	559.4703	$C_{36}H_{64}O_4$		+	-
	141.0917	$C_8H_{14}O_2$	2-Octenoic acid(D)	-	-
	165.0549	$C_9H_{10}O_3$	Phenyllactic acid (D)	-	-
	165.0913	$C_{10}H_{14}O_2$	Perillic acid(D)	-	-
	167.1070	$C_{10}H_{16}O_2$	(3E,5Z)-3,5-Decadienoic acid(D)	-	-
	167.1070	$C_{10}H_{16}O_2$	4-oxo-2E-Decenal(D)	-	-
P6	171.1020	$C_9H_{16}O_3$	9-Oxononanoic acid	+	+
	209.1174	$C_{12}H_{18}O_3$	Jasmonic acid(D)	+	-
P8	223.1344	$C_{13}H_{20}O_3$	13-Oxo-9,11-tridecadienoic acid	+	+
	237.1851	$C_{15}H_{26}O_2$	5E,9Z-Tridecadienyl acetate(D)	-	-
P3	255.2328	$C_{16}H_{32}O_2$	Palmitic acid	-	-
P4	281.2484	$C_{18}H_{34}O_2$	Oleic acid	-	-
P5	295.2267	$C_{18}H_{32}O_3$	13(S)-HODE	+	+
P7	297.2422	$C_{18}H_{34}O_3$	Hydroxy-octadecenoic acid	+	-
	337.2321	$C_{20}H_{34}O_4$	11,12-DiHETrE(D)	-	-

*The enlisted *m/z* values in this column are from deprotonated ions.

†The identities of compounds with (D) are from database search.

‡The compounds which can be found in heated linoleate or linolenate are marked with "+".

Table 3.3. A list of confirmed HQ derivatives of aldehydes.*

ID	Compounds	Formula	Derivative Formula	Exact Mass of $[M+H]^+$
I	2,4-Decadienal	$C_{10}H_{16}O$	$C_{19}H_{24}N_3^+$	294.1965
II	2-Undecenal	$C_{11}H_{20}O$	$C_{20}H_{28}N_3^+$	310.2278
III	2-Decenal	$C_{10}H_{18}O$	$C_{19}H_{26}N_3^+$	296.2121
IV	2,4-Undecadienal	$C_{11}H_{18}O$	$C_{20}H_{26}N_3^+$	308.2121
V	4-HNE	$C_9H_{16}O_2$	$C_{18}H_{24}N_3O^+$	298.1914
VI	2-Octenal	$C_8H_{14}O$	$C_{17}H_{22}N_3^+$	268.1808
VII	Pentanal	$C_5H_{10}O$	$C_{14}H_{18}N_3^+$	228.1495
VIII	Hexanal	$C_6H_{12}O$	$C_{15}H_{20}N_3^+$	242.1652
IX	Acrolein	C_3H_4O	$C_{12}H_{12}N_3^+$	198.1026
X	2,4-Heptadienal	$C_7H_{10}O$	$C_{16}H_{18}N_3^+$	252.1495
XI	2-Heptenal	$C_7H_{12}O$	$C_{16}H_{20}N_3^+$	254.1652
XII	-	$C_9H_{16}O_2$	$C_{18}H_{24}N_3O^+$	298.1914

*Information on each compound includes its molecular formula, the formula of its HQ derivative, and the exact mass of protonated HQ derivative ($[M+H]^+$). The compounds contributing to the separation of samples in Figure 3.10A were presented with their identities (ID) labeled in Figure 3.10B. The chemical structures of these compounds were confirmed by comparing their chromatographic peaks and MS/MS fragmentograms with the standards.

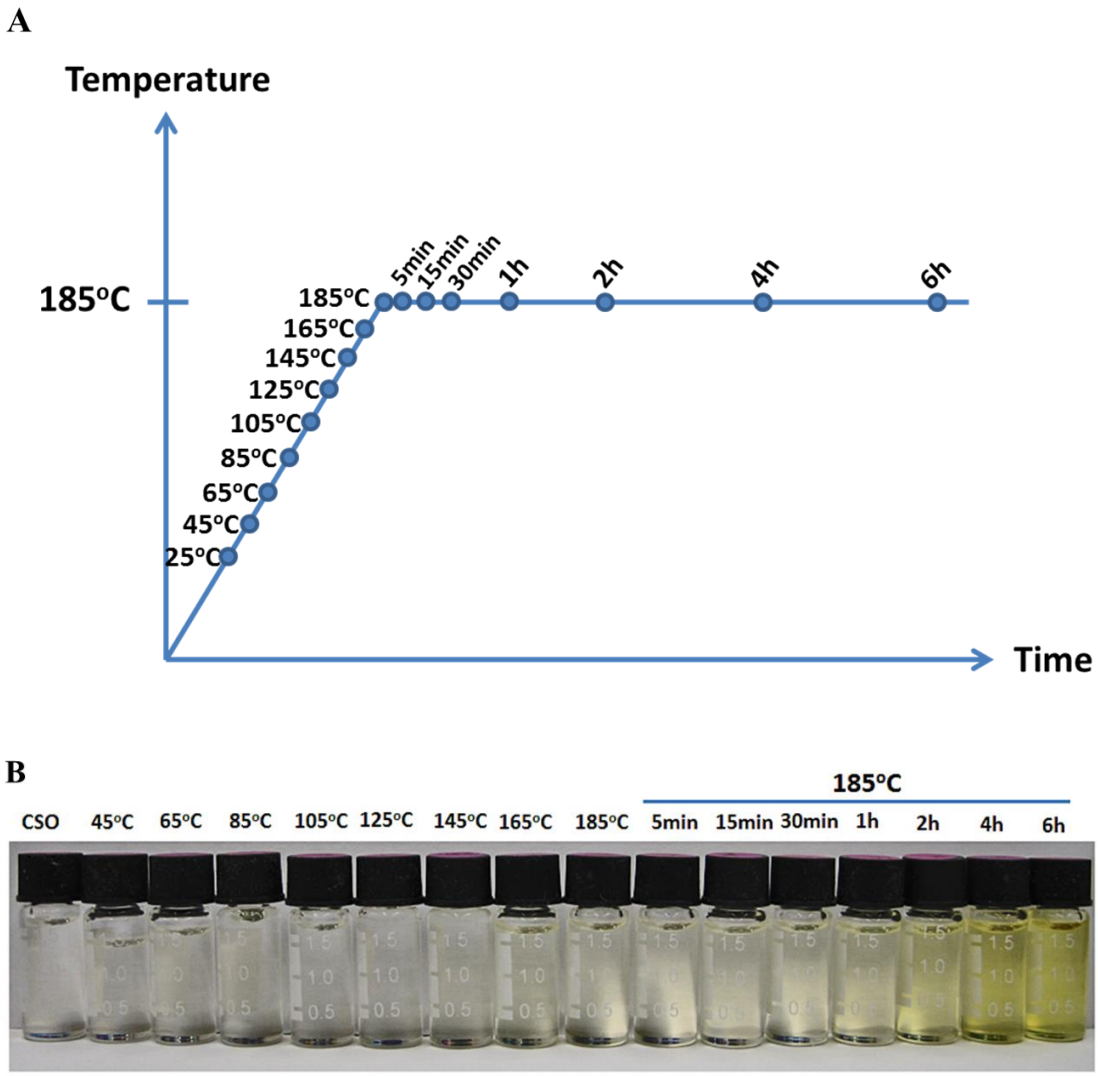

Figure 3.1. Preparation of heated soybean oil. ***A.*** The temperatures and time points of sampling. ***B.*** Heating-induced color change in soybean oil.

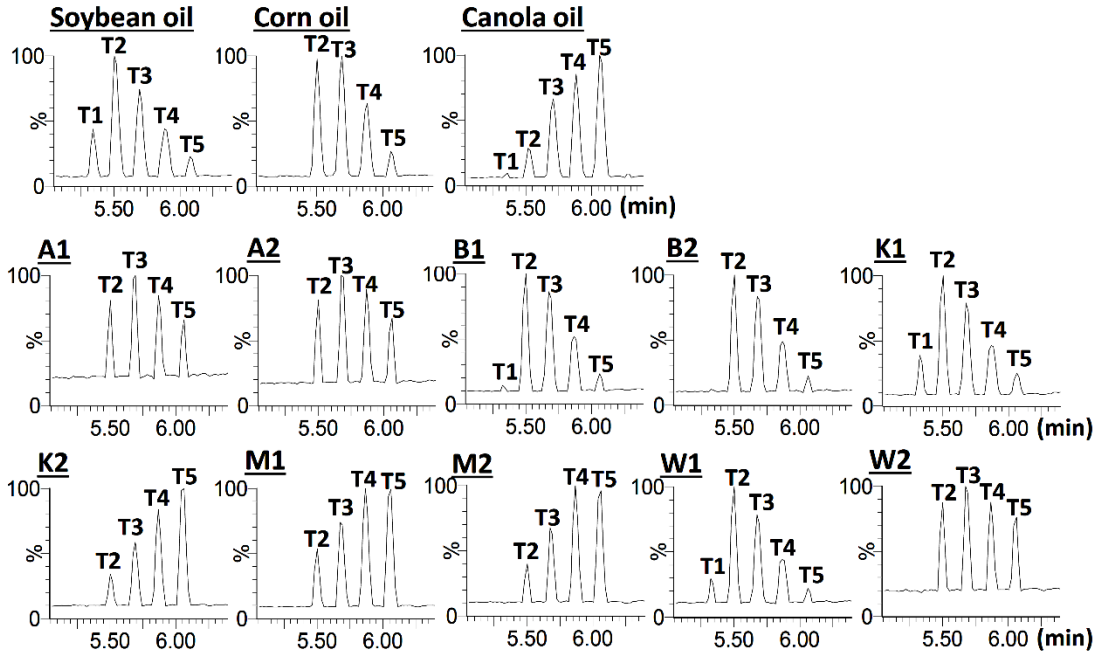

Figure 3.2. Representative base peak ion chromatograms of vegetable oils and French fries oil extracts. Major peaks are marked with their ID (detailed in **Table 3.1**). French fries samples (A1, A2, B1, B2, K1, K2, M1, M2, W1, and W2) were purchased from the restaurants of five fast food chains. Procedures and conditions of sample preparation and LC-MS measurement are described under "Materials and Methods".

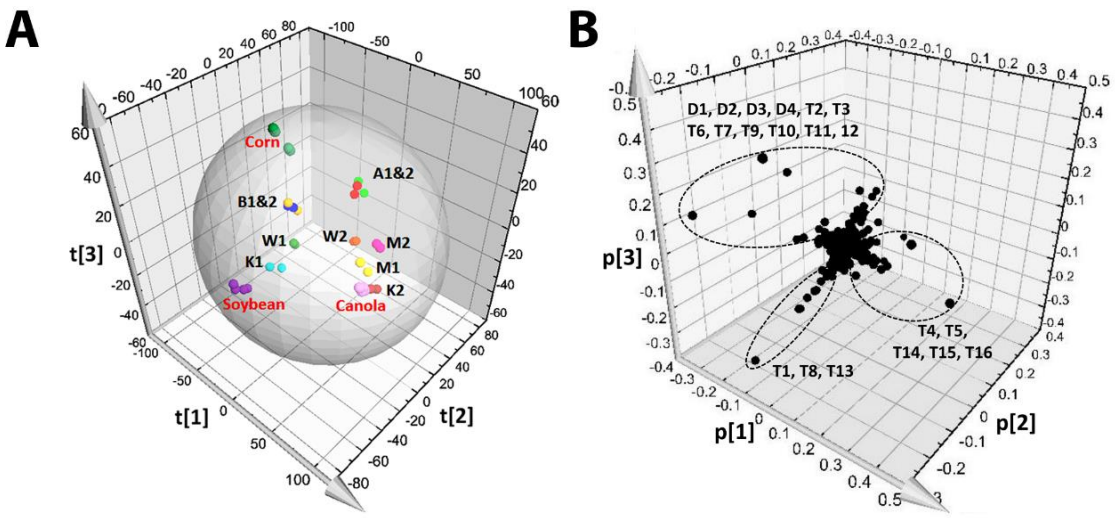

Figure 3.3. PCA modeling of vegetable oils and French fries oil extracts. Procedures of data processing and PCA are described under "Materials and Methods". ***A.*** Scores plot of a PCA model on vegetable oils and French fries oil extracts. The t[1], t[2], and t[3] values represent the scores of each sample in the principal component 1, 2 and 3, respectively. ***B.*** Loadings plot of the ions detected by LC-MS analysis. The ions contributing to the separation of vegetable oils and French fries oil extracts in the model were encircled and labeled. The p[1], p[2] and p[3] values represent the contributing weights of each ion to the principal component 1, 2 and 3 of the PCA model, respectively.

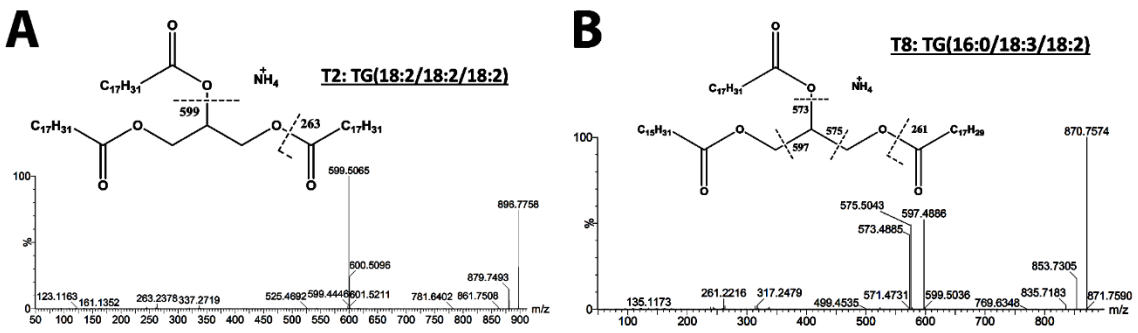

Figure 3.4. Representative collision-induced decomposition spectra of TGs. The fragmentation pattern is interpreted in the inlaid diagram ***A.*** MSMS fragmentogram of T2 [TG (18:2, 18:2, 18:2)]. ***B.*** MSMS fragmentogram of T8 [TG (16:0, 18:3, 18:2)].

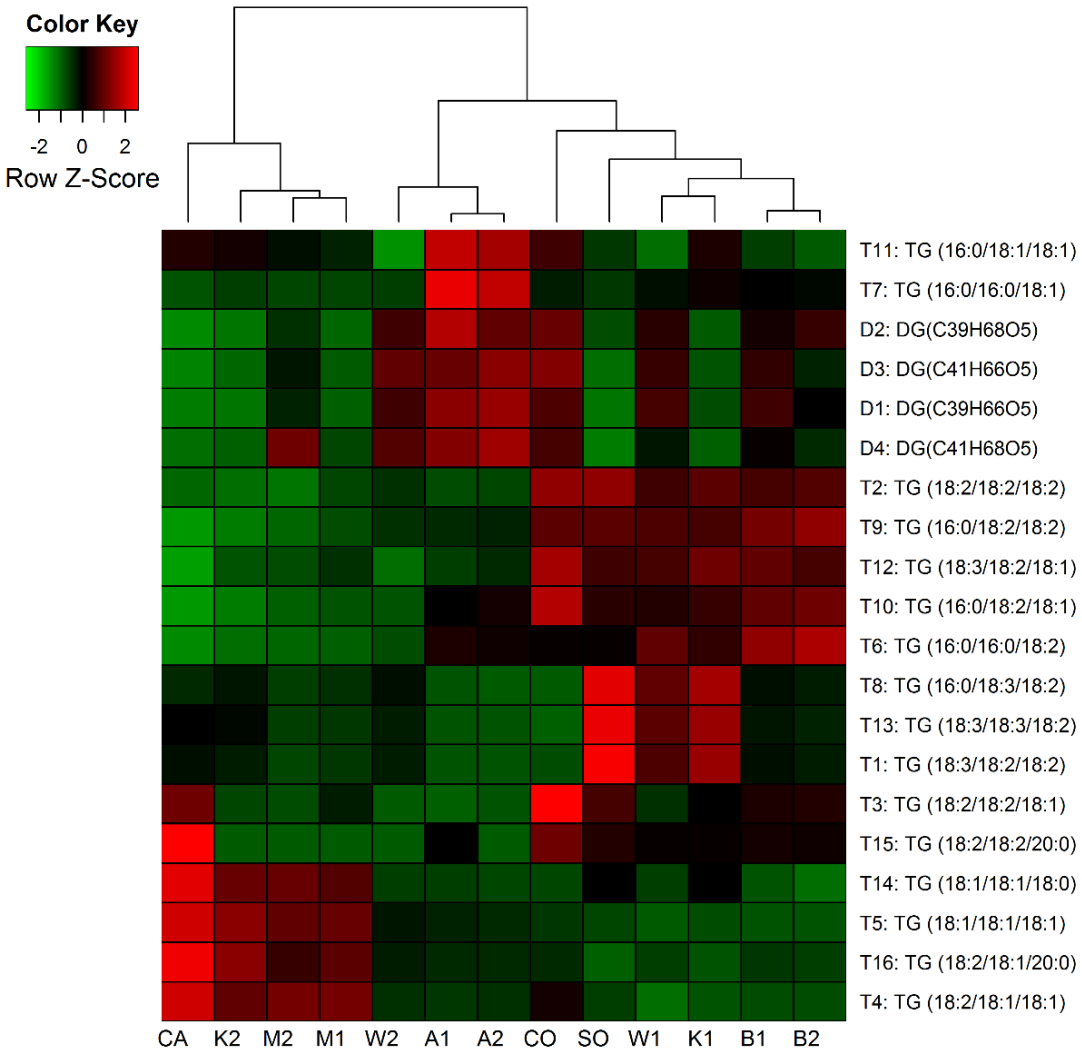

Figure 3.5. Heat map of hierarchically clustered markers that contribute to the separation of vegetable oils and French fries oil extracts in the model. Relative abundances of each marker were compared by its Z scores and are presented according to inlaid color keys.

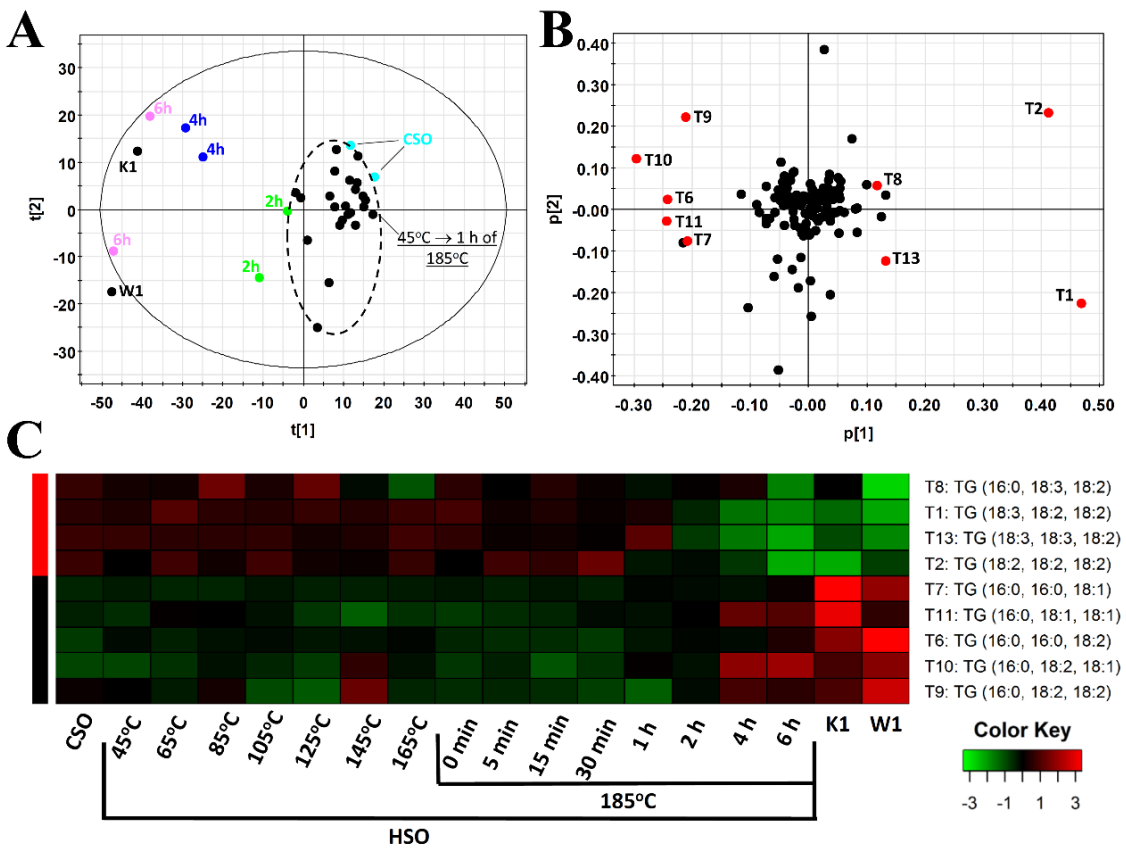

Figure 3.6. LC-MS-based chemometric analysis of thermal stress-induced changes in TG composition of soybean oil. ***A.*** Scores plot of a PCA model on W1 and K1 French fries oil extracts, CSO and HSO sample. The t[1] and t[2] values represent the scores of each sample in the principal component 1 and 2, respectively. The identities of examined samples are labeled. The HSO samples from 45ºC to 1 h of 185ºC are encircled. ***B.*** Loadings plot of the TGs detected by LC-MS analysis. Identified TG ions (T1, T2, T6-T11, and T13) contributing to the sample separation along the principal component 1 are labeled. The p[1] and p[2] values represent the contributing weights of each ion to the PC 1 and 2 of the PCA model, respectively. ***C.*** Heat map of identified markers in the model. Relative abundances of each marker were compared by its Z scores and are presented according to inlaid color keys.

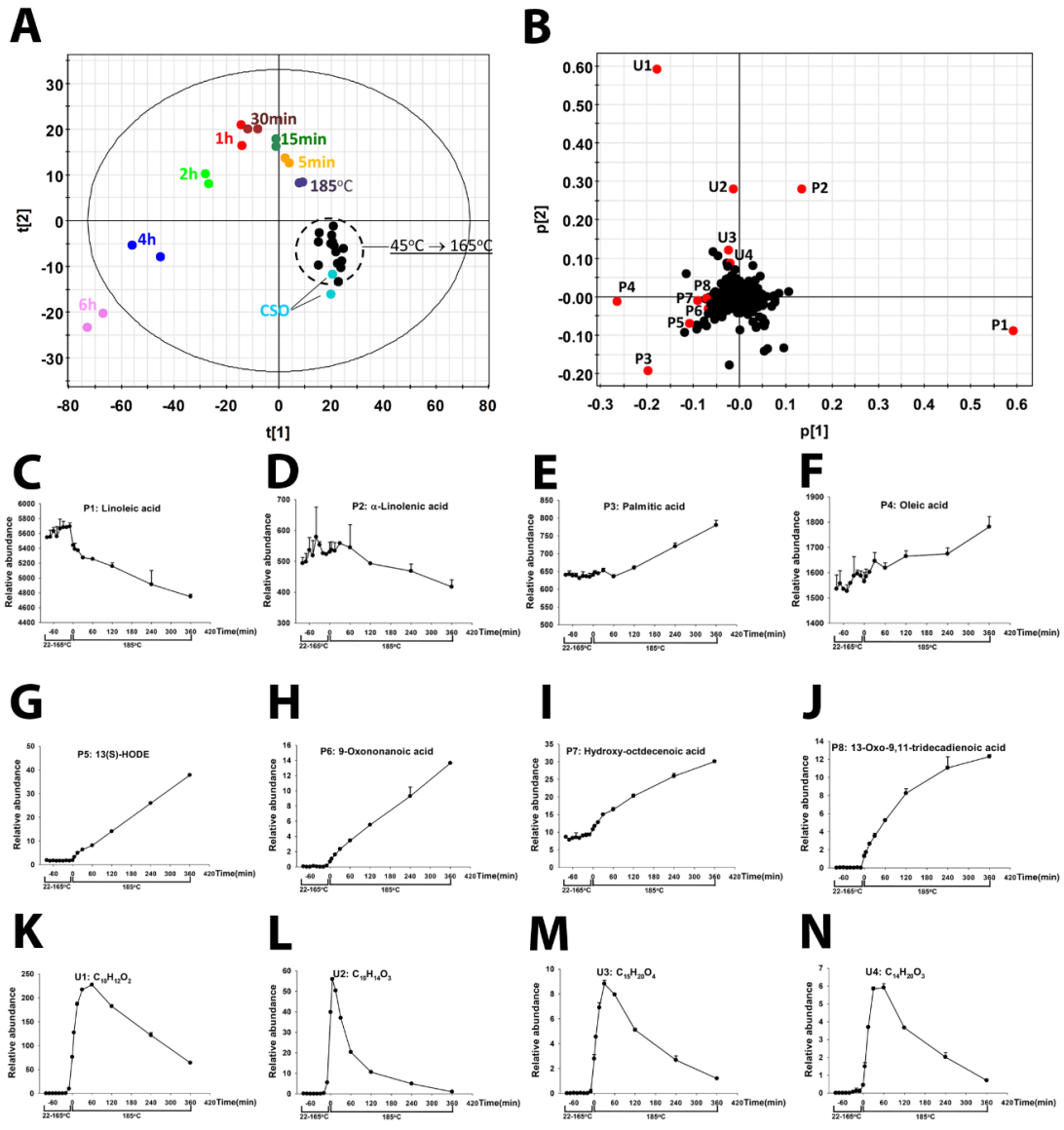

Figure 3.7. LC-MS-based chemometric analysis of free fatty acids and LOPs in soybean oil. ***A.*** Scores plot of a PCA model on CSO and HSO sample. The t[1] and t[2] values represent the scores of each sample in the principal component 1 and 2, respectively. The identities of examined samples are labeled. The HSO samples from 45ºC to 165ºC are encircled. ***B.*** Loadings plot of the ions detected by LC-MS analysis. Some of major contributing ions are labeled (P1-P8 and U1-U4). The p[1] and p[2] values represent the contributing weights of each ion to the principal components 1and 2 of the PCA model, respectively. ***C-N.*** The relative abundance of Linoleic acid (P1), α-linolenic acid (P2), palmitic acid (P3), oleic acid (P4), 13(S)-HODE (P5), 9-oxononanoic acid (P6), hydroxy-octadecenoic acid (P7), 13-oxo-9,11-tridecadienoic acid (P8), $C_{10}H_{12}O_2$ (U1), $C_{10}H_{14}O_3$ (U2), $C_{15}H_{20}O_4$ (U3), and $C_{14}H_{20}O_3$ (U4).

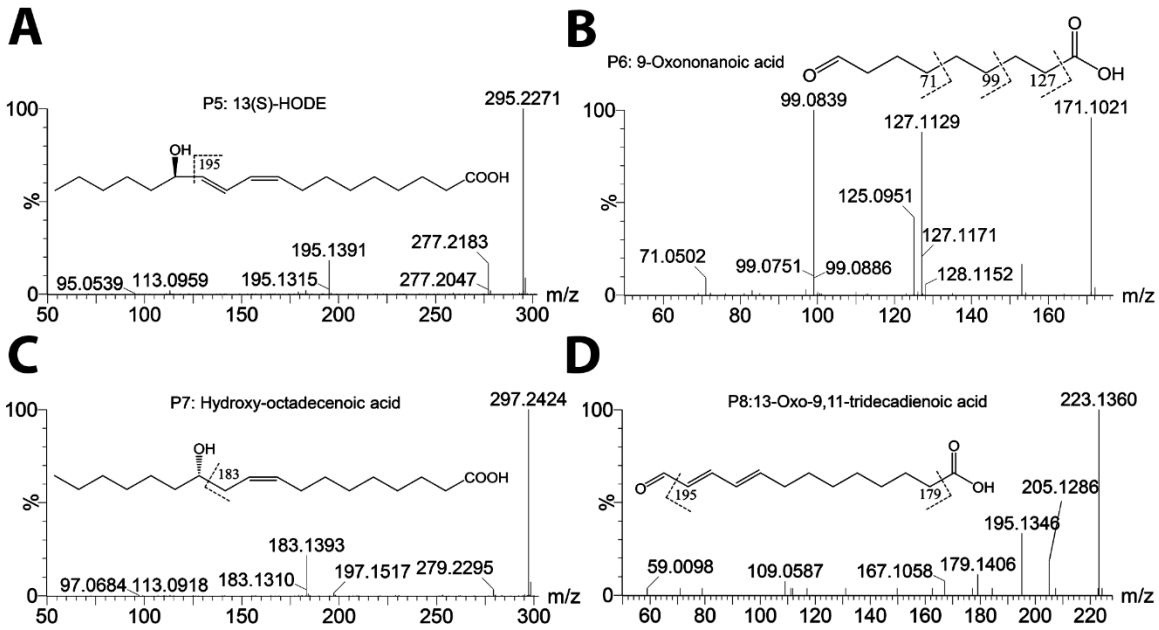

Figure 3.8. Structural elucidation of LOP markers. ***A.*** MSMS chromatograms of 13(S)-HODE from oil samples. ***B.*** MSMS chromatograms of 9-oxononanoic acid from oil samples. ***C.*** MSMS chromatograms of hydroxy-octadecenoic acid from oil samples. ***D.*** MSMS chromatograms of 13-oxo-9,11-tridecadienoic acid from oil samples.

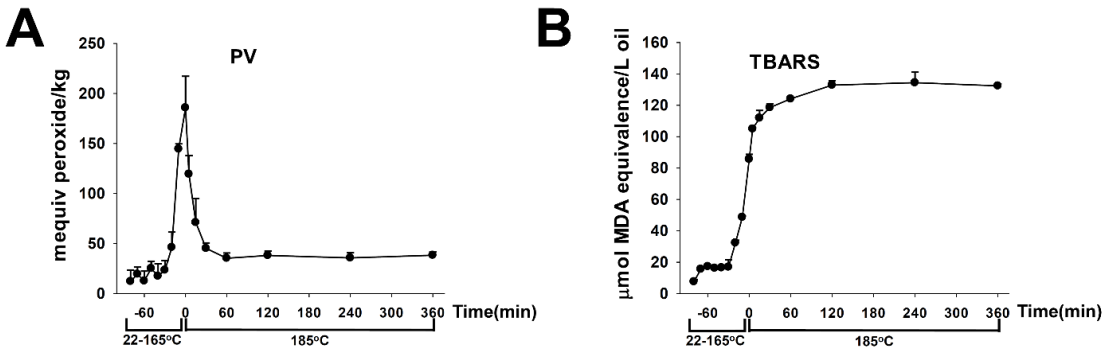

Figure 3.9. Kinetics of established lipid oxidation markers. ***A.*** PV of HSO samples. ***B.*** TBARS value of HSO samples.

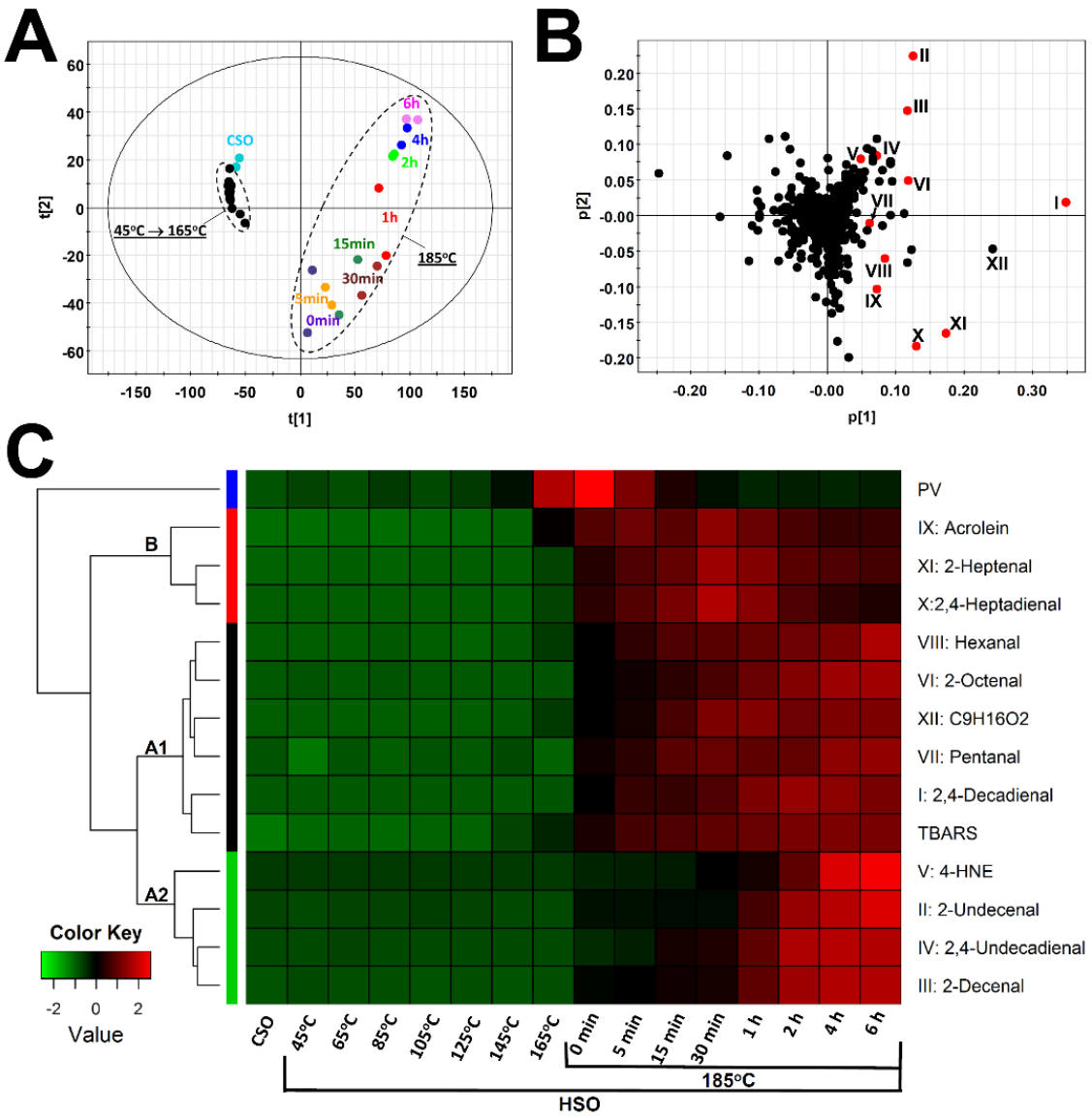

Figure 3.10. LC-MS-based chemometric analysis of aldehyde production in HSO. Aldehydes in CSO and HSO samples were derivatized by HQ prior to the LC-MS analysis. *A.* Scores plot of a PCA model on CSO and HSO sample. The t[1] and t[2] values represent the scores of each sample in the principal component 1 and 2, respectively. The identities of examined samples are labeled. The HSO samples from 45ºC to 165ºC and the samples collected at 185ºC are encircled. ***B.*** Loadings plot of the ions detected by HQ derivatization and LC-MS analysis. Major aldehyde ions (I-XII) correlated to the HSO samples are labeled. The p[1] and p[2] values represent the contributing weights of each ion to the principal component 1 and 2 of the PCA model, respectively. ***C.*** Heat map and dendrogram of aldehyde markers of thermal stress. The markers are hierarchically clustered as clusters A1, A2, and B. The relative abundance of each marker in all samples were compared by their Z scores and presented in the inlaid color key.

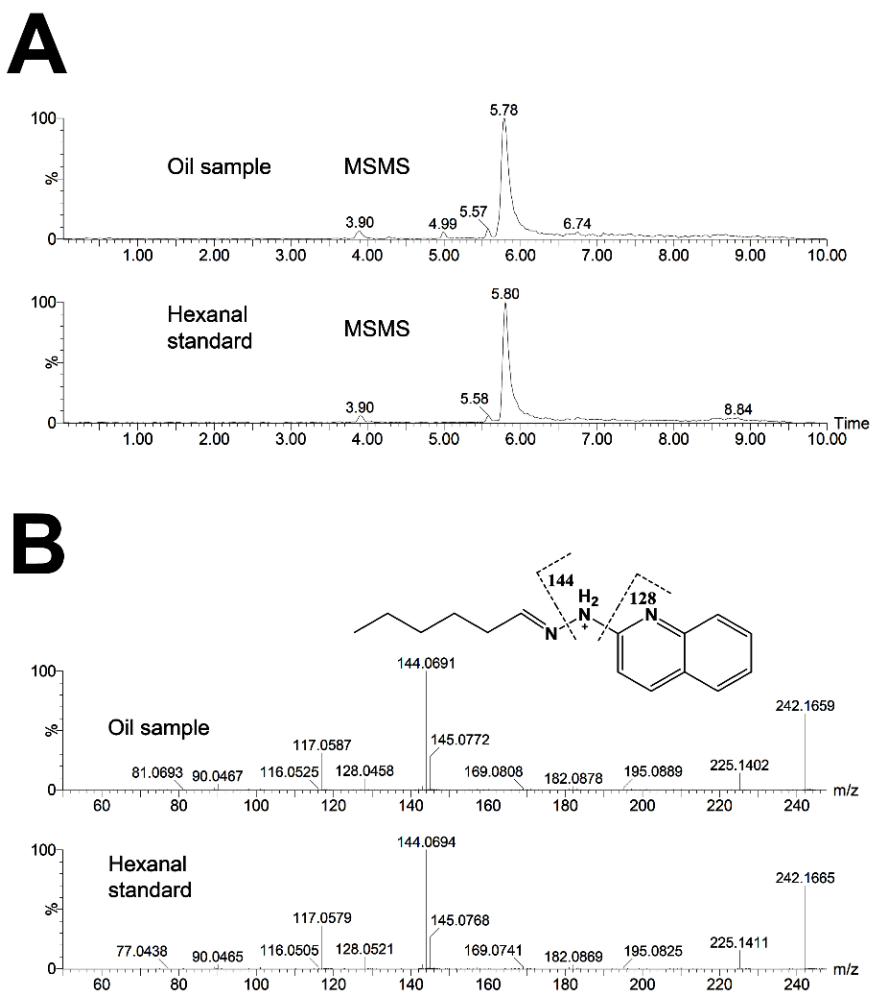

Figure 3.11. LC-MS analysis of aldehyde-HQ derivatives using hexanal as an example. ***A.*** MSMS chromatograms of hexanal-HQ derivative from oil samples and standard. ***B.*** Structure and MSMS spectrum of hexanal-HQ derivative.

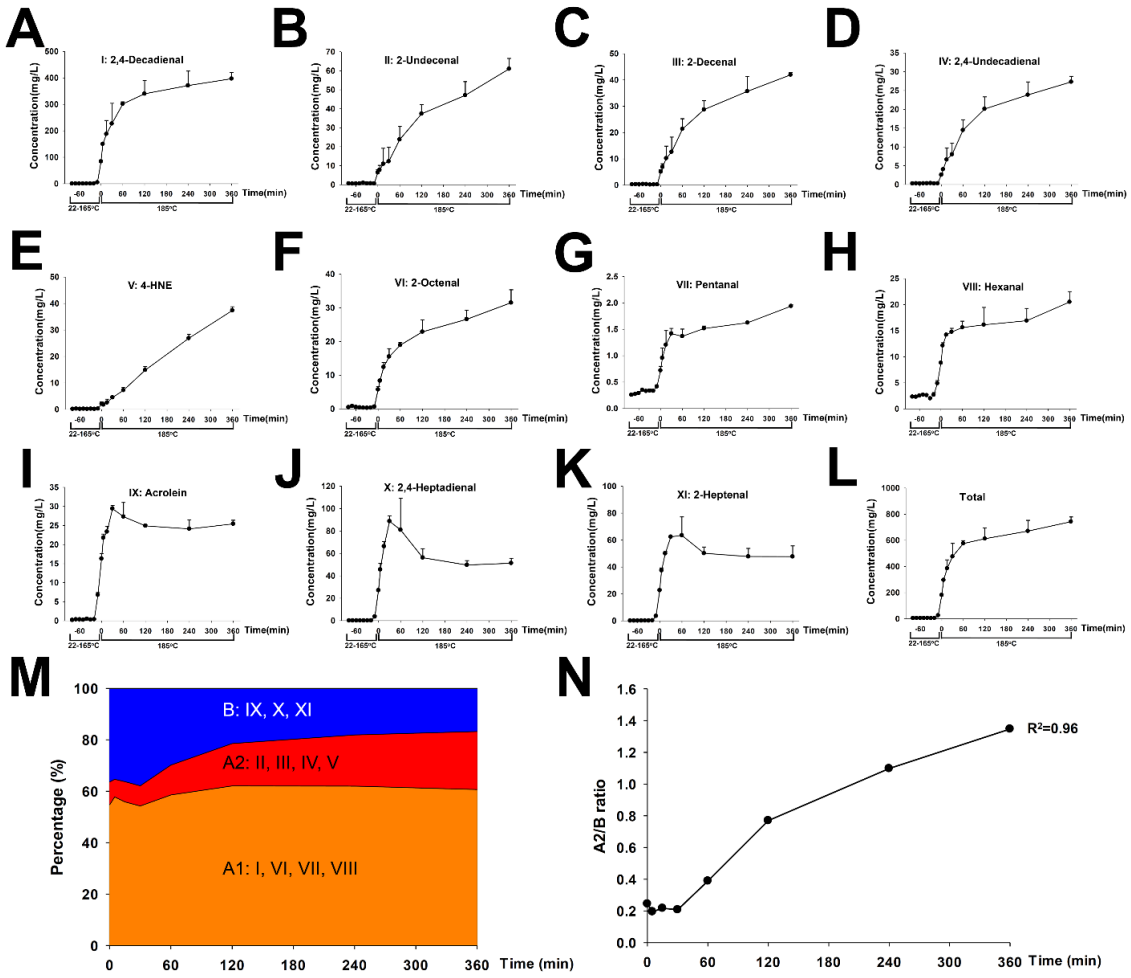

Figure 3.12. Kinetics of individual aldehyde markers (I-XI) and aldehyde clusters (A1, A2, and B). The concentrations of aldehyde markers in HSO were quantified by LC-MS analysis. ***A.*** 2,4-Decadienal. ***B.*** 2-Undecenal. ***C.*** 2-Decenal. ***D.*** 2,4-Undecadienal. ***E.*** 4-HNE. ***F.*** 2-Octenal. ***G.*** Pentanal. ***H.*** Hexanal. ***I.*** Acrolein. ***J.*** 2,4-Heptadienal. ***K.*** 2-Heptenal. ***L.*** Total aldehydes. The value is the sum of eleven aldehyde markers (I-XI). ***M.*** Kinetics of aldehyde clusters A1, A2, and B in HSO samples. Each cluster is expressed by its percentage in total aldehydes. ***N.*** Kinetics of A2/B ratio.

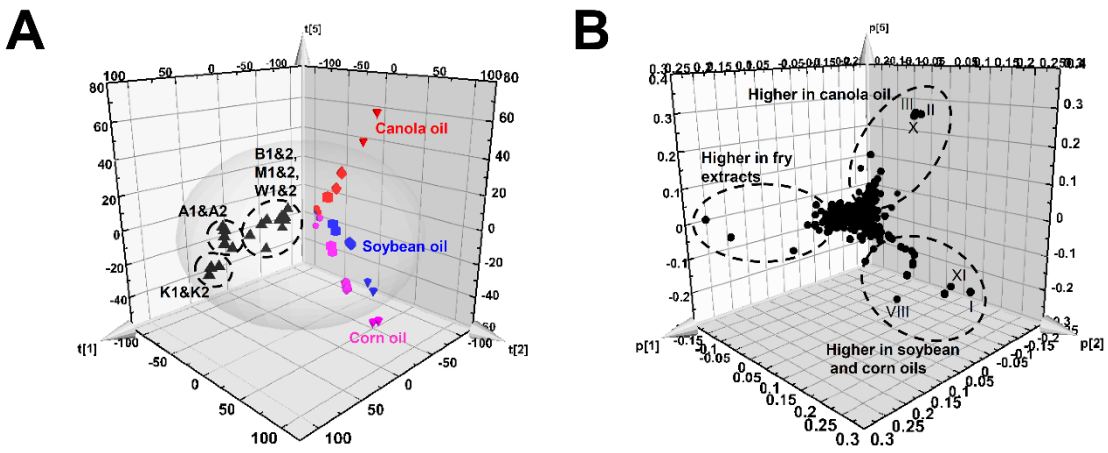

Figure 3.13. LC-MS-based chemometric analysis of aldehydes in three frying oils (soybean, corn, and canola oils) and French fry oil extracts. *A.* Scores plot of a PCA model on frying oils and French fry extracts. Each type of oil has unheated controls (●), 0 min (■), 30 min (♦), and 360 min (▼) samples collected at 185ºC frying temperature. French fry oil extracts are labeled with their sources (A, B, K, M, W). ***B.*** Loadings plot of the ions detected by HQ derivatization and LC-MS analysis. Major aldehyde markers associated with the sample groups are labeled.

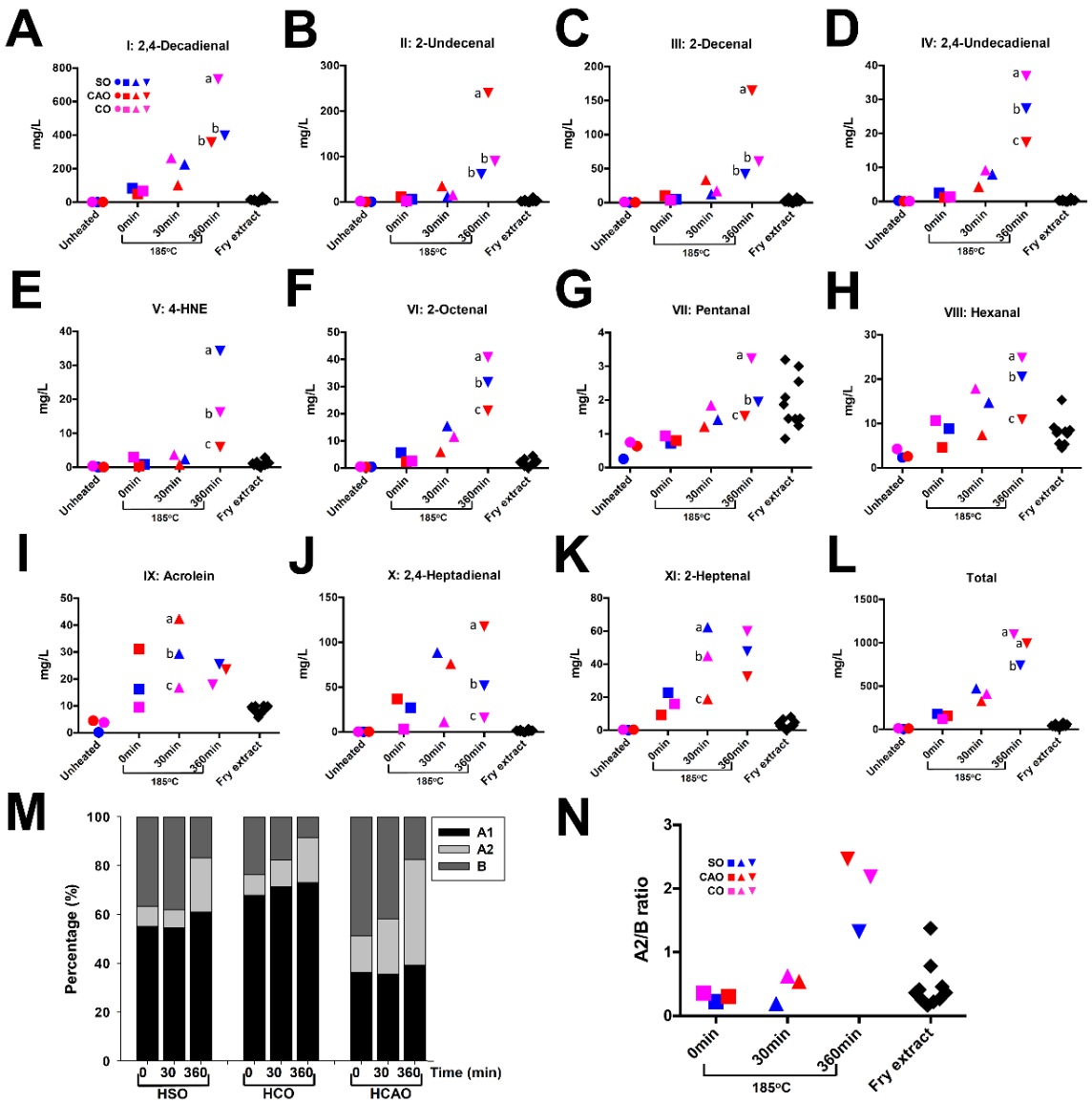

Figure 3.14. Quantification of aldehyde markers in HSO, HCO, HCAO and French fry extracts through LC-MS analysis. Each type of oil has unheated controls (●), 0 min (■), 30 min (▲), and 360 min (▼) samples collected at 185ºC frying temperature (two samples per time point per oil and duplicate measurement for each sample). The time point with the highest level of individual or total aldehydes in three frying oils was selected for statistic analysis. Different letter labels (a, b, or c) indicate significant differences from each other while the same letter no differences. ***A.*** 2,4-Decadienal. ***B.*** 2-Undecenal. ***C.*** 2-Decenal. ***D.*** 2,4-Undecadienal. ***E.*** 4-HNE. ***F.*** 2-Octenal. ***G.*** Pentanal. ***H.*** Hexanal. ***I.*** Acrolein. ***J.*** 2,4-Heptadienal. ***K.*** 2-Heptenal. ***L.*** Total aldehydes. ***M.*** Relative abundances of aldehyde clusters A1, A2, and B in HSO, HCO, and HCAO samples. Each cluster is expressed by its percentage in total aldehydes. ***N.*** The ratios of A2/B in HSO, HCO, HCAO, and French fry extracts.

CHAPTER 4. METABOLIC EFFECTS OF HEATED SOYBEAN OIL IN MOUSE REVEALED BY LC-MS-BASED METABOLOMICS

4.1 SUMMARY

Consumption of thermally-oxidized oil through fried foods has been suggested as a contributing factor in various metabolic disorders such as cancers and cardiovascular diseases. However, the underlying mechanism of this association is not fully understood. In this study, the influences of consuming heated vegetable oils on the metabolic system were examined through the metabolomics-guided biochemical analysis. Control soybean oil (CSO) diet (contain 7% fresh oil) and heated soybean oil (HSO) diet (contain 7% heated oil) were given to C57BL/6 mice for 4 weeks, respectively. The results from untargeted metabolomics analysis indicated that HSO treatment altered several groups of metabolites. The homeostasis of phospholipids species was affected by the HSO treatment. This result suggested that HSO feeding increased saturation level (16:0 and 18:0 fatty acids) but decreased unsaturation level (20:4 and 22:6 fatty acids) of serum and hepatic phospholipids. More importantly, results indicate that serum tryptophan was dramatically decreased but urinary tryptophan metabolites including kynurenic acid, nicotinamide, and nicotinamide *N*-oxide were increased by HSO treatment. Accordingly, hepatic NAD^+ level was dramatically increased by HSO treatment. The gene expression levels of three enzymes in the tryptophan-NAD^+ pathway were significantly induced by the HSO treatment. In terms of the role of NAD^+ as the indispensable cofactors or substrates of major metabolic events induced by HSO, including the detoxification of reactive aldehydes through aldehyde dehydrogenase, sustaining redox balance and DNA repair activities, and peroxisome proliferator-activated receptor α (PPARα)–mediated

metabolic reactions, the activation of tryptophan-NAD^+ pathway was identified as a central metabolic event induced by thermally-oxidized lipids.

KEYWORDS: frying oil, LC-MS, metabolomics, tryptophan, NAD^+

ABBREVIATIONS: ADG, average daily gain; ALDH, aldehyde dehydrogenases; BW, body weight; CSO, control soybean oil; D, day; DC, dansyl chloride; DEAB, 4-Diethylaminobenzaldehyde; DG, daily gain; FAA, free amino acid; FI, feed intake; G:F, gain:feed; GSH, glutathione; HCA, hierarchical clustering analysis; HMDB, human metabolome database; HPLC, high performance liquid chromatography; HQ, 2-hydrazinoquinoline; HSO, heated soybean oil; IACUC, Institutional Animal Care and Use Committee; KEGG, Kyoto encyclopedia of genes and genomes; LC-MS, liquid chromatography-mass spectrometry; LOPs, lipid oxidation products; LysoPC, lyso-phosphatidylcholines; m/z, mass to charge ratio; PC, phosphatidylcholines; PCA, principal components analysis; PE, phosphatidylethanolamine; PPARα, peroxisome proliferator-activated receptor α; QTOF, quadrupole time of flight mass spectrometry; SIC, single ion counts; TIC, total ion counts; UPLC, ultra-performance liquid chromatography.

4.2 INTRODUCTION

The health risk of consuming thermally-oxidized oils has been examined in epidemiological, clinical, and animal studies. The results from these studies suggested that moderately-oxidized oils had either limited or no detrimental effects on animals[122, 142]. However, feeding highly-oxidized oils led to apparent toxicities, including loss of appetite, diarrhea, growth retardation, increased kidney and liver weights, altered fatty acid composition of tissue lipids. These adverse effects have been attributed to the elevation of metabolic oxidative stress, the induction of peroxisome proliferator-activated receptor α (PPARα), and the impairment of intestinal function caused by consumption of thermally-oxidized oils[132, 143-148, 165, 253, 254].

The negative effects of thermally-oxidized oils are closely related to their chemical profiles. Thermal stress-induced chemical reactions extensively transform the chemical composition of heated oils, especially polyunsaturated fatty acids (PUFAs)-enriched vegetable oils[62, 216]. The lipid oxidation products (LOPs) of these reactions have been considered as major contributors to observed toxic effects of thermally oxidized oil[149]. For example, primary LOPs, such as conjugated lipid hydroperoxydienes, are acutely toxic to rodents[150], while secondary LOPs, such as 4-hydroxynonenal (4-HNE), 4-oxononenal (4-ONE), 4,5-epoxy-*trans*-2-decenal, and 9,12-dioxo-trans-10-dodecenoic acid can covalently bind to proteins and DNA, resulting in protein inactivation and DNA damage, which could contribute to the induction of disease such as cancer and cardiovascular disease[101, 131, 136, 154-161]. In addition, primary and secondary LOPs could

react with amino acids and lipids in the GI tract, thereby decreasing the digestibility of proteins and complex lipids[151].

Despite previous investigations on the biological effects of thermally-oxidized oils, many issues remain undefined, such as how thermally-oxidized oils affect nutrient metabolism *in vivo*. Instead of measuring a few traditional biomarkers, such as triacylglycerol (TAG) and cholesterol, the examination of complex metabolic events induced by thermally-oxidized oils require comprehensive evaluation of the metabolome, which could only be achieved by the high-throughput analytical platforms on small-molecule metabolites, such as metabolomics. Because of its capacity of defining metabolite profiles and fluxes in complex biological matrices as well as its capability in the identification of individual metabolite markers, metabolomics has been applied to investigate the metabolic differences and changes in many scientific fields[174-177]. However, metabolomic analysis of metabolic changes induced by the exposure of thermally-oxidized oils has not been carried out previously.

In the present study, the metabolic changes during a 4-week feeding of heated soybean oil (HSO) were evaluated by the liquid chromatography-mass spectrometry (LC-MS)-based metabolomic analysis of serum, urine, and liver extracts from the mice. The HSO-induced disruption of tryptophan metabolism was further characterized.

4.3 MATERIALS AND METHODS

4.3.1 Chemicals

LC-MS-grade water and acetonitrile (ACN) (Fisher Scientific, Houston, TX). 2-Hydrazinoquinoline (HQ) and triphenylphosphine (TPP) (Alfa Aesar, Ward Hill, MA).

2,2′-Dipyridyl disulfide (DPDS) (MP Biomedicals, Santa Ana, CA). Dansyl chloride (DC) and n-butanol (Sigma-Aldrich, St. Louis, MO). The metabolite standards used for structural confirmation were from Sigma-Aldrich, Fisher Scientific, Alfa Aesar, Ark Pharm **(**Libertyville, IL), Frontier Scientific (Logan, UT), and Steraloids (Newport, RI), respectively.

4.3.2 Preparation of experimental diets

Two experimental diets were prepared by mixing 7% (w/w) of control soybean oil (CSO) or HSO with fat-free AIN93G powder, respectively. The HSO sample were prepared based on the procedure descripted at materials and methods part in Chapter 3 (**3.3.2**). Briefly, soybean oil was placed in a round-bottom glass flask and then heated in an electric heating mantle. The temperature of soybean oil was gradually increased from room temperature (22^{o}C) to 185^{o}C in approximately 1 h with bubbling air (50 mL/min). Afterwards, the temperature was held constant at 185^{o}C for 6 h. The 6 h HSO sample was used for preparation of HSO diet. Based on the formulation of CSO and HSO diets (Table 4.1), the powders were thoroughly mixed by KitchenAid mixer Professional. After pelleting, two diets were dried and vacuum-sealed for storage at 4°C.

4.3.3 Animal experiments and sample collection

All animal protocols were approved by the Institutional Animal Care and Use Committee (IACUC) of the University of Minnesota. Ten-week-old male C57BL/6 mice were purchased from Charles River Laboratory and were housed under controlled temperature and lighting conditions (20-22°C and a 14-hour/10-hour light/dark cycle). The mice were allowed to acclimate on CSO diet before the treatment. Two separate

mouse feeding experiments were conducted to monitor growth performance and collect the samples for kinetic analysis, respectively. For growth performance, two groups of male C57BL/6 mice were fed with CSO and HSO diets, respectively, for 28 days. Body weight and food intake was monitored during the treatment. Liver samples were harvested on day 28 when the mice were sacrificed by CO_2 euthanization. For kinetic analysis, another two groups of male C57BL/6 mice were fed with CSO and HSO diets, respectively, for 28 days. Serum and urine samples were collected on day 0, 3, 7, 14, 21, and 28 of feeding. Serum samples were collected by submandibular facial bleeding while urine samples were obtained by housing mice individually in metabolic cages for 24 h. Liver samples were harvested on day 28. Cholesterol, TAG, glucose, and alanine transaminase (ALT) activity in mouse serum were measured using commercial assay kits (Pointe Scientific, Canton, MI).

4.3.4 *In vitro* analysis of HSO metabolism

Mouse liver was homogenized in ice-cold 0.25M sucrose aqueous solution containing 1% triton x-100 (W/V=10/90) to prepare the mouse liver homogenate. Then the substrates, including negative control (H_2O:DMSO=1:1), positive control (acetaldehyde:DMSO=1:1), CSO sample (CSO:DMSO=1:1) and HSO sample (HSO:DMSO=1:1), were incubated with mouse liver homogenates in sodium pyrophosphate reaction buffer with or without NAD^+ (cofactor) at 37^{o}C for 30 min. The reaction mixture was derivatized with HQ and then introduced to the LC-MS system for data collection. 4-Diethylaminobenzaldehyde (DEAB), an established aldehyde

dehydrogenases (ALDH) inhibitor [255], was used to determine whether ALDHs are responsible for the observed changes in aldehyde level after the incubation.

4.3.5 Metabolomics

LC-MS-based metabolomic analysis comprises sample preparation, chemical derivatization, LC-MS analysis, data deconvolution and processing, multivariate data analysis, and marker characterization and quantification[190].

4.3.5.1 Sample preparation

Urine sample was processed by mixing one volume of urine with 4 volumes of 50% aqueous ACN and then centrifuged at 18,000 × *g* for 10 min to obtain the supernatants. Serum sample was deproteinized and extracted by mixing one volume of serum with 19 volumes of 66% aqueous ACN. After vortexing, the mixture was centrifuged at 18,000 × *g* for 10 min to obtain the supernatants. Liver tissue samples were fractionated using a modified Bligh and Dyer method[191]. Briefly, 100 mg of liver sample was homogenized in 0.5 mL of methanol and then mixed with 0.5 mL of chloroform and 0.4 mL of water. After 10 min centrifugation at 18,000 × *g*, upper aqueous fraction was harvested while chloroform fraction was dried by nitrogen and then reconstituted in n-butanol.

4.3.5.2 Chemical derivatization

For detecting the metabolites containing amino functional group in their structures, the samples were derivatized with DC prior to the LC-MS analysis. Briefly, 5 μL of sample or standard was mixed with 5 μL of 100 μM *p*-chlorophenylalanine (internal standard), 50 μL of 10 mM sodium carbonate, and 100 μL of DC solution (3 mg/mL in acetone). The mixture was incubated at 25°C for 15 min and centrifuged at 18,000 × *g* for

10 min, the supernatant was transferred into a HPLC vial for LC-MS analysis. For detecting carboxylic acids, aldehydes and ketones, the samples were derivatized with HQ prior to the LC-MS analysis[192]. Briefly, 2 µL of sample was added into a 100 µL of freshly-prepared ACN solution containing 1 mM DPDS, 1 mM TPP and 1 mM HQ. The reaction mixture was incubated at 60°C for 30 min, chilled on ice and then mixed with 100 µL of ice-cold H_2O. After centrifugation at 18,000 × *g* for 10 min, the supernatant was transferred into a HPLC vial for LC-MS analysis.

4.3.5.3 LC-MS analysis

A 5 µl of aliquot prepared from urine, serum, and hepatic extract sample, was injected into an Acquity ultra-performance liquid chromatography (UPLC) system (Waters, Milford, MA) and separated in a BEH C18 column (Waters). The mobile phase for underivatized and DC-derivatized samples used a gradient ranging from water to 95% aqueous ACN containing 0.1% formic acid over a 10 min run, while the mobile phase for HQ-derivatized samples contained A: H_2O containing 0.05 % acetic acid (v/v) and 2 mM ammonium acetate; B: H_2O:ACN = 5:95 (v/v) containing 0.05 % acetic acid (v/v) and 2 mM ammonium acetate. LC eluant was introduced into a Xevo-G2-S quadrupole time-of-flight mass spectrometer (QTOFMS, Waters) for accurate mass measurement and ion counting. Capillary voltage and cone voltage for electrospray ionization was maintained at 3 kV and 30 V for positive-mode detection, or at -3 kV and -35 V for negative-mode detection, respectively. Source temperature and desolvation temperature were set at 120°C and 350°C, respectively. Nitrogen was used as both cone gas (50 L/h) and desolvation gas (600 L/h), and argon as collision gas. For accurate mass measurement,

the mass spectrometer was calibrated with sodium formate solution with mass-to-charge ratio (*m/z*) of 50-1,000 and monitored by the intermittent injection of the lock mass leucine enkephalin ($[M+H]^+$ = *m/z* 556.2771 and ($[M-H]^-$ = *m/z* 554.2615) in real time. Mass chromatograms and mass spectral data were acquired and processed by MassLynx^{TM} software (Waters) in centroided format. Additional structural information was obtained tandem MS (MSMS) fragmentation with collision energies ranging from 15 to 40 eV.

4.3.5.4 Data deconvolution and processing

After data acquisition in the UPLC-QTOFMS system, chromatographic and spectral data of samples were deconvoluted by MarkerLynx^{TM} software (Waters). A multivariate data matrix containing information on sample identity, ion identity (retention time and *m/z*) and ion abundance was generated through centroiding, deisotoping, filtering, peak recognition and integration. The intensity of each ion was calculated by normalizing the single ion counts (SIC) *versus* the total ion counts (TIC) in the whole chromatogram.

4.3.5.5 Multivariate data analysis

The processed data matrix was exported into SIMCA-P+^{TM} software (Umetrics, Kinnelon, NJ), transformed by *Pareto* scaling, and then analyzed by unsupervised principal components analysis (PCA), supervised partial least squares-discriminant analysis (PLS-DA), and partial least squares-discriminant analysis (OPLS-DA). Major latent variables in the data matrix were determined as the principal components of PCA model, and the relationships among examined samples were described in the scores

scatter plot. Metabolite markers of HSO treatment were identified by analyzing ions contributing to sample separation in PLS-DA and OPLS-DA model.

4.3.5.6 Marker characterization and quantification

The chemical identities of metabolite markers were determined by accurate mass measurement, elemental composition analysis, searching Human Metabolome Database (HMDB), Kyoto Encyclopedia of Genes and Genomes (KEGG), and Lipid Maps databases using MassTRIX search engine (http://masstrix3.helmholtz-muenchen.de/masstrix3/)[193], MSMS fragmentation, and comparisons with authentic standards if available. Individual metabolite concentrations were determined by calculating the ratio between the peak area of metabolite and the peak area of internal standard and fitting with a standard curve using QuanLynx^{TM} software (Waters).

4.3.6 Gene expression analysis

TRIzol reagent was used to extract total RNA from the liver samples of C57BL/6 mice. With SuperScript III Reverse Transcriptase, cDNA generated from 1 µg total RNA was used for quantitative real-time PCR (qPCR). Primers for the PCR reaction were designed using NCBI/Primer-BLAST (http://www.ncbi.nlm.nih.gov/tools/primer-blast/). SYBR green PCR master mix was used to carry out qPCR reactions in a StepOnePlus system (Applied Biosystems). Using β-actin as reference gene, the expression levels of genes were quantified using the Comparative CT method. Gene expression levels of acyl-CoA thioesterase 1 (*Acot1*), cluster of differentiation 36 (CD36), NAD(P)H dehydrogenase [quinone] 1 (*Nqo*1), phospholipid transfer protein (*Pltp*), carnitine palmitoyltransferase I (*Cpt1*), carnitine palmitoyltransferase II (*Cpt2*)**,** heme

oxygenase1(*HO1*), tryptophan 2,3-dioxygenase (*Tdo*), indoleamine 2,3-dioxygenase (*Ido2*), kynureninase (*Kynu*), kynurenine 3-monooxygenase (*Kmo*), 3-hydroxyanthranilate 3,4-dioxygenase (*Haao*), and quinolinate phosphoribosyltransferase (*Qprt*), were determined by real-time PCR analysis. The primer sequences are listed in Table 4.2.

4.3.7 Statistics

Experimental values are expressed as means ± SD. Two-tailed Student's *t*-test was used for comparisons between CSO and HSO treatments. Differences were considered significant if $P < 0.05$.

4.4 RESULTS

4.4.1 Influences of HSO on growth performance

To examine the metabolic impacts of HSO consumption, the body weight and feed intake of two groups of young mice were compared during a 4-week feeding of CSO and HSO diets. The results showed that, compared to CSO, HSO significantly decreased the average daily gain (ADG) of body weight (Figure 4.1A) even though the feed intake (FI) was comparable between these two groups (Figure 4.1B). Overall, HSO resulted in a much lower feeding efficiency than CSO, as represented by the ratio of ADG *versus* FI (Figure 4.1C). Consistent to several previous reports, these results confirmed the negative effects of thermally-oxidized lipids on the growth performance[144, 148].

4.4.2 Influences of HSO feeding on blood chemistry

To further understand the negative impacts of HSO on growth performance and physiology, serum samples collected at different time points during 4-week feeding of

CSO or HSO were analyzed for their blood chemistry. Serum glucose and TAGs levels were significantly decreased by HSO (Figure 4.2A-B). However, serum cholesterol level was not affected by HSO (Figure 4.2C). The influences of HSO feeding on the liver were also evaluated. Serum ALT activity, an enzymatic marker of liver function, was not affected by HSO (Figure 4.2D). However, the value of hepatosomatic index, which is calculated by the ratio of liver weight versus body weight, was higher in HSO-treated mice than that in CSO-treated mice (Figure 4.2E). Consistent to the changes in serum, hepatic TAG level was significantly decreased by the HSO treatment (Figure 4.2F).

4.4.3 HSO-induced changes in urine, serum, and hepatic metabolomes

The changes in growth performance, blood chemistry, and hepatic parameters indicated significant impacts of HSO on the metabolic system. To define the metabolic effects of HSO treatment, the LC-MS based metabolomics analysis was carried out to evaluate the urine, serum, and liver extract samples collected from 4-week feeding of CSO and HSO diets. Besides adopting optimized mobile phase, ionization condition and MS parameters, efficient chromatographic separation and sensitive spectroscopic detection of diverse metabolite in these samples were also facilitated by chemical derivatization in sample preparation, such as dansylation for amino-containing metabolites and HQ derivatization for carboxylic acids, aldehydes and ketones[192]. After processing the data acquired from the LC-MS analysis, the metabolomic profiles of these samples were characterized in the multivariate models. The distribution of CSO and HSO samples in the PLS-DA model on urine samples indicated that HSO induced progressive changes in the urine metabolome along the principal component 1 of the model, while the

metabolite profile of CSO urine samples were relatively stable during 4-week feeding (Figure 4.3A). Urinary metabolites contributing to the separation of CSO and HSO samples in the model were identified in a loadings plot (Figure 4.3B, Table 4.3, Table 4.4). The PLS-DA model on the serum metabolome also revealed the time-dependent changes induced by HSO (Figure 4.3C), accompanied by the changes in serum metabolites (Figure 4.3D, Table 4.4). Moreover, after 4-week feeding, the hepatic metabolome in HSO-fed mice was distinctively different from its counterpart in CSO-fed mice (Figure 4.3E). Subsequently, the liver metabolites affected by HSO were identified (Figure 4.3F, Table 4.4). Overall, more than 62 metabolites in different biological samples (urine, serum, and liver) were identified as HSO-responsive metabolites (Table 4.4). Based on their origins and biochemical properties, these metabolite markers were further categorized as the indicators of HSO exposure, lipid metabolism, and amino acid metabolism (Table 4.4).

4.4.4 Identification of exposure markers of HSO treatment

Among the metabolites contributing to the separation of HSO and CSO samples in the multivariate models (Figure 4.3), several urinary metabolites could serve as the exposure markers of HSO treatment because they barely existed in the CSO samples but were greatly increased by HSO treatment (Figure 4.4, Table 4.3). Even though the structures of these urinary markers are not fully determined yet, the results from elemental composition analysis and MSMS fragmentation indicated the existence of two clusters of HSO-derived metabolites that share similar structural features (Table 4.3). One cluster of these exposure markers are three isomers that shared the same molecular

formula of $C_{12}H_{20}NO_3^+$ and almost identical MSMS fragmentograms, but with different retention time (Table 4.3). Analyzing the fragments in MSMS fragmentograms suggested that they are likely to be the glycine conjugates of hydroxydecenoic acid (Figure 4.4A). Their levels in the urine was shown to be greatly increased by the HSO treatment (Figure 4.4B). The other cluster of 5 exposure markers shared a molecular formula of $C_nH_{2n-2}O_3$ (n=5-10) and a similar fragmentation pattern in MSMS analysis. Analyzing the fragments in MSMS fragmentograms suggested that they are likely to be hydroxyalkenoic acids, which could be formed by ALDH-mediated oxidation of hydroxyalkenals (Figure 4.4C-F). Further studies are required to confirm the structures of these exposure markers.

4.4.5 Effects of HSO treatment on lipids metabolism

The influences of HSO on lipid metabolism were revealed by the changes in phospholipids in serum and the liver. The levels of phosphatidylcholines (PC) (18:0/22:6) and PC (18:0/20:4) in serum and the liver were decreased by HSO treatment (Figure 4.5A-D). In contrast, the levels of PC (16:0/18:1) and PC (16:1/16:0) in serum and the liver were increased by HSO treatment (Figure 4.5E-H). The levels of PC (18:1/18:0) and lysophosphatidylethanolamine (LysoPE) (16:0) in the serum, while the levels of PC (16:0/20:3), PC (16:0/20:4), PC (16:0/22:6), and PC (18:1/20:4) in the liver were increased by HSO treatment (Table 4.4). On the contrary, the levels of PC (16:1/20:4), PC (18:2/22:6), PC, PC (16:1/18:2), lysophosphatidylcholine (LysoPC) (22:6), and LysoPC (18:2) in the serum, while the levels of PC (18:0/18:2), PC (16:0/18:2), phosphatidylethanolamine (PE) (18:0/22:6), PC (16:1/18:2), PE (18:2/18:1), LysoPC (18:0), and PC (18:2/22:6) in the liver were decreased by HSO treatment (Table 4.4).

This result suggested that HSO feeding increased saturation level (16:0 and 18:0 fatty acids) and decreased unsaturation level (20:4 and 22:6 fatty acids) in serum and liver lipids, which is consistent with the observed changes in the triglyceride composition of HSO (Figure 3.6).

4.4.6 Effects of HSO treatment on amino acid profile and tryptophan metabolism

Following the observation of amino acids as the metabolites affected by the HSO treatment in the multivariate model (Figure 4.3D and F), the concentrations of free amino acids in serum and the liver were quantified (Figure 4.6A, Table 4.4). Different levels of phenylalanine, citrulline, histidine, and tryptophan were observed between CSO and HSO serum samples (Figure 4.6B-E). Among them, serum tryptophan level in HSO samples was consistently lower than its level in CSO samples from day 3 of HSO feeding (Figure 4.6E), suggesting that serum tryptophan level is sensitive to HSO treatment. Interestingly, tryptophan metabolites, kynurenic acid, nicotinamide, and nicotinamide *N*-oxide, were identified as the urinary metabolites responsive to HSO feeding in the PLS-DA model of urine samples (Table 4.4). Similar to the kinetic profile of serum tryptophan, the increase of these tryptophan metabolites in urine also occurred early in 4-week HSO feeding (Figure 4.7A-C). Most importantly, hepatic NAD^+ level was dramatically increased by HSO treatment (Figure 4.7D). All together, these results suggested that tryptophan catabolism was activated by the HSO treatment. Analyzing the gene expression levels of tryptophan-metabolizing enzymes further confirmed this conclusion since the mRNA

levels of *Tdo*, *Kynu*, and *Qprt*, three enzymes in the tryptophan-NAD^+ pathway, were significantly induced by the HSO treatment (Figure 4.7E,F).

PPARα has been identified as a positive regulator of tryptophan-NAD^+ pathway in previous studies[256, 257]. To examine the underlying mechanism of HSO-induced upregulation of tryptophan-NAD^+ pathway, the expression levels of PPARα target genes in the transport and catabolism of fatty acids and lipids, including *Acot1*, *CD36*, *Pltp*, *Cpt1*, and *Cpt2*, were measured. The results showed that all these PPARα target genes were transcriptionally activated by the HSO treatment (Figure 4.8).

The significance of HSO-induced upregulation of tryptophan-NAD^+ pathway was further defined by examining the utilization of NAD^+ in the metabolism of HSO and its reactive aldehydes through *in vitro* incubations of mouse liver homogenate. The incubation of HSO with mouse liver homogenate resulted in much higher rate of NAD^+ elimination than the incubation of CSO while the coincubation of HSO with DEAB, the inhibitor of ALDHs, completely suppressed the HSO-elicited NAD^+ utilization (Figure 4.9A). Furthermore, the elimination and metabolism of 4-HNE and 2,4-decadienal, two major reactive aldehydes in HSO, were facilitated by including NAD^+ in their incubations with mouse liver homogenate (Figure 4.9B).

4.4.7 Effects of HSO treatment on redox balance and antioxidant system

Besides the changes in lipid and amino acid metabolism, HSO feeding also significantly decreased the levels of glutathione (GSH) and ascorbic acid, two important antioxidants, in the liver (Figure 4.10A). Further examination of the gene expression levels of *Nqo1* and *HO1* showed significant induction of these two marker enzymes of

antioxidant response (Figure 4.10B), suggesting that the antioxidant response system was activated by the HSO-induced oxidative stress.

4.4.8 Effects of HSO treatment on other types of metabolites.

Besides the above mentioned metabolites, HSO treatment also affected other types of metabolites. Urinary metabolite such as suberic acid, azelaic acid, phenylpyruvic acid, as well as hepatic metabolites including gluconic acid, adenosine, and adenosine monophosphate, were increased by HSO treatment. On the other side, HSO feeding decrease the levels of urinary metabolites such as octenoylglycine, 2-sec-butyl-4,5-dihydrothiazole, pantothenic acid, hippuric acid, 4-hydroxyphenylacetic acid, serum acetylcarnitine, as well as hepatic metabolites including malic acid, glycerophosphocholine, hypoxanthine, xanthine, and taurodeoxycholic acid (Table 4.4).

4.5 DISCUSSION

Decrease in growth performance has been consistently observed in previous feeding studies on oxidized lipids[148, 258-260]. Reduced feed intake was observed in some studies, but not in all studies[261, 262]. Therefore, besides feed intake, oxidized lipids-induced metabolic changes may also contribute to the decrease in growth performance. In the present study, HSO feeding decreased body weight gain and feeding efficiency (the ratio of body weight gain *versus* food intake), but had no effect on food intake (Figure 4.1). These observations further implied that HSO might affect the growth performance through the disruption of metabolic system, such as nutrient and energy metabolism.

To further evaluate the metabolic effects of HSO, the levels of serum glucose, TAGs, and cholesterol were measured. Glucose decreased after two weeks of HSO treatment.

Similar to the previous studies[162, 163], the serum level of TAGs was decreased by the HSO treatment from day 7 and the hepatic level of TAGs was also decreased. The decrease of TAGs could be attributed to the activation of nuclear receptor PPARα since the compounds generated during the heating process could serve as PPARα activators, inducing the PPARα target genes such as *Acot1*, *CD36*, *Cpt1* and *Cpt2*[163-167]. In the present study, the induction of these PPARα target genes were also observed (Figure 4.8). Serum and hepatic levels of cholesterol were not affected by the HSO treatment even though *Srebp2* was shown to be inhibited by the HSO treatment (data not shown). Despite these changes in liver metabolites, no apparent liver damage was observed as indicated by the serum ALT activity. HSO feeding in the present study induced hepatic proliferation as reflected by the enlarged liver. In the feeding studies of oxidized lipids, the enlargement of liver were recognized as a typical response to the PPARα agonists in oxidized lipids which induce peroxisome proliferation[170, 171].

Growth performance and blood chemistry reflect the general status of metabolic system, but do not reveal its exact status due to their limited coverage. Comprehensive coverage of HSO-induced metabolic changes was achieved by the LC-MS-based metabolomic analysis (Figure 4.3). The results from metabolomic analysis of diverse samples, including urine, serum, and liver, not only defined the global impacts of HSO on metabolic systems through multivariate modeling, but also revealed previously unreported changes through the identification and characterization of metabolite markers (Figure 4.3-4.7, Table 4.4). The significance of these metabolite markers are discussed based on their sources and biochemical functions.

Monitoring and measuring exposure of HSO is important to evaluate the correlation between HSO intake and biological effects of HSO treatment. The decreases of TAGs were recognized as common responses to oxidized lipid treatment. However, the change of TAGs level was caused by PPARα activation, which could also be observed in animals which were treated with other PPARα agonist such as fenofibrate. Thus, finding specific markers for treatment of oxidized lipid is important in confirming the effects of HSO treatment. In the present study, several exposure markers of HSO treatment were found through metabolomics analysis. Among them, three isomers with the masses ($[M+H]^+$ = 226.1437) were proposed to be glycine conjugation metabolites of aldehydes from the HSO. The first step of aldehydes metabolism was known to be carried out by ALDH. In the present study, *in vitro* assay showed that the aldehydes in HSO could be metabolized by ALDH with NAD^+ as cofactor (Figure 4.9). The identification of glycine conjugation metabolites suggested that the aldehydes in HSO may be metabolized by ALDH first and then be further metabolized to glycine conjugation products. At the same time, the present of a series of hydroxyalkenoic acids in the urine were proposed to be formed by ALDH-mediated oxidation of hydroxyalkenals from HSO. As one important component of HSO, aldehydes were known for causing protein inactivation and DNA damage[101, 131, 136, 154-161]. In the present study, aldehydes induced oxidative stress could be reflected by the decreased GSH and ascorbic acid in the liver (Figure 4.10A, Table 4.4) and inductions of oxidative stress scavenger genes such as *Nqo1* and *HO1* (Figure 4.10B). Thus, the identification of these exposure markers are important in evaluating the effects of HSO exposure (Figure 4.4).

Phospholipids are important components of cell membrane[201]. The observed changes in hepatic and serum phospholipids (Figure 4.3D,F, Figure 4.5, Table 4.4) implicated that HSO could disrupt plasma membrane through altering its composition. From the changing pattern of phospholipid markers, the decrease of phospholipids containing linoleic acid, arachidonic acid, and docosahexaenoic acid as well as the increase of phospholipids containing palmitic acid, palmitoleic acid, or oleic acid were found in serum and liver (Figure 4.5, Table 4.4). Considering food source is the major source of these long-chain unsaturated fatty acids, this pattern of change should be associated with the decreased unsaturation level of HSO during heating process. Because previous studies showed that blood phospholipid fatty acid concentration was associated with cardiovascular disease and cancer[263-265], the changes of phospholipids caused by HSO treatment worth further evaluations in the future.

Free amino acids (FAAs) are useful indicators of nutritional and metabolic status because they are connected with diverse metabolic pathways[194]. Several features were identified among the changes in FAAs and their associated metabolites: First, among the FAAs which were changed by the HSO treatment during 28 days, citrulline was increased in both serum and liver. Considering the decreased antioxidants level and induced antioxidant response system in liver (Figure 4.10), the increase of citrulline may indicate an increase of nitric oxide in response to the oxidative stress because the role of nitric oxide in regulating mitochondrial oxidative stress protection[266]. Second, serum tryptophan level was consistently decreased by the HSO treatment after Day 3 (Figure 4.6E). Because dietary tryptophan was shown to be related to the growth performance[267],

the reduced growth in the present study may be related to the decrease level of serum tryptophan. Since tryptophan is an essential amino acid, this pattern of changes suggests that HSO can significantly disrupt tryptophan metabolism.

In the present study, tryptophan in serum was greatly decreased by HSO treatment (Figure 4.6E), while several major catabolic metabolites of tryptophan in urine including kynurenic acid, nicotinamide, and nicotinamide *N*-oxide, were increased by HSO treatment (Figure 4.7A-C). These observations suggested that HSO treatment disrupted tryptophan metabolism. In the body, tryptophan can be metabolized through two routes. About 95% of tryptophan are metabolized via the tryptophan-kynurenine-NAD^+ pathway[268]. While the remained portion of tryptophan are metabolized through tryptophan-serotonin pathway. Following the tryptophan-NAD^+ pathway, tryptophan is metabolized by TDO primarily in the liver, or IDO predominantly in extra-hepatic tissue. Several other enzymes along NAD^+ pathway include *Kmo*, *Kynu*, *Haao*, and *Qprt*. In the present study, the selective induction of *Tdo*, *Kynu*, and *Qprt* in the liver, as well as dramatic increase of hepatic NAD^+ provide further support for the induction of tryptophan-NAD^+ metabolism pathway. The need for the induction of tryptophan-NAD^+ pathway in the body could be attributed to several reasons. First of all, as the major products of tryptophan-NAD^+ pathway, NAD^+ was needed in fatty acid β-oxidation as cofactor which was induced by the activation of PPARα. PPARα has been identified as a positive regulator of tryptophan-NAD^+ pathway in previous studies [256, 257]. In the present study, as reflected by the increased expression of several PPARα targeted genes as well

as the decrease of TAGs, pantothenic acid, and acetalcarnitine in the body, fatty acid β-oxidation was induced be HSO treatment, which demand increase needs of NAD^+. Second, the aldehyde species in HSO, once inside body, need to be metabolized to organic acids for detoxification. In this ALDH mediated process, NAD^+ plays the important role as the cofactor in the body. Thus, the demand of NAD^+ could also be contributed to this step. Third, directly in mitochondrial compartment and indirectly in other locations, NAD^+ could also function as a free radical scavenger [269, 270]. The demand of NAD^+ could also be caused by the increase of oxidative stress which was reflected by the decreased GSH and ascorbic acid in the liver, and inductions of oxidative stress scavenger genes such as *Nqo1* and *HO1* (Figure 4.10). Finally, NAD^+ has been shown to function as a substrate for poly (ADP-ribose) polymerases (PARPs) which could play multiple roles in DNA damage responses such as DNA repair [271, 272]. Higher cellular NAD^+ levels has been demonstrated to enhance the recovery of cell from DNA damage [273]. In view of secondary LOPs such as aldehydes were known to damage DNA[101, 131, 136, 154-161]. the demand for DNA recovery may be one of the reasons for activation of tryptophan-NAD^+ pathway. Thus, putting all above information together, NAD^+ was identified to be the key connecting point for the changes of metabolic system which was caused by the HSO administration.

Except the crucial NAD^+, HSO treatment also caused changes in levels of other metabolites. Adenosine can be produced from different sources including the adenine nucleotides ATP, ADP, and AMP [274, 275]. Previous study had shown that the transporting activity of adenine nucleotide translocator (ANT) which is the import in ADP/ATP

transportation in mitochondria, was inhibited by unsaturated aldehydes such as 4-HNE [276]. Since thermally oxidized oil have large varieties of unsaturated aldehydes including 4-HNE, the increase of adenosine in the livers from HSO treated mice may be caused by the interruption of ANT activity. Previous study showed that the levels of pantothenic acid and acetylcarnitine were decreased in both human and mice urine with fenofibrate administration, probably due to the need of pantothenic acid and acetylcarnitine in fatty acid β-oxidation inside mitochondria[277]. In the present study, the decrease of pantothenic acid and acetylcarnitine in HSO treatment may also be caused by the activation of PPARα. In the body, the decrease of hippuric acid could be caused by the limit availability of CoA because benzoic acid need CoA to be converted to benzoyl CoA first and then changed into hippuric acid[278]. In the mice fed with HSO, the induction of fatty acid β-oxidation via PPARα pathway increase the demand of CoA, which may be the reason for the decrease formation and excretion of hippuric acid.

In conclusion, comprehensive metabolomic analysis of diverse biological samples in this study revealed novel HSO-induced metabolic effects. Changes in identified metabolite markers indicated that HSO treatment increased saturation level of lipids and induced tryptophan-kynurenine-NAD^+ pathway in the body. All these observations warrant further investigations on the mechanism behind HSO intake induced biological effects.

Table 4.1. Ingredients and formulation of CSO and HSO diets

	Diet	
Ingredients (gram)	CSO	HSO
Casein	200.00	200.00
L-Cystine	3.00	3.00
Sucrose	100.00	100.00
Cornstarch	397.50	397.50
Dyetrose	132.00	132.00
Cellulose	50.00	50.00
Mineral Mix	35.00	35.00
Vitamin Mix	10.00	10.00
Choline Bitartrate	2.50	2.50
CSO	70.00	0.00
HSO	0.00	70.00
Total	1000.00	1000.00

Table 4.2. The primer sequences of genes.

Gene	Forward primer (from 5' to 3')	Reverse primer (from 5' to 3')
Acot1	TTGCACATGCGGTGCACGAG	AGGAAAGGGTCCAGGTTCTGG
CD36	TGAATTAGTAGAACCGGGCCAC	AGCCCATTCTCCTCGTGCAGCA
Nqo1	CTCTGGCCGATTCAGAGTGGCA	GATCTGCATGCGGGCATCTGGT
Pltp	TATAAAGGCTGCTGGACCCGCG	GGACCATGGCGACCAAGCTTA
Cpt1	ACACCACTGGCCGCATGTCAAG	TGCCGTGCTCTGCAAACATCCA
Cpt2	TGCCCAGGCTGCCTATCCCTAA	GCAGCTCCTTCCCAATGCCGTT
HO1	AGCATAGCCCGGAGCCTGAATC	CAAATCCTGGGGCATGCTGTCG
Tdo	ATGAGTGGGTGCCCGTTTG	GGCTCTGTTTACACCAGTTTGA
Ido2	CGGGGCTTCATCCTAGTGAC	TTCCCTGAACCAGGGCCTTA
Kynu	TAAGCCTACTCCAAAGCGGC	AAGGTCTCTTCCCCCTCTCG
Kmo	AGGGAAGATATTCGCGTGGC	AGGCCTGCCGTCCTCTATAA
Haao	CAGGAGGGCTCCTCTAAGGT	GCTCCCACACATACGAGGTT
Qprt	GTGGAATGTAGCAGCCTGGA	TGCAGCTCCTCAGGCTTAAA
Actin	TCCATCATGAAGTGTGACGTT	TGTGTTGGCATAGAGGTCTTTA

Table 4.3. Exposure markers of HSO treatment.

RT	Exact Mass of $[M+H]^+$	Formula of detected ions	Metabolite formula	Potential structures (based on MSMS fragmentograms)
3.50	258.1232†	$C_{14}H_{16}O_2N_3^+$	$C_5H_8O_3$	Hydroxy-pentenoic acid
3.86	272.1377†	$C_{15}H_{18}O_2N_3^+$	$C_6H_{10}O_3$	Hydroxy-hexenoic acid
5.49	286.1543†	$C_{16}H_{20}O_2N_3^+$	$C_7H_{12}O_3$	Hydroxy-heptenoic acid
4.74	300.1700†	$C_{17}H_{22}O_2N_3^+$	$C_8H_{14}O_3$	Hydroxy-octenoic acid
5.29	328.2015†	$C_{19}H_{26}O_2N_3^+$	$C_{10}H_{18}O_3$	Hydroxy-decenoic acid
3.74	226.1440	$C_{12}H_{20}NO_3^+$	$C_{12}H_{19}NO_3$	Glycine conjugate of hydroxydecenoic acid
3.94	226.1433	$C_{12}H_{20}NO_3^+$	$C_{12}H_{19}NO_3$	Glycine conjugate of hydroxydecenoic acid
4.05	226.1428	$C_{12}H_{20}NO_3^+$	$C_{12}H_{19}NO_3$	Glycine conjugate of hydroxydecenoic acid

†Information on each compound includes its retention time (RT), molecular formula, the formula of its HQ derivative, and the exact mass of protonated HQ derivative ($[M+H]^+$).

Table 4.4. Effects on HSO treatment on urinary, serum, and hepatic metabolomes.*

	Markers increased by HSO	**Markers decreased by HSO**
Urine	Hydroxy-pentenoic acid, hydroxy-hexenoic acid, hydroxy-heptenoic acid, hydroxy-octenoic acid, hydroxy-decenoic acid, glycine conjugates of hydroxydecenoic acid, kynurenic acid, nicotinamide, nicotinamide n-oxide, suberic acid, azelaic acid, phenylpyruvic acid	Octenoylglycine, 2-sec-butyl-4,5-dihydrothiazole, pantothenic acid, hippuric acid, 4-hydroxyphenylacetic acid
Serum	PC(16:0/18:1), PC(18:1/18:0), PC (16:1/16:0), LysoPE(16:0) citrulline, histidine, phenylalanine	Tryptophan, PC(16:1/20:4), PC(18:2/22:6), PC(18:0/22:6), PC(18:0/20:4), PC(16:1/18:2), LysoPC(22:6), LysoPC(18:2), acetylcarnitine
Liver	Proline, citrulline, histidine, gluconic acid, PC(16:0/20:3), PC(16:0/20:4), PC(16:0/22:6), PC(16:0/18:1), PC(16:1/16:0), PC(18:1/20:4), adenosine, adenosine monophosphate (AMP)	PC(18:0/18:2), PC(18:0/20:4), PC(18:0/22:6), PC(16:0/18:2), PE(18:0/22:6), PC(16:1/18:2), PE(18:2/18:1), LysoPC(18:0), PC(18:2/22:6), malic acid, glycerophosphocholine, GSH, ascorbic acid, hypoxanthine, xanthine, taurodeoxycholic acid

*Enlisted metabolites are the ones that were significantly affected by HSO and also had their structures identified by either authentic standards or MSMS fragmentograms.

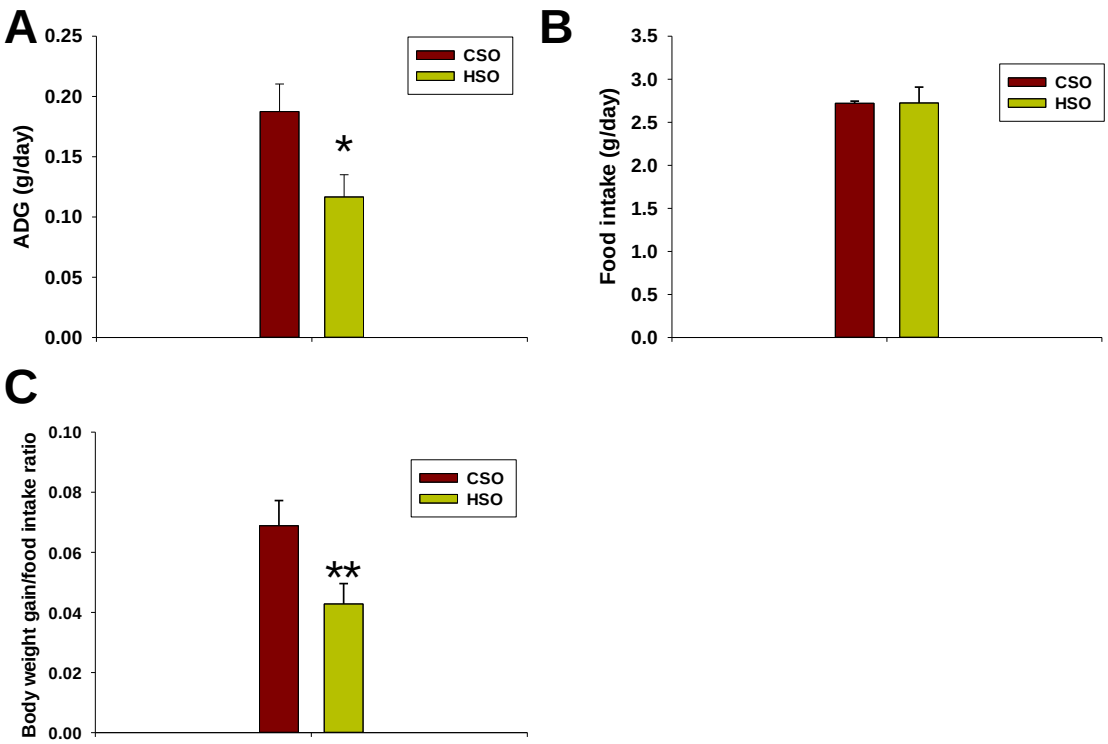

Figure 4.1. The effects of HSO treatment on growth performance. ***A.*** Average daily body weight gain ***B.*** Food intake. ***C.*** Ratio between body weight gain and food intake.

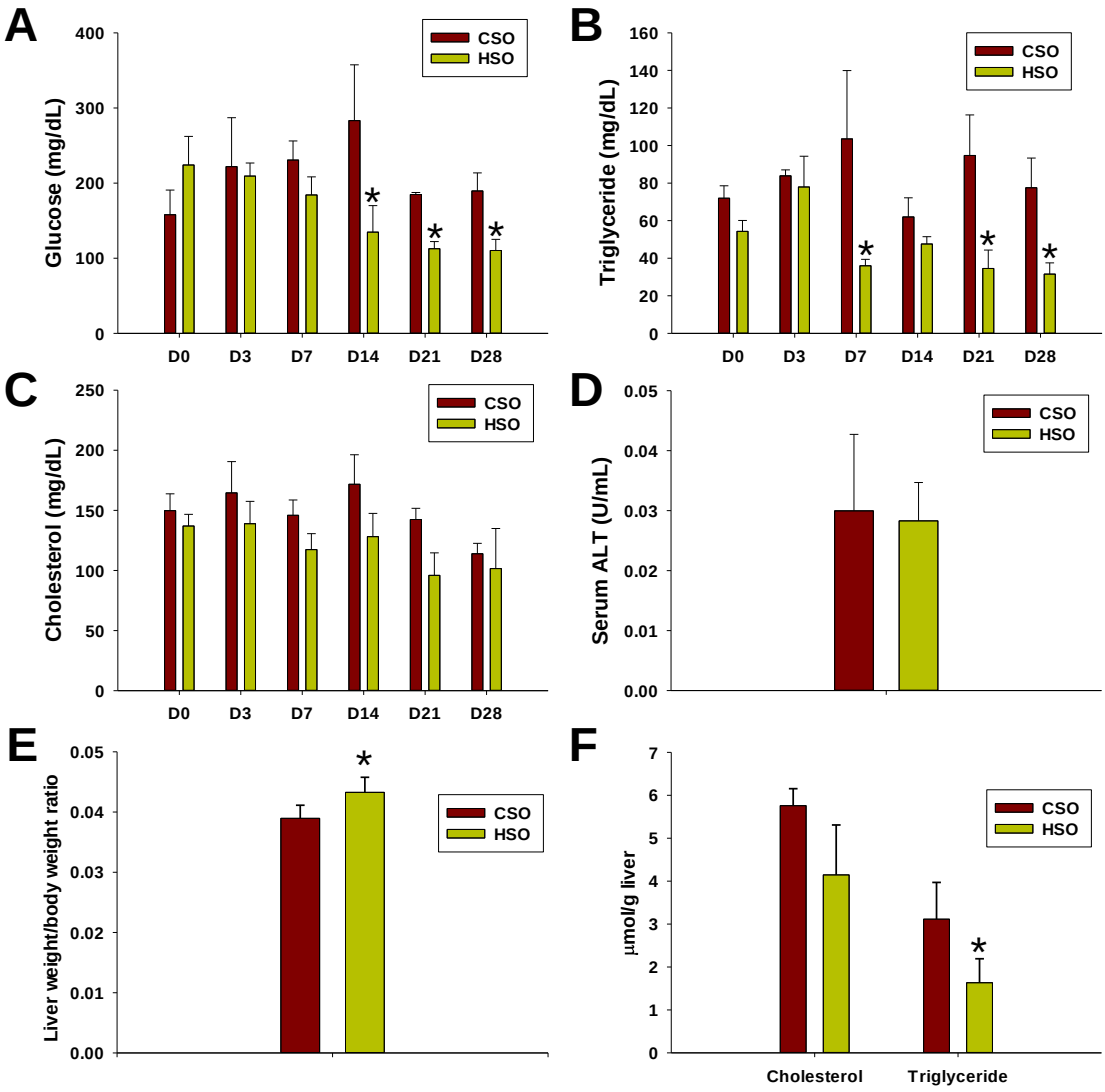

Figure 4.2. The effects of HSO treatment on general biochemical parameter and hepatosomatic index. ***A.*** Serum glucose. ***B.*** Serum triglyceride. ***C.*** Serum cholesterol. ***D.*** Serum ALT activity. ***E.*** Hepatosomatic index. ***F.*** Hepatic cholesterol and triglyceride.

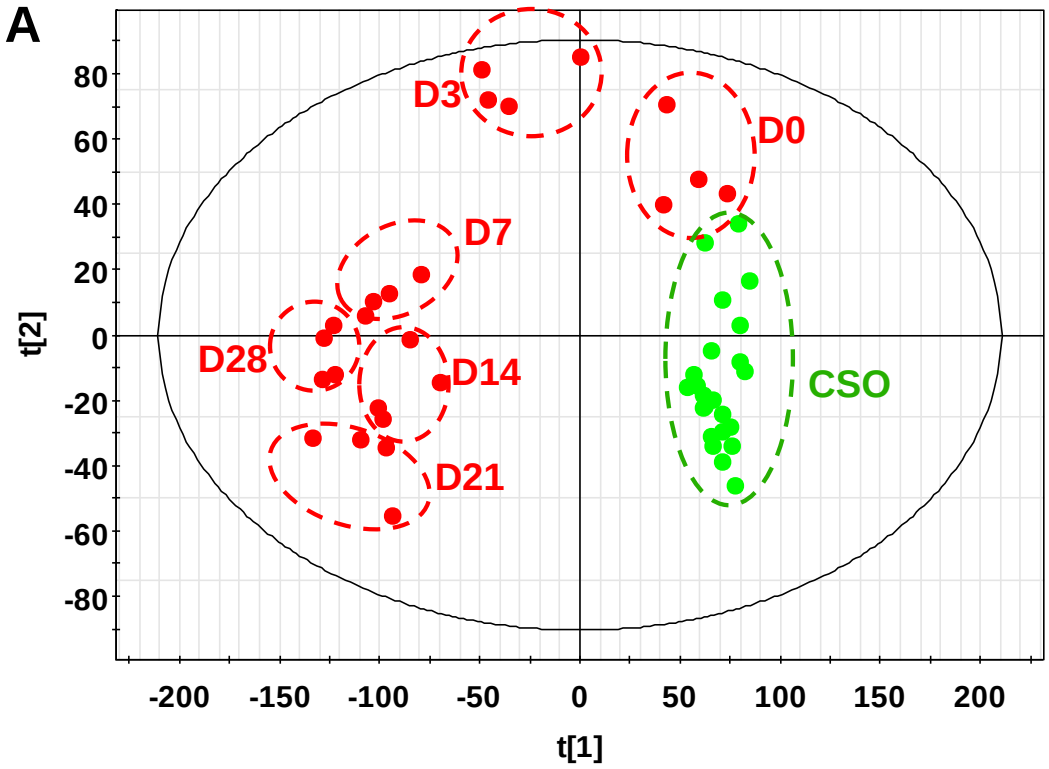
A
D3
D0
D7
D28
D14
CSO
D21
t[2]
t[1]
80
60
40
20
0
-20
-40
-60
-80
-200
-150
-100
-50
0
50
100
150
200

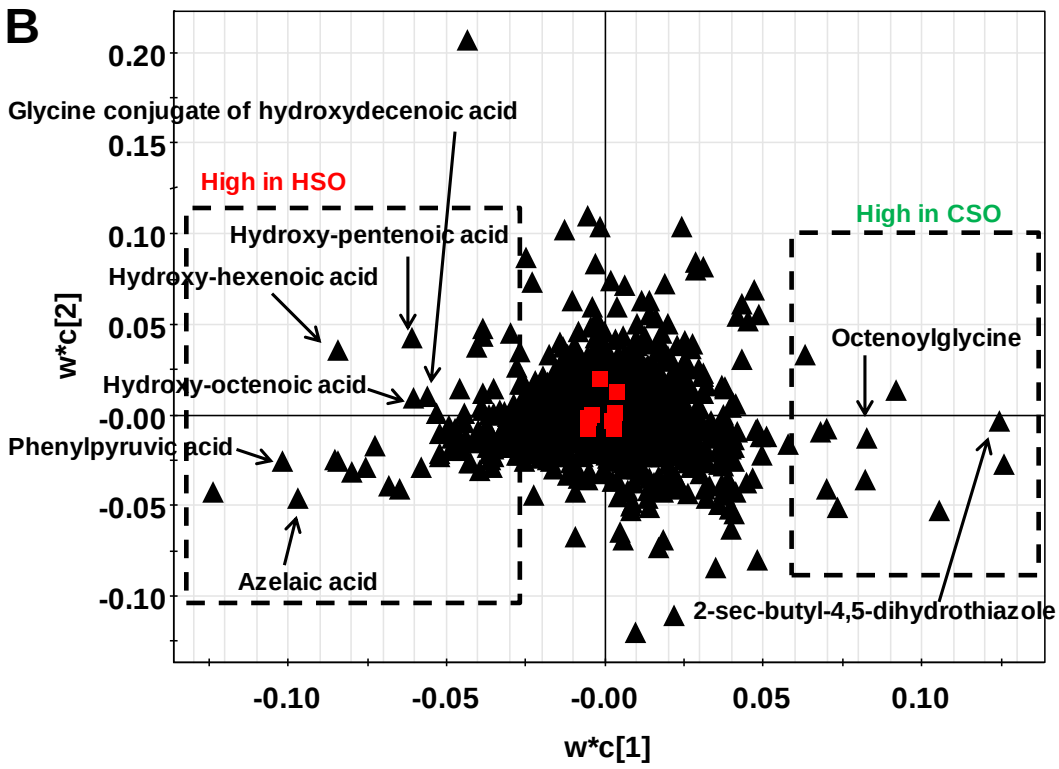
B
Glycine conjugate of hydroxydecenoic acid
High in HSO
High in CSO
Hydroxy-pentenoic acid
Hydroxy-hexenoic acid
Octenoylglycine
Hydroxy-octenoic acid
Phenylpyruvic acid
Azelaic acid
2-sec-butyl-4,5-dihydrothiazole
w*c[2]
w*c[1]
0.20
0.15
0.10
0.05
-0.00
-0.05
-0.10
-0.10
-0.05
-0.00
0.05
0.10

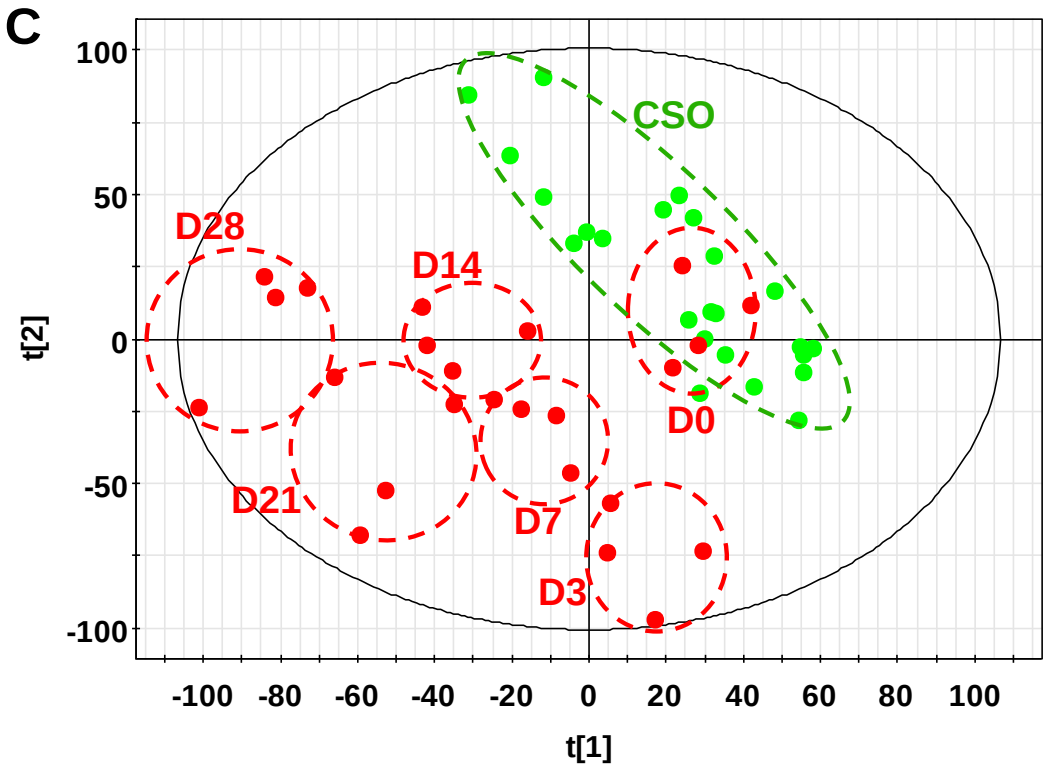
C
CSO
D28
D14
D0
D21
D7
D3
t[2]
t[1]
100
50
0
-50
-100
-100 -80 -60 -40 -20 0 20 40 60 80 100

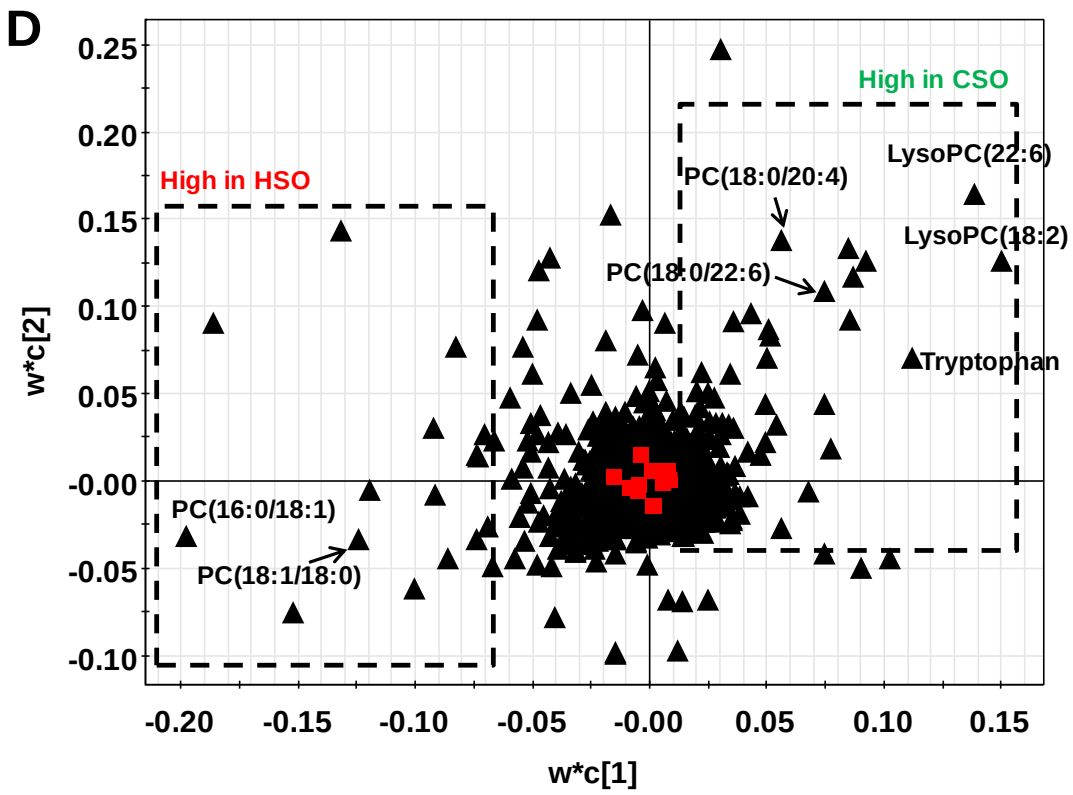
D
High in CSO
High in HSO
LysoPC(22:6)
PC(18:0/20:4)
LysoPC(18:2)
PC(18:0/22:6)
Tryptophan
PC(16:0/18:1)
PC(18:1/18:0)
w*c[2]
w*c[1]
0.25
0.20
0.15
0.10
0.05
-0.00
-0.05
-0.10
-0.20 -0.15 -0.10 -0.05 -0.00 0.05 0.10 0.15

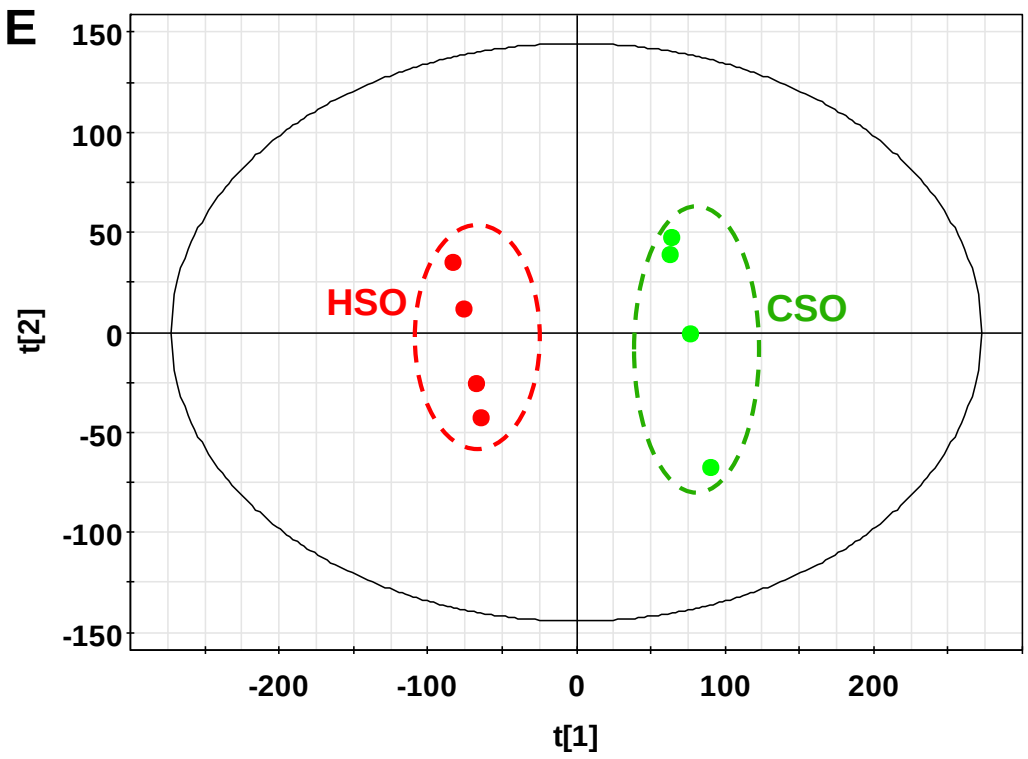
E
150
100
50
0
-50
-100
-150
t[2]
HSO
CSO
-200
-100
0
100
200
t[1]

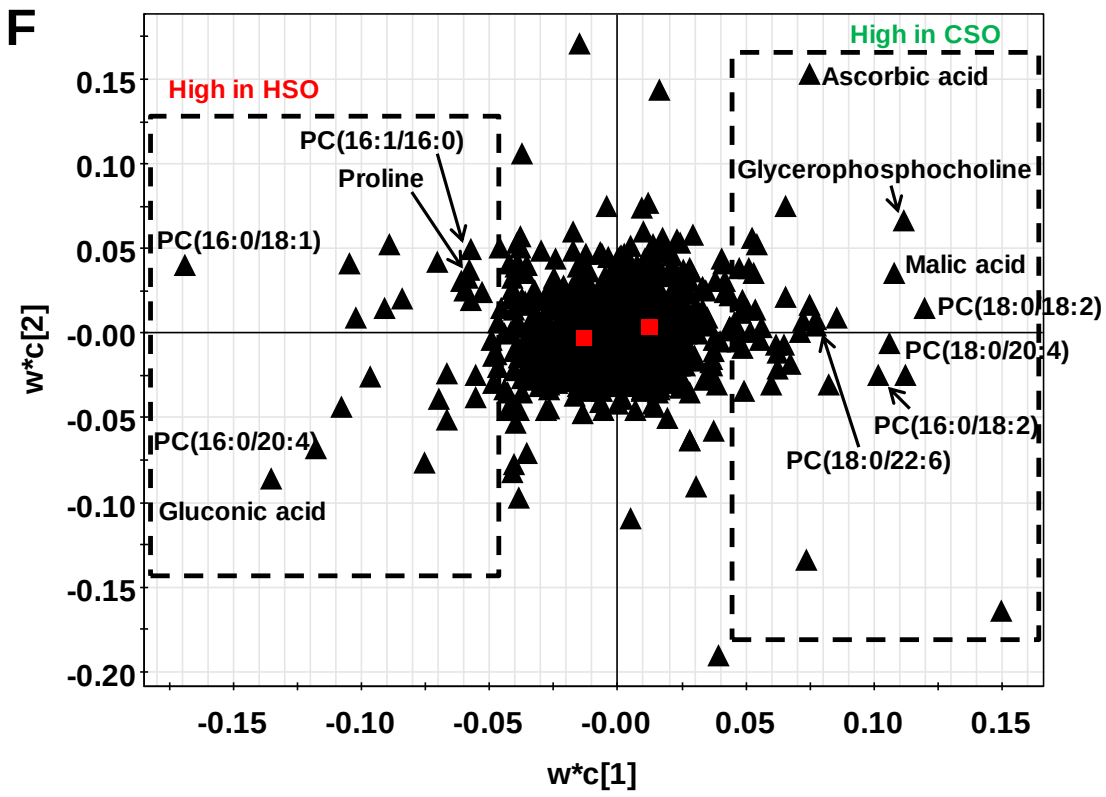
F
High in HSO
High in CSO
PC(16:1/16:0)
Proline
PC(16:0/18:1)
PC(16:0/20:4)
Gluconic acid
Ascorbic acid
Glycerophosphocholine
Malic acid
PC(18:0/18:2)
PC(18:0/20:4)
PC(16:0/18:2)
PC(18:0/22:6)
0.15
0.10
0.05
-0.00
-0.05
-0.10
-0.15
-0.20
w*c[2]
-0.15
-0.10
-0.05
-0.00
0.05
0.10
0.15
w*c[1]

Figure 4.3. The effects of HSO on urine, serum and hepatic metabolome. Green and red indicate CSO and HSO samples, respectively. ***A.*** The scores plot of a PLS-DA model on metabolites in the urine samples from CSO and HSO treatments. ***B.*** Identification of urinary metabolites contributing to the separation of CSO and HSO samples in a loadings plot of a PLS-DA model. ***C.*** The scores plot of a PLS-DA model on metabolites in the serum samples from CSO and HSO treatments. ***D.*** Identification of serum metabolites contributing to the separation of CSO and HSO samples in a loadings plot of a PLS-DA model. ***E.*** The scores plot of a PLS-DA model on metabolites in the liver samples from CSO and HSO treatments. ***F.*** Identification of hepatic metabolites contributing to the separation of CSO and HSO samples in a loadings plot of a PLS-DA model.

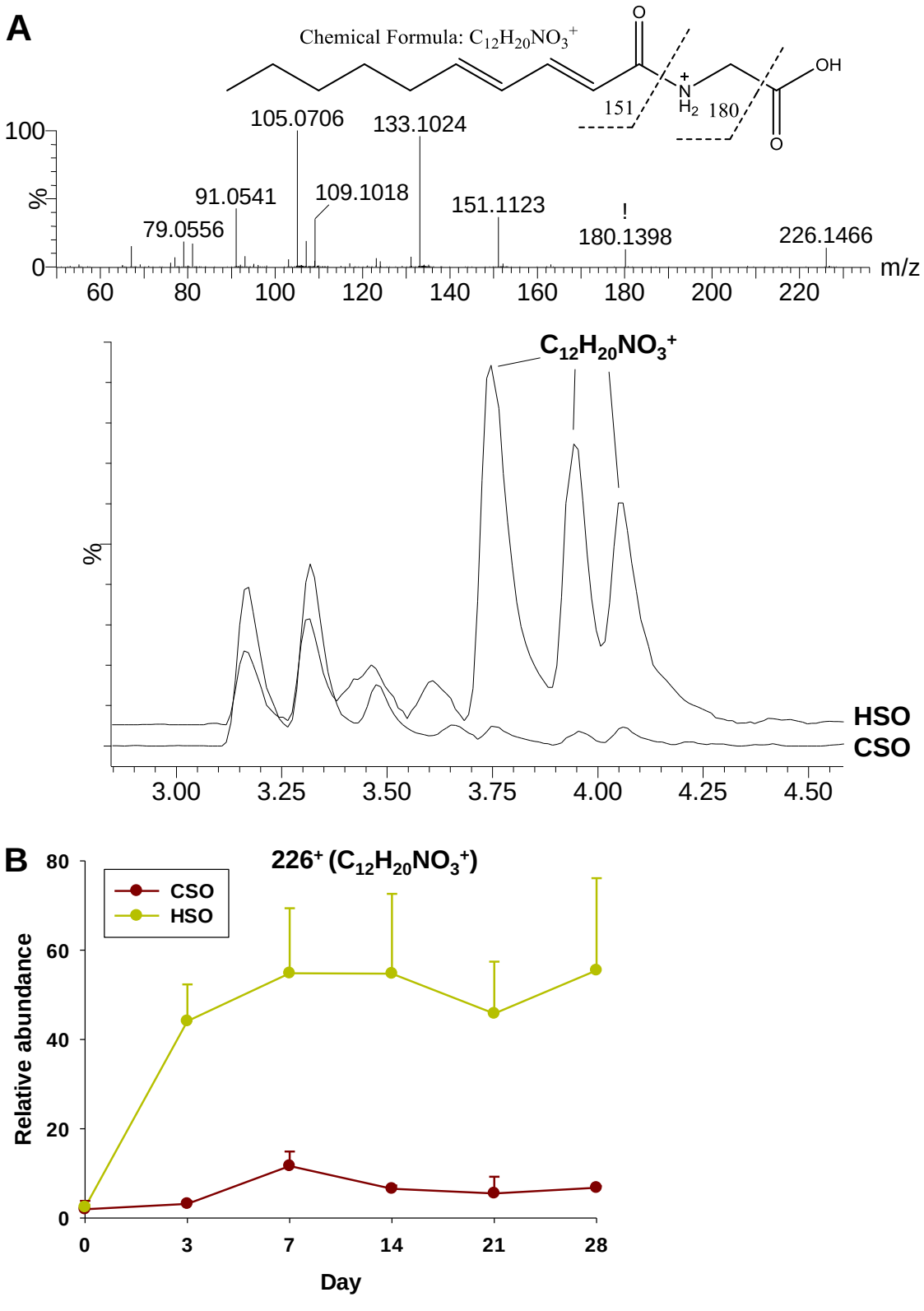
A
Chemical Formula: $C_{12}H_{20}NO_3^+$
105.0706
133.1024
91.0541
109.1018
151.1123
79.0556
180.1398
226.1466
151
180
100
%
0
m/z
60
80
100
120
140
160
180
200
220
$C_{12}H_{20}NO_3^+$
HSO
CSO
3.00
3.25
3.50
3.75
4.00
4.25
4.50
B
226^+ ($C_{12}H_{20}NO_3^+$)
CSO
HSO
Relative abundance
Day
0
3
7
14
21
28

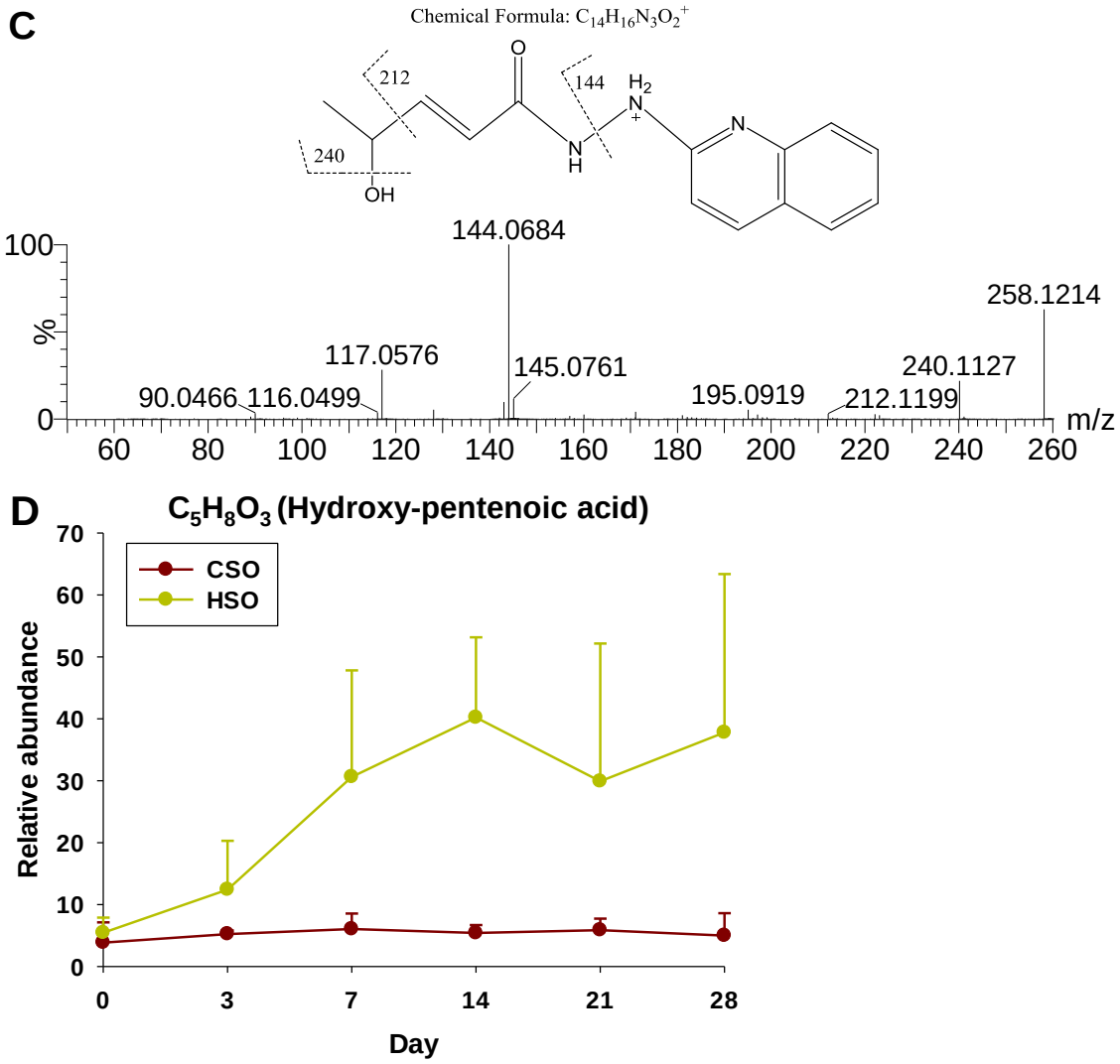
C
Chemical Formula: $C_{14}H_{16}N_3O_2^+$
212
144
240
O
OH
N
H
H_2
N
+
N
100
%
0
144.0684
258.1214
117.0576
145.0761
240.1127
90.0466
116.0499
195.0919
212.1199
m/z
60
80
100
120
140
160
180
200
220
240
260
D
$C_5H_8O_3$ (Hydroxy-pentenoic acid)
CSO
HSO
Relative abundance
70
60
50
40
30
20
10
0
0
3
7
14
21
28
Day

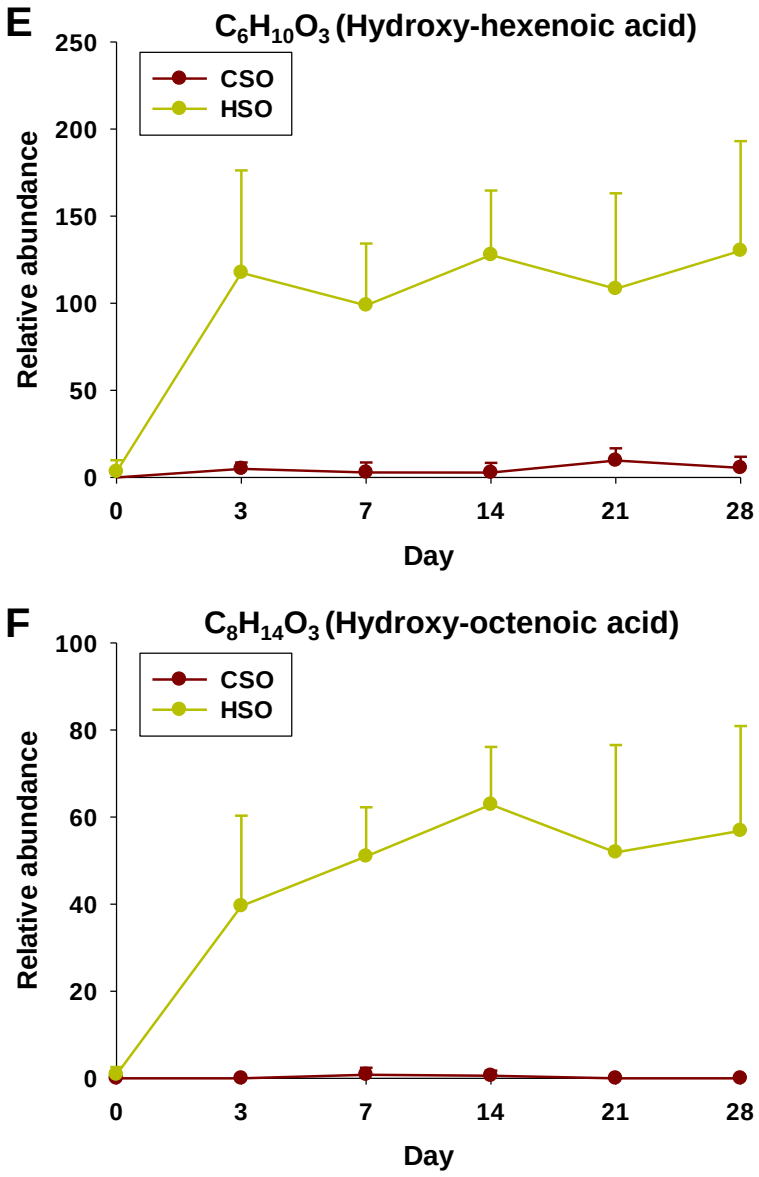

Figure 4.4. Exposure markers of HSO treatment. ***A.*** Chromatogram and structural elucidation of 226^{+}. ***B.*** Relative abunance of 226^{+}. ***C.*** Structural elucidation of HQ derivatized hydroxy-pentenoic acid. ***D.*** Relative abunance of hydroxy-pentenoic acid. ***E.*** Relative abunance of hydroxy-hexenoic acid. ***F.*** Relative abunance of hydroxy-octenoic acid.

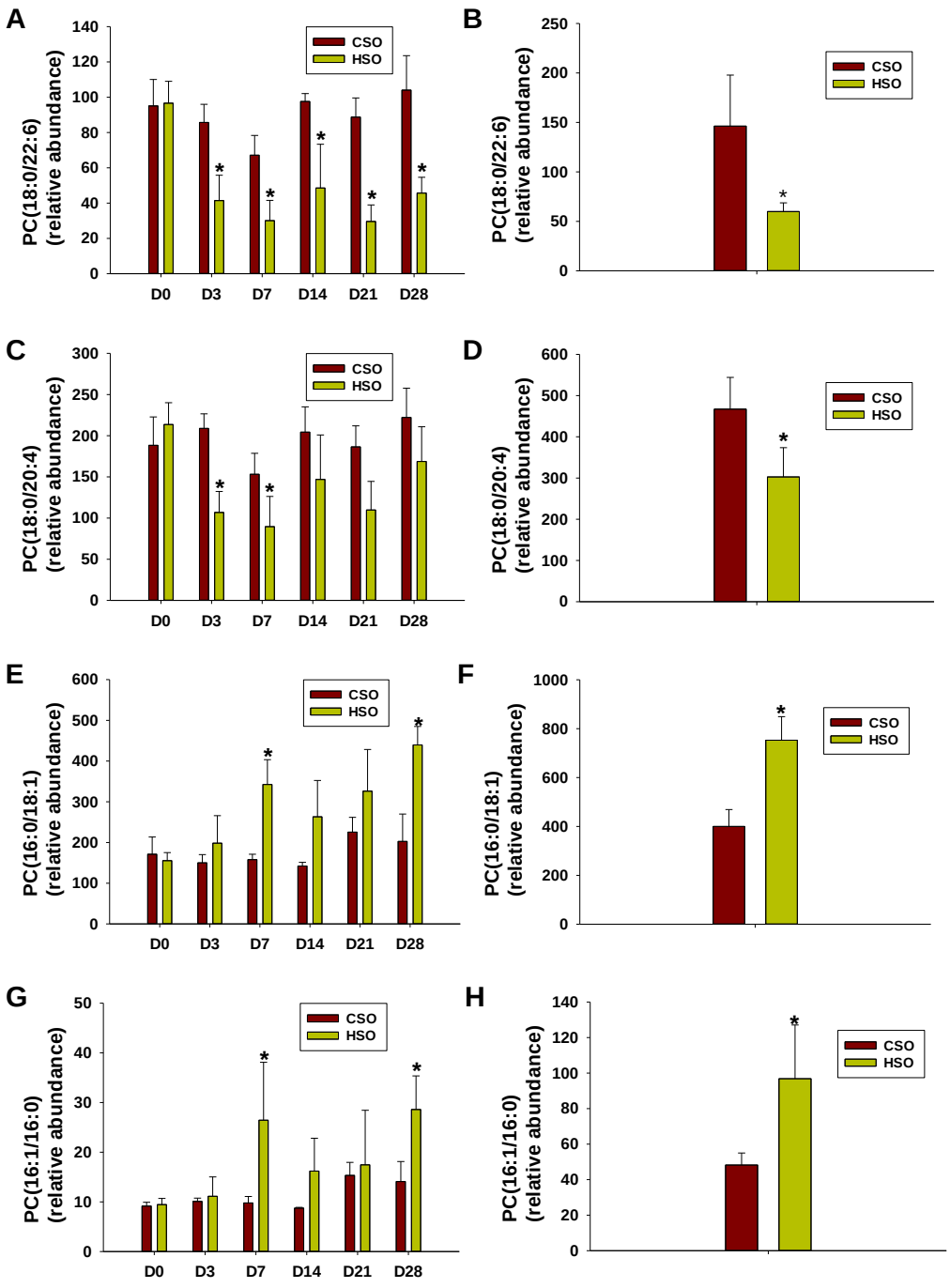

Figure 4.5. HSO-induced changes of lipid markers in serum and liver. ***A.*** Relative abunance of PC(18:0/22:6) in serum. ***B.*** Relative abunance of PC(18:0/22:6) in liver. ***C.*** Relative abunance of PC(18:0/20:4) in serum. ***D.*** Relative abunance of PC(18:0/20:4) in liver. ***E.*** Relative abunance of PC(16:0/18:1) in serum. ***F.*** Relative abunance of PC(16:0/18:1) in liver. ***G.*** Relative abunance of PC(16:1/16:0) in serum. ***H.*** Relative abunance of PC(16:1/16:0) in liver.

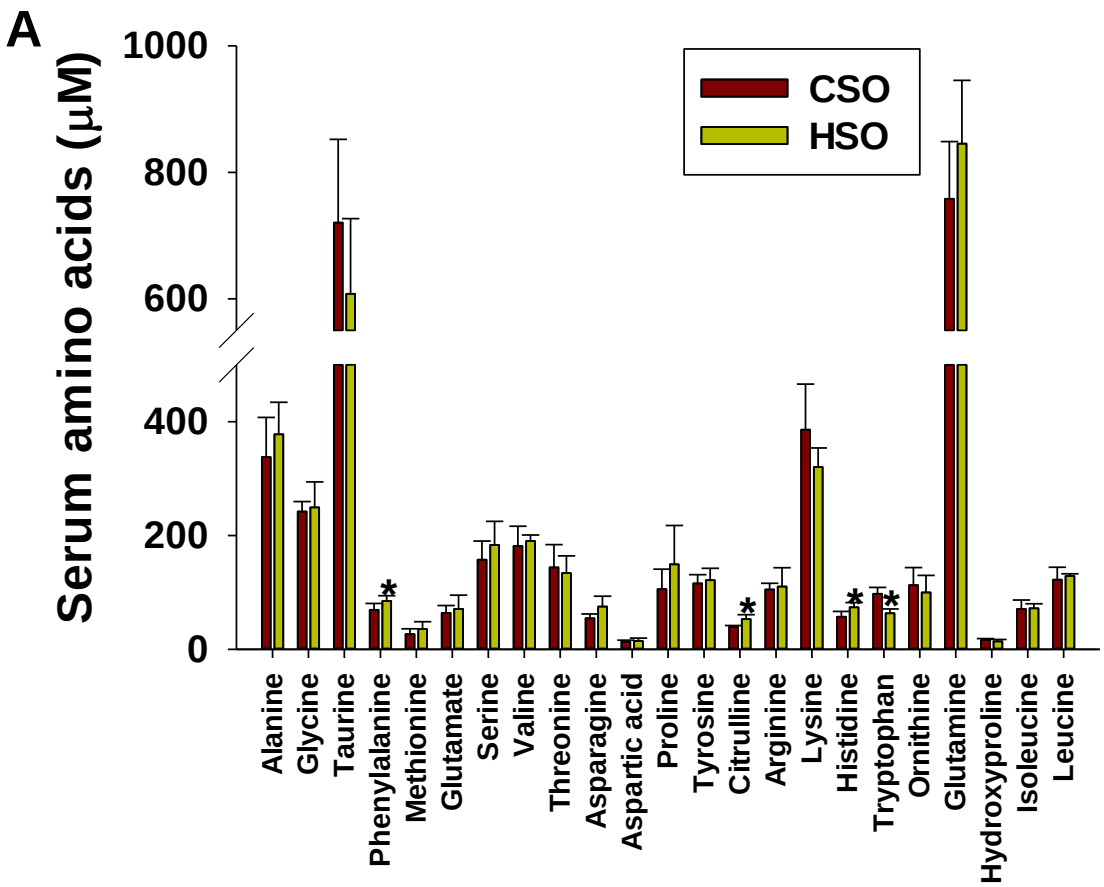
A
Serum amino acids (μM)
1000
800
600
400
200
0
CSO
HSO
*
*
*
Alanine
Glycine
Taurine
Phenylalanine
Methionine
Glutamate
Serine
Valine
Threonine
Asparagine
Aspartic acid
Proline
Tyrosine
Citrulline
Arginine
Lysine
Histidine
Tryptophan
Ornithine
Glutamine
Hydroxyproline
Isoleucine
Leucine

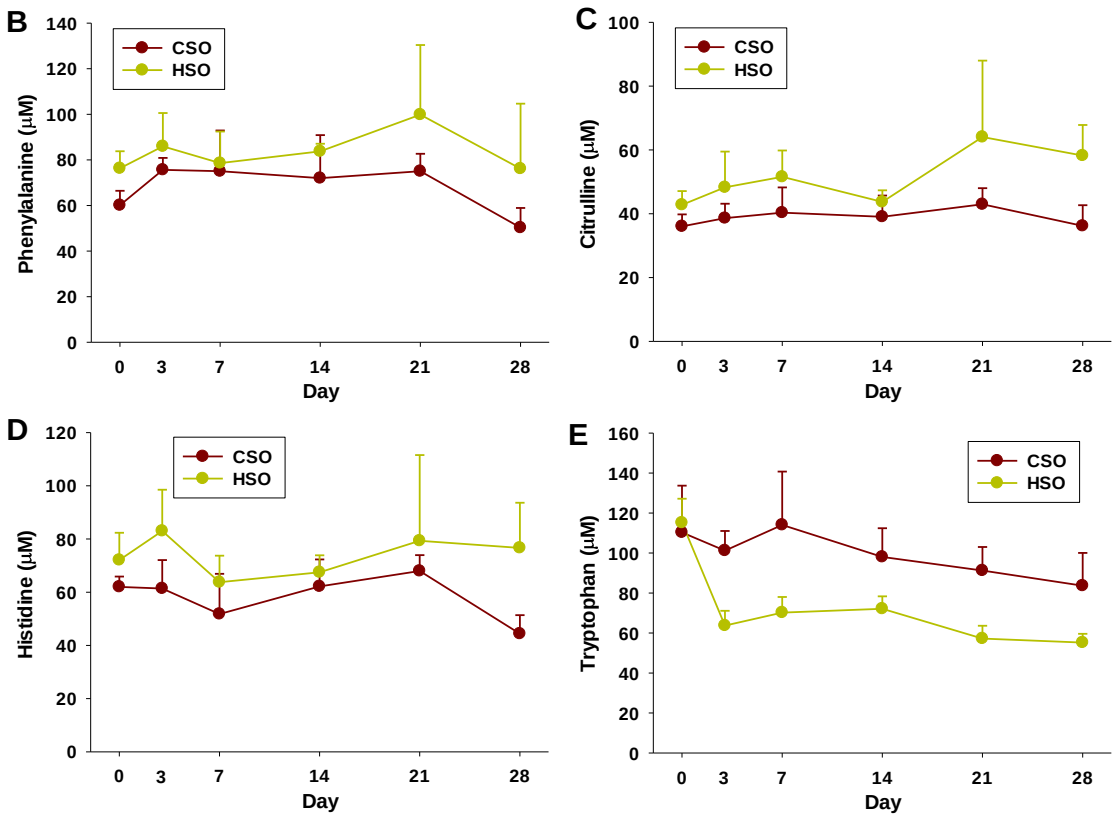

Figure 4.6. HSO-induced changes of amino acids in serum. ***A.*** Amino acids in serum during 28 day treatment. The concentrations are the means of serum samples belonging to CSO and HSO treatment. ***B.*** Phenylalanine in serum sample. ***C.*** Citrulline in serum sample. ***D.*** Histidine in serum sample. ***E.*** Tryptophan in serum sample.

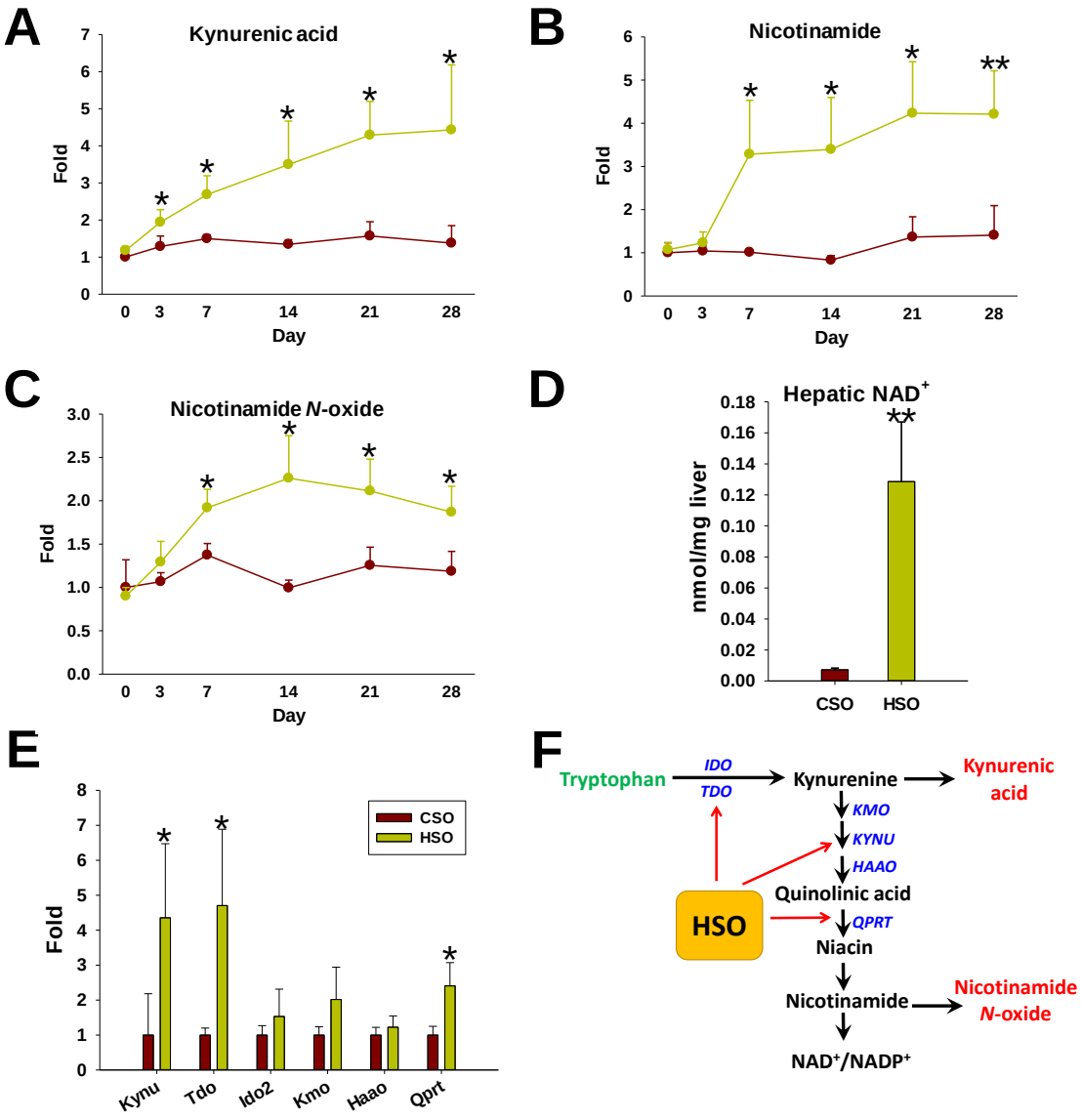

Figure 4.7. The effects of HSO on tryptophan metabolism. ***A.*** Kynurenic acid in urine. ***B.*** Nicotinamide in urine. ***C.*** Nicotinamide *N*-oxide in urine. ***D.*** Hepatic NAD^+. ***E.*** Gene expression levels of metabolizing enzymes in tryptophan-NAD^+ pathway. ***F.*** Summary on effects of HSO on tryptophan-NAD^+ pathway.

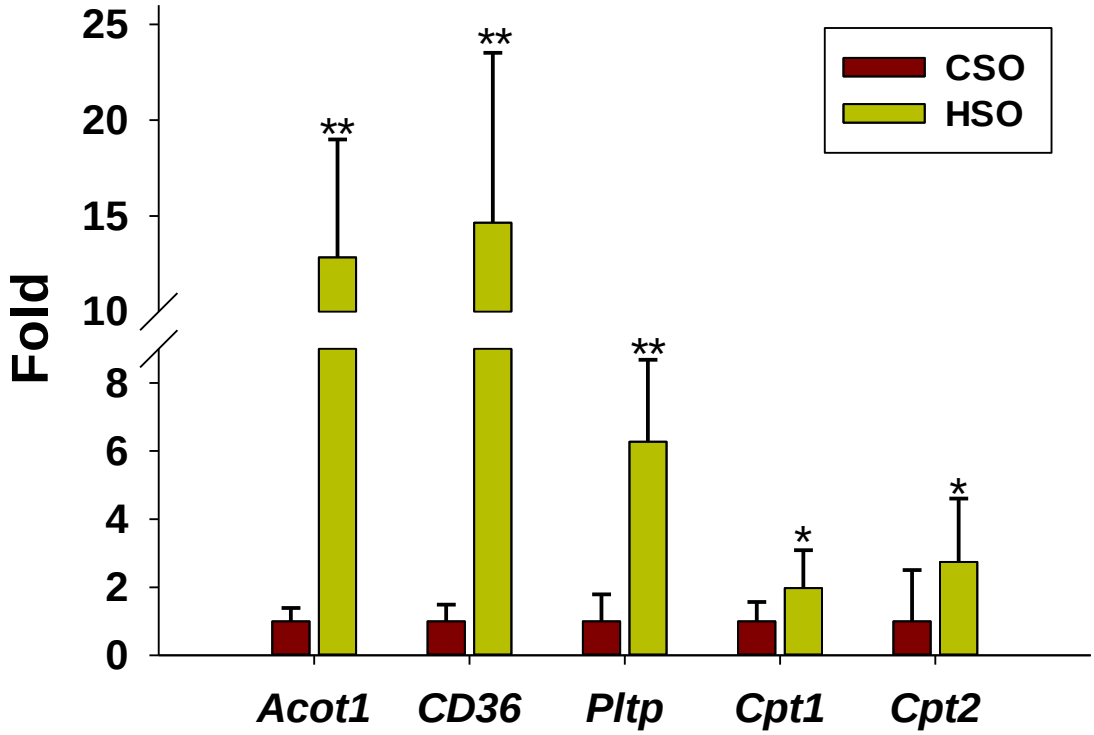

Figure 4.8. Expression levels of PPARα target genes related to fatty acid oxidation.

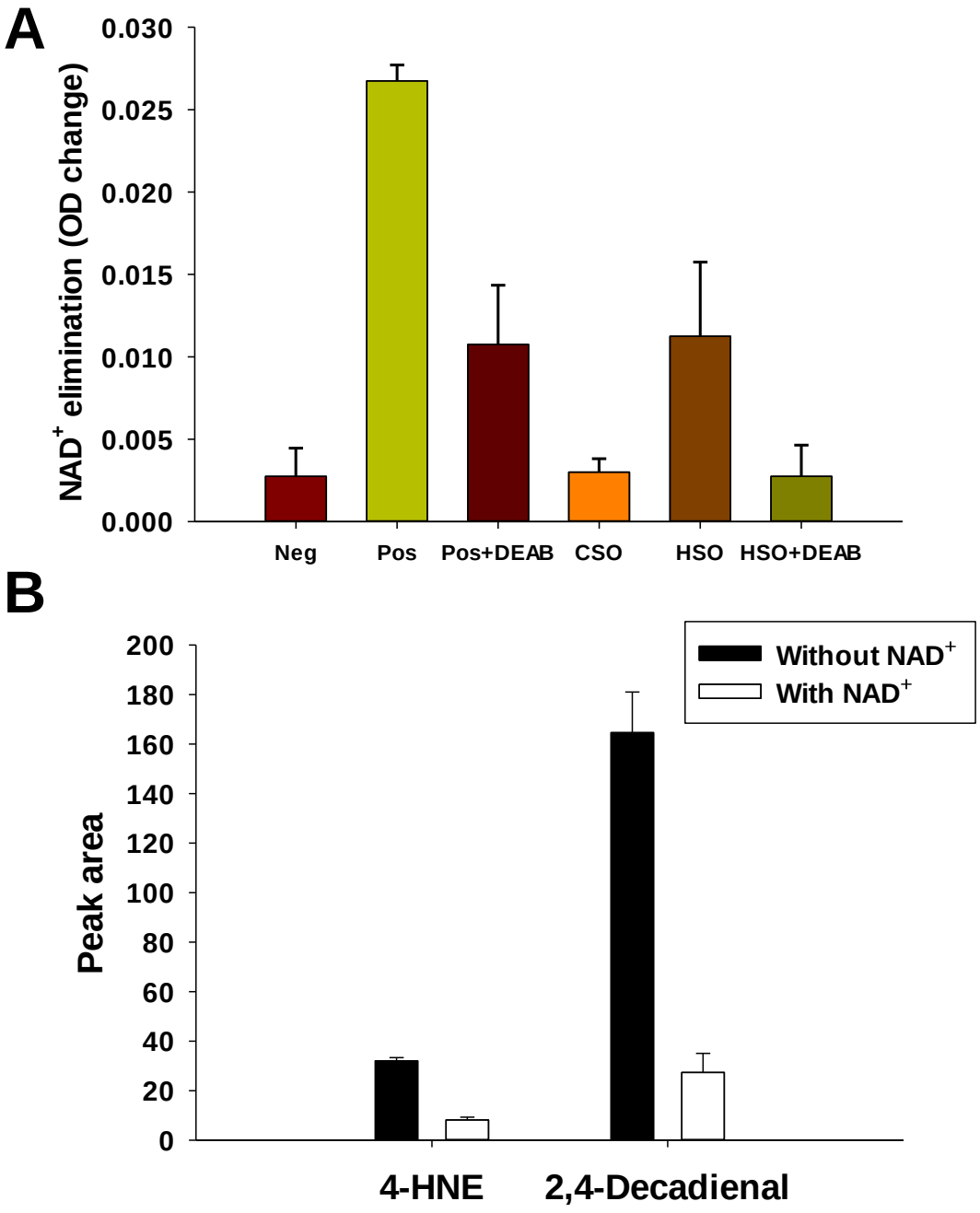

Figure 4.9. ***In vitro*** **analysis of ALDHs-mediated metabolism of HSO.** ***A.*** NAD^+ elimination by different substrate incubating with mouse liver homogenate. Negative control sample (H_2O:DMSO=1:1), Positive control sample (acetaldehyde:DMSO=1:1), CSO sample (CSO:DMSO=1:1) and HSO sample (HSO:DMSO=1:1). ***B.*** The levels of 4-HNE and 2,4-decadienal in HSO after incubating with mouse liver homogenate.

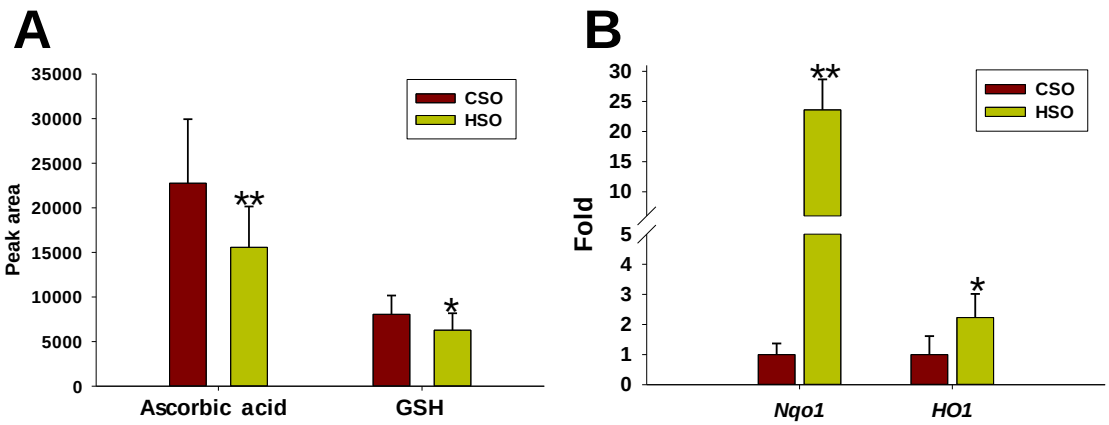

Figure 4.10. HSO treatment induced oxidative stress. *A*. Hepatic ascorbic acid and GSH. ***B.*** Expression levels of genes related to oxidative stress.

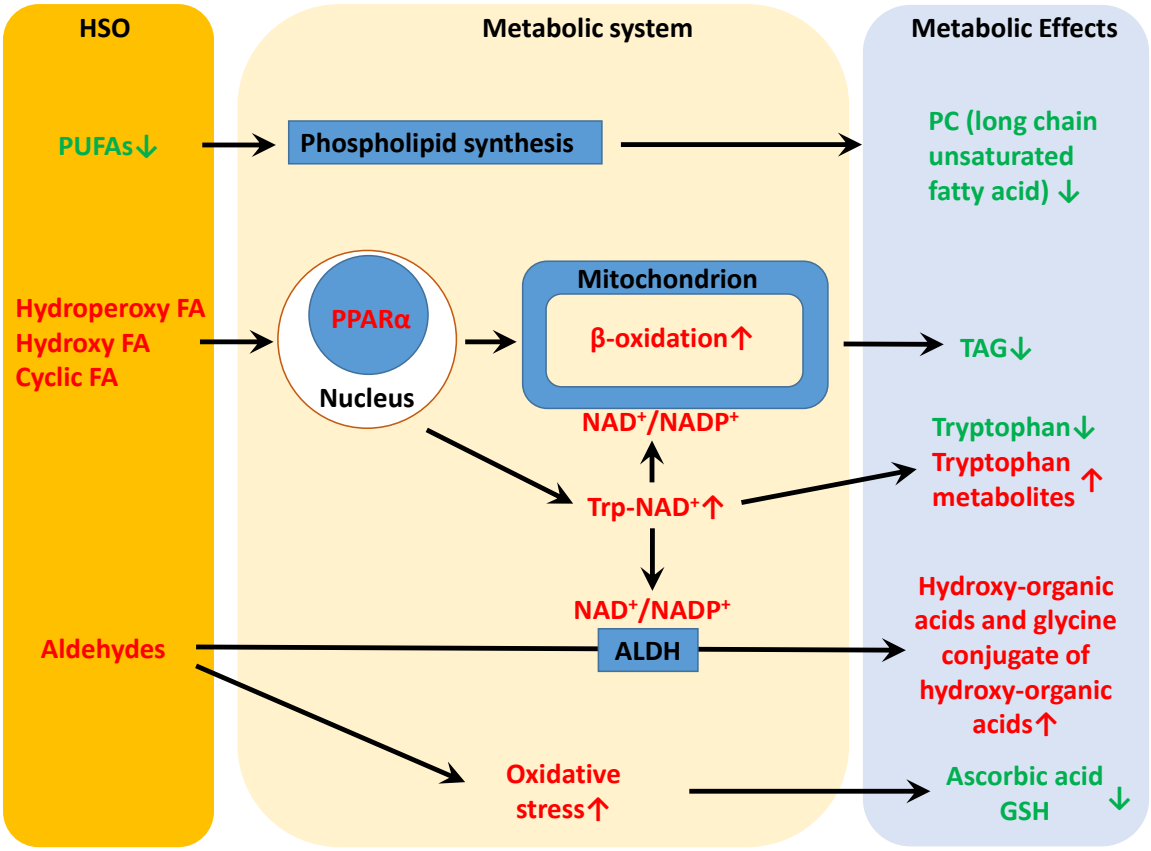

Figure 4.11. Summary of major HSO-induced metabolic changes. Green and red indicate decrease and increase, respectively.

REFERENCES

(1) Hwang, I. G.; Shin, Y. J.; Lee, S.; Lee, J.; Yoo, S. M. Effects of Different Cooking Methods on the Antioxidant Properties of Red Pepper (Capsicum annuum L.). *Prev Nutr Food Sci.* **2012**, *17*, 286-92.

(2) Jimenez-Monreal, A. M.; Garcia-Diz, L.; Martinez-Tome, M.; Mariscal, M.; Murcia, M. A. Influence of cooking methods on antioxidant activity of vegetables. *J Food Sci.* **2009**, *74*, H97-H103.

(3) Jagerstad, M.; Skog, K. Genotoxicity of heat-processed foods. *Mutat Res.* **2005**, *574*, 156-72.

(4) Changnon, S. A.; Kunkel, K. E.; Reinke, B. C. Impacts and responses to the 1995 heat wave: A call to action. *B Am Meteorol Soc.* **1996**, *77*, 1497-1506.

(5) Leon, L. R.; Helwig, B. G. Heat stroke: role of the systemic inflammatory response. *Journal of applied physiology.* **2010**, *109*, 1980-8.

(6) Renaudeau, D.; Gourdine, J. L.; St-Pierre, N. R. A meta-analysis of the effects of high ambient temperature on growth performance of growing-finishing pigs. *Journal of animal science.* **2011**, *89*, 2220-30.

(7) Hansen, P. J. Effects of heat stress on mammalian reproduction. *Philosophical transactions of the Royal Society of London. Series B, Biological sciences.* **2009**, *364*, 3341-50.

(8) Kovats, R. S.; Hajat, S. Heat stress and public health: a critical review. *Annu Rev Public Health.* **2008**, *29*, 41-55.

(9) Wallace, R. F.; Kriebel, D.; Punnett, L.; Wegman, D. H.; Amoroso, P. J. Prior heat illness hospitalization and risk of early death. *Environ Res.* **2007**, *104*, 290-5.

(10) Katsouyanni, K.; Trichopoulos, D.; Zavitsanos, X.; Touloumi, G. The 1987 Athens Heatwave. *Lancet.* **1988**, *2*, 573-573.

(11) di Leonardo, M. Heat wave: A social autopsy of disaster in Chicago. *Nation.* **2002**, *275*, 31-+.

(12) St-Pierre, N. R.; Cobanov, B.; Schnitkey, G. Economic Losses from Heat Stress by US Livestock Industries. *J Dairy Sci.* **2003**, *86*, E52-E77.

(13) Silanikove, N.; Koluman, N. Impact of climate change on the dairy industry in temperate zones: Predications on the overall negative impact and on the positive role of dairy goats in adaptation to earth warming. *Small Ruminant Res.* **2015**, *123*, 27-34.

(14) Anderson, M. Climate Change 2014: Synthesis Report. *Libr J.* **2016**, *141*, 28-28.

(15) Patience, J. F.; Umboh, J. F.; Chaplin, R. K.; Nyachoti, C. M. Nutritional and physiological responses of growing pigs exposed to a diurnal pattern of heat stress. *Livest Prod Sci.* **2005**, *96*, 205-214.

(16) Kellogg, D. L., Jr.; Crandall, C. G.; Liu, Y.; Charkoudian, N.; Johnson, J. M. Nitric oxide and cutaneous active vasodilation during heat stress in humans. *Journal of applied physiology.* **1998**, *85*, 824-9.

(17) Dokladny, K.; Moseley, P. L.; Ma, T. Y. Physiologically relevant increase in temperature causes an increase in intestinal epithelial tight junction permeability. *American journal of physiology. Gastrointestinal and liver physiology.* **2006**, *290*, G204-12.

(18) Pearce, S. C.; Sanz-Fernandez, M. V.; Hollis, J. H.; Baumgard, L. H.; Gabler, N. K. Short-term exposure to heat stress attenuates appetite and intestinal integrity in growing pigs. *Journal of animal science.* **2014**, *92*, 5444-54.
(19) Toivola, D. M.; Strnad, P.; Habtezion, A.; Omary, M. B. Intermediate filaments take the heat as stress proteins. *Trends Cell Biol.* **2010**, *20*, 79-91.
(20) Sonna, L. A.; Fujita, J.; Gaffin, S. L.; Lilly, C. M. Invited Review: Effects of heat and cold stress on mammalian gene expression. *Journal of applied physiology.* **2002**, *92*, 1725-1742.
(21) Welch, W. J.; Suhan, J. P. Morphological-Study of the Mammalian Stress Response - Characterization of Changes in Cytoplasmic Organelles, Cytoskeleton, and Nucleoli, and Appearance of Intranuclear Actin-Filaments in Rat Fibroblasts after Heat-Shock Treatment. *J Cell Biol.* **1985**, *101*, 1198-1211.
(22) Patriarca, E. J.; Maresca, B. Acquired Thermotolerance Following Heat-Shock Protein-Synthesis Prevents Impairment of Mitochondrial Atpase Activity at Elevated-Temperatures in Saccharomyces-Cerevisiae. *Exp Cell Res.* **1990**, *190*, 57-64.
(23) Kuhl, N. M.; Rensing, L. Heat shock effects on cell cycle progression. *Cell Mol Life Sci.* **2000**, *57*, 450-463.
(24) Richter, K.; Haslbeck, M.; Buchner, J. The Heat Shock Response: Life on the Verge of Death. *Mol Cell.* **2010**, *40*, 253-266.
(25) Baumgard, L. H.; Rhoads, R. P., Jr. Effects of heat stress on postabsorptive metabolism and energetics. *Annual review of animal biosciences.* **2013**, *1*, 311-37.
(26) Aggarwal, A.; Upadhyay, R. *Heat stress and animal productivity*. Springer India: 2013; p 27-42.
(27) McGuire, M. A.; Beede, D. K.; Collier, R. J.; Buonomo, F. C.; DeLorenzo, M. A.; Wilcox, C. J.; Huntington, G. B.; Reynolds, C. K. Effects of acute thermal stress and amount of feed intake on concentrations of somatotropin, insulin-like growth factor (IGF)-I and IGF-II, and thyroid hormones in plasma of lactating Holstein cows. *Journal of animal science.* **1991**, *69*, 2050-6.
(28) Rhoads, R. P.; La Noce, A. J.; Wheelock, J. B.; Baumgard, L. H. Alterations in expression of gluconeogenic genes during heat stress and exogenous bovine somatotropin administration. *J Dairy Sci.* **2011**, *94*, 1917-21.
(29) Stallings, J. D.; Ippolito, D. L.; Rakesh, V.; Baer, C. E.; Dennis, W. E.; Helwig, B. G.; Jackson, D. A.; Leon, L. R.; Lewis, J. A.; Reifman, J. Patterns of gene expression associated with recovery and injury in heat-stressed rats. *BMC genomics.* **2014**, *15*, 1058.
(30) Victoria Sanz Fernandez, M.; Johnson, J. S.; Abuajamieh, M.; Stoakes, S. K.; Seibert, J. T.; Cox, L.; Kahl, S.; Elsasser, T. H.; Ross, J. W.; Isom, S. C.; Rhoads, R. P.; Baumgard, L. H. Effects of heat stress on carbohydrate and lipid metabolism in growing pigs. *Physiological reports.* **2015**, *3*.
(31) Ippolito, D. L.; Lewis, J. A.; Yu, C.; Leon, L. R.; Stallings, J. D. Alteration in circulating metabolites during and after heat stress in the conscious rat: potential biomarkers of exposure and organ-specific injury. *BMC physiology.* **2014**, *14*, 14.
(32) Malmendal, A.; Overgaard, J.; Bundy, J. G.; Sorensen, J. G.; Nielsen, N. C.; Loeschcke, V.; Holmstrup, M. Metabolomic profiling of heat stress: hardening and

recovery of homeostasis in Drosophila. *American journal of physiology. Regulatory, integrative and comparative physiology.* **2006**, *291*, R205-12.
(33) Belhadj Slimen, I.; Najar, T.; Ghram, A.; Abdrrabba, M. Heat stress effects on livestock: molecular, cellular and metabolic aspects, a review. *J Anim Physiol Anim Nutr (Berl).* **2015**.
(34) Vigh, L.; Maresca, B.; Harwood, J. L. Does the membrane's physical state control the expression of heat shock and other genes? *Trends Biochem Sci.* **1998**, *23*, 369-374.
(35) van Meer, G.; Voelker, D. R.; Feigenson, G. W. Membrane lipids: where they are and how they behave. *Nat Rev Mol Cell Bio.* **2008**, *9*, 112-124.
(36) Balogh, G.; Peter, M.; Glatz, A.; Gombos, I.; Torok, Z.; Horvath, I.; Harwood, J. L.; Vigh, L. Key role of lipids in heat stress management. *Febs Lett.* **2013**, *587*, 1970-1980.
(37) Walter, S.; Buchner, J. Molecular chaperones - Cellular machines for protein folding. *Angew Chem Int Edit.* **2002**, *41*, 1098-1113.
(38) Van Brocklyn, J. R.; Williams, J. B. The control of the balance between ceramide and sphingosine-1-phosphate by sphingosine kinase: Oxidative stress and the seesaw of cell survival and death. *Comp Biochem Phys B.* **2012**, *163*, 26-36.
(39) Kagan, V. E.; Borisenko, G. G.; Tyurina, Y. Y.; Tyurin, V. A.; Jiang, J. F.; Potapovich, A. I.; Kini, V.; Amoscato, A. A.; Fujii, Y. Oxidative lipidomics of apoptosis: Redox catalytic interactions of cytochrome C with cardiolipin and phosphatidylserine. *Free Radical Bio Med.* **2004**, *37*, 1963-1985.
(40) Bochkov, V. N.; Oskolkova, O. V.; Birukov, K. G.; Levonen, A. L.; Binder, C. J.; Stockl, J. Generation and Biological Activities of Oxidized Phospholipids. *Antioxid Redox Sign.* **2010**, *12*, 1009-1059.
(41) Zhang, M. Q.; Jiang, M.; Bi, Y.; Zhu, H.; Zhou, Z. M.; Sha, J. H. Autophagy and Apoptosis Act as Partners to Induce Germ Cell Death after Heat Stress in Mice. *Plos One.* **2012**, *7*.
(42) Imik, H.; Ozlu, H.; Gumus, R.; Atasever, M. A.; Urcar, S.; Atasever, M. Effects of ascorbic acid and -lipoic acid on performance and meat quality of broilers subjected to heat stress. *Brit Poultry Sci.* **2012**, *53*, 800-808.
(43) Packer, L.; Witt, E. H.; Tritschler, H. J. Alpha-Lipoic Acid as a Biological Antioxidant. *Free Radical Bio Med.* **1995**, *19*, 227-250.
(44) Smith, A. R.; Shenvi, S. V.; Widlansky, M.; Suh, J. H.; Hagen, T. M. Lipoic acid as a potential therapy for chronic diseases associated with oxidative stress. *Curr Med Chem.* **2004**, *11*, 1135-1146.
(45) Moini, H.; Packer, L.; Saris, N. E. Antioxidant and prooxidant activities of alpha-lipoic acid and dihydrolipoic acid. *Toxicology and applied pharmacology.* **2002**, *182*, 84-90.
(46) Mirzaei, M.; Ghorbani, G. R.; Khorvash, M.; Rahmani, H. R.; Nikkhah, A. Chromium improves production and alters metabolism of early lactation cows in summer. *J Anim Physiol Anim Nutr (Berl).* **2011**, *95*, 81-9.
(47) Sahin, K.; Ozbey, O.; Onderci, M.; Cikim, G.; Aysondu, M. H. Chromium supplementation can alleviate negative effects of heat stress on egg production, egg quality and some serum metabolites of laying Japanese quail. *Journal of Nutrition.* **2002**, *132*, 1265-1268.

(48) Toghyani, M.; Toghyani, M.; Shivazad, M.; Gheisari, A.; Bahadoran, R. Chromium Supplementation Can Alleviate the Negative Effects of Heat Stress on Growth Performance, Carcass Traits, and Meat Lipid Oxidation of Broiler Chicks without Any Adverse Impacts on Blood Constituents. *Biol Trace Elem Res.* **2012**, *146*, 171-180.
(49) Sahin, K.; Sahin, N.; Kucuk, O.; Hayirli, A.; Prasad, A. S. Role of dietary zinc in heat-stressed poultry: a review. *Poultry science.* **2009**, *88*, 2176-83.
(50) Sahin, K.; Kucuk, O. Zinc supplementation alleviates heat stress in laying Japanese quail. *The Journal of nutrition.* **2003**, *133*, 2808-11.
(51) Hollis, G. R.; Carter, S. D.; Cline, T. R.; Crenshaw, T. D.; Cromwell, G. L.; Hill, G. M.; Kim, S. W.; Lewis, A. J.; Mahan, D. C.; Miller, P. S.; Stein, H. H.; Veum, T. L.; Nutrition, N. C. R. C. o. S. Effects of replacing pharmacological levels of dietary zinc oxide with lower dietary levels of various organic zinc sources for weanling pigs. *Journal of animal science.* **2005**, *83*, 2123-9.
(52) Sahin, K.; Smith, M. O.; Onderci, M.; Sahin, N.; Gursu, M. F.; Kucuk, O. Supplementation of zinc from organic or inorganic source improves performance and antioxidant status of heat-distressed quail. *Poultry science.* **2005**, *84*, 882-7.
(53) Wapnir, R. A.; Stiel, L. Zinc intestinal absorption in rats: specificity of amino acids as ligands. *The Journal of nutrition.* **1986**, *116*, 2171-9.
(54) Powell, S. R. The antioxidant properties of zinc. *The Journal of nutrition.* **2000**, *130*, 1447S-54S.
(55) Parmesan, C.; Yohe, G. A globally coherent fingerprint of climate change impacts across natural systems. *Nature.* **2003**, *421*, 37-42.
(56) Pedreschi, F.; Moyano, P.; Kaack, K.; Granby, K. Color changes and acrylamide formation in fried potato slices. *Food Res Int.* **2005**, *38*, 1-9.
(57) Briefel, R. R.; Johnson, C. L. Secular trends in dietary intake in the United States. *Annual review of nutrition.* **2004**, *24*, 401-31.
(58) U.S. Department of Agriculture, A. R. S. Nutrient Intakes from Food: Mean Amounts Consumed per Individual, by Gender and Age, What We Eat in America, NHANES 2009-2010. Available: www.ars.usda.gov/ba/bhnrc/fsrg. **2012**.
(59) Dietary Assessment of Major Trends in U.S. Food Consumption, 1970-2005. Available: http://www.ers.usda.gov/media/210681/eib33_1_.pdf. *United States Department of Agriculture Economic Research Service.* **2008**.
(60) Agriculture Fact Book. Available: http://www.usda.gov/factbook/2002factbook.pdf. *United States Department of Agriculture Office of Communications.* **2001-2002**.
(61) Groschen, R. Overview of: The Feasibility of Biodiesel from Waste/Recycled Greases and Animal Fats. **2002**.
(62) Choe, E.; Min, D. B. Chemistry of deep-fat frying oils. *Journal of Food Science.* **2007**, *72*, R77-R86.
(63) Boskou, D.; Elmadfa, I. *Frying of food: oxidation, nutrient and non-nutrient antioxidants, biologically active compounds and high temperatures, second edition*. 2nd ed.; CRC Press: Boca Raton, 2011; p 318.
(64) Zhang, Q.; Saleh, A. S.; Chen, J.; Shen, Q. Chemical alterations taken place during deep-fat frying based on certain reaction products: a review. *Chemistry and physics of lipids.* **2012**, *165*, 662-81.

(65) Frega, N.; Mozzon, M.; Lercker, G. Effects of free fatty acids on oxidative stability of vegetable oil. *J Am Oil Chem Soc.* **1999**, *76*, 325-329.
(66) Chung, J.; Lee, J.; Choe, E. Oxidative stability of soybean and sesame oil mixture during frying of flour dough. *Journal of Food Science.* **2004**, *69*, C574-C578.
(67) Dana, D.; Blumenthal, M. M.; Saguy, I. S. The protective role of water injection on oil quality in deep fat frying conditions. *Eur Food Res Technol.* **2003**, *217*, 104-109.
(68) Romero, A.; Cuesta, C.; Sanchez-Muniz, F. J. Effect of oil replenishment during deep-fat flying of frozen foods in sunflower oil and high-oleic acid sunflower oil. *J Am Oil Chem Soc.* **1998**, *75*, 161-167.
(69) Stevenson, S. G.; Vaiseygenser, M.; Eskin, N. A. M. Quality-Control in the Use of Deep Frying Oils. *J Am Oil Chem Soc.* **1984**, *61*, 1102-1108.
(70) Erickson, M. D. *Deep Frying - Chemistry, Nutrition, and Practical Applications (2nd Edition).* . AOCS Press: 2007; p 329-342.
(71) Sebastian, A.; Ghazani, S. M.; Marangoni, A. G. Quality and safety of frying oils used in restaurants. *Food Res Int.* **2014**, *64*, 420-423.
(72) Melton, S. L.; Jafar, S.; Sykes, D.; Trigiano, M. K. Review of Stability Measurements for Frying Oils and Fried Food Flavor. *J Am Oil Chem Soc.* **1994**, *71*, 1301-1308.
(73) Steel, C. J.; Dobarganes, M. C.; Barrera-Arellano, D. Formation of polymerization compounds during thermal oxidation of cottonseed oil, partially hydrogenated cottonseed oil and their blends. *Grasas Aceites.* **2006**, *57*, 284-291.
(74) TasioulaMargari, M.; MarquezRuiz, G.; Dobarganes, M. C. Fractionation of oligomeric triacylglycerides and the relation to rejection limits for used frying oils. *J Am Oil Chem Soc.* **1996**, *73*, 1579-1584.
(75) Christopoulou, C. N.; Perkins, E. G. Isolation and Characterization of Dimers Formed in Used Soybean Oil. *J Am Oil Chem Soc.* **1989**, *66*, 1360-1370.
(76) Byrdwell, W. C.; Neff, W. E. Electrospray ionization MS of high MW TAG oligomers. *J Am Oil Chem Soc.* **2004**, *81*, 13-26.
(77) Choe, E.; Min, D. B. Mechanisms and factors for edible oil oxidation. *Compr Rev Food Sci F.* **2006**, *5*, 169-186.
(78) Velasco, J.; Dobarganes, C. Oxidative stability of virgin olive oil. *Eur J Lipid Sci Tech.* **2002**, *104*, 661-676.
(79) Frankel, E. N. Lipid Oxidation - Mechanisms, Products and Biological Significance. *J Am Oil Chem Soc.* **1984**, *61*, 1908-1917.
(80) Peers, K. E.; Swoboda, P. A. T. Deterioration of Sunflower Seed Oil under Simulated Frying Conditions and during Small-Scale Frying of Potato-Chips. *J Sci Food Agr.* **1982**, *33*, 389-395.
(81) Cuesta, C.; Sanchezmuniz, F. J.; Garridopolonio, C.; Lopezvarela, S.; Arroyo, R. Thermooxidative and Hydrolytic Changes in Sunflower Oil Used in Fryings with a Fast Turnover of Fresh Oil. *J Am Oil Chem Soc.* **1993**, *70*, 1069-1073.
(82) Choe, E.; Min, D. B. Chemistry and reactions of reactive oxygen species in foods. *Journal of Food Science.* **2005**, *70*, R142-R159.
(83) Shurson, G. C.; Kerr, B. J.; Hanson, A. R. Evaluating the quality of feed fats and oils and their effects on pig growth performance. *J Anim Sci Biotechno.* **2015**, *6*.

(84) Shahidi, F.; Zhong, Y. Lipid Oxidation: Measurement Methods. In *Bailey's Industrial Oil and Fat Products*, Shahidi, F., Eds.; Wiley: Hoboken, NJ, 2005.
(85) Bezzi, S.; Loupassaki, S.; Petrakis, C.; Kefalas, P.; Calokerinos, A. Evaluation of peroxide value of olive oil and antioxidant activity by luminol chemiluminescence. *Talanta.* **2008**, *77*, 642-646.
(86) Dhaouadi, A.; Monser, L.; Sadok, S.; Adhoum, N. Flow-injection methylene blue-based spectrophotometric method for the determination of peroxide values in edible oils. *Anal Chim Acta.* **2006**, *576*, 270-4.
(87) Gotoh, N.; Miyake, S.; Takei, H.; Sasaki, K.; Okuda, S.; Ishinaga, M.; Wada, S. Simple Method for Measuring the Peroxide Value in a Colored Lipid. *Food Anal Method.* **2011**, *4*, 525-530.
(88) Lomanno, S. S.; Nawar, W. W. Effect of heating temperature and time on the volatile oxidative decomposition of linolenate. *Journal of Food Science.* **1982**, *47*, 744-&.
(89) Liu, P.; Kerr, B. J.; Chen, C.; Weber, T. E.; Johnston, L. J.; Shurson, G. C. Methods to create thermally oxidized lipids and comparison of analytical procedures to characterize peroxidation. *Journal of animal science.* **2014**, *92*, 2950-2959.
(90) Gray, J. I. Measurement of lipid oxidation: A review. *Journal of the American Oil Chemists' Society.* **1978**, *55*, 539-546.
(91) Shahidi, F.; Wanasundara, U. N. Methods for measuring oxidative rancidity in fats and oils. In *Food Lipids: Chemistry, Nutrition, and Biotechnology*, 3rd ed.; Akoh, C. C.; Min, D. B., Eds.; Marcel Dekker Incorporated: New York, 2008.
(92) Grotto, D.; Maria, L. S.; Valentini, J.; Paniz, C.; Schmitt, G.; Garcia, S. C.; Pomblum, V. J.; Rocha, J. B. T.; Farina, M. Importance of the Lipid Peroxidation Biomarkers and Methodological Aspects for Malondialdehyde Quantification. *Quim Nova.* **2009**, *32*, 169-174.
(93) Papastergiadis, A.; Mubiru, E.; Van Langenhove, H.; De Meulenaer, B. Malondialdehyde Measurement in Oxidized Foods: Evaluation of the Spectrophotometric Thiobarbituric Acid Reactive Substances (TBARS) Test in Various Foods. *J Agr Food Chem.* **2012**, *60*, 9589-9594.
(94) Tompkins, C.; Perkins, E. G. The evaluation of frying oils with the p-anisidine value. *J Am Oil Chem Soc.* **1999**, *76*, 945-947.
(95) Nuchi, C.; Guardiola, F.; Bou, R.; Bondioli, P.; Della Bella, L.; Codony, R. Assessment of the Levels of Degradation in Fat Co-and Byproducts for Feed Uses and Their Relationships with Some Lipid Composition Parameters. *J Agr Food Chem.* **2009**, *57*, 1952-1959.
(96) Barriuso, B.; Astiasaran, I.; Ansorena, D. A review of analytical methods measuring lipid oxidation status in foods: a challenging task. *Eur Food Res Technol.* **2013**, *236*, 1-15.
(97) Srivastava, Y.; Semwal, A. D. A study on monitoring of frying performance and oxidative stability of virgin coconut oil (VCO) during continuous/prolonged deep fat frying process using chemical and FTIR spectroscopy. *J Food Sci Tech Mys.* **2015**, *52*, 984-991.
(98) Alavijeh, S. G.; Goli, S. A. H.; Kadivar, M. Deep-fat frying performance of palm olein enriched with conjugated linoleic acid (CLA). *J Food Sci Tech Mys.* **2015**, *52*, 7369-7376.
(99) Mariod, A.; Matthaeus, B.; Eichner, K.; Hussein, I. H. Frying quality and oxidative stability of two unconventional oils. *J Am Oil Chem Soc.* **2006**, *83*, 529-538.

(100) Blair, I. A. DNA adducts with lipid peroxidation products. *Journal of Biological Chemistry.* **2008**, *283*, 15545-15549.
(101) Guillen, M. D.; Goicoechea, E. Toxic oxygenated alpha,beta-unsaturated aldehydes and their study in foods: A review. *Crit Rev Food Sci.* **2008**, *48*, 119-136.
(102) Dobarganes, M. C.; Marquez-Ruiz, G. Regulation of used frying fats and validity of quick tests for discarding the fats. *Grasas Aceites.* **1998**, *49*, 331-335.
(103) Caldwell, J. D.; Cooke, B. S.; Greer, M. K. High Performance Liquid Chromatography-Size Exclusion Chromatography for Rapid Analysis of Total Polar Compounds in Used Frying Oils. *J Am Oil Chem Soc.* **2011**, *88*, 1669-1674.
(104) Zainal; Isengard, H. D. Determination of total polar material in frying oil using accelerated solvent extraction. *Lipid Technology.* **2010**, *22*, 134-136.
(105) Kuligowski, J.; Quintas, G.; Garrigues, S.; de la Guardia, M. Monitoring of Polymerized Triglycerides in Deep-Frying Oil by On-Line GPC-FTIR Spectrometry Using the Science Based Calibration Multivariate Approach. *Chromatographia.* **2010**, *71*, 201-209.
(106) Sánchez-Muniz, F.; Cuesta, C.; Garrido-Polonio, C. Sunflower oil used for frying: combination of column, gas and high-performance size-exclusion chromatography for its evaluation. *Journal of the American Oil Chemists' Society.* **1993**, *70*, 235-240.
(107) Dobarganes, M. C.; Velasco, J.; Dieffenbacher, A. Determination of polar compounds, polymerized and oxidized triacylglycerols, and diacylglycerols in oils and fats - Results of collaborative studies and the standardized method (Technical Report). *Pure Appl Chem.* **2000**, *72*, 1563-1575.
(108) Takeoka, G. R.; Full, G. H.; Dao, L. T. Effect of heating on the characteristics and chemical composition of selected frying oils and fats. *J Agr Food Chem.* **1997**, *45*, 3244-3249.
(109) Gertz, C. Chemical and physical parameters as quality indicators of used frying fats. *Eur J Lipid Sci Tech.* **2000**, *102*, 566-572.
(110) Marmesat, S.; Rodrigues, E.; Velasco, J.; Dobarganes, C. Quality of used frying fats and oils: comparison of rapid tests based on chemical and physical oil properties. *Int J Food Sci Tech.* **2007**, *42*, 601-608.
(111) Goodridge, C. F.; Beaudry, R. M.; Pestka, J. J.; Smith, D. M. Solid phase microextraction-gas chromatography for quantifying headspace hexanal above freeze-dried chicken myofibrils. *J Agr Food Chem.* **2003**, *51*, 4185-4190.
(112) Jensen, P. N.; Christensen, J.; Engelsen, S. B. Oxidative changes in pork scratchings, peanuts, oatmeal and muesli viewed by fluorescence, near-infrared and infrared spectroscopy. *Eur Food Res Technol.* **2004**, *219*, 294-304.
(113) Shermer, W. D.; Giesen, A. F. Quality control methods to montior oxidative status of fats: What do fat tests tell you? *Feed Managment.* **1997**, *48*, 55-58.
(114) Jebe, T. A.; Matlock, M. G.; Sleeter, R. T. Collaborative study of the oil stability index analysis. *Journal of the American Oil Chemists' Society.* **1993**, *70*, 1055-1061.
(115) Frankel, E. N. In Search of Better Methods to Evaluate Natural Antioxidants and Oxidative Stability in Food Lipids. *Trends Food Sci Tech.* **1993**, *4*, 220-225.
(116) Warner, K.; Eskin, N. A. M. *Methods to assess quality and stability of oils and fat-containing foods*. AOCS Press: Champaign, Ill., 1995; p vii, 220 p.

(117) Laubli, M. W.; Bruttel, P. A. Determination of the Oxidative Stability of Fats and Oils - Comparison between the Active Oxygen Method (Aocs Cd 12-57) and the Rancimat Method. *J Am Oil Chem Soc.* **1986**, *63*, 792-795.
(118) Shahidi, F.; Zhong, Y. Lipid oxidation: measurement methods. *In Bailey's Industrial Oil and Fat Products; Wiley and Blackwell: Hoboken, NJ.* **2005**, *1*, 357−385.
(119) Liu, P.; Kerr, B. J.; Chen, C.; Weber, T. E.; Johnston, L. J.; Shurson, G. C. Methods to create thermally oxidized lipids and comparison of analytical procedures to characterize peroxidation. *Journal of animal science.* **2014**, *92*, 2950-9.
(120) Iqbal, J.; Hussain, M. M. Intestinal lipid absorption. *American journal of physiology. Endocrinology and metabolism.* **2009**, *296*, E1183-94.
(121) Combe, N.; Constantin, M. J.; Entressangles, B. Lymphatic Absorption of Non-Volatile Oxidation-Products of Heated Oils in the Rat. *Lipids.* **1981**, *16*, 8-14.
(122) Kok, T. S.; Harris, P. G.; Alexander, J. C. Heated Canola Oil and Oxidative Stress in Rats. *Nutr Res.* **1988**, *8*, 673-684.
(123) Porsgaard, T.; Zhang, H.; Nielsen, R. G.; Hoy, C. E. Absorption in rats of rapeseed, soybean, and sunflower oils before and following moderate heating. *Lipids.* **1999**, *34*, 727-732.
(124) Arroyo, R.; SanchezMuniz, F. J.; Cuesta, C.; Burguillo, F. J.; SanchezMontero, J. M. Hydrolysis of used frying palm olein and sunflower oil catalyzed by porcine pancreatic lipase. *Lipids.* **1996**, *31*, 1133-1139.
(125) Yoshida, H.; Alexander, J. C. Enzymatic-Hydrolysis of Fractionated Products from Oils Thermally Oxidized in the Laboratory. *Lipids.* **1983**, *18*, 402-407.
(126) Bergan, J. G.; Draper, H. H. Absorption and metabolism of 1-14C-methyl linoleate hydroperoxide. *Lipids.* **1970**, *5*, 976-82.
(127) Nakatsugawa, K. K., T. Absorption of methyl linoleate hydroperoxides in rabbits. *Yukagaku.* **1980**, *30*, 74-77.
(128) Grootveld, M.; Atherton, M. D.; Sheerin, A. N.; Hawkes, J.; Blake, D. R.; Richens, T. E.; Silwood, C. J. L.; Lynch, E.; Claxson, A. W. D. In vivo absorption, metabolism, and urinary excretion of au,P-Unsaturated aldehydes in experimental animals - Relevance to the development of cardiovascular diseases by the dietary ingestion of thermally stressed polyunsaturate-rich culinary oils. *J Clin Invest.* **1998**, *101*, 1210-1218.
(129) Kanazawa, K.; Ashida, H. Dietary hydroperoxides of linoleic acid decompose to aldehydes in stomach before being absorbed into the body. *Bba-Lipid Lipid Met.* **1998**, *1393*, 349-361.
(130) Oarada, M.; Miyazawa, T.; Kaneda, T. Distribution of C-14 after Oral-Administration of (U-C-14)Labeled Methyl Linoleate Hydroperoxides and Their Secondary Oxidation-Products in Rats. *Lipids.* **1986**, *21*, 150-154.
(131) Loureiro, A. P. M.; Di Mascio, P.; Medeiros, M. H. G. Exocyclic DNA adducts: Implications in mutagenesis and carcinogenesis. *Quim Nova.* **2002**, *25*, 777-793.
(132) Kanazawa, K.; Kanazawa, E.; Natake, M. Uptake of Secondary Autoxidation Products of Linoleic-Acid by the Rat. *Lipids.* **1985**, *20*, 412-419.
(133) Goicoechea, E.; Van Twillert, K.; Duits, M.; Brandon, E. D. F. A.; Kootstra, P. R.; Blokland, M. H.; Guillen, M. D. Use of an in vitro digestion model to study the

bioaccessibility of 4-hydroxy-2-nonenal and related aldehydes present in oxidized oils rich in omega-6 acyl groups. *J Agr Food Chem.* **2008**, *56*, 8475-8483.
(134) Siu, G. M.; Draper, H. H. Metabolism of malonaldehyde in vivo and in vitro. *Lipids.* **1982**, *17*, 349-55.
(135) McGirr, L. G.; Hadley, M.; Draper, H. H. Identification of N alpha-acetyl-epsilon-(2-propenal)lysine as a urinary metabolite of malondialdehyde. *The Journal of biological chemistry.* **1985**, *260*, 15427-31.
(136) Lee, S. H.; Blair, I. A. Characterization of 4-oxo-2-nonenal as a novel product of lipid peroxidation. *Chem Res Toxicol.* **2000**, *13*, 698-702.
(137) Kuiper, H. C.; Miranda, C. L.; Sowell, J. D.; Stevens, J. F. Mercapturic acid conjugates of 4-hydroxy-2-nonenal and 4-oxo-2-nonenal metabolites are in vivo markers of oxidative stress. *Journal of Biological Chemistry.* **2008**, *283*, 17131-17138.
(138) Alary, J.; Gueraud, F.; Cravedi, J. P. Fate of 4-hydroxynonenal in vivo: disposition and metabolic pathways. *Molecular aspects of medicine.* **2003**, *24*, 177-87.
(139) Niki, E. Lipid peroxidation: physiological levels and dual biological effects. *Free radical biology & medicine.* **2009**, *47*, 469-84.
(140) Jackson, B.; Brocker, C.; Thompson, D. C.; Black, W.; Vasiliou, K.; Nebert, D. W.; Vasiliou, V. Update on the aldehyde dehydrogenase gene (ALDH) superfamily. *Human genomics.* **2011**, *5*, 283-303.
(141) Perozich, J.; Nicholas, H.; Wang, B. C.; Lindahl, R.; Hempel, J. Relationships within the aldehyde dehydrogenase extended family. *Protein science : a publication of the Protein Society.* **1999**, *8*, 137-46.
(142) Hageman, G.; Verhagen, H.; Schutte, B.; Kleinjans, J. Biological effects of short-term feeding to rats of repeatedly used deep-frying fats in relation to fat mutagen content. *Food and chemical toxicology : an international journal published for the British Industrial Biological Research Association.* **1991**, *29*, 689-98.
(143) Alexander, J. C. Chemical and biological properties related to toxicity of heated fats. *Journal of toxicology and environmental health.* **1981**, *7*, 125-38.
(144) Alexander, J. C.; Valli, V. E.; Chanin, B. E. Biological observations from feeding heated corn oil and heated peanut oil to rats. *Journal of toxicology and environmental health.* **1987**, *21*, 295-309.
(145) Izaki, Y.; Yoshikawa, S.; Uchiyama, M. Effect of ingestion of thermally oxidized frying oil on peroxidative criteria in rats. *Lipids.* **1984**, *19*, 324-31.
(146) Borsting, C. F.; Engberg, R. M.; Jakobsen, K.; Jensen, S. K.; Andersen, J. O. Inclusion of Oxidized Fish-Oil in Mink Diets .1. The Influence on Nutrient Digestibility and Fatty-Acid Accumulation in Tissues. *J Anim Physiol an N.* **1994**, *72*, 132-145.
(147) Hochgraf, E.; Mokady, S.; Cogan, U. Dietary oxidized linoleic acid modifies lipid composition of rat liver microsomes and increases their fluidity. *The Journal of nutrition.* **1997**, *127*, 681-6.
(148) Lopez-Varela, S.; Sanchez-Muniz, F. J.; Cuesta, C. Decreased food efficiency ratio, growth retardation and changes in liver fatty acid composition in rats consuming thermally oxidized and polymerized sunflower oil used for frying. *Food and chemical toxicology : an international journal published for the British Industrial Biological Research Association.* **1995**, *33*, 181-9.

(149) Haywood, R. M.; Claxson, A. W.; Hawkes, G. E.; Richardson, D. P.; Naughton, D. P.; Coumbarides, G.; Hawkes, J.; Lynch, E. J.; Grootveld, M. C. Detection of aldehydes and their conjugated hydroperoxydiene precursors in thermally-stressed culinary oils and fats: investigations using high resolution proton NMR spectroscopy. *Free radical research.* **1995**, *22*, 441-82.
(150) Cortesi, R.; Privett, O. S. Toxicity of fatty ozonides and peroxides. *Lipids.* **1972**, *7*, 715-21.
(151) Nielsen, H. K.; Finot, P. A.; Hurrell, R. F. Reactions of Proteins with Oxidizing Lipids .2. Influence on Protein-Quality and on the Bioavailability of Lysine, Methionine, Cyst(E)Ine and Tryptophan as Measured in Rat Assays. *Brit J Nutr.* **1985**, *53*, 75-86.
(152) Dianzani, M. U. 4-hydroxynonenal from pathology to physiology. *Molecular aspects of medicine.* **2003**, *24*, 263-72.
(153) Zarkovic, N.; Ilic, Z.; Jurin, M.; Schaur, R. J.; Puhl, H.; Esterbauer, H. Stimulation of HeLa cell growth by physiological concentrations of 4-hydroxynonenal. *Cell biochemistry and function.* **1993**, *11*, 279-86.
(154) Zarkovic, N. 4-hydroxynonenal as a bioactive marker of pathophysiological processes. *Molecular aspects of medicine.* **2003**, *24*, 281-91.
(155) Parola, M.; Pinzani, M.; Casini, A.; Albano, E.; Poli, G.; Gentilini, A.; Gentilini, P.; Dianzani, M. U. Stimulation of lipid peroxidation or 4-hydroxynonenal treatment increases procollagen alpha 1 (I) gene expression in human liver fat-storing cells. *Biochemical and biophysical research communications.* **1993**, *194*, 1044-50.
(156) Jurgens, G.; Chen, Q.; Esterbauer, H.; Mair, S.; Ledinski, G.; Dinges, H. P. Immunostaining of human autopsy aortas with antibodies to modified apolipoprotein B and apoprotein(a). *Arteriosclerosis and thrombosis : a journal of vascular biology / American Heart Association.* **1993**, *13*, 1689-99.
(157) Hu, W.; Feng, Z.; Eveleigh, J.; Iyer, G.; Pan, J.; Amin, S.; Chung, F. L.; Tang, M. S. The major lipid peroxidation product, trans-4-hydroxy-2-nonenal, preferentially forms DNA adducts at codon 249 of human p53 gene, a unique mutational hotspot in hepatocellular carcinoma. *Carcinogenesis.* **2002**, *23*, 1781-9.
(158) Li, L.; Hamilton, R. F., Jr.; Kirichenko, A.; Holian, A. 4-Hydroxynonenal-induced cell death in murine alveolar macrophages. *Toxicology and applied pharmacology.* **1996**, *139*, 135-43.
(159) Castellani, R. J.; Perry, G.; Siedlak, S. L.; Nunomura, A.; Shimohama, S.; Zhang, J.; Montine, T.; Sayre, L. M.; Smith, M. A. Hydroxynonenal adducts indicate a role for lipid peroxidation in neocortical and brainstem Lewy bodies in humans. *Neuroscience letters.* **2002**, *319*, 25-8.
(160) Lee, S. H.; Arora, J. A.; Oe, T.; Blair, I. A. 4-Hydroperoxy-2-nonenal-induced formation of 1,N2-etheno-2'-deoxyguanosine adducts. *Chem Res Toxicol.* **2005**, *18*, 780-6.
(161) Jian, W. Y.; Arora, J. S.; Oe, T.; Shuvaev, V. V.; Blair, I. A. Induction of endothelial cell apoptosis by lipid hydroperoxide-derived bifunctional electrophiles. *Free Radical Bio Med.* **2005**, *39*, 1162-1176.
(162) Eder, K. The effects of a dietary oxidized oil on lipid metabolism in rats. *Lipids.* **1999**, *34*, 717-25.

(163) Chao, P. M.; Chao, C. Y.; Lin, F. J.; Huang, C. Oxidized frying oil up-regulates hepatic acyl-CoA oxidase and cytochrome P450 4 A1 genes in rats and activates PPARalpha. *The Journal of nutrition.* **2001**, *131*, 3166-74.
(164) Sulzle, A.; Hirche, F.; Eder, K. Thermally oxidized dietary fat upregulates the expression of target genes of PPARa in rat liver. *Journal of Nutrition.* **2004**, *134*, 1375-1383.
(165) Ringseis, R.; Piwek, N.; Eder, K. Oxidized fat induces oxidative stress but has no effect on NF-kappa B-mediated proinflammatory gene transcription in porcine intestinal epithelial cells. *Inflamm Res.* **2007**, *56*, 118-125.
(166) Ringseis, R.; Gutgesell, A.; Dathe, C.; Brandsch, C.; Eder, K. Feeding oxidized fat during pregnancy up-regulates expression of PPAR alpha-responsive genes in the liver of rat fetuses. *Lipids Health Dis.* **2007**, *6*.
(167) Luci, S.; Konig, B.; Giemsa, B.; Huber, S.; Hause, G.; Kluge, H.; Stangl, G. I.; Eder, K. Feeding of a deep-fried fat causes PPAR alpha activation in the liver of pigs as a non-proliferating species. *Brit J Nutr.* **2007**, *97*, 872-882.
(168) Konig, B.; Eder, K. Differential action of 13-HPODE on PPAR alpha downstream genes in rat Fao and human HepG2 hepatoma cell lines. *J Nutr Biochem.* **2006**, *17*, 410-418.
(169) Martin, J. C.; Caselli, C.; Broquet, S.; Juaneda, P.; Nour, M.; Sebedio, J. L.; Bernard, A. Effect of cyclic fatty acid monomers on fat absorption and transport depends on their positioning within the ingested triacylglycerols. *J Lipid Res.* **1997**, *38*, 1666-79.
(170) Peters, J. M.; Cheung, C.; Gonzalez, F. J. Peroxisome proliferator-activated receptor-alpha and liver cancer: where do we stand? *J Mol Med-Jmm.* **2005**, *83*, 774-785.
(171) Holden, P. R.; Tugwood, J. D. Peroxisome proliferator-activated receptor alpha: Role in rodent liver cancer and species differences. *J Mol Endocrinol.* **1999**, *22*, 1-8.
(172) Koch, A.; Konig, B.; Luci, S.; Stangl, G. I.; Eder, K. Dietary oxidised fat up regulates the expression of organic cation transporters in liver and small intestine and alters carnitine concentrations in liver, muscle and plasma of rats. *Brit J Nutr.* **2007**, *98*, 882-889.
(173) Koch, A.; Konig, B.; Spielmann, J.; Leitner, A.; Stangl, G. I.; Eder, K. Thermally oxidized oil increases the expression of insulin-induced genes and inhibits activation of sterol regulatory element-binding protein-2 in rat liver. *The Journal of nutrition.* **2007**, *137*, 2018-23.
(174) Kaddurah-Daouk, R.; Kristal, B. S.; Weinshilboum, R. M. Metabolomics: a global biochemical approach to drug response and disease. *Annu Rev Pharmacol Toxicol.* **2008**, *48*, 653-83.
(175) Patti, G. J.; Yanes, O.; Siuzdak, G. Innovation: Metabolomics: the apogee of the omics trilogy. *Nat Rev Mol Cell Biol.* **2012**, *13*, 263-9.
(176) Wang, L.; Chen, C. Emerging applications of metabolomics in studying chemopreventive phytochemicals. *AAPS J.* **2013**, *15*, 941-50.
(177) Chen, C.; Kim, S. LC-MS-based Metabolomics of Xenobiotic-induced Toxicities. *Comput Struct Biotechnol J.* **2013**, *4*, e201301008.
(178) Zhu, J. Q.; Fan, X. H.; Cheng, Y. Y.; Agarwal, R.; Moore, C. M. V.; Chen, S. T.; Tong, W. D. Chemometric Analysis for Identification of Botanical Raw Materials for Pharmaceutical Use: A Case Study Using Panax notoginseng. *Plos One.* **2014**, *9*.

(179) Katajamaa, M.; Oresic, M. Data processing for mass spectrometry-based metabolomics. *Journal of chromatography. A.* **2007**, *1158*, 318-28.
(180) Sysi-Aho, M.; Katajamaa, M.; Yetukuri, L.; Oresic, M. Normalization method for metabolomics data using optimal selection of multiple internal standards. *Bmc Bioinformatics.* **2007**, *8*.
(181) Schlotterbeck, G.; Ross, A.; Dieterle, F.; Senn, H. Metabolic profiling technologies for biomarker discovery in biomedicine and drug development. *Pharmacogenomics.* **2006**, *7*, 1055-1075.
(182) Trygg, J.; Holmes, E.; Lundstedt, T. Chemometrics in metabonomics. *J Proteome Res.* **2007**, *6*, 469-479.
(183) Iijima, Y.; Nakamura, Y.; Ogata, Y.; Tanaka, K.; Sakurai, N.; Suda, K.; Suzuki, T.; Suzuki, H.; Okazaki, K.; Kitayama, M.; Kanaya, S.; Aoki, K.; Shibata, D. Metabolite annotations based on the integration of mass spectral information. *Plant J.* **2008**, *54*, 949-62.
(184) Kind, T.; Fiehn, O. Metabolomic database annotations via query of elemental compositions: mass accuracy is insufficient even at less than 1 ppm. *Bmc Bioinformatics.* **2006**, *7*, 234.
(185) Victoria Sanz Fernandez, M.; Johnson, J. S.; Abuajamieh, M.; Stoakes, S. K.; Seibert, J. T.; Cox, L.; Kahl, S.; Elsasser, T. H.; Ross, J. W.; Isom, S. C.; Rhoads, R. P.; Baumgard, L. H. Effects of heat stress on carbohydrate and lipid metabolism in growing pigs. *Physiological reports.* **2015**, *3*, e12315.
(186) Carlson, M. S.; Hill, G. M.; Link, J. E. Early- and traditionally weaned nursery pigs benefit from phase-feeding pharmacological concentrations of zinc oxide: effect on metallothionein and mineral concentrations. *Journal of animal science.* **1999**, *77*, 1199-207.
(187) Lynch, C. J.; Patson, B. J.; Goodman, S. A.; Trapolsi, D.; Kimball, S. R. Zinc stimulates the activity of the insulin- and nutrient-regulated protein kinase mTOR. *American journal of physiology. Endocrinology and metabolism.* **2001**, *281*, E25-34.
(188) Hedemann, M. S.; Jensen, B. B.; Poulsen, H. D. Influence of dietary zinc and copper on digestive enzyme activity and intestinal morphology in weaned pigs. *Journal of animal science.* **2006**, *84*, 3310-20.
(189) Maret, W. Zinc Biochemistry: From a Single Zinc Enzyme to a Key Element of Life. *Adv Nutr.* **2013**, *4*, 82-91.
(190) Chen, C.; Gonzalez, F. J.; Idle, J. R. LC-MS-based metabolomics in drug metabolism. *Drug metabolism reviews.* **2007**, *39*, 581-97.
(191) Bligh, E. G.; Dyer, W. J. A rapid method of total lipid extraction and purification. *Canadian journal of biochemistry and physiology.* **1959**, *37*, 911-7.
(192) Lu, Y.; Yao, D.; Chen, C. 2-Hydrazinoquinoline as a derivatization agent for LC-MS-based metabolomic investigation of diabetic ketoacidosis. *Metabolites.* **2013**, *3*, 993-1010.
(193) Suhre, K.; Schmitt-Kopplin, P. MassTRIX: mass translator into pathways. *Nucleic acids research.* **2008**, *36*, W481-4.
(194) Abumrad, N. N.; Miller, B. The physiologic and nutritional significance of plasma-free amino acid levels. *JPEN. Journal of parenteral and enteral nutrition.* **1983**, *7*, 163-70.

(195) Seltzer, J. L.; Eisen, A. Z.; Bauer, E. A.; Morris, N. P.; Glanville, R. W.; Burgeson, R. E. Cleavage of type VII collagen by interstitial collagenase and type IV collagenase (gelatinase) derived from human skin. *The Journal of biological chemistry.* **1989**, *264*, 3822-6.
(196) Thomas, J.; Crowhurst, T. Exertional heat stroke, rhabdomyolysis and susceptibility to malignant hyperthermia. *Internal medicine journal.* **2013**, *43*, 1035-8.
(197) Shimomura, Y.; Murakami, T.; Nakai, N.; Nagasaki, M.; Harris, R. A. Exercise promotes BCAA catabolism: effects of BCAA supplementation on skeletal muscle during exercise. *The Journal of nutrition.* **2004**, *134*, 1583S-1587S.
(198) Kellogg, D. L., Jr.; Zhao, J. L.; Friel, C.; Roman, L. J. Nitric oxide concentration increases in the cutaneous interstitial space during heat stress in humans. *Journal of applied physiology.* **2003**, *94*, 1971-7.
(199) Daghigh, F.; Fukuto, J. M.; Ash, D. E. Inhibition of rat liver arginase by an intermediate in NO biosynthesis, NG-hydroxy-L-arginine: implications for the regulation of nitric oxide biosynthesis by arginase. *Biochemical and biophysical research communications.* **1994**, *202*, 174-80.
(200) Torrallardona, D.; Harris, C. I.; Fuller, M. F. Lysine synthesized by the gastrointestinal microflora of pigs is absorbed, mostly in the small intestine. *American journal of physiology. Endocrinology and metabolism.* **2003**, *284*, E1177-80.
(201) Fadeel, B.; Xue, D. The ins and outs of phospholipid asymmetry in the plasma membrane: roles in health and disease. *Critical reviews in biochemistry and molecular biology.* **2009**, *44*, 264-77.
(202) Torok, Z.; Crul, T.; Maresca, B.; Schutz, G. J.; Viana, F.; Dindia, L.; Piotto, S.; Brameshuber, M.; Balogh, G.; Peter, M.; Porta, A.; Trapani, A.; Gombos, I.; Glatz, A.; Gungor, B.; Peksel, B.; Vigh, L., Jr.; Csoboz, B.; Horvath, I.; Vijayan, M. M.; Hooper, P. L.; Harwood, J. L.; Vigh, L. Plasma membranes as heat stress sensors: from lipid-controlled molecular switches to therapeutic applications. *Biochimica et biophysica acta.* **2014**, *1838*, 1594-618.
(203) Jenkins, B.; West, J. A.; Koulman, A. A review of odd-chain fatty acid metabolism and the role of pentadecanoic Acid (c15:0) and heptadecanoic Acid (c17:0) in health and disease. *Molecules.* **2015**, *20*, 2425-44.
(204) Foulon, V.; Sniekers, M.; Huysmans, E.; Asselberghs, S.; Mahieu, V.; Mannaerts, G. P.; Van Veldhoven, P. P.; Casteels, M. Breakdown of 2-hydroxylated straight chain fatty acids via peroxisomal 2-hydroxyphytanoyl-CoA lyase: a revised pathway for the alpha-oxidation of straight chain fatty acids. *The Journal of biological chemistry.* **2005**, *280*, 9802-12.
(205) Fujitani, K.; Manami, H.; Nakazawa, M.; Oida, T.; Kawase, T. Preparation of polycarboxylic acids by oxidative cleavage with oxygen / Co-Mn-Br system. *Journal of oleo science.* **2009**, *58*, 629-37.
(206) King, J. C.; Shames, D. M.; Woodhouse, L. R. Zinc homeostasis in humans. *The Journal of nutrition.* **2000**, *130*, 1360S-6S.
(207) Weigand, E.; Kirchgessner, M. Total true efficiency of zinc utilization: determination and homeostatic dependence upon the zinc supply status in young rats. *The Journal of nutrition.* **1980**, *110*, 469-80.

(208) Weigand, E.; Kirchgessner, M. Homeostatic adjustments in zinc digestion to widely varying dietary zinc intake. *Nutrition and metabolism.* **1978**, *22*, 101-12.
(209) Cragg, R. A.; Phillips, S. R.; Piper, J. M.; Varma, J. S.; Campbell, F. C.; Mathers, J. C.; Ford, D. Homeostatic regulation of zinc transporters in the human small intestine by dietary zinc supplementation. *Gut.* **2005**, *54*, 469-78.
(210) King, J. C. Assessment of zinc status. *The Journal of nutrition.* **1990**, *120 Suppl 11*, 1474-9.
(211) Katouli, M.; Melin, L.; Jensen-Waern, M.; Wallgren, P.; Mollby, R. The effect of zinc oxide supplementation on the stability of the intestinal flora with special reference to composition of coliforms in weaned pigs. *Journal of applied microbiology.* **1999**, *87*, 564-73.
(212) Surjawidjaja, J. E.; Hidayat, A.; Lesmana, M. Growth inhibition of enteric pathogens by zinc sulfate: an in vitro study. *Medical principles and practice : international journal of the Kuwait University, Health Science Centre.* **2004**, *13*, 286-9.
(213) Gika, H. G.; Theodoridis, G. A.; Plumb, R. S.; Wilson, I. D. Current practice of liquid chromatography-mass spectrometry in metabolomics and metabonomics. *Journal of pharmaceutical and biomedical analysis.* **2014**, *87*, 12-25.
(214) Xu, F.; Zou, L.; Liu, Y.; Zhang, Z.; Ong, C. N. Enhancement of the capabilities of liquid chromatography-mass spectrometry with derivatization: general principles and applications. *Mass spectrometry reviews.* **2011**, *30*, 1143-72.
(215) Wishart, D. S. Advances in metabolite identification. *Bioanalysis.* **2011**, *3*, 1769-82.
(216) Pokorny, J.; Dostalova, J. Changes in nutrients, antinutritional factors, and contaminants at frying temperatures. In *Frying of Food: Oxidation, Nutrient and Non-Nutrient Antioxidants, Biologically Active Compounds, and High Temperatures*, 2nd ed.; Boskou, D.; Elmadfa, I., Eds.; CRC Press: Boca Raton, FL, 2011; pp 71-104.
(217) Zhang, Q.; Saleh, A. S.; Chen, J.; Shen, Q. Chemical alterations taken place during deep-fat frying based on certain reaction products: a review. *Chem. Phys. Lipids.* **2012**, *165*, 662-681.
(218) Warner, K.; Neff, W. E.; Byrdwell, W. C.; Gardner, H. W. Effect of oleic and linoleic acids on the production of deep-fried odor in heated triolein and trilinolein. *J Agric Food Chem.* **2001**, *49*, 899-905.
(219) Bordin, K.; Kunitake, M. T.; Aracava, K. K.; Trindade, C. S. F. Changes in food caused by deep fat frying - A review. *Arch Latinoam Nutr.* **2013**, *63*, 5-13.
(220) Pegg, R. B. Measurement of primary lipid oxidation products. *Current Protocols in Food Analytical Chemistry.* **2001**, D:D2:D2.1.
(221) Botsoglou, N. A.; Fletouris, D. J.; Papageorgiou, G. E.; Vassilopoulos, V. N.; Mantis, A. J.; Trakatellis, A. G. Rapid, sensitive, and specific thiobarbituric acid method for measuring lipid-peroxidation in animal tissue, food, and feedstuff samples. *J Agr Food Chem.* **1994**, *42*, 1931-1937.
(222) Bird, S. S.; Marur, V. R.; Sniatynski, M. J.; Greenberg, H. K.; Kristal, B. S. Serum Lipidomics Profiling Using LC-MS and High-Energy Collisional Dissociation Fragmentation: Focus on Triglyceride Detection and Characterization. *Anal Chem.* **2011**, *83*, 6648-6657.

(223) Shah, K. J.; Venkatesan, T. K. Aqueous Isopropyl-Alcohol for Extraction of Free Fatty-Acids from Oils. *J Am Oil Chem Soc.* **1989**, *66*, 783-787.
(224) Zhao, S. L.; Guo, Y.; Sheng, Q. H.; Shyr, Y. Advanced heat map and clustering analysis using heatmap3. *Biomed Res Int.* **2014**.
(225) Karakaya, S.; Simsek, S. Changes in total polar compounds, peroxide value, total phenols and antioxidant activity of various oils used in deep fat frying. *J Am Oil Chem Soc.* **2011**, *88*, 1361-1366.
(226) Ollivier, D.; Artaud, J.; Pinatel, C.; Durbec, J. P.; Guerere, M. Triacylglycerol and fatty acid compositions of French virgin olive oils. Characterization by chemometrics. *J Agric Food Chem.* **2003**, *51*, 5723-31.
(227) Zribi, A.; Jabeur, H.; Aladedunye, F.; Rebai, A.; Matthaus, B.; Bouaziz, M. Monitoring of quality and stability characteristics and fatty acid compositions of refined olive and seed oils during repeated pan- and deep-frying using GC, FT-NIRS, and chemometrics. *J Agric Food Chem.* **2014**, *62*, 10357-67.
(228) Ng, C. L.; Wehling, R. L.; Cuppett, S. L. Method for determining frying oil degradation by near-infrared spectroscopy. *J Agric Food Chem.* **2007**, *55*, 593-7.
(229) Engelsen, S. Explorative spectrometric evaluations of frying oil deterioration. *Journal of the American Oil Chemists' Society.* **1997**, *74*, 1495-1508.
(230) Zhou, B.; Xiao, J. F.; Tuli, L.; Ressom, H. W. LC-MS-based metabolomics. *Molecular bioSystems.* **2012**, *8*, 470-81.
(231) Sandra, P.; Medvedovici, A.; Zhao, Y.; David, F. Characterization of triglycerides in vegetable oils by silver-ion packed-column supercritical fluid chromatography coupled to mass spectroscopy with atmospheric pressure chemical ionization and coordination ion spray. *Journal of chromatography. A.* **2002**, *974*, 231-41.
(232) Leskinen, H.; Suomela, J. P.; Kallio, H. Quantification of triacylglycerol regioisomers in oils and fat using different mass spectrometric and liquid chromatographic methods. *Rapid communications in mass spectrometry : RCM.* **2007**, *21*, 2361-73.
(233) Aparicio, R.; Aparicio-Ruiz, R. Authentication of vegetable oils by chromatographic techniques. *Journal of Chromatography A.* **2000**, *881*, 93-104.
(234) Garcia-Gonzalez, D. L.; Viera, M.; Tena, N.; Aparicio, R. Evaluation of the methods based on triglycerides and sterols for the detection of hazelnut oil in olive oil. *Grasas Aceites.* **2007**, *58*, 344-350.
(235) Piravi-Vanak, Z.; Ghavami, M.; Ezzatpanah, H.; Arab, J.; Safafar, H.; Ghasemi, J. B. Evaluation of Authenticity of Iranian Olive Oil by Fatty Acid and Triacylglycerol Profiles. *J Am Oil Chem Soc.* **2009**, *86*, 827-833.
(236) Schneider, C.; Boeglin, W. E.; Yin, H. Y.; Stec, D. F.; Hachey, D. L.; Porter, N. A.; Brash, A. R. Synthesis of dihydroperoxides of linoleic and linolenic acids and studies on their transformation to 4-hydroperoxynonenal. *Lipids.* **2005**, *40*, 1155-1162.
(237) Schneider, C.; Porter, N. A.; Brash, A. R. Autoxidative transformation of chiral omega6 hydroxy linoleic and arachidonic acids to chiral 4-hydroxy-2E-nonenal. *Chem Res Toxicol.* **2004**, *17*, 937-41.
(238) Schneider, C.; Tallman, K. A.; Porter, N. A.; Brash, A. R. Two distinct pathways of formation of 4-hydroxynonenal - Mechanisms of nonenzymatic transformation of the 9-

and 13-hydroperoxides of linoleic acid to 4-hydroxyalkenals. *Journal of Biological Chemistry.* **2001**, *276*, 20831-20838.
(239) Yamauchi, Y.; Furutera, A.; Seki, K.; Toyoda, Y.; Tanaka, K.; Sugimoto, Y. Malondialdehyde generated from peroxidized linolenic acid causes protein modification in heat-stressed plants. *Plant Physiol Bioch.* **2008**, *46*, 786-793.
(240) Gutteridge, J. M. C. The HPTLC separation of malondialdehyde from peroxidised linoleic acid. *Journal of High Resolution Chromatography.* **1978**, *1*, 311-312.
(241) Ho, C. T.; Chen, Q. Y. Lipids in food flavors - an overview. *Acs Sym Ser.* **1994**, *558*, 2-14.
(242) Bax, S.; Hakka, M. H.; Glaude, P. A.; Herbinet, O.; Battin-Leclerc, F. Experimental study of the oxidation of methyl oleate in a jet-stirred reactor. *Combust Flame.* **2010**, *157*, 1220-1229.
(243) Endo, Y.; Hayashi, C.; Yamanaka, T.; Takayose, K.; Yamaoka, M.; Tsuno, T.; Nakajima, S. Linolenic acid as the main source of acrolein formed during heating of vegetable oils. *J Am Oil Chem Soc.* **2013**, *90*, 959-964.
(244) Nielsen, G. S.; Larsen, L. M.; Poll, L. Formation of volatile compounds in model experiments with crude leek (Allium ampeloprasum Var. Lancelot) enzyme extract and linoleic acid or linolenic acid. *J Agric Food Chem.* **2004**, *52*, 2315-21.
(245) Neff, W. E.; Mounts, T. L.; Rinsch, W. M.; Konishi, H. Photooxidation of soybean oils as affected by triacylglycerol composition and structure. *J Am Oil Chem Soc.* **1993**, *70*, 163-168.
(246) Esterbauer, H.; Schaur, R. J.; Zollner, H. Chemistry and biochemistry of 4-hydroxynonenal, malonaldehyde and related aldehydes. *Free radical biology & medicine.* **1991**, *11*, 81-128.
(247) Seppanen, C. M.; Csallany, A. S. Formation of 4-hydroxynonenal, a toxic aldehyde, in soybean oil at frying temperature. *J Am Oil Chem Soc.* **2002**, *79*, 1033-1038.
(248) Csallany, A. S.; Han, I.; Shoeman, D. W.; Chen, C.; Yuan, J. Y. 4-Hydroxynonenal (HNE), a toxic aldehyde in French fries from fast food restaurants. *J Am Oil Chem Soc.* **2015**, *92*, 1413-1419.
(249) Kim, Y. S.; Ho, C. T. Formation of pyridines from thermal interaction of glutamine or glutamic acid with a mixture of alkadienals in aqueous and oil media. *Journal of Food Lipids.* **1998**, *5*, 173-182.
(250) Kim, Y. S.; Hartman, T. G.; Ho, C. T. Formation of 2-pentylpyridine from the thermal interaction of amino acids and 2,4-decadienal. *J Agr Food Chem.* **1996**, *44*, 3906-3908.
(251) Uchida, K. Histidine and lysine as targets of oxidative modification. *Amino acids.* **2003**, *25*, 249-57.
(252) Stevens, J. F.; Maier, C. S. Acrolein: sources, metabolism, and biomolecular interactions relevant to human health and disease. *Mol Nutr Food Res.* **2008**, *52*, 7-25.
(253) Rosero, D. S.; Odle, J.; Moeser, A. J.; Boyd, R. D.; van Heugten, E. Peroxidised dietary lipids impair intestinal function and morphology of the small intestine villi of nursery pigs in a dose-dependent manner. *Br J Nutr.* **2015**, *114*, 1985-92.
(254) Ringseis, R.; Eder, K. Regulation of genes involved in lipid metabolism by dietary oxidized fat. *Mol Nutr Food Res.* **2011**, *55*, 109-21.

(255) Koppaka, V.; Thompson, D. C.; Chen, Y.; Ellermann, M.; Nicolaou, K. C.; Juvonen, R. O.; Petersen, D.; Deitrich, R. A.; Hurley, T. D.; Vasiliou, V. Aldehyde Dehydrogenase Inhibitors: a Comprehensive Review of the Pharmacology, Mechanism of Action, Substrate Specificity, and Clinical Application. *Pharmacol Rev.* **2012**, *64*, 520-539.
(256) Delaney, J.; Hodson, M. P.; Thakkar, H.; Connor, S. C.; Sweatman, B. C.; Kenny, S. P.; McGill, P. J.; Holder, J. C.; Hutton, K. A.; Haselden, J. N.; Waterfield, C. J. Tryptophan-NAD(+) pathway metabolites as putative biomarkers and predictors of peroxisome proliferation. *Arch Toxicol.* **2005**, *79*, 208-223.
(257) Shin, M.; Ohnishi, M.; Iguchi, S.; Sano, K.; Umezawa, C. Peroxisome-proliferator regulates key enzymes of the tryptophan-NAD(+) pathway. *Toxicology and applied pharmacology.* **1999**, *158*, 71-80.
(258) Penumetcha, M.; Schneider, M. K.; Cheek, H. A.; Karabina, S. A diet containing soybean oil heated for three hours increases adipose tissue weight but decreases body weight in C57BL/6 J mice. *Lipids Health Dis.* **2013**, *12*.
(259) Liu, P.; Chen, C.; Kerr, B. J.; Weber, T. E.; Johnston, L. J.; Shurson, G. C. Influence of thermally oxidized vegetable oils and animal fats on growth performance, liver gene expression, and liver and serum cholesterol and triglycerides in young pigs. *Journal of animal science.* **2014**, *92*, 2960-2970.
(260) Hanson, A. R.; Urriola, P. E.; Wang, L.; Johnston, L. J.; Chen, C.; Shurson, G. C. Dietary peroxidized maize oil affects the growth performance and antioxidant status of nursery pigs. *Anim Feed Sci Tech.* **2016**, *216*, 251-261.
(261) Boler, D. D.; Fernandez-Duenas, D. M.; Kutzler, L. W.; Zhao, J.; Harrell, R. J.; Campion, D. R.; McKeith, F. K.; Killefer, J.; Dilger, A. C. Effects of oxidized corn oil and a synthetic antioxidant blend on performance, oxidative status of tissues, and fresh meat quality in finishing barrows. *Journal of animal science.* **2012**, *90*, 5159-5169.
(262) DeRouchey, J. M.; Hancock, J. D.; Hines, R. H.; Maloney, C. A.; Lee, D. J.; Cao, H.; Dean, D. W.; Park, J. S. Effects of rancidity and free fatty acids in choice white grease on growth performance and nutrient digestibility in weanling pigs. *Journal of animal science.* **2004**, *82*, 2937-2944.
(263) Matthan, N. R.; Ooi, E. M.; Van Horn, L.; Neuhouser, M. L.; Woodman, R.; Lichtenstein, A. H. Plasma Phospholipid Fatty Acid Biomarkers of Dietary Fat Quality and Endogenous Metabolism Predict Coronary Heart Disease Risk: A Nested Case-Control Study Within the Women's Health Initiative Observational Study. *J Am Heart Assoc.* **2014**, *3*.
(264) Khaw, K. T.; Friesen, M. D.; Riboli, E.; Luben, R.; Wareham, N. Plasma Phospholipid Fatty Acid Concentration and Incident Coronary Heart Disease in Men and Women: The EPIC-Norfolk Prospective Study. *Plos Med.* **2012**, *9*.
(265) Crowe, F. L.; Allen, N. E.; Appleby, P. N.; Overvad, K.; Aardestrup, I. V.; Johnsen, N. F.; Tjonneland, A.; Linseisen, J.; Kaaks, R.; Boeing, H.; Kroger, J.; Trichopoulou, A.; Zavitsanou, A.; Trichopoulos, D.; Sacerdote, C.; Palli, D.; Tumino, R.; Agnoli, C.; Kiemeney, L. A.; Bueno-de-Mesquita, H. B.; Chirlaque, M. D.; Ardanaz, E.; Larranaga, N.; Quiros, J. R.; Sanchez, M. J.; Gonzalez, C. A.; Stattin, P.; Hallmans, G.; Bingham, S.; Khaw, K. T.; Rinaldi, S.; Slimani, N.; Jenab, M.; Riboli, E.; Key, T. J. Fatty acid composition of plasma phospholipids and risk of prostate cancer in a case-control analysis

nested within the European Prospective Investigation into Cancer and Nutrition. *Am J Clin Nutr.* **2008**, *88*, 1353-1363.
(266) Borniquel, S.; Valle, I.; Cadenas, S.; Lamas, S.; Monsalve, M. Nitric oxide regulates mitochondrial oxidative stress protection via the transcriptional coactivator PGC-1 alpha. *Faseb J.* **2006**, *20*, 1889-+.
(267) Shen, Y. B.; Voilque, G.; Kim, J. D.; Odle, J.; Kim, S. W. Effects of increasing tryptophan intake on growth and physiological changes in nursery pigs. *Journal of animal science.* **2012**, *90*, 2264-2275.
(268) Oxenkrug, G. F. Genetic and hormonal regulation of tryptophan-kynurenine metabolism - Implications for vascular cognitive Impairment, major depressive disorder, and aging. *Ann Ny Acad Sci.* **2007**, *1122*, 35-49.
(269) Kamat, J. P.; Devasagayam, T. P. Methylene blue plus light-induced lipid peroxidation in rat liver microsomes: inhibition by nicotinamide (vitamin B3) and other antioxidants. *Chem Biol Interact.* **1996**, *99*, 1-16.
(270) Kirsch, M.; De Groot, H. NAD(P)H, a directly operating antioxidant? *Faseb J.* **2001**, *15*, 1569-74.
(271) Surjana, D.; Halliday, G. M.; Damian, D. L. Role of nicotinamide in DNA damage, mutagenesis, and DNA repair. *J Nucleic Acids.* **2010**, *2010*.
(272) Oliver, F. J.; Menissier-de Murcia, J.; de Murcia, G. Poly(ADP-ribose) polymerase in the cellular response to DNA damage, apoptosis, and disease. *Am J Hum Genet.* **1999**, *64*, 1282-8.
(273) Jacobson, E. L.; Shieh, W. M.; Huang, A. C. Mapping the role of NAD metabolism in prevention and treatment of carcinogenesis. *Mol Cell Biochem.* **1999**, *193*, 69-74.
(274) Peng, Z.; Borea, P. A.; Wilder, T.; Yee, H.; Chiriboga, L.; Blackburn, M. R.; Azzena, G.; Resta, G.; Cronstein, B. N. Adenosine signaling contributes to ethanol-induced fatty liver in mice. *J Clin Invest.* **2009**, *119*, 582-594.
(275) Fredholm, B. B. Adenosine, an endogenous distress signal, modulates tissue damage and repair. *Cell Death Differ.* **2007**, *14*, 1315-1323.
(276) Chen, J. J.; Bertrand, H.; Yu, B. P. Inhibition of Adenine-Nucleotide Translocator by Lipid-Peroxidation Products. *Free Radical Bio Med.* **1995**, *19*, 583-590.
(277) Patterson, A. D.; Slanar, O.; Krausz, K. W.; Li, F.; Hofer, C. C.; Perlik, F.; Gonzalez, F. J.; Idle, J. R. Human Urinary Metabolomic Profile of PPAR alpha Induced Fatty Acid beta-Oxidation. *J Proteome Res.* **2009**, *8*, 4293-4300.
(278) Emudianughe, T. S.; Bickle, Q. D.; Taylor, M. G.; Andrews, B. Effect of Plasmodium berghei infection on benzoic acid metabolism in mice. *Experientia.* **1985**, *41*, 1407-9.